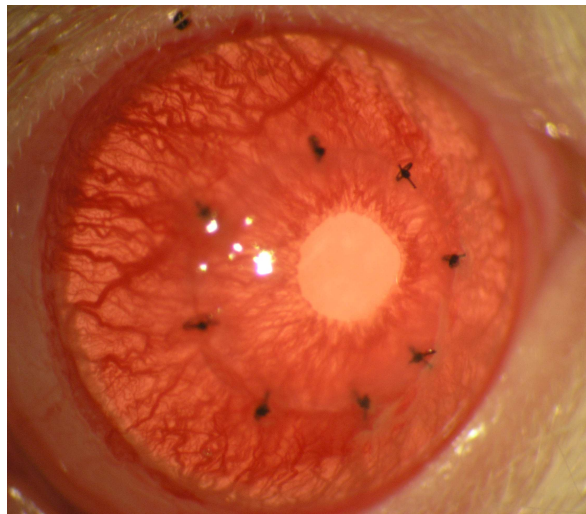


# REGIONAL IMMUNOSUPPRESSION FOR CORNEAL TRANSPLANTATION

**SARAH L BRICE**

B. Biotech (Hons)



Thesis submitted for the degree of

Doctor of Philosophy

January 2010

Faculty of Health Sciences

School of Medicine

Flinders University of SA

Adelaide, Australia

## TABLE OF CONTENTS

ABSTRACT .....	x
CONFERENCE PRESENTATIONS ARISING FROM THIS THESIS .....	xiii
DECLARATION.....	xiv
ACKNOWLEDGEMENTS .....	xv
ABBREVIATIONS .....	xvii
<b>CHAPTER 1: INTRODUCTION.....</b>	<b>1</b>
1.1 INTRODUCTION OVERVIEW .....	2
1.2 THE HUMAN CORNEA.....	2
1.2.a. Anatomy of the human cornea.....	2
1.2.b. Proliferative capacity of the human corneal endothelium.....	4
1.3. CORNEAL TRANSPLANTATION.....	5
1.4 ANIMAL MODELS OF CORNEAL TRANSPLANTATION .....	7
1.5 MECHANISMS OF CORNEAL GRAFT REJECTION .....	8
1.6 IMMUNOLOGY OF CORNEAL TRANSPLANTATION .....	9
1.6.a. T cells .....	9
1.6.b. Antigen presenting cells (APCs) in the eye.....	13
1.6.c. Allorecognition.....	20
1.6.d. Ocular lymphatic drainage .....	21
1.6.e. Immune privilege in the eye .....	27
1.7 THERAPIES FOR CORNEAL GRAFT REJECTION .....	29
1.7.a. Topical application of glucocorticosteroids .....	29
1.7.b. HLA-matching.....	29
1.7.c. Systemic immunosuppression using calcineurin blockers .....	30
1.7.d. Antibodies and antibody fragments.....	30

1.8 GENE THERAPY .....	34
1.8.a. Gene therapy overview .....	34
1.8.b. Gene transfer to the corneal endothelium.....	35
1.8.c. Lentivirus biology.....	37
1.8.d. Recombinant lentiviral vectors for gene transfer .....	38
1.8.e. The Anson HIV-1 vector system .....	44
1.9 BIOSAFETY ISSUES ASSOCIATED WITH GENE THERAPY .....	46
1.9.a. The first gene therapy death .....	46
1.9.b. Insertional mutagenesis .....	47
1.9.c. Immune reactivity of viral vectors.....	48
1.9.d. Gene therapy for the treatment of non-life threatening disease .....	48
1.9.e. Ocular gene therapy .....	49
1.9.f. Summary of the biosafety issues associated with gene therapy.....	49
1.10 SUMMARY AND AIMS.....	50
<b>CHAPTER 2: MATERIALS AND METHODS .....</b>	<b>53</b>
2.1 MATERIALS .....	54
2.1.a. General chemicals.....	54
2.1.b. Antibodies .....	54
2.1.c. Antibody fragments .....	54
2.1.d. Antibiotics .....	54
2.1.e. <i>Escherichia coli</i> ( <i>E. coli</i> ) strains.....	56
2.1.f. Plasmids .....	56
2.1.g. Molecular biology reagents .....	56
2.1.h. Polymerase chain reaction (PCR) primers .....	56
2.1.i. Mammalian cell culture reagents .....	56

2.1.j. Animals .....	61
2.1.k. Miscellaneous reagents.....	61
2.1.l. Filter cube specifications on fluorescence microscopes .....	61
2.2 MOLECULAR METHODS .....	63
2.2.a. Plasmid DNA preparation .....	63
2.2.b. Restriction endonuclease digestion .....	64
2.2.c. Dephosphorylation with shrimp alkaline phosphatase (SAP) .....	64
2.2.d. Purification of digested and/or SAP-treated DNA .....	65
2.2.e. Ligations .....	65
2.2.f. Purification of ligation products .....	65
2.2.g. Agarose gel electrophoresis.....	66
2.2.h. Preparation of electrocompetent cells ( <i>E. coli</i> strains).....	66
2.2.i. Electroporation of <i>E. coli</i> strains DH5 $\alpha$ and GM48.....	67
2.2.j. End-point polymerase chain reaction (PCR).....	68
2.2.k. Total RNA extraction .....	69
2.2.l. DNase I treatment of RNA.....	70
2.2.m. cDNA synthesis.....	71
2.3 QUANTITATIVE REAL-TIME PCR (QPCR) .....	71
2.3.a. Primers for qPCR.....	71
2.3.b. qPCR set up.....	72
2.3.c. Determination of primer pair amplification efficiency.....	73
2.3.d. Gene expression analysis.....	73
2.4 CELL CULTURE METHODS .....	74
2.4.a. Maintenance of cell lines.....	74
Table 2.9: Cell lines.....	75



2.4.b. Freezing cell lines.....	75
2.4.c. Thawing cells.....	75
2.4.d. Cell viability determinations .....	76
2.4.e. Liposome-mediated transfection of mammalian cells.....	76
2.4.f. Transduction of mammalian cells with lentiviral vectors .....	77
2.4.g. Flow cytometry to detect scFv binding .....	77
2.4.h. Flow cytometry for eYFP detection in transfected or transduced cells .....	79
2.4.i. Fluorescence microscopy of cell lines .....	80
2.4.j. Human endostatin::kringle-5 (EK5) detection in culture supernatant by ELISA.....	80
2.4.k. Determination of endotoxin levels in viral preparations .....	80
2.5 LENTIVIRAL VECTOR PRODUCTION AND TESTING .....	81
2.5.a. Large scale lentiviral vector preparations.....	81
2.5.b. Medium scale lentiviral vector preparations .....	83
2.5.c. Detection of replication-competent lentivirus .....	84
2.5.d. Titration of lentiviral vector preparations .....	84
2.6 ADENOVIRAL VECTOR PREPARATION .....	87
2.6.a. Adenoviral vector production.....	87
2.6.b. Titration of adenoviral vector preparations .....	89
2.7 ANIMAL AND TISSUE METHODS .....	90
2.7.a. Conventional histology.....	90
2.7.b. Nuclear staining of tissues.....	90
2.7.c. Fluorescence microscopy of rat tissues .....	91
2.7.d. Transduction of rat tissues with viral vectors.....	92
2.7.e. Rat orthotopic corneal transplantation.....	94

2.7.f. Post-operative assessment of corneal grafts.....	95
2.7.g. Collection of rat blood by tail tipping .....	97
2.7.h. Lymphadenectomy of cervical lymph nodes.....	97
2.8 STATISTICAL ANALYSIS .....	98
2.8.a. Statistical analysis of transgene expression.....	98
2.8.b. Statistical analysis of corneal graft survival and inflammation data.....	98
<b>CHAPTER 3: CONSTRUCTION AND CHARACTERISATION</b>	
<b>OF LENTIVIRAL VECTORS .....</b>	<b>99</b>
3.1 ABSTRACT .....	100
3.2 INTRODUCTION.....	101
3.2.a. Gene transfer to the eye .....	101
3.2.b. Lentiviral vectors for gene transfer .....	101
3.2.c. CD4 as a target for T cell activation.....	102
3.2.d. ScFv as a potential treatment to the cornea.....	102
3.2.e. The Foot and Mouth Disease Virus (FMDV) 2A self-processing sequence	103
3.2.f. Specific aims .....	103
3.3 RESULTS.....	104
3.3.a. Construction of lentiviral plasmids.....	104
3.3.b. Analysis of lentiviral vector titration.....	123
3.3.c. Transgene expression from single-gene and dual-gene vectors .....	128
3.4: SUMMARY AND DISCUSSION .....	139
3.4.a. Summary.....	139
3.4.b. Titration of lentiviral vector preparations .....	140
3.4.c. Multigenic expression using the 2A self-processing sequence .....	146

<b>CHAPTER 4: EXPRESSION OF ANTI-RAT CD4 SCFV AT POTENTIAL SITES OF ANTIGEN PRESENTATION.....</b>	<b>154</b>
4.1 ABSTRACT .....	155
4.2 INTRODUCTION.....	156
4.2.a. Corneal graft rejection.....	156
4.2.b. Regional immunosuppression .....	156
4.2.c. Anti-rat CD4 scFv as an immunosuppressive agent.....	158
4.2.d. Specific aims .....	159
4.3 RESULTS.....	160
4.3.a Lentiviral transduction of the corneal endothelium.....	160
4.3.b. Lentiviral transduction of the cervical lymph nodes.....	182
4.3.c. Bilateral lymphadenectomy of the cervical lymph nodes .....	185
4.4 SUMMARY AND DISCUSSION .....	189
4.4.a. Summary.....	189
4.4.b. Immunosuppression produced by the corneal endothelium.....	192
4.4.c. Immunosuppression within the anterior segment.....	195
4.4.d. Immunosuppression within the cervical lymph nodes .....	198
4.4.e. Regional immunosuppression for corneal transplantation in the rat .....	201
<b>CHAPTER 5: FINAL DISCUSSION.....</b>	<b>203</b>
5.1 SUMMARY OF THE MAJOR FINDINGS FROM THIS THESIS .....	204
5.2 MULTI-GENE EXPRESSION USING THE 2A SELF-PROCESSING SEQUENCE .....	205
5.2.a. Expression of multiple transgenes from a single lentiviral construct.....	205
5.2.b. Stoichiometry of upstream and downstream proteins expressed from 2A vectors .....	207

5.2.c. The use of the 2A self-processing sequence to prevent corneal allograft rejection .....	210
<b>5.3 ANTIGEN PRESENTATION DURING CORNEAL TRANSPLANTATION.</b>	<b>211</b>
5.3.a. Antigen travels from the eye to the secondary lymphoid organs in soluble form .....	211
5.3.b. Evidence for antigen presentation within the anterior segment of the eye .	215
5.3.c. A proposed model of antigen presentation during corneal transplantation in rodents .....	217
5.3.d. Inhibition of antigen presentation with anti-CD4 antibodies and antibody fragments in rodents .....	222
5.3.e. The outcome of corneal allograft survival after bilateral lymphadenectomy of the cervical lymph nodes in rodents .....	224
5.3.f. Regional immunosuppression for human corneal transplantation.....	228
<b>APPENDIX 1: BUFFERS AND SOLUTIONS .....</b>	<b>230</b>
A1.1 Chrome-alum-subbed microscope slides.....	231
A1.2 DEPC-H <sub>2</sub> O .....	231
A1.3 DMEM (high glucose).....	231
A1.4 Eosin stain .....	231
A1.5 FACS fixative .....	232
A1.6 GelRed <sup>TM</sup> agarose plates .....	232
A1.7 Haematoxylin solution.....	232
A1.8 HEPES-buffered RPMI medium .....	233
A1.9 HEPES-buffered Saline .....	233
A1.10 LB medium .....	233
A1.11 LB agar plates .....	234

A1.12 Low salt LB medium .....	234
A1.13 PBS (10x) .....	234
A1.14 PBS-azide .....	235
A1.15 RBC lysis solution (10X) .....	235
A1.16 SOC medium .....	235
A1.17 Sodium azide 4M stock .....	235
A1.18 TBE (10x) .....	236
A1.19 Trypan blue stock .....	236
A1.20 Trypsin-EDTA .....	236
<b>APPENDIX 2: VECTOR MAPS .....</b>	<b>237</b>
A2.1: pBS-CD55-F2A-CD59 vector map .....	238
A2.2: pHIV-eYFP vector map .....	239
A2.3 fHSSOX38scFv in pAdtrackCMV vector map .....	240
A2.4 pHIV-EK5 vector map .....	241
A2.5 pBLAST41-hEndoKring5 vector map .....	242
<b>APPENDIX 3: CONSTRUCTION OF pHIV-CD4scFv .....</b>	<b>243</b>
<b>APPENDIX 4: SEQUENCE ANALYSIS .....</b>	<b>251</b>
A4.1 Sequence analysis of pHIV-CD4scFv_F2A_eYFP .....	253
A4.2 Sequence analysis of pHIV-eYFP_F2A_CD4scFv .....	255
A4.3 Sequence analysis of pHIV-CD4scFv_F2A .....	257
A4.4 Sequence analysis of pHIV-CD4scFv_F2A_EK5 .....	259
<b>REFERENCES .....</b>	<b>251</b>

## ABSTRACT

Corneal transplantation is performed to restore vision or to relieve pain in patients with damaged or diseased corneas. However, approximately 40% of corneal allografts fail after 10 years. The most common cause of graft failure is irreversible immunological rejection, primarily mediated by CD4<sup>+</sup> T cells, despite the topical application of glucocorticosteroids. The aim of this project was to investigate the anatomic site of antigen presentation during corneal transplantation in the rat, by using a lentiviral vector to express an anti-CD4 antibody fragment at potential sites of antigen presentation, including the donor corneal endothelium, the anterior segment of the eye and the cervical lymph nodes.

Dual-gene lentiviral vectors were constructed by inserting the 2A self-processing sequence between two transgenes. This allowed expression of two transgenes within a single open reading frame. *In vitro* characterisation of the dual-gene vectors was performed in cell culture experiments, which showed that transgenic proteins were expressed at lower levels from dual-gene vectors compared to the expression from single-gene vectors and expression was lowest when the transgene was situated downstream of the 2A self-processing sequence.

To locate the anatomic site of antigen presentation during corneal transplantation in rats, a lentiviral vector carrying an anti-CD4 antibody fragment was delivered to the corneal endothelium either immediately prior to corneal transplantation by *ex vivo* transduction of the donor corneas, or 5 days prior to corneal transplantation by anterior chamber injection into both the recipient and the donor rats. A separate group of recipient rats received intranodal injections of the lentiviral vector carrying

an anti-CD4 antibody fragment into the cervical lymph nodes 2 days prior to corneal transplantation. Another group of rats underwent bilateral lymphadenectomy of the cervical lymph nodes 7 days prior to corneal transplantation. Corneal allografts were scored daily for opacity, inflammation and neovascularisation. Expression of the anti-CD4 antibody fragment from transduced tissues was detected using flow cytometry and polymerase chain reaction. Modest, but significant prolongation of corneal allograft survival was experienced by rats that received *ex vivo* transduction of the donor corneas with a lentiviral vector carrying an anti-CD4 antibody fragment immediately prior to corneal transplantation, but all grafts did eventually reject. Anterior chamber injection of the lentiviral vector carrying the anti-CD4 antibody fragment 5 days prior to corneal transplantation into both recipient and donor eyes did not prolong allograft survival. Intranodal injection of a lentiviral vector carrying an anti-CD4 antibody fragment did not prolong the survival of the corneal allografts, nor did bilateral lymphadenectomy of the cervical lymph nodes 7 days prior to corneal transplantation.

Neither expression of the anti-CD4 antibody fragment in the cervical lymph nodes nor the removal of these nodes was able to prolong corneal allograft survival in rats, suggesting that T cell sensitisation could potentially occur elsewhere in the body. However, expression of the anti-CD4 antibody fragment from the donor corneal endothelium was able to prolong corneal allograft survival, suggesting that some antigen presentation might occur within the anterior segment of the eye. Based on the findings described in this thesis and those of others, I propose that antigen presentation in the rat occurs within anterior segment of the eye and within the secondary lymphoid tissues such as the cervical lymph nodes, and that inhibiting

antigen presentation at one of these sites will delay graft rejection. However, to completely abolish antigen presentation during corneal transplantation in the rat, I hypothesise that antigen presentation within both the anterior segment of the eye and within the secondary lymphoid tissues must be inhibited.



**CONFERENCE PRESENTATIONS ARISING FROM THIS THESIS**

**Brice S.L.**, Mortimer L.M., Marshall K.A., Brereton H.M., Williams K.A. Lentiviral-mediated gene transfer of anti-CD4 scFv prolongs corneal allograft survival. 2009 May 29-April 1, Australian Gene Therapy Society meeting, Sydney, poster presentation.

**Brice S.L.**, Mortimer L.M., Brereton H.M., Williams K.A. Lentiviral gene transfer to the rat cornea. 2008 August 9-14, The Transplantation Society – XXII International Congress, Sydney, poster presentation.

## **DECLARATION**

I certify that this thesis does not incorporate without acknowledgement any material previously submitted for a degree or diploma in any university; and that to the best of my knowledge and belief it does not contain any material previously published or written by another person except where due reference is made in the text.

Sarah L Brice

## ACKNOWLEDGEMENTS

This project would not have been possible without the technical assistance provided by the following people:

- Kirsty Kirk who performed all the rat corneal grafts and histology for this project.
- The staff of the Gene Technology Unit at the Women's and Children's Hospital, including Donald Anson, Stanley Tan and Sue Ping Lim for their assistance with lentivirus production.
- Lauren Mortimer for setting up lentiviral titration and RCR assays at Flinders.
- Yazad Irani who assisted with the cloning of one of the vectors used in this project.

I would like to thank my principal supervisor Keryn Williams for taking me on as a student. Keryn, I feel privileged to have had the opportunity to learn from you. It took a while, but thanks to your persistence, I feel more able to critically analyse both my own work, and the work of others.

I would also like to thank Helen Brereton for her supervision and guidance throughout my project. Helen, your knowledge of cloning and molecular biology has been an invaluable resource for my project.

I would like to especially mention Kirsty Kirk who performed all of the corneal grafts and histology for my project. Kirsty, your technical prowess was truly phenomenal, even while wearing your "Darth Vader" mask. I will miss your infectious, bubbly personality.

I would like to thank Lauren Mortimer for all the long days she has put in with virus production, titration and associated procedures. Lauren, I have been very grateful for your meticulous problem solving abilities and dedication to your work. We have been studying and working together for such a long time now, I am really going to miss you as a colleague and a friend.

I would also like to thank the entire Department of Ophthalmology at Flinders University for being an inviting, helpful and friendly group of people to work with. Thank you to Alison, Dave, Kath, Yazad, Sonja, Margaret, Mel, Shiwani, Sarah and Paul for our team room discussions and for being more than just work colleagues and becoming real friends.

To Claire Jessup, thank you for taking me under your wing, mentoring me through the early stages of my project and providing me with a house to live in. I would also like to thank Melinda Tea for being a wonderful house mate, PhD buddy and supportive friend. I really will miss working and living with you.

To my friends Susan, Lisa, Row, Helen, Michelle, Loretta and Jelena, thank you for being there for me when I needed to some non-thesis time. I look forward to seeing a lot more of you now. I would like to acknowledge my godparents Auntie Sue and Uncle Kent, for showing a real interest in my studies and to my brother Nathaniel, thank you for always being only a phone call away despite the distance between us. I would like to thank Oscar my beautiful cat, for all the cuddles and affection when I needed it.

I would like to thank my parents for encouraging me to be the best I can be, for installing the drive in me to never give up and to always finish what I start. Thank you to Richie, for loving and caring for me even through my crazy moments and for looking after me when I wasn't even looking after myself. Your support has meant the world to me.

Lastly, I would like to dedicate this thesis to my grandparents who have always believed in me. You have been my inspiration and Grandpa I wish you were able to see the final product.

**ABBREVIATIONS**

>	greater than
<	less than
°C	degrees Celsius
µg	microgram
µl	microlitre
µm	micrometre
A549	human lung adenocarcinoma epithelial cell line
AAV	adeno-associated viral vector
AC	anterior chamber
ACAID	anterior chamber-associated immune deviation
Adv	adenoviral vector
AE	amplification efficiency
Ag	antigen
AIDS	acquired immunodeficiency syndrome
APC	antigen presenting cell
ARBP	acidic ribosomal phosphoprotein
bp	base pair
BSS	balanced salt solution
CaCl <sub>2</sub>	calcium chloride
CALT	conjunctiva-associated lymphoid tissue
CB-Dx	cascade blue dextran
CCTS	The American Collaborative Corneal Transplant Study
CH	constant domain of immunoglobulin heavy chain
CHO	Chinese hamster ovarian cell line

CD	cluster of differentiation
CD40L	CD40 ligand
cDNA	complementary deoxyribonucleic acid
CGD	chronic granulomatous disease
CL	constant domain of immunoglobulin light chain
CLN	cervical lymph node
cm	centimetre
CMV	cytomegalovirus immediate early promoter
CPE	cytopathic effects
cPPT	central polypurine tract
CT	cycle threshold
CTL	cytotoxic T lymphocyte
CTLA-4	cytotoxic T lymphocyte-associated protein-4 (CD152)
Da	Dalton
DC	dendritic cell
DDH <sub>2</sub> O	double distilled water
DEPC	diethylpyrocarbonate
DMEM	Dulbecco's Modified Eagle Medium
DMSO	dimethyl sulphoxide
DNA	deoxyribonucleic acid
dNTP	dinucleotide triphosphate
ds	double stranded
DTH	delayed type hypersensitivity
DTT	dithiothreitol
eGFP	enhanced green fluorescent protein

eYFP	enhanced yellow fluorescent protein
ECACC	European Collection of Cell Cultures
<i>E. Coli</i>	<i>Escherichia coli</i>
EK5	human endostatin::kringle-5 fusion protein
ELISA	enzyme-linked immunosorbent assay
ETDA	ethylene diamine tetra acetic acid
EU	endotoxin unit
F2A	FMDV 2A self-processing sequence with a furin cleavage site immediately upstream of 2A, and a 2B proline residue at its C-terminus
F344	Fisher 344 inbred rat strain
Fab	monomeric antigen binding fragment
FACS	fluorescence-activated cell sorting
FasL	Fas-ligand (CD95L)
Fc	crystallisable fragment
FCS	fetal calf serum
FDA	Food and Drug Administration
fHSS	factor H secretory sequence
FITC	fluorescein isothiocyanate
FMDV	foot and mouth disease virus
g	gram
g	unit of gravity
gDNA	genomic deoxyribonucleic acid
GFP	green fluorescent protein
HeBS	HEPES-buffered saline

HEK-293A	human embryonic kidney cell line with E1- region of adenovirus 5
HEK-293T	human embryonic kidney cell line that constitutively expresses the SV40 large T cell antigen
HEPES	N-2-hydroxyethylpiperazine-N-2-ethanesulphonic acid
HIS6 tag	6 histidine tag
HIV	human immunodeficiency virus
HLA	human leucocyte antigen
HRP	horseradish peroxidase
HPRT	hypoxanthine guanine phosphoribosyl-transferase
Hz	Hertz
IFN- $\gamma$	interferon gamma
Ig	immunoglobulin
IL	interleukin
IRES	internal ribosome entry sites
IU/ml	international units/ml
kb	kilobase
kDa	kilodalton
L	litre
LB	luria bertani
LC	Langerhans cells
LCA2	Leber's congenital amaurosis type 2
LIP	liposome-incorporated
log	logarithm
log <sub>e</sub>	natural logarithm
LTR	long terminal repeat



LV	lentiviral vector
LYVE-1	lymphatic vessel endothelial hyaluronan receptor 1
M	Molar
mAb	monoclonal antibody
MLN	mesenteric lymph node
MFI	mean fluorescence intensity
mg	milligram
MHC	major histocompatibility complex
ml	millilitre
MLR	mixed lymphocyte reaction
MLV	Molony murine leukaemia viral vector
mm	millimetre
MOI	multiplicity of infection
mRNA	messenger ribonucleic acid
MW	molecular weight
NIH	National Institutes of Health
ng	nanogram
NHMRC	National Health and Medical Research Council
NK	natural killer cell
NTC	no template control
OD	optical density
ORF	open reading frame
OVA	ovalbumin peptide
pA	polyadenylation signal
PBL	peripheral blood lymphocytes

PBS	phosphate buffered saline
PC2	physical containment level 2
PCR	polymerase chain reaction
PE	phycoerythrin
pfu	plaque forming unit
pg	pictogram
PGK	phosphoglycerate kinase
pmol	picomole
polyA	polyadenylation site
PPT	polypurine tract
qPCR	quantitative real-time polymerase chain reaction
qRT-PCR	quantitative reverse transcription real-time polymerase chain reaction
RBC	red blood cells
RCR	replication competent recombinant
RNA	ribonucleic acid
RPMI	Roswell Park Memorial Institute
RRE	rev response element
RRExt	extended rev response element
RT	reverse transcription
SAP	shrimp alkaline phosphatase
SAPE	streptavidin R-phycoerythrin
SCID-X1	x-linked severe combined immunodeficiency disorder
scFv	single chain fragment variable
SD	standard deviation
sFlt-1	soluble vascular endothelial growth factor receptor 1

SIN	self inactivating
SOC	Super Optimal Broth with 20 mM glucose. 'C' stands for catabolite repression, reflective of the added glucose.
SOE-PCR	splice overlap extension polymerase chain reaction
ss	single stranded
SV40	simian-like virus type-40 early promoter
Tc	cytotoxic response
TCID <sub>50</sub>	tissue culture infectious dose method
TCR	T cell receptor
TGF- $\beta$	transforming growth factor beta
Th	T helper response
T <sub>m</sub>	melting temperature
TNF	tumour necrosis factor
TU	transducing units
UV light	ultraviolet light
v/v	volume per volume
VEGF	vascular endothelial growth factor
VEGFR	vascular endothelial growth factor receptor
VH	variable domain of immunoglobulin heavy chain
VL	variable domain of immunoglobulin light chain
VSV	vesicular stomatitis virus
VSV-G	vesicular stomatitis virus glycoprotein G
whv	woodchuck hepatitis virus post-transcriptional element
w/v	weight per volume
WF	Wistar Furth inbred rat strain

WT      wild type

## **CHAPTER 1: INTRODUCTION**

## 1.1 INTRODUCTION OVERVIEW

This chapter will start with a discussion on the human cornea, its lack of proliferative ability *in vivo*, and how corneal transplantation can be performed to restore vision. The use animal models of corneal transplantation to understand the mechanisms of immunological rejection will be considered. The immunology of corneal transplantation will be discussed as well as the current prevention and treatment strategies for corneal graft rejection. The use of gene therapy as a potential novel strategy to prevent corneal graft failure will be examined along with the current biosafety issues associated with it. This chapter will finish with the aims of this thesis and how regional immunosuppression for corneal transplantation using gene therapy has the potential to be an effective new preventative strategy for corneal graft rejection.

## 1.2 THE HUMAN CORNEA

### 1.2.a. Anatomy of the human cornea

The cornea is an avascular transparent dome-shaped tissue that forms the anterior surface of the eye. In humans the cornea is approximately ½ mm thick and is comprised of several layers (Figure 1.1). On the anterior surface is the epithelium which is attached to the Bowman's membrane. Underneath the Bowman's membrane lies a stroma of ordered collagen fibrils interspersed with fibroblast-like keratocytes. Attached to the second cell basement membrane (Descemet's membrane) lies the endothelial monolayer. The metabolically-active endothelium regulates the hydration of the cornea and is thus critical for corneal transparency. Failure of the endothelial pump can lead to oedema, which can disrupt the ordered alignment of collagen fibrils

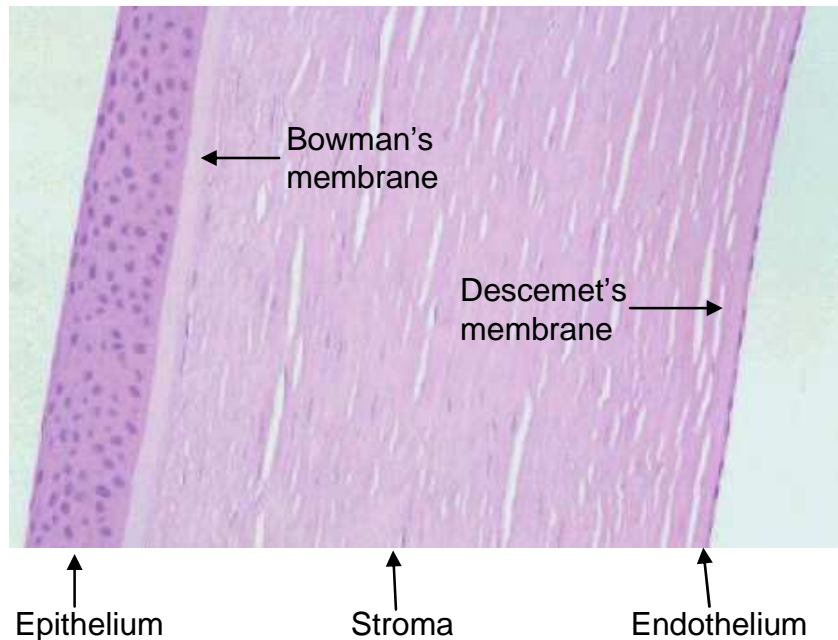


**Figure 1.1: A cross section of a human cornea stained with haematoxylin and eosin.** The human cornea is comprised of several layers. On the anterior surface of the cornea lies the epithelium which is 5-6 cells thick. This epithelial layer is attached to the first cell basement membrane (Bowman's membrane). Underneath the epithelium is the stroma which consists of keratocytes and orthogonally arranged collagen lamellae. Attached to the second cell basement membrane (Descemet's membrane), is an endothelial monolayer which forms the posterior surface of the cornea and is bathed in aqueous humour.

within the stroma and can result in corneal opacity. Since the adult human corneal endothelium has minimal replicative ability *in vivo*, the damage is irreversible.<sup>1</sup>

### **1.2.b. Proliferative capacity of the human corneal endothelium**

Joyce and colleagues have shown that the human corneal endothelium does have the capacity to proliferate, but is arrested in the G1-phase of the cell cycle and proliferation *in vivo* is minimal.<sup>1</sup> Cell density studies have shown that the human corneal endothelium does not replicate *in vivo* at a rate sufficient to negate cell loss,<sup>2</sup> and morphological studies have revealed an age-related decrease in endothelial-cell density.<sup>1</sup> However, the corneal endothelium is able to repair endothelial cell loss by mechanisms other than proliferation, including monolayer spreading<sup>3</sup> and cell migration.<sup>4-6</sup>

Senoo and Joyce and colleagues have performed a study that compared cell cycle kinetics of the human corneal endothelium of young donors (<30 year old) compared to old donors (<50 years old).<sup>7</sup> This study revealed that corneal endothelial cells from old donors were able to enter and complete cell cycle, however they required a longer time in the G1-phase and needed stronger mitogenic stimulation than cells from younger donors.<sup>7</sup> There is evidence to suggest that exogenous transforming growth factor- $\beta$  (TGF- $\beta$ ) and TGF- $\beta$  within the aqueous humour, suppress S-phase entry of corneal endothelial cells,<sup>8-9</sup> and cell-cell contact during corneal development appears to inhibit human endothelial cell proliferation.<sup>10</sup>

In summary, because the corneal endothelium has very minimal proliferative capacity *in vivo*, the most effective treatment currently available for irreversible



endothelial cell loss is corneal transplantation and will be discussed in the following section.

### **1.3. CORNEAL TRANSPLANTATION**

Disease of the cornea is the second most common cause of blindness worldwide.<sup>11</sup> When irreversible damage to the cornea does occur through disease or trauma, a surgical procedure known as corneal transplantation can be performed. This involves the removal of the damaged or diseased cornea from the patient and replacing it with healthy corneal tissue from an eye donor (Figure 1.2).

The first successful human corneal allograft was reported in 1906. The cornea from a young male donor was transplanted into a male patient who was left blind following a chemical burn.<sup>12</sup> Today with the use of corticosteroids and antibiotics, corneal grafts experience high survival rates of >90% at one year post surgery.<sup>13</sup> However, within Australia, the survival rate drops considerably within ten years post surgery, with a ten-year Kaplan Meier corneal graft survival of 60%,<sup>14</sup> and the most common cause of corneal graft failure is irreversible immunological rejection.<sup>13</sup> Within the last 20 years, there has been only modest improvement to the survival rate of corneal allografts.<sup>13</sup> In contrast, over the same period, vascularised organ transplantation has seen significant improvement in graft survival rates, largely attributed to improved therapies for prevention and treatment of rejection.<sup>15-16</sup> Therefore, to improve the

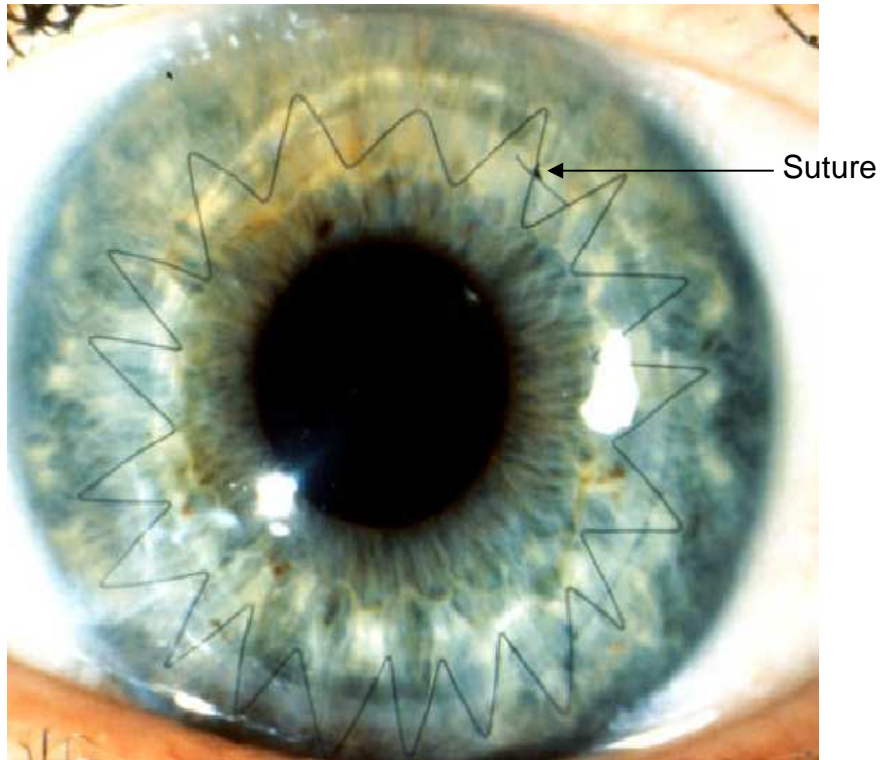


**Figure 1.2: The eye of a patient who has received a successful corneal allograft.** The donor corneal tissue was taken from an eye donor and grafted into the recipient corneal bed using a continuous suture (marked on diagram). The graft is transparent and avascular.

survival rates of corneal allografts, improved strategies for the prevention and treatment of corneal allograft rejection are necessary.

#### **1.4 ANIMAL MODELS OF CORNEAL TRANSPLANTATION**

Animal models of corneal transplantation can be used to study the mechanisms of corneal graft acceptance and failure and can be used to develop novel therapies for the prevention and treatment of rejection. Animal models of corneal transplantation have been developed in small animals such as mice<sup>17</sup> and rats,<sup>18</sup> and in large animals such as rabbits,<sup>19</sup> cats,<sup>20</sup> sheep<sup>21</sup> and monkeys.<sup>22</sup>

Animal models of corneal transplantation in cats, sheep and monkeys closely mimic corneal graft rejection seen in humans, however surgery in these animals can be difficult and the upkeep of housing these larger animals can be expensive. The inbred strains of mice and rats allow for many combinations of minor and major histocompatibility antigen differences to be studied, which can be useful when investigating the immunology behind graft acceptance and failure,<sup>23-25</sup> and is not possible in outbred species such as rabbits, cats, sheep and monkeys. The use of transgenic murine strains (that express a reporter gene such as green fluorescence protein (GFP)) allows for tracking of donor cells or antigen within a non-transgenic recipient.<sup>26</sup> Furthermore, the abundance of available reagents (such as monoclonal antibodies) also makes rodents appealing for animal studies.

The proliferative ability of the corneal endothelium varies greatly between species. The corneal endothelium of rabbits<sup>27</sup> and rats<sup>28</sup> have shown the ability to proliferate during wound healing. However, cats<sup>27</sup> and monkeys<sup>29</sup> have shown minimal

proliferation of the corneal endothelium in response to wound healing *in vivo*, similar to what has been reported in humans (Section 1.2.b). It is important to be aware of these species differences when using animals for models of corneal transplantation.

A well established rat model of corneal transplantation was used in this study, which makes use of inbred strains with both minor and major histocompatibility mismatches,<sup>18</sup> with most unmodified allografts rejecting within 2-3 weeks. Only 1 corneal allograft from >90 corneal allografts performed in this project survived indefinitely, therefore the proliferative capacity of the rat corneal endothelium was considered a negligible issue in these experiments.

## 1.5 MECHANISMS OF CORNEAL GRAFT REJECTION

Under normal conditions, the ocular environment is an immune privileged site.<sup>30</sup> However, with the onset of disease or trauma to the cornea, inflammation through the expression of proinflammatory cytokines, such as IL-1 and tumour necrosis factor- $\alpha$  (TNF-  $\alpha$ ),<sup>31</sup> can result in the break-down of the physical and immunological barriers of immune privilege.

Inflammation stimulates neovascularisation<sup>32</sup> and has been shown in humans, rats and mice to allow trafficking of infiltrating leucocytes, including antigen presenting cells (APCs), T cells, neutrophils and natural killer (NK) cells to the donor cornea,<sup>33-35</sup> which can lead to corneal allograft rejection. Expression of the anti-angiogenic molecule, soluble vascular endothelial growth factor receptor 1 (sFlt-1) from an adeno-associated virus (AAV), was able to inhibit cautery-induced corneal neovascularisation in rats.<sup>36</sup> In addition, transduction of donor corneas using a

lentiviral vector carrying the anti-angiogenic fusion protein endostatin::kringle-5 (EK5), was able inhibit neovascularisation and prolong corneal allograft survival in rabbits.<sup>37</sup>

In humans, inflammation either before or as a consequence of corneal transplantation, greatly increases the risk of corneal graft rejection.<sup>14</sup> The following sections will discuss the immunology of acceptance and rejection of corneal allografts.

## **1.6 IMMUNOLOGY OF CORNEAL TRANSPLANTATION**

### **1.6.a. T cells**

#### ***1.6.a.1. T cell overview***

T cells are produced in the bone marrow and migrate to the thymus to mature. After maturation, T cells express a cell surface molecule known as the T cell receptor (TCR) which recognises a unique processed peptide bound to a major histocompatibility complex (MHC) molecule. Essential to the process of antigen presentation are the glycoproteins CD4 and CD8, which are expressed on the surface of T cells and prolong the interaction between the MHC molecule and the TCR during antigen presentation.<sup>38-39</sup> There are two main subsets of T cells distinguishable by the expression of either CD4 or CD8. CD4+ T cells recognise and respond to foreign antigen when it is associated with MHC class II,<sup>38</sup> and are commonly involved in T helper (Th) responses. CD8+ T cells respond to self- or viral-antigen when it is associated with MHC class I,<sup>40</sup> and are commonly involved in cytotoxic (Tc) responses.

### **1.6.a.2. T cell activation and costimulation**

T cell activation (Figure 1.3) is achieved when the TCR-CD3 complex interacts with an antigen-loaded MHC molecule on an APC.<sup>41</sup> Full activation of the T cell does not take place unless secondary signals occur through costimulation.<sup>42</sup> If costimulation does not occur, T cells become anergic or apoptotic. Costimulation can result from the interaction between CD28 (a T cell surface molecule) and CD80 or CD86 (cell surface molecules expressed on APCs),<sup>43</sup> or the interaction between CD40 ligand (CD40L) (expressed on activated T cells) with CD40 (expressed on numerous cells including APCs).<sup>44</sup>

### **1.6.a.3. Th1 and Th2 responses**

Traditionally, populations of CD4+ T helper cells are divided into two groups based on the cytokines they produce. Th1 cells predominately produce IL-2 and IFN- $\gamma$  and commonly mediate delayed type hypersensitivity (DTH) responses. Th2 cells produce IL-4, IL-6, IL-10 and IL-13 and are commonly involved in immunomodulatory responses.<sup>45</sup>

Several studies have characterised the development of DTH after corneal transplantation in mice.<sup>24-25,46-47</sup> Interestingly, Sano and co-workers found that DTH developed in all mice that received corneal allografts, regardless of whether they had accepted or rejected the grafts.<sup>24</sup> This suggests that other immunologic processes may also influence acceptance and rejection of corneal allografts.

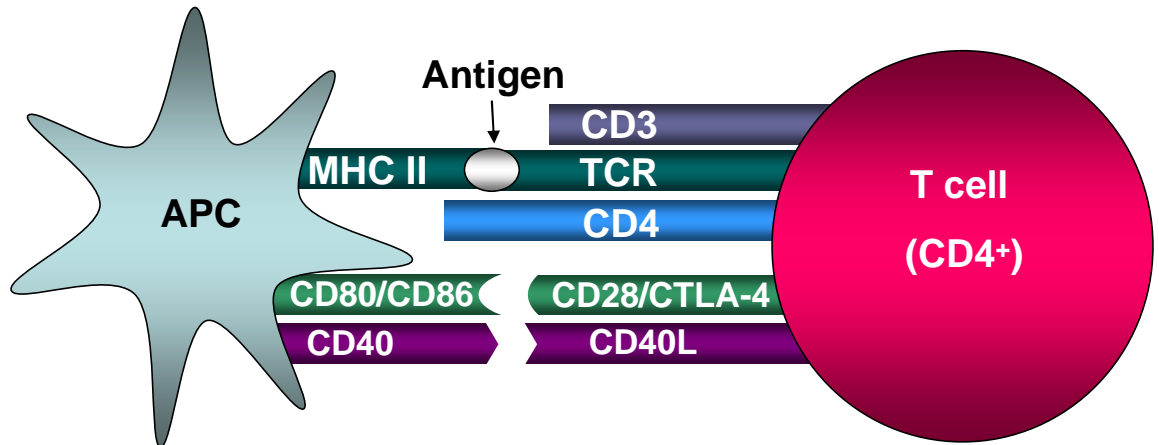


**Figure 1.3: Antigen presentation and T cell activation.** Full activation of a naïve T cell requires two signals. The first signal comes from the interaction between the TCR/CD3 complex associating with an antigen-loaded MHC molecule. The second signal can come from either the interaction between CD28 with CD80 or CD86 or the interaction between CD40L with CD40. CTLA-4 is a competitive inhibitor of CD28 and can interact with CD80 or CD86 to prevent T cell activation.

Kuffova and colleagues demonstrated that the first cells to infiltrate the donor cornea after transplantation were recipient APCs (with some APCs expressing high levels of MHC class II, CD40 and CD86), followed by the infiltration of CD4<sup>+</sup> T cells and CD8<sup>+</sup> T cells, all within 24 hours of transplantation.<sup>33</sup> The levels of CD4<sup>+</sup> and CD8<sup>+</sup> T cells were low within the donor cornea until immediately prior to corneal allograft rejection, when the number of CD8<sup>+</sup> T cells increased within the grafted tissue.<sup>33</sup> The results of Kuffova *et al.*,<sup>33</sup> coupled with the findings of Sano *et al.*,<sup>24</sup> suggest that initial indirect allorecognition of CD4<sup>+</sup> T cells causes the induction of both a DTH response and a cytotoxic T cell response (by CD8<sup>+</sup> T cells), which can lead to corneal allograft rejection. Moreover, Larkin and colleagues demonstrated that B cells were not part of the cellular infiltrate found in rejected corneal allografts in humans<sup>34</sup> or rats,<sup>35</sup> and several studies have revealed that although alloantibody production can damage the donor corneal endothelium, there is no correlation with antibody production and corneal allograft rejection,<sup>48</sup> highlighting that the rejection of corneal allografts is T cell mediated.

Th1 and Th2 cells are able to regulate one another mutually through their cytokine pattern.<sup>49</sup> The Th1 cytokine IFN- $\gamma$  can inhibit proliferation of Th2 cells whilst the Th2 cytokine IL-10 can inhibit cytokine synthesis by Th1 cells. Several studies have shown that Th2 cytokines can modulate corneal allograft rejection. Delivery of adenoviral vectors carrying IL-10 either to the donor corneal endothelium in sheep<sup>50</sup> or systemically in rats<sup>51</sup> has prolonged corneal allograft survival. This indicates that it is possible to modulate the Th1 response using Th2 cytokines. However, Hargrave and co-workers have revealed that corneal allograft rejection can still occur in IFN- $\gamma$  knockout mice in a Th2 manner.<sup>52</sup>



More recent murine experiments have changed the Th1/Th2 paradigm with the discovery that CD4<sup>+</sup> T cells can also differentiate into Th17 cells which produce IL-17. Th17 cells play a role in inflammation in autoimmune disease<sup>53-55</sup> and have also been associated with acute renal and cardiac rejection in mice.<sup>56-57</sup> Chen and colleagues have demonstrated that in mice, IL-17 was expressed highly in both the corneal allograft and the draining cervical lymph nodes in the early stages of rejection, whilst the Th1 cytokine, IFN- $\gamma$  was produced in the later stages of rejection.<sup>58</sup> In addition, corneal allograft survival in recipient IL-17 knockout mice showed delayed rejection kinetics.<sup>58</sup> These results reveal that Th1 and Th17 cells play a role in corneal allograft rejection in mice.

The above discussion suggests that corneal allograft rejection is predominantly initiated by CD4<sup>+</sup> T cells (via Th1 and Th17 responses) and CD8<sup>+</sup> T cells appear to be involved in the effector arm of the immune response.

### **1.6.b. Antigen presenting cells (APCs) in the eye**

APCs play a crucial role in both innate and adaptive immunity. There are two main classes of professional APCs, dendritic cells (DCs) and macrophages. The role APCs play in immunity within the eye will be discussed below.

#### **1.6.b.1. Dendritic cells (DCs)**

DCs are potent APCs as they are able to induce primary immune responses and are thus critical for the development of immunological memory.<sup>59-61</sup> A continuous production of DCs occurs within the bone marrow from haematopoietic stem cells, and immature DCs selectively migrate to lymphoid and non-lymphoid tissues where

they take up, process and present antigen to T cells.<sup>59,62-64</sup> Immature DCs have high capacity for antigen uptake,<sup>65</sup> and express low levels of MHC class II and the required costimulatory molecules for T cell activation, such as CD40, CD80 and CD86.<sup>65-66</sup> Upon maturation, DCs express very high levels of MHC class II and costimulatory molecules such as CD40, CD80 and CD86 and are subsequently highly effective as activators of T cells, however, their capacity to capture antigen is diminished.<sup>65-67</sup> Both immature and mature DCs have been identified within the cornea,<sup>26,68-74</sup> uveal tract,<sup>75-79</sup> limbus<sup>80</sup> and conjunctiva.<sup>81</sup>

### **1.6.b.2. Macrophages**

Macrophages are derived from bone-marrow monocytes and reside in most tissues. Compared to activated DCs, the expression of MHC class II and co-stimulatory molecules is relatively low on macrophages, however, resident macrophages are able to function as APCs and secrete proinflammatory cytokines.<sup>82</sup> Macrophages take up and process antigen effectively, but are less effective than DC in inducing primary immune responses.<sup>83</sup> Resident ocular macrophages have been identified in the cornea,<sup>69,71-72,84</sup> uveal tract,<sup>76,83,85-86</sup> limbus<sup>80</sup> and conjunctiva.<sup>81</sup>

### **1.6.b.3. Antigen presenting cells within the uveal tract**

Many studies have reported the presence of resident APCs within the uveal tract (iris, ciliary body and choroid).<sup>75,77-78,87-88</sup> The majority of these APCs have been characterised as resident macrophages that express low levels or no MHC class II.<sup>76,86</sup> A smaller population of MHC class II+ DCs has also been identified within the uveal tract.<sup>75-76,79,83,86</sup>

For many years it was believed that APCs within the uveal tract had reduced immunostimulatory abilities due to the immune privilege status of the eye and because of the involvement of resident iris and ciliary body APCs in deviant immune responses.<sup>89</sup> However more recent studies have shown the contrary.<sup>83</sup> The majority of antigen uptake after antigen injection into the anterior chamber is performed by macrophages in the iris and ciliary body.<sup>76,85,90</sup> A DC population (CD11c+MHC class II+) has also been reported to phagocytose antigen,<sup>91</sup> but at lower levels compared to macrophages.<sup>86</sup>

Stephens and colleagues showed potent allostimulatory abilities of resident iris DCs that were able to activate resting T cells *in vitro*.<sup>83</sup> However, iris macrophages displayed negligible stimulating activity on resting T cells, but could induce proliferation of primed T cells in an antigen specific manner,<sup>83</sup> suggesting a role in secondary immune responses.

The direct interaction between antigen-loaded APCs and T cells has been reported in the iris,<sup>92</sup> and these APCs do not appear to migrate after antigen uptake.<sup>91-92</sup> These studies suggest that uveal tract APCs are not involved in T cell priming in the draining lymph nodes and that antigen presentation of ocular antigens may occur within the eye itself.

Uveal tract APCs have been seen to play an immunomodulatory role through the induction of deviant immune responses.<sup>89</sup> Li *et al.*, have also shown that after injection of antigen into the anterior chamber, CD11c+ DCs are able to suppress DTH by activating regulatory CD8+ T cells in mice.<sup>87</sup>

In summary, the evidence suggests that uveal tract APCs play a role in immunomodulatory responses. Firstly, even though uveal tract APCs have potent allostimulatory abilities, resident uveal tract APCs do not appear to migrate after antigen uptake. Secondly, there is extensive evidence highlighting the role uveal tract APCs play in the induction of deviant immune responses.

#### **1.6.b.4. Antigen presenting cells in the cornea**

APCs have been identified in both the central corneal stroma<sup>69,71-72,84</sup> and the central corneal epithelium,<sup>70,73-74,93-94</sup> in humans and in animal studies. This section will outline the different APC populations identified within the corneal stroma and the corneal epithelium.

APCs were first identified in the corneal epithelium of humans, mice, guinea pigs and rats by Chandler and Gillette in the 1980s.<sup>93-94</sup> In more recent years, the identification of APC-specific markers and improvements in tissue processing and confocal microscopy have resulted in further characterisation of the APC population in the corneal epithelium of mice<sup>70</sup> and humans.<sup>73-74</sup>

Within the murine corneal epithelium, a DC population (CD45+CD11c+CD11b-MHC class II+) was characterised in the central and peripheral regions.<sup>70</sup> Upon inflammation, MHC class II, CD80 and CD86 expression was up-regulated in these cells.<sup>70</sup> In humans, Yamagami *et al.* characterised a DC population (CD45+CD11c+HLA-DR+) which was mainly situated in the basal cell layer but partly in the more superficial layer of the human corneal epithelium.<sup>73</sup> In addition, Zhivov and colleagues performed a study on 112 healthy humans using *in vivo*

confocal microscopy in which they identified epithelial DCs known as Langerhans cells (LCs) within both the central and peripheral regions of the corneal epithelium in 30 of these volunteers.<sup>74</sup>

APCs have been identified in murine<sup>69,71,84</sup> and human studies<sup>72</sup> of the corneal stroma. Brissette-Storkus *et al.* identified a macrophage population which was present within the central region of the murine corneal stroma.<sup>84</sup> The majority of these APCs were CD45+CD11b+ monocytes and macrophages, and MHC class II expression was detected at low levels in 30% of these cells.<sup>84</sup>

Hamrah *et al.*, identified a combination of DCs and macrophages within the mouse corneal stroma.<sup>69</sup> The DC population (CD45+CD11c+CD11b+ ) was identified throughout the central, and peripheral regions of the anterior stroma, with 50% of these corneal DCs seen to express MHC class II and the costimulatory molecule CD80.<sup>69</sup> The macrophage population (CD45+CD11b+CD11c-) was restricted to the posterior stroma.<sup>69</sup> Yamagami and colleagues characterised an APC population within the human corneal stroma in both central and peripheral regions.<sup>72</sup> These APCs were CD45+CD11b+CD11c+CD14+HLA (human leucocyte antigen)-DR+ with mainly round or spindle morphology. It is currently unclear whether these cells are immature macrophages and/or DCs.<sup>72</sup>

The bone marrow origins of resident corneal APCs have been directly investigated.<sup>71,95</sup> Bone marrow cells<sup>71,95</sup> or bone marrow-derived haematopoietic stem/progenitor cells<sup>71</sup> from transgenic GFP-expressing mice were transplanted into irradiated wild type mice and the distribution of these cells within the corneal stroma

was studied for 8 weeks<sup>95</sup> or up to 6 months.<sup>71</sup> Both studies found GFP+ bone marrow-derived cells within the corneal stroma 2 weeks post reconstitution,<sup>71,95</sup> and Chinnery and colleagues characterised these cells to be predominantly within the anterior stroma.<sup>95</sup> By 8 weeks<sup>71,95</sup> these GFP+ bone marrow-derived cells were distributed evenly throughout the corneal stroma and were detected 6 months after reconstitution.<sup>71</sup>

For many years it was believed that one of the factors necessary for immune privilege of the cornea was the lack of resident corneal APCs. However, from the studies discussed previously, it is evident that many APCs reside within the normal cornea. Now it is speculated that the characteristics of the resident corneal APCs provide the cornea with its immune privilege status.<sup>59</sup> These characteristics include the immature state of corneal APCs<sup>26</sup> and their reduced allostimulatory capacity when activated.<sup>26</sup> On the other hand, there is also evidence to suggest that APCs within the cornea are involved in corneal lymphangiogenesis and antigen uptake and this will be discussed in this section.

Cursiefen *et al.* showed that secretion of vascular endothelial growth factor (VEGF)-C and VEGF-D by activated resident corneal macrophages in response to inflammation, promoted corneal lymphangiogenesis<sup>96</sup> by binding to VEGF receptor-3 (VEGR-3) which is critical for lymphangiogenesis.<sup>97</sup> In mice, depletion of macrophages either within the eye or by whole-body irradiation prevented corneal lymphangiogenesis.<sup>96</sup> In addition, resident corneal CD11b+ macrophages have been shown to form tube-like aggregates within the stroma of an inflamed cornea that grow towards and connect to existing lymphatic vessels in the limbus.<sup>98</sup>

Furthermore, nanotubes are long membrane structures that connect mammalian cells and it has been speculated that they function in intercellular communication between distant cells. Chinnery and colleagues have identified nanotubular membrane structures on DCs within the central corneal stroma in mice and the frequency of these nanotubes was significantly increased in response to inflammation.<sup>99</sup> Chinnery and colleagues hypothesised that nanotube-bearing DCs within the central corneal stroma may act as a potential means of cell-cell signalling through the transfer of antigen-receptor complexes between widely separated DCs.<sup>99</sup>

In the context of corneal transplantation, Liu and colleagues characterised a DC population (CD11c+MHC class II-) within the murine cornea, which became MHC class II+ in a time dependent manner after corneal transplantation or placement in culture.<sup>26</sup> These resident corneal DCs had only modest allostimulatory capacity *in vitro* suggesting that their immunostimulatory capacity was being suppressed.<sup>26</sup> In addition, this study revealed migration of donor APCs to the draining cervical lymph nodes within 24 hours after surgery under normal conditions and within 6 hours when grafting was performed within an inflamed corneal bed.

Kuffova *et al.* also studied antigen transport after corneal transplantation to the draining cervical lymph nodes in mice.<sup>100</sup> An APC population (CD45+CD11b+CD11c-) within the central cornea (the area used for corneal transplantation) was identified,<sup>100</sup> however these cells were not detected in the draining cervical lymph nodes. Instead, host antigen loaded-CD11c+ APCs were detected as early as 6 hours after allografting within the draining cervical lymph nodes and these host APCs

stimulated antigen specific T cell activation and clonal expansion within the draining lymph nodes.<sup>100</sup>

In summary, corneal APCs appear to be involved in the erosion of ocular immune privilege. Firstly, macrophages have been shown to play an important role in inflammation-induced lymphangiogenesis,<sup>96-98</sup> and DCs are able to form nanotube-structures which might be involved in cell-cell signalled between widely spread DCs within the central cornea.<sup>99</sup> Secondly, the studies from Liu *et al.*<sup>26</sup> and Kuffova *et al.*<sup>100</sup> reveal that both donor and host APCs might be involved in mediating the immune response against corneal allografts by activating T cells in the draining cervical lymph nodes.

### **1.6.c. Allorecognition**

Allorecognition of T cells against alloantigens can occur either by direct or indirect pathways.<sup>101</sup> Direct recognition occurs when a recipient T cell recognises intact donor MHC complexed with peptide on donor APCs. Indirect recognition occurs when a recipient APC processes alloantigen before presenting it to recipient T cells in a self-restricted manner.

In animal models, the indirect pathway appears to be the main method of alloantigen presentation after corneal transplantation<sup>47</sup> and minor histocompatibility rather than major histocompatibility alloantigens are more successful at triggering DTH and corneal allograft rejection.<sup>24-25,47</sup> This contrasts with what is seen with the rejection of vascularised organs where MHC alloantigens are the primary target of DTH and allograft rejection.<sup>102</sup>



Boisgerault and colleagues have shown that only CD4+ (and not CD8+) T cells are able to mediate corneal allograft rejection in mice after antigen presentation via the indirect pathway.<sup>103</sup> Kuffova and colleagues also revealed that antigen presentation of corneal alloantigens occurred via the indirect pathway, followed by T cell priming, activation and clonal expansion in the draining cervical lymph nodes.<sup>100</sup> In contrast, Liu *et al.* demonstrated trafficking of donor APCs to the draining cervical lymph nodes of mice,<sup>26</sup> and Huq and colleagues revealed that in the high-risk setting (grafting into inflamed recipient corneal bed), the direct pathway of antigen presentation can take place within the draining cervical lymph nodes during corneal transplantation and can lead to rejection.<sup>104</sup>

These results show that in murine studies, the majority of antigen presentation in response to corneal transplantation occurs via the indirect pathway.<sup>47,100,103</sup> However, the direct pathway has also been implicated in the inflamed setting.<sup>26,104</sup>

#### **1.6.d. Ocular lymphatic drainage**

Patterns of lymphatic drainage in the rat were first described by Tilney.<sup>105</sup> This study identified lymphatic drainage from the head and neck to the cervical lymph nodes, including the superficial cervical, facial and internal jugular lymph nodes (Figure 1.4).<sup>105</sup>

It is important to note that many rodent studies refer to the submandibular lymph node separately to the superficial cervical lymph node.<sup>106-112</sup> In this thesis, the submandibular and the superficial cervical lymph node will both be referred to as the

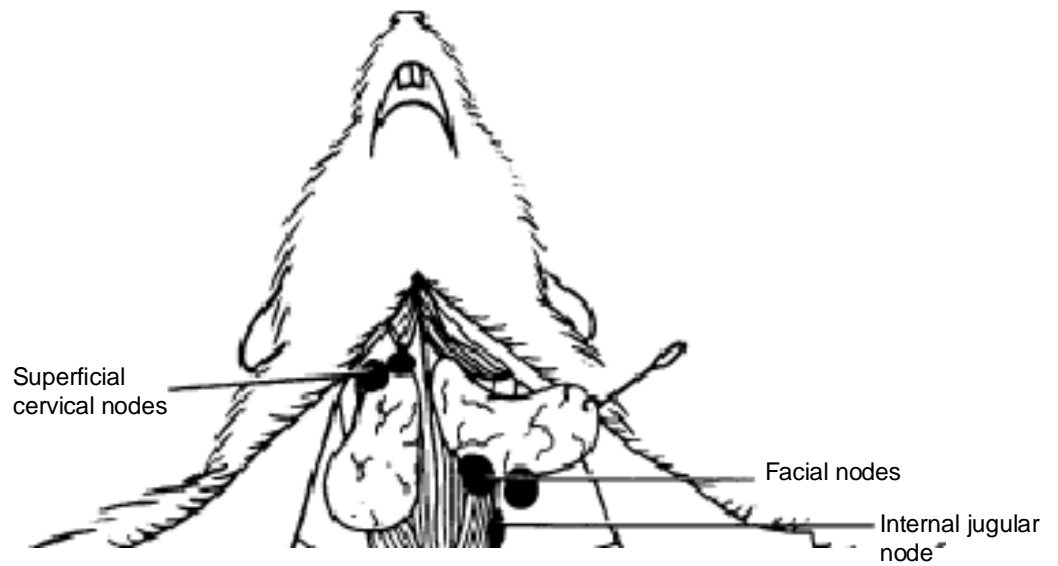


**Figure 1.4: Diagrammatic representation of the regional head and neck lymph nodes in the rat.** Adapted from Tilney.<sup>105</sup>

superficial cervical lymph nodes as depicted in Figure 1.4, which is consistent with the nomenclature used by Tilney.<sup>105</sup>

#### **1.6.d.1. Corneal lymphatics**

In the mouse, inflammation stimulates the growth of both blood and lymph vessels within the healthy avascular cornea.<sup>32</sup> When haemangiogenesis and lymphangiogenesis are inhibited, prolonged corneal allograft survival occurs.<sup>32</sup> Until recently, little was known about lymphatic growth in response to inflammation within the cornea. Recent studies have characterised lymphangiogenesis within the cornea using lymphatic-specific markers such as prospero-related homeobox1 (Prox1) transcription factor,<sup>113</sup> VEGF-C<sup>114</sup> and its receptor VEGFR-3,<sup>97,114-115</sup> lymphatic vessel endothelial hyaluronan receptor 1 (LYVE-1)<sup>32,96,114</sup> and popoplanin.<sup>114</sup>

Cursiefen and colleagues revealed that 8% of vessels within vascularised human corneas stained for lymphatic specific markers (LYVE-1 and popoplanin).<sup>114</sup> Lymphangiogenesis occurred only in association with haemangiogenesis, was more common in early neovascularisation and was always associated with stromal inflammatory cells.<sup>114</sup>

In mice, the growth of blood and lymph vessels was similar after corneal transplantation into normal recipient beds in both allogeneic and syngeneic grafts,<sup>32</sup> indicating that the promotion of vessel growth was through the trauma of surgery rather than the allogeneic tissue.<sup>32</sup> In a mouse model of corneal neovascularisation,

blood vessels were still present 6 months after trauma, whereas lymph vessels were not, indicating that lymph vessels regress earlier than blood vessels.<sup>116</sup>

Moreover, VEGF-A recruitment of macrophages was critical for the growth of blood and lymph vessels, and systemic and local depletion of bone-marrow derived cells significantly inhibited haemangiogenesis and lymphangiogenesis within the inflamed mouse cornea.<sup>96</sup> In addition, delivery of VEGF Trap, (a receptor-based fusion protein which binds to and neutralises VEGF-A), significantly reduced haemangiogenesis and lymphangiogenesis, and mice that underwent treatment with VEGF Trap experienced prolonged corneal allograft survival.<sup>96</sup>

The extracellular matrix protein integrin  $\alpha 5$  plays a crucial role in lymphangiogenesis.<sup>117</sup> Dietrich and colleagues have shown that integrin  $\alpha 5$  blockade inhibits lymphangiogenesis more potently than haemangiogenesis in mouse corneas.<sup>117</sup>

The collective data reveal that lymphangiogenesis occurs in the inflamed cornea, creating a pathway for leucocytes to access corneal alloantigens, and that inhibiting lymphangiogenesis can prolong corneal allograft survival.

#### ***1.6.d.2. Lymphatic drainage from the eye to the cervical lymph nodes***

Lymphatic drainage from the eye to the cervical lymph nodes has been well documented in recent years and the uveoscleral pathway appears to be the main lymphatic drainage route from the eye to these lymph nodes in rodents.<sup>106-107,110-112</sup>

Bilateral lymphadenectomy of the cervical lymph nodes prior to corneal transplantation has proven to be a successful strategy to prolong corneal allograft survival in mice.<sup>118-121</sup> Yamagami *et al.* reported indefinite survival of all allografts into normal recipient corneal beds,<sup>120</sup> whilst Plskova showed prolonged survival in a similar study.<sup>118</sup> Prolonged allograft survival was also reported after bilateral lymphadenectomy of the cervical lymph nodes prior to corneal transplantation into prevascularised recipient corneal beds.<sup>119,121</sup> These studies suggest that the cervical lymph nodes are a site of ocular antigen drainage, especially as their removal delays<sup>121</sup> and even prevents<sup>120</sup> the onset of DTH to alloantigen. However, a study by Schulte *et al.* revealed that mice that underwent bilateral cervical lymphadenectomy prior to corneal transplantation did *not* experience prolonged corneal allograft survival,<sup>111</sup> which contradicts the findings of others,<sup>118-121</sup> and an explanation for these differences will be considered in the final discussion (Section 5.3.e).

Hoffmann and colleagues performed several tracer studies using radioactive <sup>99m</sup>Tc colloidal albumin (Nanocoll) to investigate drainage from the eye in mice.<sup>110-112</sup> They showed that the majority of aqueous humour outflow drained into the *ipsilateral* cervical lymph nodes and not the *contralateral* cervical lymph nodes.<sup>110</sup> In addition, both the lower lid and the subconjunctival outflow drained to the *ipsilateral* cervical lymph nodes.<sup>112</sup> Removal of the *ipsilateral* cervical lymph nodes led to dramatically increased accumulation of radioactive antigen in the *contralateral* lymph nodes and failed to significantly prolong corneal allograft survival.<sup>111</sup> This indicated that under certain conditions, the *contralateral* cervical lymph nodes could functionally replace the *ipsilateral* lymph nodes. Furthermore, a considerable increase in antigen specific IFN- $\gamma$  production was observed in the *contralateral* lymph nodes in mice that had

their *ipsilateral* cervical lymph nodes removed. This suggests that drainage of antigenic material and the expression of a Th1 immune response was occurring in these lymph nodes.<sup>111</sup>

Boonman and colleagues studied the drainage of ocular tumour-antigen in mice and found that intraocular tumour-antigen drained to the superficial cervical lymph nodes where antigen-specific cytotoxic T lymphocyte (CTL) activation occurred.<sup>122</sup>

McMenamin and co-workers investigated the distribution of fluorescent dextran after injection into the anterior chamber by following its migration to the lymphoid tissues of rats.<sup>106-107</sup> Using confocal microscopy, antigen-positive cells were identified within various lymphoid organs, including draining *ipsilateral* cervical lymph nodes (superficial cervical lymph node and deep cervical lymph node) as well as in the marginal zone of the spleen and in the mesenteric lymph nodes.<sup>106-107</sup> The majority of antigen-positive cells within the various lymphoid organs were phenotypically characterised as macrophages.<sup>107</sup>

Egan and co-workers showed that antigen injected into the posterior chamber of the eye could initiate the activation and clonal expansion of antigen-specific T cells in the *ipsilateral* superficial cervical lymph nodes within three days after antigen exposure in mice.<sup>109</sup> The proliferating T cells secreted IL-2, indicating that an immunogenic rather than an immunomodulatory response was generated against the ocular antigen.<sup>109</sup>

Liu and colleagues revealed that alloantigen from corneal grafts in mice was able to trigger T cell proliferation in the draining cervical lymph nodes.<sup>123</sup> This was

observed in both allografts that had been accepted and allografts that had been rejected, which correlates with another study that revealed that a DTH response was generated regardless of acceptance or rejection of a corneal allograft.<sup>24</sup> However, only mice with rejected allografts showed production IFN- $\gamma$  and IL-12 within the draining cervical lymph nodes, indicating a Th1 immune response.<sup>123</sup>

The weight of the evidence suggests that ocular lymphatic drainage in rodents occurs through the uveoscleral pathway to the *ipsilateral* cervical lymph nodes. APCs appear to activate T cells in an antigen-specific manner within the draining *ipsilateral* cervical lymph nodes in response to corneal alloantigens. Therefore, preventing lymphatic drainage to the cervical lymph nodes (a possible site of T cell sensitisation) could be a potential strategy which may prolong corneal allograft survival in the rat.

#### **1.6.e. Immune privilege in the eye**

Immune privilege was first reported by Medawar in 1948 when he showed long term survival of skin when grafted into areas such as the anterior chamber of the eye and the brain of rabbits.<sup>124</sup> A number of physical and immunological factors are involved in the maintenance of ocular immune privilege. The physical factors that contribute to ocular immune privilege include the blood-ocular barrier and the avascular nature of the healthy cornea.<sup>30</sup>

Soluble factors in the aqueous humour can inhibit the onset of DTH in response to corneal alloantigens. These factors include transforming growth factor- $\beta$  (TGF- $\beta$ ),<sup>125-</sup><sup>126</sup>  $\alpha$ -melanocyte-stimulating hormone,<sup>127</sup> vasoactive intestinal peptide<sup>128</sup> and

calcitonin gene-related protein,<sup>129</sup> and have been hypothesised to inhibit the migratory ability of iris APCs.<sup>91</sup>

The widespread expression of Fas ligand (FasL)<sup>130-131</sup> and TRAIL<sup>132-133</sup> on the surface of most ocular cells plays a large role in immune privilege within the eye. FasL and TRAIL are members of the tumour necrosis factor family of membrane proteins and both cause the induction of apoptosis in inflammatory cells.<sup>130-133</sup>

Streilein and colleagues discovered and characterised the phenomenon termed anterior chamber-associated immune deviation (ACAID). ACAID results in the suppression of a DTH response upon secondary exposure to antigen after injection of antigen or shedding of antigen from a corneal allograft into the anterior chamber.<sup>89,134-136</sup> ACAID is induced when ocular APCs take up and process antigen within the anterior chamber. The antigen-loaded APCs then migrate to the spleen where a series of complex cellular interactions takes place between the ocular APCs, NK T cells, B cells and CD8+ T cells and leads to the production of CD8+ regulatory T cells. CD4+ CD25+ regulatory T cells are also involved in ACAID, but their role is unclear. The subsequent result of ACAID is the suppression of Th1 and Th2 responses in the eye.<sup>30,137</sup>

In summary, under normal conditions the eye is an immune privileged site. However, inflammation and neovascularisation can erode this privilege and can result in irreversible immunological corneal allograft rejection. The next section will discuss the therapies currently available for the prevention and treatment of allograft rejection.



## **1.7 THERAPIES FOR CORNEAL GRAFT REJECTION**

### **1.7.a. Topical application of glucocorticosteroids**

Topical application of glucocorticosteroids is currently the most widely used and most effective therapy for prevention and treatment of corneal graft rejection in humans.<sup>14</sup> Glucocorticosteroids inhibit leucocyte migration in the cornea and can prevent or even reverse corneal graft rejection.<sup>138</sup> However, despite their universal use, approximately 40% of all corneal allografts reject within 10 years.<sup>13</sup> To improve the survival rate of corneal allografts, an adjunctive therapy is needed. Potential adjunctive therapies include those which have been able to improve the survival of vascularised organs, including human leucocyte antigen (HLA)-matching<sup>16</sup> and systemic immunosuppression.<sup>15</sup> Another more novel therapy for the prevention and treatment of corneal allograft rejection is the use of immunosuppressive agents such as monoclonal antibodies (mAbs) or antibody fragments. These potential therapies will be discussed in more detail in the upcoming sections.

### **1.7.b. HLA-matching**

HLA-matching has been used successfully to prevent renal allograft rejection.<sup>16</sup> However, the effectiveness of matching for HLA determinants for corneal transplantation has been an area for debate. The American Collaborative Corneal Transplant Study (CCTS) reported no benefit from matching HLA class I or class II antigens in corneal transplantation.<sup>139</sup> However, benefits of HLA-matching on corneal allograft survival have been reported from Canada,<sup>140</sup> Holland,<sup>141</sup> Germany<sup>142</sup> and the United Kingdom.<sup>143</sup>

In summary, the benefits of HLA-matching for corneal transplantation are still unclear, and consequently, HLA-matching is not a widely used method for prevention of corneal allograft rejection.

### **1.7.c. Systemic immunosuppression using calcineurin blockers**

Calcineurin blockers such as cyclosporine and FK506 prevent IL-2-controlled T cell expansion<sup>138</sup> and systemic immunosuppression using calcineurin blockers has been highly successful at preventing and treating rejection of vascularised organs.<sup>15</sup> However, there are conflicting reports on the effectiveness of systemic immunosuppression for preventing corneal transplantation.<sup>144-148</sup> Some studies have shown beneficial effects of systemic cyclosporine on corneal allograft survival,<sup>144,148</sup> whilst other studies have revealed that its use failed to prolong corneal allograft survival.<sup>145-147</sup> In addition, systemic delivery of calcineurin blockers is associated with serious side effects. Therefore, systemic delivery of calcineurin blockers is not a widely used treatment for prevention or treatment of corneal graft rejection.

### **1.7.d. Antibodies and antibody fragments**

The use of immunosuppressive antibodies for the treatment and prevention of corneal allograft rejection is a relatively novel field and has shown success in animal models<sup>149</sup> and in humans.<sup>150</sup> Systemic delivery of CAMPATH-1H, (a humanised mAb against CD52) in humans, has been proven to reduce ocular inflammation in patients including those with corneal grafts, with no adverse side effects observed.<sup>150</sup>

Systemic delivery of antibodies and antibody fragments that target molecules involved in antigen presentation and early T cell activation, has been a successful

method for prolonging corneal allograft survival in animal models (Table 1.1). Systemic delivery of anti-CD4 mAb has prolonged corneal graft survival in mice<sup>151-152</sup> and rats.<sup>153-154</sup> Moreover, cytotoxic T-lymphocyte antigen-4 (CTLA-4) is a competitive inhibitor of CD28 and binds to CD80 and CD86 which are expressed on APCs. Delivery of a soluble CTLA-4 construct or an anti-CD28 mAb has prolonged corneal graft survival in mice,<sup>112,155-156</sup> rats<sup>157-158</sup> and rabbits.<sup>159</sup> In addition, systemic delivery of anti-CD40L mAb has prolonged corneal allograft survival in mice.<sup>155,160</sup>

#### **1.7.d.1. Single chain fragment variables**

With the exception of one study,<sup>161</sup> the topical application of whole antibodies to the cornea has shown limited success at prolonging corneal allograft survival in animal models.<sup>149</sup> This is most likely due to the structure of the cornea, which forms a barrier to many therapeutics, including whole antibodies.<sup>149,162</sup>

Genetic engineering has allowed for the isolation of the cDNA that encodes the variable heavy and the variable light regions from a whole antibody, which can be connected together using a linker peptide. These monomeric antibody fragments are referred to as single chain fragment variables (scFv) (Figure 1.5) and have been shown to penetrate pig corneas *in vitro* and rabbit corneas *in vivo*.<sup>162-163</sup> In addition, scFv have reduced immunogenicity compared to whole antibodies, because they do not have an Fc region. ScFv are small enough to penetrate the corneal epithelium, however, one of their limitations as therapeutic agents is their rapid clearance.<sup>163</sup>

**Table 1.1: Studies that have reported prolonged allograft survival by inhibiting early T cell activation.**

Target	Mode of action	Delivery	Species	Reference
CD4	anti-CD4 mAb	systemic	rat	154
CD4	anti-CD4 mAb	systemic	rat	153
CD4	anti-CD4 mAb	systemic	mouse	151
CD4	anti-CD4 mAb	systemic	mouse	152
CD4	LIP anti-CD4 mAb	topical	rat	161
CD28	CTLA4-fusion protein	systemic	rat	158
CD28	anti-CD28 mAb	systemic	rat	158
CD28	CTLA4-Ig	systemic	mouse	155
CD28	CTLA4-Ig	ex vivo	rabbit	159
CD28	AdCTLA	ex vivo	rat	157
CD28	AdCTLA	systemic	rat	157
CD28	CTLA4-Ig	ex vivo	rat	157
CD28	CTLA4-Ig	systemic	rat	157
CD28	CTLA4-Ig + IL-4	ballistic transfer	mouse	112
CD28	CTLA4-Ig + IL-4	ballistic transfer	mouse	156
CD40L	anti-CD40L mAb	systemic	mouse	160
CD40L	anti-CD40L mAb	systemic	mouse	155

LIP, liposome-incorporated; AdCTLA, adenoviral vector encoding CTLA-4 cDNA

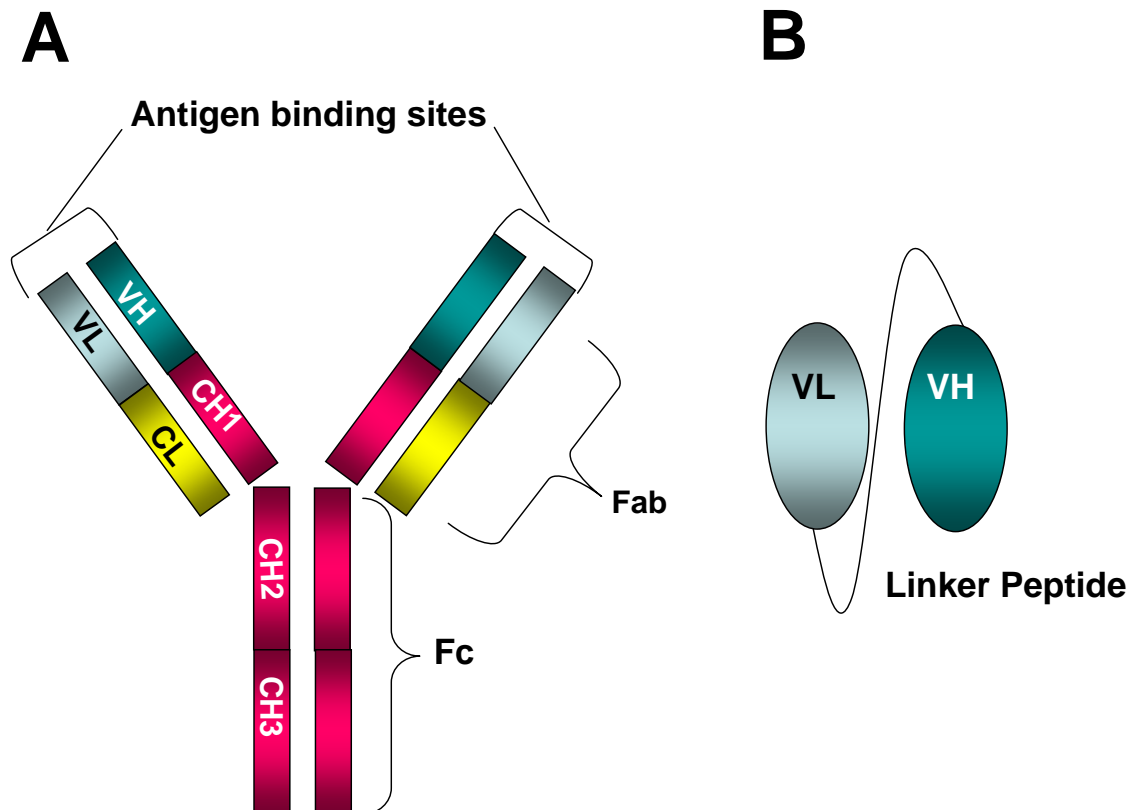


**Figure 1.5: (A) A whole IgG antibody is approximately 146 kDa and (B) a single chain fragment variable is approximately 28 kDa (scFv).** The variable heavy (VH), variable light (VL), constant heavy (CH) and constant light (CL) regions are labelled. Antigen binding occurs at the Fab, as marked on (A). The scFv does not contain the inflammatory Fc region and allows for better tissue penetration because it is approximately 1/5 of the size of a whole IgG antibody.

In summary, scFv have good tissue penetration and negligible immunogenicity. Strategies need to be developed to overcome their rapid clearance after administration, as this will potentially increase their efficacy. One such method could be gene therapy and this will be discussed in the next section.

## **1.8 GENE THERAPY**

### **1.8.a. Gene therapy overview**

The first use of gene transfer in a clinical trial was reported by Rosenberg and colleagues in 1990.<sup>164</sup> A retroviral vector was used to transfer a neomycin resistance marker into tumour-infiltrating lymphocytes from 5 patients with metastatic melanoma. The lymphocytes were expanded *in vitro* and re-infused into the patients.<sup>164</sup> Since this first trial, gene transfer has been used to treat an assortment of diseases including cancer, cardiovascular diseases, monogenic inherited disorders, ocular disease and many others. Approximately 1% of all gene therapy clinical trials worldwide are for the treatment of ocular diseases, including age-related macular degeneration, diabetic macular oedema, glaucoma, retinitis pigmentosa and superficial corneal opacity.<sup>165</sup>

Delivery of transgenes can be performed using viral or non-viral vectors. Viral vectors make use of the natural ability of a virus to infect a target cell. For this reason, gene transfer is very efficient and almost 70% of clinical trials worldwide involve their use.<sup>165</sup> There are concerns for the biosafety of viral vectors including the risk of insertional mutagenesis, their immunogenicity and the potential for replication competent recombinants (RCR) to develop during vector production. Viral vectors commonly used for gene transfer are adenoviral vectors, adeno-

associated viral vectors (AAV) and retroviral vectors such as Molony murine leukaemia viral vectors (MLV) and lentiviral vectors.

Non-viral vectors are currently far less efficient at gene transfer than viral vectors, but they are much safer.<sup>166</sup> Ballistic transfer can be used to deliver plasmid DNA carrying a transgene to the target tissue using brute force.<sup>156</sup> Another non-viral gene transfer method uses cationic lipids to coat the plasmid DNA and this is referred to as lipofection.<sup>167</sup>

Gene therapy has the potential to produce sustained delivery of a scFv to the site of interest. This could be achieved by cloning the scFv gene into a gene transfer vector, then delivering the gene transfer vector to the target cells, which would then express the scFv protein. This strategy has the potential to produce sustained protein expression of a therapeutic scFv at the site where it is needed after a single intervention.

### **1.8.b. Gene transfer to the corneal endothelium**

Gene transfer to the corneal endothelium has been performed using a variety of methods, including viral vectors<sup>168</sup> and non-viral vectors.<sup>156</sup> The use of gene therapy to prolong corneal allograft survival using viral vectors such as lentiviral, adenoviral and AAV vectors has been recently reviewed.<sup>168</sup>

Adenoviral vectors have been used extensively as gene transfer vectors to the cornea, as they produce rapid, strong transgene expression, high titre yields, have a large transgene capacity and are able to transduce non-dividing cells<sup>169</sup> (Table 1.2).

**Table 1.2: Characteristics of adenoviral and lentiviral vectors**

Characteristic	Adenoviral vector	Lentiviral vector
Genetic material	dsDNA	ssRNA
Chromosomal integration	Episomal	Integrated
Transgene expression	Rapid and transient	Slow and long term
Transgene capacity	~30 kb	~9 kb
Inflammatory potential	High	Low
Ability to transduce dividing and non-dividing cells	Yes	Yes
Biosafety risks	Systemic toxicity	Insertional mutagenesis

ds, double stranded; ss, single stranded



However, adenoviral vectors have their limitations for use as gene transfer vectors to the corneal endothelium. Firstly, adenoviral vectors are immunogenic, especially in ocular tissue.<sup>170</sup> The development of “guttated” adenoviral vectors (vectors that are produced without viral sequences) has reduced the adaptive immune response to these constructs, but they have still been reported to generate innate immunity.<sup>171-172</sup> The second limitation is the transient transgene expression produced by these vectors, which is due to the episomal nature of the virus.<sup>173</sup>

Lentiviral vectors possess many of the desirable characteristics of adenoviral vectors, such as the ability to transduce non-dividing cells, to produce high titre yields and they have a relatively large transgene capacity.<sup>174</sup> Lentiviral vectors also possess features that the adenoviral vectors do not, which makes them an attractive alternative for use as a gene transfer vector for the corneal endothelium (Table 1.2). Firstly, lentiviral vectors have low inflammatory potential in ocular tissue.<sup>170,175</sup> Secondly, lentiviral vectors integrate into the host genome, therefore producing long-term stable transgene expression.

### **1.8.c. Lentivirus biology**

Lentiviruses are a genus in the family retroviridae and typically infect terminally differentiated cells.<sup>176-177</sup> There are five serotypes of the lentivirus genus, each categorised by the host mammal with which the virus is associated, including bovine, equine, feline, ovine and primate. The most characterised of the lentivirus genus is the human immunodeficiency virus-1 (HIV-1), which infects human T cells and can lead to the development of acquired immunodeficiency syndrome (AIDS). HIV-1 particles consist of a lipid-envelope, with a homodimer of linear positive-sense,

single-stranded RNA genome which is approximately 9.7 kb. These particles are approximately 110 nm in diameter.<sup>178</sup> A schematic representation of a HIV-1 particle is shown in Figure 1.6 (A). Unlike simple gammaretroviruses, lentiviruses possess the ability to transduce non-dividing cells.<sup>179</sup>

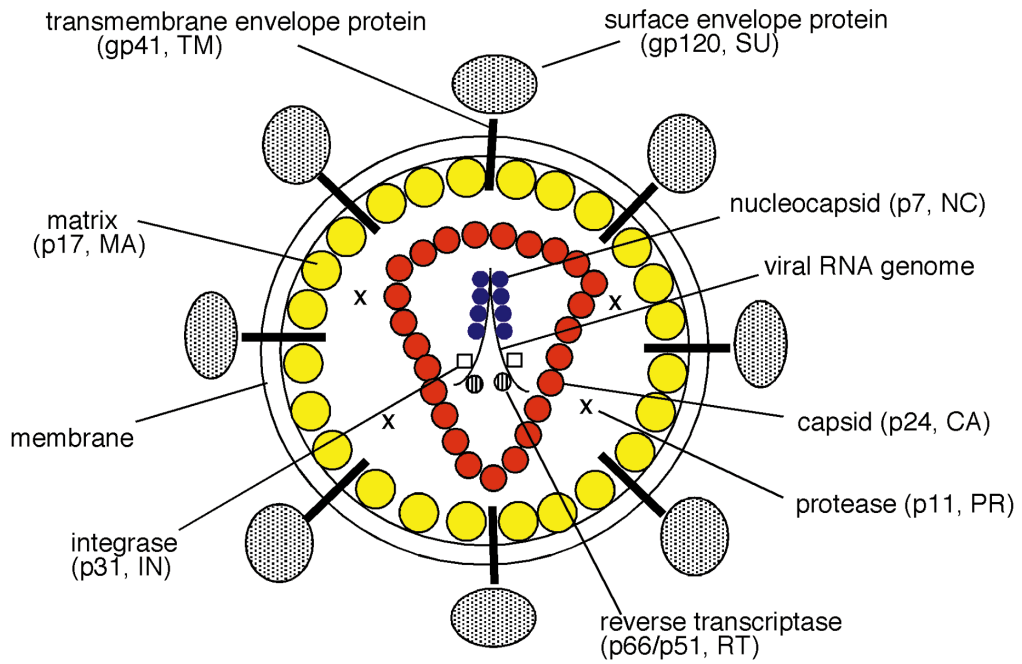
A schematic representation of the HIV-1 genome is shown in Figure 1.6 (B). The cis-acting elements of the HIV-1 genome are common to all retroviruses and include two long terminal repeats (LTRs) which flank the *gag*, *pol* and *env* genes (Table 1.3). The HIV-1 genome encodes regulatory genes such as *tat* and *rev*, which are necessary for HIV-1 replication (Table 1.3) and accessory genes such as *vif*, *vpr*, *vpu*, and *nef* (Table 1.3) which are not essential for viral replication but are critical for pathogenesis.<sup>180</sup>

#### **1.8.d. Recombinant lentiviral vectors for gene transfer**

The development of recombinant lentiviral vectors for gene transfer has been reviewed elsewhere.<sup>174</sup> The design of recombinant lentiviral vectors is based on the separation of the cis-acting sequences that are necessary for transfer of the viral genome to the target cell from the trans-acting sequences that encode the viral proteins.<sup>174,181-182</sup> This is achieved by linking the cis-acting sequences to the expression vector containing the transgene of interest (the transfer vector construct), whilst the viral proteins that are required for the assembly of the viral particles are expressed from separate packaging constructs. Both cis- and trans-acting constructs are introduced in the same cell to produce vector particles. The non-replicative nature

**Figure 1.6: Schematic representation of (A) an HIV-1 particle (adapted from Freed, 1998)<sup>183</sup> and (B) the HIV-1 genome (adapted from Freed, 2001).<sup>184</sup>** HIV-1 particles consist of a lipid-envelope, with a homodimer of linear positive-sense, single-stranded RNA genome. LTRs flank the *gag*, *pol* and *rev* genes. The *gag* gene encodes structural proteins including the matrix protein (MA or p17), the nucleocapsid protein (NC or p7), the capsid protein, (CA or p24) the p6 protein and the spacer proteins p1 and p2. The enzymatic proteins such as reverse transcriptase (RT), protease (PR) and integrase (IN) are encoded by the *pol* gene. The envelope proteins including gp120 and gp41 are encoded on the *env* gene. The regulatory genes *tat* and *rev* are essential for viral replication. The accessory genes *vif*, *vpr*, *vpu* and *nef* are not essential for viral replication but are critical for pathogenesis.

# A



# B

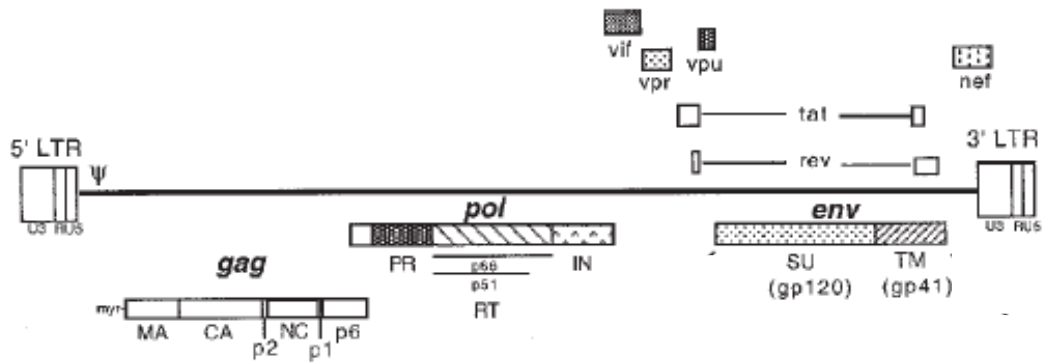


**Table 1.3 HIV-1 genes and their protein products**

Gene	Protein products	Function	Essential for infectivity
<i>gag</i>	matrix (MA or p17)	Structural	Yes
	capsid (CA or p24)	Structural	Yes
	nucleocapsid (NC or p7)	Structural	Yes
	p6 protein	Structural	Yes
	p2 (spacer)	Structural	Yes
	p1 (spacer)	Structural	Yes
<i>pol</i>	viral protease (PR)	Enzyme	Yes
	reverse transcriptase (RT)	Enzyme	Yes
	integrase (IN)	Enzyme	Yes
<i>env</i>	gp120	Structural	Yes
	gp41 (transmembrane glycoprotein)	Structural	Yes
<i>rev</i>	rev	Regulatory	Yes
<i>tat</i>	tat	Regulatory	Yes
<i>vif</i>	vif (viral infectivity factor)	Accessory	No
<i>vpr</i>	vpr (viral protein r)	Accessory	No
<i>vpu</i>	vpu (viral protein u)	Accessory	No
<i>nef</i>	nef (negative factor)	Accessory	No

of these recombinant lentiviral vectors is due to the fact that only a single round of infection (transduction) is possible, because the recombinant particles can only encapsidate the transfer construct (which lacks the trans-acting viral sequences required for replication).<sup>174</sup> Lentiviral vectors can be pseudotyped with an envelope protein from another virus such as vesicular stomatitis virus (VSV) enabling broader tropism and vector stability.<sup>179,185-187</sup>

Since the initial development of first generation HIV-1 vectors for gene transfer by Naldini and colleagues in 1996,<sup>179</sup> there has been continuous development into improving the biosafety and efficiency of these vectors. First generation HIV-1 vectors consisted of a single packaging cassette that contained all the regulatory and accessory genes. The transfer vector construct carried the transgene. There was considerable risk of RCR developing from first generation HIV-1 vectors because of the sequence similarities with wild-type HIV-1 virus. In addition, because the first generation HIV-1 vectors contained the accessory genes, eventual RCR could have pathogenic properties. Methods used to improve the biosafety while maintaining the efficiency of the recombinant lentiviral vectors have focused on segregating the cis- and trans-acting functions of the viral genome,<sup>174</sup> summarised in Table 1.4.

The accessory genes *vif*, *vpr*, *vpu* and *nef* are not essential for HIV-1 replication. Thus, HIV-1 vectors were designed without these accessory genes and were termed second generation HIV-1 vectors (Table 1.4).<sup>188</sup> The removal of accessory genes greatly improved the biosafety of the recombinant HIV-1 vectors because if a RCR arose during vector production, it would not be pathogenic.

**Table 1.4: Advances in recombinant HIV-1 vector biosafety**

Advancement	References	Method	Improved biosafety
2nd generation	188	Removal of accessory genes	Eliminated pathogenic lentiviral properties
3rd generation	189	Deletion of <i>tat</i> and expression of <i>rev</i> in a separate non-overlapping expression construct	Removal of <i>tat</i> and separation of <i>rev</i> further decreased risk of RCR development
SIN	190,191,192	Deletion in U3 region of LTR, results in transcriptional inactivation of LTR	Diminished risk of oncogene activation by promoter insertion and reduces risk of vector mobilisation and recombination with WT

SIN, self inactivating; WT, wild type; RCR, replication competent recombinant; LTR, long terminal repeat

Further biosafety improvements were achieved with the development of third generation HIV-1 vectors (Table 1.4).<sup>189</sup> These vectors did not encode the transcriptional activator gene, *tat*. Instead, strong constitutive promoters with elements of the HIV-1 LTR upstream of transfer vector allowed for the production of enough RNA for efficient encapsidation and transfer by the vector particles.<sup>174</sup> In addition, the third generation HIV-1 vectors were designed with the expression of the *rev* gene in a separate non-overlapping expression construct, which further decreased the likelihood of recombination with wild type HIV-1. If an RCR were to develop, the only features shared with the eventual RCR and the parental virus would be those dependent on the *gag* and *pol* genes.

Deletion of viral enhancer and promoter sequences in the LTR brought about further improvement in terms to biosafety with the development of self inactivating (SIN) transfer vectors (Table 1.4).<sup>190-192</sup> SIN vectors greatly reduced the risk of oncogene activation by promoter insertion, because transgene expression from SIN vectors were controlled completely by an internal promoter, which allowed for the use of tissue-specific promoters<sup>193</sup> or regulatable promoters<sup>194</sup> without interference from the LTR.

#### **1.8.e. The Anson HIV-1 vector system**

Anson and colleagues have developed an HIV-1 vector system designed for optimal safety and large-scale production.<sup>195-197</sup> The Anson HIV-1 vector system (Figure 1.7) has a transfer construct carrying the transgene of interest with codon optimised cis-acting sequences necessary for transduction of target cells, including LTRs, central



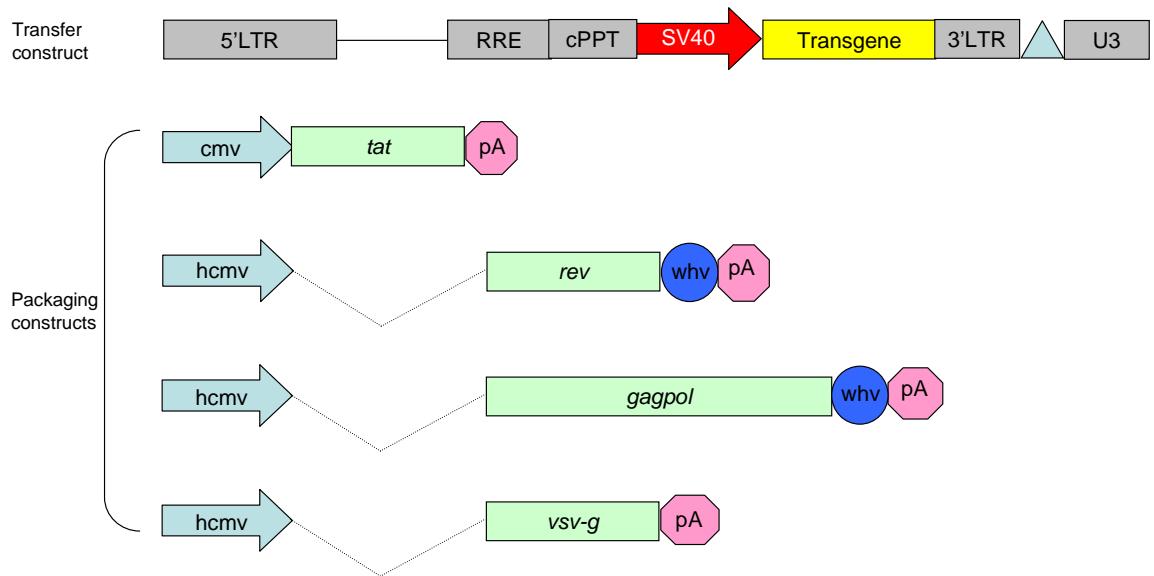


**Figure 1.7: Schematic of the transfer and packaging constructs that make up the Anson HIV-1 vector system.**<sup>195-197</sup> LTR, long terminal repeat; RRE, rev response element; cPPT, central polypurine tract; SV40, simian-like virus early promoter;  $\Delta$ , deletion in U3; cmv, cytomegalovirus promoter; hCMV; human CMV; whv, woodchuck hepatitis virus post-transcriptional element, pA, polyadenylation signal; vsv-g, vesicular stomatitis virus G protein; dashed lines represent splicing signals from the rabbit  $\beta$ -globin gene. For more details on the viral genes *tat*, *rev* and *gagpol* refer to Table 1.3.

poly purine tract (cPPT), rev response element (RRE), 3' poly purine tract (PPT) and 550 bp of the gag gene.<sup>197</sup> It also has a deletion in the U3 sequence in 3'LTR, making it a SIN vector. The coding regions of the structural and regulatory proteins including *gagpol*, *tat*, *rev* and *vsv-g* are provided on separate packaging constructs.<sup>195</sup> The Anson HIV-1 vector system is not *tat* independent. However, because all viral sequences are encoded on separate plasmids, this increases the number of steps required for RCR to occur during virus production, thus ensuring that biosafety is not compromised for viral efficiency.

Using a construct containing the reporter gene enhanced yellow fluorescent protein (eYFP), the Anson HIV-1 vector system has been shown to transduce the rat, sheep and human corneal endothelium effectively.<sup>198</sup>

## **1.9 BIOSAFETY ISSUES ASSOCIATED WITH GENE THERAPY**

### **1.9.a. The first gene therapy death**

Since the first gene therapy clinical trial in 1990,<sup>164</sup> over 1340 clinical trials have taken place or have been approved world-wide.<sup>165</sup> Gene therapy has treated many diseases including immunodeficiencies<sup>199-200</sup> and blood clotting disorders.<sup>201</sup> However, the success of gene therapy has been limited by biosafety issues associated with the viral vectors used to deliver the therapeutic transgenes. The first death associated with gene therapy was that of Jesse Gelsinger in September 1999, who was part of a clinical trial at the University of Pennsylvania.<sup>202</sup> Jesse Gelsinger, an 18 year old male, died from a massive immune response after systemic delivery of a modified serotype 5 adenoviral vector. After Gelsinger's death, all gene therapy trials

were subject to more stringent regulation by the National Institutes of Health (NIH) and the Food and Drug Administration (FDA).<sup>166</sup>

### **1.9.b. Insertional mutagenesis**

In Paris, 2000, Cavazzana-Calvo and colleagues reported the successful use of gene transfer using an MLV vector carrying a gene for a missing cytokine chain in patients who suffered from severe combined immunodeficiency disorder (SCID-X1).<sup>199</sup> Shortly after, Thrasher and colleagues reported the same success in a separate trial in London.<sup>200</sup> However, between the two clinical trials, 5 of the 18 patients developed T cell leukaemia between 31-68 months after gene therapy.<sup>203-204</sup> In all 5 patients that developed leukaemia, proto-oncogenes (LMO2, BMI1, or CCND2) were activated as a result of vector integration.<sup>203</sup> Two of the five patients that developed leukaemia have now died.

Gammaretroviruses such as MLV favour integration near the 5' ends of transcription start sites and associated CpG islands.<sup>205</sup> Consequently, the viral enhancers of the gammaretroviruses have the potential to alter the expression of nearby genes, which appears to be the case with the SCID-X1 patients.<sup>206-208</sup> In contrast, lentiviruses favour integration within active transcription sites and do not show any preference for integration near gene 5' ends.<sup>205</sup> There is evidence to show that HIV integration in active transcription sites is optimal for proviral gene expression. Conversely, it is unclear why gammaretroviruses integrate near the 5' ends of transcription start sites. Consequently, there has been much research into how and why this occurs.<sup>203,206-209</sup> Lentiviral vectors currently appear to be a safer alternative to gammaretroviruses due to the random nature of their integration into active transcription sites.

### **1.9.c. Immune reactivity of viral vectors**

Besides insertional mutagenesis, other issues have hampered the clinical success of gene therapy. Immune reactivity against the cells transduced with integrative viral vectors including MLV<sup>210</sup> and AAV<sup>201</sup> has subsequently resulted in only transient expression of the therapeutic genes. In April 2006, a male participant died in a gene therapy clinical trial in which an MLV vector was used to deliver a therapeutic gene for the treatment of chronic granulomatous disease (CGD). The death was attributed to a decrease in the expression of the therapeutic transgene, as the patient died from complications associated with CGD.<sup>210</sup> This was likely to be a consequence of an immune response against the cells transduced with the MLV. Moreover, in a clinical trial to treat haemophilia by gene transfer using an AAV, the gene therapy was successful for only 8 weeks. After this, levels of the therapeutic gene dropped significantly.<sup>201</sup> The decrease in transgene expression was caused by a cell-mediated immunity generated against the AAV capsid. It has been suggested that future gene therapy studies in humans may require the use of immunosuppressive drugs to prevent immune reactivity against the viral vectors.<sup>201</sup>

### **1.9.d. Gene therapy for the treatment of non-life threatening disease**

The use of gene therapy for the treatment of non-life threatening diseases is an area for debate. In July 2007 a 36 year old women died in a rheumatoid arthritis gene therapy clinical trial after the administration of the second dose of the treatment.<sup>211</sup> An AAV vector carrying the therapeutic transgene was injected into the patient's knee. This was the first clinical trial using an AAV vector where the viral vector was readministered. There was not enough evidence to link the gene transfer to her death, however readministration of the AAV vector could have led to severe immunologic

reaction in the now-sensitised patient, despite the use of immunosuppressive drugs.<sup>211</sup> Another possibility is that the patient's death was related to her systemic immunosuppression.<sup>211</sup>

#### **1.9.e. Ocular gene therapy**

Gene therapy for the treatment of ocular disease has also been performed in humans. In 2008, 3 separate gene therapy clinical trials began for the treatment of Leber's congenital amaurosis type 2 (LCA2). LCA2 is a recessive inherited rod-cone dystrophy caused by a single gene defect and is characterised by moderate vision impairment in infancy that progresses to complete blindness by early to mid adulthood.<sup>212-214</sup> In all three clinical trials, an AAV vector was used to deliver the retinal pigment epithelium-specific protein 65 kDa to the subretinal space. To date, some patients have shown increases in light sensitivity and visual acuity in all three studies,<sup>215</sup> and so far no adverse events have been reported. For example, immune reactivity against the AAV vector and the transgene has been minimal and biodistribution levels have been negative thus far.<sup>215</sup> These trials have paved the way for future gene therapy trials for the treatment of eye disease.

#### **1.9.f. Summary of the biosafety issues associated with gene therapy**

Gene therapy is a very young field and has the potential to cure many diseases that were thought once to be incurable. Gene therapy has enabled patients suffering from immunodeficiencies<sup>199</sup> and blood clotting disorders<sup>201</sup> to be cured after a single administration. Many would argue that the benefits of gene therapy outweigh its risks. The question arises as to whether the potential risks associated with gene therapy outweigh its use for the treatment of non-life threatening diseases including

ocular disease. However, the loss of vision is not a trivial matter and continued research into the development of safer more efficient gene transfer vectors will hopefully reduce or eliminate the biosafety concerns associated with gene therapy.

### **1.10 SUMMARY AND AIMS**

The evidence provided in this chapter, highlights the need for improvements to the current therapies for the prevention of irreversible immunological corneal allograft rejection. Firstly, there has been no improvement in the survival rate of corneal allografts in humans over the last 20 years, and despite the universal use of topical glucocorticosteroids, approximately 40% of corneal allografts reject after 10 years.<sup>13</sup> Secondly, the therapies that have been able to greatly improve the survival rate of vascularised organ allografts including HLA-matching<sup>16</sup> and systemic immunosuppression using calcineurin blockers<sup>15</sup> have had mixed results for the prevention of corneal allograft rejection in humans.<sup>139-148</sup> Thus a need for a novel therapy for the prevention of corneal allograft rejection is evident.

Systemic delivery of antibodies and antibody fragments targeting antigen presentation and early T cell activation has proven to be a successful strategy for prolonging corneal allograft survival in animals models (Table 1.1). The CD4 molecule might to be a suitable target for the prevention of corneal allograft rejection using immunosuppressive therapy because (1) CD4 is expressed abundantly on the surface of CD4+ T cells,<sup>38</sup> which are primarily responsible for generating an immune response against corneal allografts,<sup>47</sup> and (2) CD4 is essential for antigen presentation and early T cell activation, therefore inhibiting its function will inhibit

these processes and (3) inhibiting the function of CD4 at a specific anatomic site could potentially allow for the actual site of antigen presentation within the body to be determined.

A regional immunosuppressive strategy, using an anti-CD4 antibody fragment could be a novel approach to prevent corneal allograft rejection. This could be achieved by delivering the antibody fragment to the actual site where the immune response is being generated. Regional immunosuppression has the potential to have a more potent effect, be more cost effective and may further reduce any potential side effects compared to systemic delivery of such an agent.

Ideally, an immunosuppressive agent should modulate the targeted immune response without any undesired side effects. ScFv are small monomeric antibody fragments that have good tissue penetration and have low immunogenicity, however they do have rapid clearance from ocular tissue.<sup>163</sup> ScFv appear to be a good choice for a regional immunosuppressive therapy.

Gene delivery using an integrative vector such as a recombinant lentiviral vector, has the potential to produce sustained long term expression of a transgene after a single intervention.<sup>179</sup> Thus, constitutive expression of an anti-CD4 scFv from lentiviral-transduced tissue, would reduce the problem of rapid clearance associated with scFv, because the scFv would be constitutively expressed at the site of interest.

Before regional immunosuppression can be performed, the best site for the delivery of an immunosuppressive agent (such as an anti-CD4 scFv) must first be identified.

It is still unclear as to whether this may be within the eye, the draining cervical lymph nodes or elsewhere in the body. Studies in rodents have revealed the importance of the cervical lymph nodes in relation to ocular antigen drainage (section 1.6.d.). In mice, one study has shown that the cervical lymph nodes are essential for corneal allograft rejection.<sup>120</sup> In addition, the ocular environment may also be an important site of antigen presentation of ocular antigen, including within the cornea,<sup>34-35</sup> or the uveal tract.<sup>92</sup>

The aims of the work described in this thesis were:

- (1) to construct single-gene and dual-gene lentiviral vectors carrying the cDNA for an anti-rat CD4 scFv and the reporter gene eYFP;
- (2) to characterise the expression of the anti-rat CD4 scFv and eYFP from the single-gene and dual-gene lentiviral vectors;
- (3) to optimise the methods used to titrate lentiviral vector preparations that do not carry a reporter gene;
- (4) to use a lentiviral vector carrying the anti-rat CD4 scFv to investigate the potential sites where antigen presentation may occur in response to corneal transplantation in the rat. This was achieved by transducing the sites of interest, including the corneal endothelium and the cervical lymph nodes, with a lentiviral vector carrying the anti-rat CD4 scFv and assessing corneal allograft survival.



## **CHAPTER 2: MATERIALS AND METHODS**

## **2.1 MATERIALS**

### **2.1.a. General chemicals**

Chemicals were obtained from Sigma, St Louis, MO, USA Chemical Company (St Louis, MO, USA), AJAX Chemicals (Auburn, NSW, Australia) or BDH Chemicals (Kilsyth, Vic, Australia) and were analytical reagent grade unless otherwise stated. Recipes for buffers and solutions are detailed in Appendix 1. Water for irrigation (Baxter, Old Toongabbie), NSW, Australia) was used to prepare buffers and solutions.

### **2.1.b. Antibodies**

Sources of antibodies are listed in Table 2.1.

### **2.1.c. Antibody fragments**

Anti-rat CD4 antibody fragments were prepared by Mrs S Taylor (CSL Laboratories, Melbourne, Vic, Australia). Single-chain antibody fragments (scFv, derived from hybridoma OX38) were produced in bacteria and purified as previously described.<sup>163</sup> ScFv constructs with 20 amino acid (20-mer) linker sequence were generated. Fractions of scFv protein were eluted from an anion exchange column and concentrated to 2.3 mg/ml in buffer (20 mM HEPES, pH 8.0 with 50 mM NaCl), filter sterilised and stored at 4°C.

### **2.1.d. Antibiotics**

Ampicillin (50 mg/ml; Boehringer, Mannheim, Germany) and kanamycin (10 mg/ml; Sigma, St Louis, MO, USA) stocks were prepared in sterile water and used at working concentrations of 100 µg/ml and 50 µg/ml, respectively. Chloramphenicol stocks (Sigma

**Table 2.1 Antibodies**

Designation	Specificity	Antibody	Format	Source (Accession number)
X63	Unknown (negative control)	Monoclonal mouse IgG <sub>1</sub>	Hybridoma supernatant	H. Zola, Women's Children's Health Research Institute, North Adelaide, SA
Sal5	Salmonella epitope (negative control)	Monoclonal mouse IgG <sub>2a</sub>	Hybridoma supernatant	H. Zola, Women's Children's Health Research Institute, North Adelaide, SA
JJ319	Rat CD28	Monoclonal mouse IgG <sub>1</sub>	Hybridoma supernatant	T. Hunig, Institute of Virology and Immunology, University of Wurzburg, Germany
OX38	Rat CD4	Monoclonal mouse IgG <sub>2a</sub>	Hybridoma supernatant	ECACC (88051303)
OX35	Rat CD4	Monoclonal mouse IgG <sub>2a</sub>	Hybridoma supernatant	ECACC (86100904)
Anti- polyhistidine	Polyhistidine tag	Monoclonal mouse IgG <sub>2a</sub>	Ascites fluid, clone HIS-1	Sigma Chemical Company, St Louis, MO, USA
Biotinylated goat anti-mouse	Mouse Ig	Goat Ig	Purified, absorbed to human Ig and cow serum	DakoCytomation, CA, USA
Anti-CD3-FITC	Rat CD3	Monoclonal mouse IgM	Purified, fluorescein isothiocyanate conjugate	Serotec, Oxford, UK

ECACC, European Collection of Cell Cultures, Porton Down, Wiltshire, UK.; Ig, immunoglobulin

St Louis, MO, USA) were prepared in ethanol (34 mg/ml) and used at 34 µg/ml. All antibiotic stocks were stored at -20°C until required.

#### **2.1.e. *Escherichia coli* (*E. coli*) strains**

The *Escherichia coli* (*E. coli*) strains used in this project are listed in Table 2.2.

#### **2.1.f. Plasmids**

A list of plasmids used in this project can be found in Table 2.3.

#### **2.1.g. Molecular biology reagents**

Reagents used for molecular biology are listed in Table 2.4.

#### **2.1.h. Polymerase chain reaction (PCR) primers**

Polymerase chain reaction (PCR) primers used for both endpoint PCR and quantitative real-time PCR (qPCR) were constructed by GeneWorks Pty Ltd, (Thebarton, SA, Australia) to sequencing grade and are listed in Table 2.5.

#### **2.1.i. Mammalian cell culture reagents**

Tissue culture flasks, disposable pipettes and disposable graduated tubes were obtained from Nunclon (Copenhagen, Denmark) or Falcon (Franklin Lakes, NJ, USA). Powdered media for mammalian cell culture were obtained from Thermo Electron (Melbourne, Vic, Australia) and GIBCO BRL (Gaithersburg, MD, USA). HEPES-buffered RPMI and DMEM were prepared as described in Appendix 1 in endotoxin-low glassware treated

**Table 2.2: *E. coli* strains**

Strain	Genotype	Details
DH5 $\alpha$	<i>supE44</i> $\Delta$ <i>lacU169</i> ( $\Phi$ 80 <i>lacZ</i> $\Delta$ <i>M15</i> ) <i>hsdr17</i> <i>recA1</i> <i>endA1</i> <i>gyrA96</i> <i>thi-1</i> <i>relA1</i>	A recombination-deficient suppressing strain used for plating and growth of plasmids and cosmids. The $\Phi$ 80 <i>lacZ</i> $\Delta$ <i>M15</i> permits $\alpha$ - complementation with the amino acid terminus of $\beta$ -galactosidase encoded in pUC vectors.
GM48	<i>dam-3</i> <i>dcm-6</i> <i>thr-1</i> <i>leuB6</i> <i>ara-14</i> <i>tonA31</i> <i>lacY1</i> <i>tsx-78</i> <i>supE44</i> <i>galK2</i> <i>galT22</i> <i>thi-1</i>	The prototype <i>dam dcm</i> double mutant. Transformed at high efficiency by plasmid DNA. Does not lack any restriction system.

---

**Table 2.3: Plasmids**

Designation	Description	Sequence(s) of interest	Resistance	Source
pHIV-eYFP	HIV-1 lentiviral vector plasmid encoding eYFP under SV40 promoter control	SV40 promoter + eYFP	Chloramphenicol	D. Anson, Women's and Children's Hospital, Adelaide, SA
pBS-CD55_F2A_CD59	Plasmid encoding CD55 and CD59 with a furin cleavage site and a FMDV 2A sequence in between the two genes	2A sequence + furin cleavage site	Ampicillin	P. J. Cowan, St Vincent's Health, Melbourne, Vic
fHSSOX38scFv in pAdtrackCMV	Adenoviral shuttle vector encoding fHSS and anti-rat CD4 scFv controlled by the CMV promoter	fHSS + anti-rat CD4 scFv	Kanamycin	C. Jessup, Flinders University, Adelaide, SA
pAdEasy-1 (pAdeasy)	E1-, E3-deleted adenovirus serotype-5 backbone	Adenoviral sequences	Ampicillin	B. Vogelstein, Johns Hopkins University, Baltimore, MD, USA
pcDNA3.1tat101ml	Helper plasmid encoding HIV-1 Tat	HIV-1 Tat	Chloramphenicol	D. Anson, Women's and Children's Hospital, Adelaide, SA
pHCMVwhvrevml	Helper plasmid encoding HIV-1 Rev	HIV-1 Rev	Chloramphenicol	D. Anson, Women's and Children's Hospital, Adelaide, SA
pHCMVwhvgagpolml	Helper plasmid encoding HIV-1 GagPol	HIV-1 GagPol	Chloramphenicol	D. Anson, Women's and Children's Hospital, Adelaide, SA
pHCMV-G	Helper plasmid encoding VSV-G	VSV-G	Chloramphenicol	D. Anson, Women's and Children's Hospital, Adelaide, SA
pBLAST41-hEndoKringle5	Expression vector containing EK5	EK5	Blasticidin	InvivoGen, San Diego, CA, USA
pHIV-EK5	HIV-1 plasmid encoding EK5 under SV40 promoter control	EK5	Chloramphenicol	L. Mortimer, Dept of Ophthalmology, Flinders University, Adelaide SA
pHIV-CD4scFv_F2A	HIV-1 plasmid encoding anti-rat CD4 scFv and F2A under SV40 promoter control	anti-rat CD4 scFv + F2A	Chloramphenicol	eYFP was removed from pHIV-CD4scFv_F2A_eYFP
pHIV-CD4scFv_F2A_eYFP	HIV-1 plasmid encoding anti-rat CD4 scFv, F2A and eYFP under SV40 promoter control	anti-rat CD4 scFv + F2A + eYFP	Chloramphenicol	anti-rat CD4 scFv cloned into pHIV-eYFP
pHIV-eYFP_F2A_CD4scFv	HIV-1 plasmid encoding eYFP, F2A and anti-rat CD4 scFv under SV40 promoter control	eYFP + F2A + anti-rat CD4 scFv	Chloramphenicol	eYFP + F2A cloned into pHIV-CD4scFv
pHIV-CD4scFv_F2A_EK5	HIV-1 plasmid encoding anti-rat CD4 scFv, F2A and EK5 under SV40 promoter control	anti-rat CD4scFv + F2A + EK5	Chloramphenicol	EK5 was cloned into pHIV-CD4scFv_F2A_eYFP after the removal of eYFP

eYFP, enhanced yellow fluorescent protein; SV40, simian-like virus type-40 early promoter; FMDV, foot and mouth disease virus; fHSS, factor H secretory sequence; CMV, cytomegalovirus; VSV-G, vesicular stomatitis virus glycoprotein G; EK5, human endostatin::kringle-5

**Table 2.4: Molecular biology reagents**

Reagent	Manufacturer
GelRed™ (10 000X)	Biotium Inc (Hayward, CA, USA)
6X Loading dye	Promega (Madison, WI, USA)
20 bp ladder (20 bp-1 kb)	Geneworks (Thebarton, SA, Australia)
2 log DNA ladder (100 bp-10 kb)	New England Biolabs (Beverly, MA, USA)
Restriction endonucleases	New England Biolabs (Beverly, MA, USA)
Restriction endonuclease reaction buffers (NEBuffers, 1,2,3,4)	New England Biolabs (Beverly, MA, USA)
One-Phor-All® restriction endonuclease buffer	Amersham Biosciences Corporation, (Piscataway, NJ, USA)
T4 DNA ligase (2 000 000 units/ml)	New England Biolabs (Beverly, MA, USA)
10X T4 DNA Ligase Reaction Buffer (containing 10 mM ATP)	New England Biolabs (Beverly, MA, USA)
Elongase®	Invitrogen (Carlsbad, CA, USA)
Platinum® Taq DNA polymerase	Invitrogen (Carlsbad, CA, USA)
10X PCR buffer (specific for either Platinum® Taq or Elongase®)	Invitrogen (Carlsbad, CA, USA)
dNTPs (10 mM for each: dATP, dCTP, dGTP and dTTP)	Amersham Biosciences Corporation, (Piscataway, NJ, USA)
TURBO DNA-free™ DNase I	Ambion (Austin TX, USA)
SuperScript III® First-Strand Synthesis System	Invitrogen (Carlsbad, CA, USA)
Quantitect™ SYBR Green Master Mix	Qiagen (Hilden, Germany)
Shrimp Alkaline Phosphatase (1000 U/ml)	USB (Cleveland, Ohio, USA)
Klenow Fragment of DNA polymerase I (10 units/μl)	Geneworks (Thebarton, SA, Australia)

---

 bp, base pairs

**Table 2.5: PCR primers**

Designation	Sense/ Antisense	Sequence (5' → 3')	bp
ClaI fHSS for	sense	GTATCGATCAAAAAATGAGACTTCTAGCAAAGATT	35
NdeI scFv rev2	antisense	CACATATGCTAATGATGGTGATGATGGTGATCGGCC	36
CD4 2A for	sense	ACCATCATTCTAGAGCCAAACGCGCTCCCGTGAAGC	36
CD4 2A rev 2	antisense	CGTTTGGCTCTAGAATGATGGTGATGATGGTGATCG	36
ClaI 2A rev 3	antisense	AGATCGATGCCAGGGTTGGACTCGACGTCGCCGGC	35
anti-CD4 scFv for 2	sense	GCCATGGCGGACTACAAA	18
anti-CD4 scFv rev 2	antisense	TGCAGGAAAGACTGACGCTAT	21
human ARBP for	sense	TCATCAACGGGTACAAACGA	20
human ARBP rev	antisense	GCAGATGGATCAGCCAAGA	19
eYFP2 for	sense	TATATCATGGCCGACAAGCA	20
eYFP2 rev	antisense	GGGTGTTCTGCTGGTAGTGG	20
ovine $\beta$ actin for	sense	CACCCAGCACGATGAAGAT	19
ovine $\beta$ actin rev	antisense	CAGGTGGAAGGTCGTCTAC	19
human transferrin for	sense	GCCCTGCCTGCCTACA	16
human transferrin rev	antisense	CAGGTTGTGCTTCTGACTCACT	22
gag for	sense	AGCTAGAACGATTCGAGTTGAT	24
gag rev	antisense	CCAGTATTTGTCTACAGCCTTCTGA	25
rat ARBP for	sense	AAAGGGTCTGGCTTTGTCT	20
rat ARBP rev	antisense	GCAAATGCAGATGGATCG	18
rat HPRT for	sense	TTGTTGGATATGCCCTTGACT	21
rat HPRT rev	antisense	CCGCTGTCTTTTAGGCTTTG	20
pHIV1SV for2	sense	CTCGGCCTCTGAGCTATTC	19
pHIV1SV rev2	antisense	CAAGCGCGCAATTAACCCTC	20
seq-VLfor	antisense	GGAGCCGCCGCCCA	16
seq-VHback	sense	GGCTCCGGTGGTGGTGGGA	18
C+D NdeIn rev	antisense	AAGTGGCTAAGATCCATAGCATA	23
GFP-Taq5'	sense	CCGACCACATGAAGCAGCA	19
GFP-Taq3'	antisense	GTGCGCTCCTGGACGTAGC	19
EK5 for2	sense	CCATCGTCAACCTCAAGGAC	20
AgeI EK5 for	sense	TCCACCGGTATGTACAGGATGCAACTCCTGTCTT	35
NdeI EK5 rev	antisense	GGAATTCCATATGCTAATCAAATGAAGGGGCCGCACA	37

for, forward; rev, reverse; bp, base pairs; ClaI, ATCGAT; NdeI, CATATG; AgeI, ACCGGT; ARBP, acidic ribosomal phosphoprotein; HPRT hypoxanthine guanine phosphoribosyl-transferase



with E-toxa-Clean™ (Sigma, St Louis, MO, USA) according to the manufacturer's instructions, and 0.22 µm filter sterilised prior to use.

### **2.1.j. Animals**

Fischer 344 (F344, RT<sup>lv1</sup> inbred albino) and Wistar Furth (WF, RT<sup>lu</sup> inbred albino) rats were kept in an approved animal house facility. Animals were housed at 21°C in 50% humidity with a 12 hour light/12 hour dark cycle with water *ad libitum* and dry ration ("New Joint Stock" Ridley Agriproducts, Murray Bridge, SA, Australia). Experimental protocols were developed in accordance with the NHMRC guidelines for the use of animals in research. All adenoviral and lentiviral-treated animals were housed in a PC2 facility in the animal house. Approval for all experimentation was obtained from the institutional Animal Welfare Committee of Flinders University. Approval for viral treatment of animals was obtained from the institutional Biosafety Committee of Flinders University and the Office of the Gene Technology Regulator, Canberra, Australia.

### **2.1.k. Miscellaneous reagents**

Miscellaneous reagents are listed in Table 2.6

### **2.1.l. Filter cube specifications on fluorescence microscopes**

Filter cube specifications for Olympus BX50 and Olympus IX71 fluorescence microscopes (Olympus Optical Co., Japan) can be found in Table 2.7.

**Table 2.6: Miscellaneous reagents**

Reagent	Description	Source
Water for irrigation	Sterile, nonpyrogenic	Baxter (Old Toongabbie, NSW Australia)
Glycogen	20 mg/ml in distilled water	Roche (Mannheim, Germany)
Tween-20	Polyethylene sorbitan monolaurate	Sigma (St Louis, MO, USA)
Hoechst-33258 dye	Nuclear stain	Sigma (St Louis, MO, USA)
2-Mercaptoethanol	$\beta$ -mercaptoethanol $\geq 98\%$ (M-7154)	Sigma (St Louis, MO, USA)
DEPC	Diethylpyrocarbonate $\geq 97\%$ (D-5758)	Sigma (St Louis, MO, USA)
Limulus amoebocyte lysate assay	Sensitivity: 0.06 EU/ml (N283-06)	BioWhittaker, (Walkersville, MD, USA)
Virkon tablets	Postassium monopersulphate 50.4% active (174023)	Antec International - A DuPont Company, (Sudbury, Suffolk, UK)
SAPE	Streptavidin R-phycoerythrin conjugate, 1 mg/ml in 0.1 M NaP, 0.1 M NaCl, pH 7.5, 2 mM azide	Invitrogen (Carlsbad, CA, USA)
Concentrating filters	Centricon® Centrifugal Filter Units, 10 kDa cut off pore size (YM-10)	Billerica (MA, USA)
Bartels Buffered Glycerol Mounting Medium	60% glycerol, pH 8.0-8.4 (B1029-45B)	Trinity Biotech plc (Bray, Co. Wicklow, Ireland)

**Table 2.7: Filter cube specifications on fluorescence microscopes**

Microscope	Label	Filter name	Wavelength		
			Excitation	Dichroic	Emission
Olympus BX50	UV light	Olympus U-MNUA	360-370	400	420-460
Olympus BX50	Blue light	Chroma 31001	465-495	505	515-555
Olympus IX71	Blue light	Olympus U-MWIBA3	460-495	505	510-550

## 2.2 MOLECULAR METHODS

### 2.2.a. Plasmid DNA preparation

All plasmids were grown in DH5- $\alpha$  *E. coli* unless digestion with the ClaI restriction enzyme was required. In this case, plasmids were grown in GM48 (dam-) *E. coli* (Table 2.2), because the ClaI restriction site is dam methylated.

All plasmid preparations were prepared using Qiagen kits (Qiagen, Hilden, Germany). Small-scale plasmid preparations were prepared using the QIAprep<sup>®</sup> Spin Miniprep Kit (Qiagen, Hilden, Germany). A 2 ml overnight culture (LB medium plus antibiotic) was incubated at 37°C with vigorous shaking. Cells were pelleted at 10 000 g. The supernatant was completely removed. Pellets were stored at -20°C or used immediately as per the manufacturer's instructions to extract and purify the plasmid DNA. Medium-scale plasmid preparations were prepared using the QIAfilter<sup>™</sup> Plasmid Midi Kit (Qiagen, Hilden, Germany). A 2 ml starter culture was incubated at 37°C with shaking for 6-8 hours. The starter culture (50  $\mu$ l) was used to inoculate 50 ml LB medium (plus antibiotic) and was incubated at 37°C with vigorous shaking overnight. Cells were pelleted at 6000 g in 30 ml Oakridge tubes (Nalge Company, Rochester, NY, USA) at 4°C for 10 minutes. Supernatant was completely removed and discarded. Pellets were stored at -20°C or used immediately to extract and purify the plasmid using the methods described by the manufacturer. Large-scale endotoxin free plasmid preparations were prepared for virus production using the Endofree

Plasmid Mega Kit (Qiagen, Hilden, Germany). A 3 ml starter culture (LB medium plus antibiotic) was incubated for 8 hours at 37°C with vigorous shaking. The starter culture was diluted 1/500 by adding 1 ml of starter culture to 500 ml of LB (plus antibiotic) and was incubated overnight at 37°C with vigorous shaking. Cells were pelleted at 6000 g in 500 ml centrifuge tubes (Sorvall® Centrifuges, Asheville, NC, USA) at 4°C for 10 minutes. Supernatant was completely removed and discarded. Pellets were stored at -20°C or used immediately to extract and purify the plasmid using the protocol outlined by the manufacturer.

### **2.2.b. Restriction endonuclease digestion**

Restriction digests were performed using the manufacturer's instructions in 1.5 ml tubes. Between 500 ng to 5 µg of DNA was digested in each reaction. Solutions were mixed thoroughly and centrifuged for 5 seconds at 7000 g. Between 50 ng to 100 ng of each digest was analysed by agarose gel electrophoresis (Section 2.2.g.) to check for complete digestion.

### **2.2.c. Dephosphorylation with shrimp alkaline phosphatase (SAP)**

Shrimp alkaline phosphatase (SAP) (USB Corporation, Ohio, USA) was used to dephosphorylate double-digested, linearised vector ends to prevent re-ligation without an insert. One unit of SAP per 1 pmol of DNA ends was used. Treatment with SAP was performed immediately after restriction digestion by incubating the digest reaction plus the SAP enzyme at 37°C for 60 minutes. SAP was inactivated immediately after dephosphorylation by incubating the reaction at 65°C for 15 minutes.

#### **2.2.d. Purification of digested and/or SAP-treated DNA**

Digested plasmid (with or without SAP-treatment), and PCR product were purified using the QIAquick PCR Purification Kit (Qiagen, Hilden, Germany) as per the manufacturer's instructions, before use in ligation reactions.

#### **2.2.e. Ligations**

Ligation reactions were performed on digested vector (200 ng) with digested insert (at 1:1 or 1:3 vector:insert molar ratio) using 2 units of T4 DNA ligase (New England Biolabs, Beverly, MA, USA) in a 20  $\mu$ l reaction volume. Ligations were incubated overnight at 4°C in 0.5 ml tubes.

#### **2.2.f. Purification of ligation products**

Ligation reactions were diluted to a 200  $\mu$ l volume and cleaned up by ethanol precipitation. Ethanol precipitation was performed by adding 2  $\mu$ l of glycogen (20 mg/ml; Roche, Mannheim, Germany) and 20  $\mu$ l of 3M sodium acetate to each ligation and tubes were vortex-mixed. Ice cold ethanol (100%) was added to each ligation to make a final concentration of 70% ethanol (550  $\mu$ l) and tubes were vortex-mixed. Ligations were incubated at -20°C for 30 minutes to allow for DNA precipitation. Reactions were centrifuged at >10 000 g for 15 minutes and the supernatant was removed. Ligations were washed twice in ice cold 70% ethanol (500  $\mu$ l) and spun at >10 000g. DNA pellets were air dried for 15 minutes, or until the pellet had completely dried. Ligations were dissolved in 10  $\mu$ l water and 5  $\mu$ l of each ligation was run on an agarose gel (Section 2.2.g.) to assess whether the ligation had been successful.

### **2.2.g. Agarose gel electrophoresis**

Agarose gels were prepared by dissolving agarose (Promega, WI, USA) in 0.5X TBE buffer (Appendix 1) by brief warming in a microwave. GelRed™ (8 µl of 10 000X stock; Biotium Inc, Hayward, CA, USA) was added to 80 ml of molten agarose/0.5X TBE solution. Agarose gels were set at room temperature. The molecular weight markers, 2 log DNA ladder (New England Biolabs, Beverley, MA, USA) and/or 20 bp ladder (Geneworks, Thebarton, SA, Australia) were used to estimate the size of DNA fragments electrophoresed at 100 volts/cm for 60 minutes. DNA fragments were visualised under ultraviolet (UV) light using GeneGenius gel documentation and imaging software (Syngene, Cambridge, England).

### **2.2.h. Preparation of electrocompetent cells (*E. coli* strains)**

Two single colonies of *E. coli* strains DH5α or GM48 were picked and used to inoculate 2 x 10 ml LB media. Cultures were incubated overnight at 37°C with vigorous shaking. The two overnight cultures were combined into one tube to make a total volume of 20 ml and were used to inoculate 1 L of low salt LB medium (Appendix 1), which was divided into 2 x 500 ml volumes into 1.5 L flasks. Cultures were incubated at 37°C and harvested when the optical density at 660 nm (OD<sub>660</sub>) was between 0.6-0.8 which usually occurred after 3 hours. The two cultures were combined into one flask and mixed well. The mixed culture was evenly divided into 500 ml centrifuge tubes (Sorvall® Centrifuges, Asheville, NC, USA) and centrifuged at 2000 g for 15 minutes at 4°C. Each cell pellet was resuspended in 250 ml of chilled sterile water (Baxter, Old Toongabbie, NSW, Australia) and centrifuged at 2000 g for 15 minutes at 4°C. Each cell pellet was resuspended in 62 ml of chilled sterile water (Baxter, Old Toongabbie, NSW, Australia) and combined into one tube. Cells were centrifuged at 2000 g for 15 minutes at 4°C and resuspended in 10 ml

chilled 10% glycerol. Cells were transferred into a 30 ml Oakridge tube (Nalge Company, Rochester, NY, USA) and centrifuged at 2000 g for 15 minutes at 4°C. Cells were resuspended in 1 ml chilled 10% glycerol, making a final suspension which was approximately 60% cells. Cells were distributed into 70 µl aliquots in 1.5 ml tubes and were snap-frozen in liquid nitrogen. Electrocompetent cells were stored at -80°C until required.

### **2.2.i. Electroporation of *E. coli* strains DH5α and GM48**

Aliquots of electrocompetent *E. coli* strains DH5α or GM48 (70 µl in a 1.5 ml tube) were thawed on ice for 20 minutes. Once thawed, 2 µl of a cleaned ligation reaction was added to the cells which were lightly mixed by gentle tapping on the tube and returned to ice for 5 minutes. Cells with added ligation reaction were transferred to a pre-cooled 0.1 cm electrode Gene Pulser® (Bio-Rad Laboratories, Hercules, CA, USA) cuvette. The electroporation was performed at 1.8 volts using a Gene Pulser® (Bio-Rad Laboratories, Hercules, CA, USA) and the time constant was recorded. Ideal time constants ranged from 3.5-5.0. SOC medium (1 ml; Appendix 1) was added to the cells in the cuvette and mixed by gentle pipetting, and then transferred back to the original 1.5 ml tube. Electroporated cells were incubated in a heat block at 37°C for 60 minutes. Cells were centrifuged at 2000 g for 5 minutes. Supernatant (800 µl) was removed and discarded. The remaining 200 µl of supernatant was used to gently resuspend the cell pellet. Cells were spread onto an LB agar plate (plus antibiotic) and incubated overnight at 37°C. Colonies were counted and picked for plasmid preparation.

### **2.2.j. End-point polymerase chain reaction (PCR)**

Unless otherwise specified, end-point polymerase chain reactions (PCR) were set up using 100  $\mu$ M dNTPs, 1.5-2 mM  $MgCl_2$ , 1  $\mu$ M of each primer and 1 U Platinum® Taq DNA polymerase or Elongase Enzyme Mix (Invitrogen, Carlsbad, CA, USA) in a total reaction volume of 25  $\mu$ l. Thermal cycles were performed in a Corbett Research Palm-Cycler™ (Corbett Research Pty Ltd, NSW, Australia) using the following cycling conditions, denaturation at 94°C for 15 minutes, followed by 30-35 cycles of 94°C denaturation for 1 minute, annealing at 55-65°C for 1 minute and 72°C extension for 2 minutes. A final extension step was performed at 72°C for 15 minutes. The number of amplification cycles and annealing temperature was modified depending on the specific PCR. PCR products were analysed and/or purified by agarose gel electrophoresis (Section 2.2.g.).

Splice-overlap-extension (SOE)-PCR was used to assemble gene constructs. Methods were based on those described previously.<sup>216</sup> Two initial thermal cycles were performed without primers as follows: 92°C for 1 minute, 63°C for 30 seconds, 58°C for 50 seconds and 72°C for 1 minute, with 1:1 molar ratio of each template to be joined. These initial cycles allowed the templates to anneal to each other at their complementary regions. After these initial cycles, 50 pmol of the outer primers were added to amplify the entire spliced construct and the reaction was cycled 35 times as follows: 92°C for minute, 60°C for 30 seconds and 72°C for 1 minute. SOE-PCR reactions included 1.5 mM  $MgCl_2$  and 2 U of Elongase Enzyme Mix (Invitrogen, Carlsbad, CA, USA). Tubes containing template DNA with pairs of internal primers alone served as positive PCR controls. SOE-PCR products were analysed and purified by agarose gel electrophoresis (Section 2.2.g.).



## **2.2.k. Total RNA extraction**

### ***2.2.k.1. Total RNA extraction from cell lines***

Cell monolayers in 9.5 cm<sup>2</sup> wells (on a 6 well plate) were washed in 1 ml phosphate buffered saline (PBS). Cell detachment was achieved by the addition of 500 µl of Trypsin-EDTA (Appendix 1) and cells were incubated for 3 minutes at 37°C. Once cells were detached, 1 ml of 1% fetal calf serum (FCS) in phosphate buffered saline (PBS) was added to neutralise the Trypsin-EDTA. Cells were suspended by gentle pipette mixing and transferred into 1.5 ml tubes. Cells were centrifuged at 3000 g for 5 minutes. The supernatant was removed and the cells were washed in 1 ml PBS. Total cellular RNA was either extracted immediately, or cell pellets were snap-frozen in liquid nitrogen and stored at -80°C until required. Total cellular RNA was isolated from mammalian cells using a QIAshredder and RNeasy Mini Kit (both Qiagen, Hilden, Germany), using the methods described by the manufacturer.

### ***2.2.k.2. Total RNA extraction from rat lymph nodes***

Rats were euthanised by isoflurane overdose and lymph nodes were placed in an autoclaved 1.5 ml screw capped tube using RNaseZap®- (Ambion Applied Biosystems, Austin, Texas, USA), treated forceps, snap frozen in liquid nitrogen and stored at -80°C until required. Frozen lymph nodes were thawed on ice for 20 minutes. Once thawed, lymph nodes were placed in a 10 cm petri dish (Techno-plas, St Marys, SA) and 600 µl of RLT lysis buffer (from Qiagen kit) was added. A disposable 26 G needle and RNaseZap®-treated forceps were used to “tease” out the cells within the lymph node into the RLT lysis buffer. The lysed cells were transferred to a 1.5 ml tube and RNA was extracted using a QIAshredder and RNeasy Mini Kit (both Qiagen, Hilden, Germany) as per the manufacturer’s instructions.

### **2.2.k.3. Total RNA extraction from rat corneas**

Rats were euthanised by isoflurane overdose and corneas were excised using RNaseZap®-treated instruments, placed into autoclaved 1.5 ml screw capped tubes, snap frozen in liquid nitrogen and stored at -80°C until required. Frozen corneas were transferred into autoclaved 2 ml round bottom tubes containing a 5 mm stainless steel bead (Qiagen, Hilden, Germany) and 350 µl of RLT lysis buffer (from Qiagen kit). Tubes were placed in the outermost positions in the TissueLyser (Qiagen, Hilden, Germany) and corneas were homogenised for 3 minutes at 30 Hz. Homogenisation was repeated for 3 minutes at 30 Hz with tubes placed in the innermost positions (rearranging the tubes ensured uniform disruption and homogenisation of samples). RNase-free water (590 µl; from Qiagen kit) and 10 µl of proteinase K (20 mg/ml; Sigma-Aldich Inc, St Louis, MO, USA) was added to each homogenised lysate and mixed thoroughly by pipetting. Lysates were centrifuged for 3 minutes at 10 000 g and the supernatants were transferred to new tubes (being careful not to disrupt the fatty layer on top or the pellet at the bottom). Ethanol (100%; 0.5 volumes) was added to cleared lysates and mixed by pipetting. The RNeasy Mini Kit (Qiagen, Hilden, Germany) was used to extract the RNA from the corneal lysates as per the manufacturer's instructions.

### **2.2.l. DNase I treatment of RNA**

To remove contaminating viral or genomic DNA, total RNA was treated with TURBO DNA-free™ (Ambion Applied Biosystems, Austin, Texas, USA) as described by the manufacturer, prior to reverse transcription. Total RNA (up to 10 µg) was digested with 2 units of TURBO DNase with 0.1 volume of 10X TURBO DNase I buffer and incubated at 37°C for 30 minutes. DNase Inactivation Reagent (0.1 volumes) was added and incubated for 2 minutes at room temperature with

occasional mixing. Tube contents were centrifuged at 13 000 g for 90 seconds at room temperature and then the supernatant was transferred to a fresh autoclaved 0.5 ml tube and stored at -20°C.

### **2.2.m. cDNA synthesis**

The synthesis of cDNA from DNaseI-treated RNA was performed through reverse transcription (RT) using the SuperScript™ III First-Strand Synthesis for RT-PCR (Invitrogen, Carlsbad, CA, USA), using the methods outlined by the manufacturer. In addition, a “non-reverse transcribed” control was prepared for every cDNA synthesis reaction to identify genomic or viral DNA contamination. Oligo dT primer (50 µM) (1 µl) was added to 1.5 µg DNase I-treated RNA in a total volume of 10 µl and incubated at 65°C for 5 minutes. Reactions were placed on ice immediately for at least 1 minute. The following components were added to each reaction, 2 µl 10X RT buffer, 4 µl 25 mM MgCl<sub>2</sub>, 2 µl 0.1 M DTT, 1 µl RNase OUT (40 U/µl) and 1 µl SuperScript III RT (200 U/µl) or 1 µl water (for “non-reverse transcribed” control). Tube contents were gently pipette mixed and incubated at 50°C for 50 minutes. Reactions were terminated by incubating at 85°C for 5 minutes and immediately chilled on ice. RNase H (1 µl; 2 U/µl) was added to the reaction and incubated for 20 minutes at 37°C. The cDNA samples were stored at -20°C until required.

## **2.3 QUANTITATIVE REAL-TIME PCR (QPCR)**

### **2.3.a. Primers for qPCR**

Primers were designed using Primer3 software (Whitehead Institute for Biomedical Research, Cambridge, MA, USA) using the parameters outlined in Table 2.8 and all other parameters were set to default. Primers were designed to cross intron/exon

boundaries and were synthesised by GeneWorks (Thebarton, SA, Australia) at sequencing grade (refer to Table 2.5 for primer sequences).

**Table 2.8: Parameters for qPCR primer design using Primer3**

Parameter	Parameter range		
	Minimum	Optimum	Maximum
Product size (bp)	80	100	120
Primer size (bp)	18	20	24
Primer $T_m$ (°C)	58	60	62
Primer G/C%	30	-	70

PCR, polymerase chain reaction; bp, base pairs;  $T_m$ , melting temperature

### 2.3.b. qPCR set up

All qPCRs were performed on a Rotor-Gene 6000 real-time thermal cycler (Corbett Research, Mortlake, NSW, Australia). Reactions were made up in a 20  $\mu$ l volume, including 10  $\mu$ l QuantiTech™ SYBR green master mix containing hot start Taq DNA polymerase, SYBR Green I, dNTPs and PCR buffer (5 mM MgCl<sub>2</sub>, Tris-Cl, KCl, (NH<sub>4</sub>)<sub>2</sub>SO<sub>4</sub> pH 8.7) (Qiagen, Hilden, Germany), 2  $\mu$ l of sense and antisense primers (0.5  $\mu$ M final concentration) and 6  $\mu$ l cDNA sample diluted 1/100 with Ultra Pure water (Fisher Biotech, West Perth, WA). Reactions underwent the following cycling conditions: initial denaturation (95°C, 15 minutes), 50 cycles of denaturation (94°C, 20 seconds), annealing (47.4°C, 20 seconds), extension (72°C, 30 seconds), final extension (72°C, 4 minutes, followed by 25°C, 5 minutes). A melt profile was performed on all qPCR products ranging from 60-99°C at 0.5°C increments every 5 seconds. A pre-melt conditioning hold was performed at 60°C prior to the first increment. Every cDNA sample was tested in triplicate and a standard cDNA pool was included in triplicate in each qPCR run. A single reverse transcription (RT) control for each sample and two no template (water) controls were included in each qPCR run.

### 2.3.c. Determination of primer pair amplification efficiency

Standard curves were prepared for each primer pair on seven three-fold serial dilutions of a standard cDNA sample, made from a pool of experimental samples from each treatment group and controls. Each dilution of cDNA was run in triplicate in two individual qPCR runs. The mean threshold cycle (Ct) values of the triplicates of each cDNA dilution were plotted as a linear function against the logarithm ( $\log_e$ ) of the cDNA dilution. Primer pair amplification efficiencies were determined using the gradient of the standard curve regression line as seen below.

$$AE = [e^{(1/-g)}]-1 \quad [217]$$

AE is the amplification efficiency (the percentage change in fluorescence per cycle of PCR)

e is Euler's number (where the natural logarithm [ $\log_e$ ] was used to transform cDNA concentration values)

g is the gradient of the standard curve regression line

### 2.3.d. Gene expression analysis

The method used for gene expression analysis was based on the  $\Delta$  Ct method of relative quantification of Livak and Schmittgen.<sup>218</sup> Modifications to this method were based on the quantification algorithm described in the public domain software GeNorm,<sup>219</sup> and allowed for the separation of the normalisation step, which enabled the use of multiple reference (housekeeping) genes and differences in amplification efficiencies of primer pairs.

The delta Ct method of quantification

Step 1:

$$Q = (AE + 1)^{(Cts - CtA)}$$

Q is the relative quantity of each gene.

AE is the amplification efficiency.

Cts is the geometric mean of the standard sample replicates.

CtA is the threshold cycle of a sample of interest

Step 2: Normalisation step

$$X_A = Q/NF$$

$X_A$  is the normalised relative quantity of each gene.

NF is the normalisation factor (the geometric mean of the relative quantities (Q) of the reference genes).

## 2.4 CELL CULTURE METHODS

### 2.4.a. Maintenance of cell lines

A list of cell lines can be found in Table 2.9. HEK-293A, HEK-293T and A549 were cultured in DMEM (5-10% vol/vol FCS) and CHO cells were cultured in HEPES-buffered RPMI (5-10% FCS). Cells were maintained in 75 cm<sup>2</sup> tissue culture flasks (Nunclon, Copenhagen, Denmark). Upon confluency, cells were passaged by washing once in 5 ml PBS and then cells were detached from plastic by incubating in 2 ml Trypsin-EDTA (Appendix 1) for 5 minutes at 37°C. Once cells had detached, 8 ml of fresh medium was added to trypsinised cells to make a single cell suspension and either 1 ml of cells (1:10 split) or 2 ml of cells (1:5 split) was added to a new 75 cm<sup>2</sup> flask containing fresh medium. Cell lines were incubated at 37°C, 5% CO<sub>2</sub> in air.

**Table 2.9: Cell lines**

Designation	Description	Growth	Source
HEK-293A	Human embryonic kidney cell line with E1- region of adenovirus 5	Adherent	Qbiogene Inc, Carlsbad, CA
HEK-293T	Human embryonic kidney cell line that constitutively expresses the SV40 large T cell antigen	Adherent	ATCC, CRL 11269
A549	Human lung adenocarcinoma epithelial cell line	Adherent	ATCC, CCL 185
CHO-K1	Chinese hamster ovary cell line	Adherent	ATCC, CCL-61

---

ATCC, American Type Culture Collection, Manassas, VA, USA

### 2.4.b. Freezing cell lines

Cells were resuspended in growth medium with an additional 50% FCS at a density of  $2 \times 10^7$  cells/ml. An equal volume of 30% dimethyl sulphoxide (DMSO) in growth medium was added dropwise at a rate of 1 ml per minute. Cell were dispensed into freezing vials (1.8 ml, Nunc, Roskilde, Denmark) and frozen slowly in insulated containers kept in the vapour phase of liquid nitrogen overnight, before being placed into liquid nitrogen for long-term storage.

### 2.4.c. Thawing cells

Cells were thawed from liquid nitrogen in a 37°C water bath. An equal volume (approximately 1 ml) of warm growth medium (5-10% FCS) was slowly added dropwise over 10 minutes. A further 10 ml of growth medium was added over 10 minutes. Cells were pelleted (200 g for 5 min), resuspended in growth medium and placed in tissue culture flasks.

#### **2.4.d. Cell viability determinations**

Cell suspensions were diluted and mixed 1:1 with 0.1% Trypan Blue (Appendix 1). After 2 minutes cells were counted in a haemocytometer and viability and cell densities were determined. Non-viable cells were determined by the Trypan Blue staining.

#### **2.4.e. Liposome-mediated transfection of mammalian cells**

The adherent mammalian cells lines HEK-293A and CHO were transfected with recombinant plasmid using Lipofectamine 2000 (Invitrogen, Carlsbad, CA, USA). Transfections were performed in 6 well plates at a confluency of 80% ( $8 \times 10^5$  total cells) in either DMEM (5% FCS) or HEPES-buffered RPMI (5% FCS). Recombinant plasmid DNA (1.6  $\mu\text{g}$ ) was diluted in 200  $\mu\text{l}$  serum-free OptiMEM medium (Life Technologies™ Gibco BRL, Gaithersburg, MD, USA). Lipofectamine (8  $\mu\text{l}$ ) was added to the diluted DNA and incubated for 20 minutes at room temperature. Concurrently, the old medium was aspirated off the cells and 960  $\mu\text{l}$  serum-free OptiMEM medium was added and incubated at 37°C for at least 10 minutes. The Lipofectamine-DNA mix was added drop-wise to the prepared well of cells and incubated at 37°C with 5% CO<sub>2</sub> in air for 6 hours. The Lipofectamine-DNA mix was removed and replaced with 6 ml of DMEM (5% FCS) or HEPES-buffered RPMI (5% FCS) and transfected cells were cultured for up to 7 days at 37°C, 5% CO<sub>2</sub> in air. Expression of eYFP from transfected cells was visualised by fluorescence microscopy (Section 2.4.i.) and quantified using flow cytometry (Section 2.4.h.). Culture medium from transfected cells was collected and the presence of the secreted products, anti-rat CD4 scFv and EK5 was performed using flow cytometry (Section 2.4.g.1.) and ELISA (Section 2.4.j.) respectively.



#### **2.4.f. Transduction of mammalian cells with lentiviral vectors**

The adherent cells line HEK293A was transduced with lentiviral vectors. Transductions were performed in 6 well plates at a confluency of 30-40% ( $6.25 \times 10^5$  total cells) in DMEM (5% FCS). Cells were transduced at a multiplicity of infection (MOI) of 5, which equates to  $3.13 \times 10^5$  transducing units (TU)/well. Transductions were performed for 24 hours at 37°C, 5% CO<sub>2</sub> in air. After this time, the transduction medium was removed and replaced with fresh DMEM (5% FCS). The transduced cells were cultured for 5 days at 37°C, 5% CO<sub>2</sub> in air. Expression of eYFP from transduced cells was visualised by fluorescence microscopy (Section 2.4.i.) and quantified using flow cytometry (Section 2.4.h.). Culture medium from transduced cells was collected and the presence of the secreted product, anti-rat CD4 scFv, was performed using flow cytometry (Section 2.4.g.1).

#### **2.4.g. Flow cytometry to detect scFv binding**

##### ***2.4.g.1. ScFv detection in culture supernatant and rat plasma***

Histidine-tagged anti-rat CD4 scFv in cell culture medium, corneal organ culture medium or rat plasma was detected by flow cytometry following binding to CD4-positive thymocytes. The thymus from a <12 week old rat was collected and placed in 20 ml of PBS. Cells were scraped from the thymus in a laminar flow hood using an 18G needle and forceps in a 10 cm petri dish (Techno-plas, St Marys, SA). Cells and PBS in the 10 cm Petri dish were transferred into a 25 ml v-bottomed tube and the dish was washed with an extra 10 ml PBS to collect as many cells as possible. The cell suspension (6 ml) was transferred into a 30 ml flat-bottomed tube and 20 ml Lymphoprep™ (Axis-Shield, PoC AS, Oslo, Norway) (prepared for rat cells by adding 5 ml Angiografín® (Schering, AG, Germany ) to 100 ml Lymphoprep) was added under the cell suspension using a 20 ml syringe and a mixing cannula.

Lymphoprep<sup>TM</sup>-treated cells were centrifuged at 800 g for 20 minutes at 4°C. Thymocytes were collected at the medium/lymphoprep interface and placed into a 25 ml v-bottomed tube. Thymocytes were washed in 20 ml ice-cold PBS-azide (Appendix 1) and centrifuged at 800 g for 10 minutes at 4°C. Supernatant was removed and discarded and cells were resuspended in 10 ml PBS-azide and mixed by inversion. The cells were counted using a haemocytometer and diluted to a concentration of  $2 \times 10^7$  cells/ml.

To each tube,  $1 \times 10^6$  cells (50 µl of diluted cells suspension) was added. Supernatant and control antibodies were added to the thymocytes and mixed by brief vortexing followed by a 30 minute incubation on ice. Cells were washed in 3 ml PBS-azide and centrifuged at 500 g for 5 minutes at 4°C. Supernatant was aspirated using suction. Primary antibody, 50 µl anti-polyhistidine (Sigma-Aldich Inc, St Louis, MO, USA) was diluted 1/250 in PBS-azide and was added to each tube and incubated for 30 minutes at 4°C. Cells were washed as above and incubated with 50 µl of secondary biotinlyated goat anti-mouse antibody (DakoCytomation, Glostrup, Denmark) (diluted 1/100 in PBS-azide) for 30 minutes at 4°C. Thymocytes were washed as above and incubated with 50 µl of Streptavidin R-phycoerythrin conjugate (SAPE) (Molecular Probes, Eugene, Oregon, USA) (diluted 1/100 in PBS-azide) for 30 minutes at 4°C. Thymocytes were washed as above, resuspended in 50 µl FACS fixative (Appendix 1) and stored at 4°C until analysis at the FACScan using Cell-Quest software v3.01f (Becton Dickinson, Franklin Lakes, NJ, USA).

#### **2.4.g.2. ScFv detection on rat peripheral blood lymphocytes (PBL)**

Bound anti-rat CD4 scFv was detected on peripheral blood lymphocytes (PBL) through the HIS6 tag using flow cytometry. Primary antibody, 50 µl anti-polyhistidine (Sigma-Aldrich Inc, St Louis, MO, USA) was diluted 1/250 in PBS-azide and was added to each tube containing whole blood cells (50 µl) and incubated for 30 minutes on ice. Whole blood cells were washed in 3 ml PBS-azide and centrifuged at 500 g for 5 minutes at 4°C. Supernatant was aspirated using suction. Secondary antibody, biotinylated goat anti-mouse antibody (DakoCytomation, Glostrup, Denmark) (diluted 1/100 in PBS-azide) was added to each tube containing whole blood cells and incubated for 30 minutes on ice. Whole blood cells were washed as above and incubated with 50 µl of SAPE (Molecular Probes, Eugene, Oregon, USA) (diluted 1/100 in PBS-azide) for 30 minutes on ice. Red blood cells (RBC) were lysed by the addition of 3 ml RBC lysis solution (Appendix 1) and incubated for 10 minutes at room temperature. Cells were centrifuged at 500 g for 5 minutes, washed in 3 ml PBS-azide, resuspended in 50 µl FACS fixative (Appendix 1) and stored at 4°C until analysis at the FACScan using Cell-Quest software v3.01f.

#### **2.4.h. Flow cytometry for eYFP detection in transfected or transduced cells**

Flow cytometry was used to detect eYFP expression from transfected or transduced cells. After 5 days in culture, transduced cells were trypsinised, transferred to a 10 ml FACS tube and washed in 2.5 ml 1% FCS in PBS (to neutralise the trypsin). Cells were centrifuged at 500 g for 3 minutes and the supernatant was aspirated. Cells were washed in 3 ml PBS, centrifuged at 500 g for 3 minutes and the supernatant was aspirated. Cells were resuspended in 100 µl of fluorescence-activated cell sorting

(FACS) fixative (Appendix 1) and stored at 4°C until analysis at the FACScan using Cell-Quest software v3.01f.

#### **2.4.i. Fluorescence microscopy of cell lines**

Fluorescence imaging of adherent cell lines was performed using the IX71 fluorescence inverted microscope (Olympus Optical Co., Japan). Images were taken in 5 central fields within the 9.5 cm<sup>2</sup> well (in a 6 well plate) using brightfield light (to visualise all cells) and blue light (to visualise eYFP expressing cells). Images were taken using the F-view digital camera and AnalySIS® getIT Software Imaging System (Olympus Soft Imaging Solutions GmbH, Münster, Germany). Filter cube specifications for the IX71 fluorescence inverted microscope can be found in Table 2.7.

#### **2.4.j. Human endostatin::kringle-5 (EK5) detection in culture supernatant by ELISA**

A commercially available human endostatin ELISA Kit (R&D Systems, Minneapolis, MN, USA) was used to detect EK5 in the culture supernatant of transfected cells as per the manufacturer's instructions.

#### **2.4.k. Determination of endotoxin levels in viral preparations**

Endotoxin levels were determined in adenoviral and lentiviral vector preparations using the commercially available Limulus Amebocyte Lysate assay (BioWhittaker, Walkersville, MD, USA) as per the manufacturer's instructions. The sensitivity of the assay was 0.06 endotoxin units (EU)/ml (or 6 pg/ml). Samples (10 µl) were diluted in a total volume of 100 µl, enabling the test to detect 0.6 EU/ml (60 pg/ml)

in the original sample. Water for irrigation (Baxter, Old Toongabbie, NSW, Australia) was used as the negative control and to prepare dilutions.

## **2.5 LENTIVIRAL VECTOR PRODUCTION AND TESTING**

Lentiviral vectors were produced at the Gene Technology Unit, Dept of Genetic Medicine, Women's and Children's Hospital, Adelaide, SA, using methods based on those previously described.<sup>195-197</sup> All procedures involving production and use of lentivirus were conducted with approval of the institutional Biosafety Committee of Flinders University and the Office of the Gene Technology Regulator in a PC2 containment laboratory.

### **2.5.a. Large scale lentiviral vector preparations**

To produce approximately 3 ml of purified, concentrated lentiviral vector stock, HEK-293T (SD3515, American Type Collection, Manassas, VA, USA) cells were seeded on 20 x 245 mm<sup>2</sup> plates (Corning Incorporated, Corning, NY, USA) at a density of  $3.75 \times 10^5$  cells/ml in 105 ml of DMEM (5% FCS) per plate. Transfection of HEK-293T cells was performed by calcium phosphate co-precipitation. This involved the use of 4 helper plasmids: pHCMV-G (encoding vesicular stomatitis virus glycoprotein G), pcDNA3tat101ml (encoding HIV-1 Tat), pHCMVwhvrevml (encoding HIV-1 Rev), and pHCMVwhvgagpolml (encoding HIV-1 GagPol), as well as a transfer construct carrying the transgene of interest. Cells were transfected using the ratios shown in Table 2.10.

**Table 2.10: Lentiviral plasmid ratios for transfection of HEK-293T cells**

Plasmid	Amount of DNA per plate* ( $\mu\text{g}$ )
Transfer construct	158
pcDNA3.1tat101ml	3.16
pHCMVwhvrevml	3.16
pHCMVwhvgagpolml	15.8
pHCMV-G	7.9

\* Calculated for a 245 mm<sup>2</sup> plate with  $4 \times 10^7$  cells in total.

All solutions were used at room temperature. Transfection was performed by adding one volume (6.5 ml) of DNA/2.5 M CaCl<sub>2</sub> solution to one volume of 2 x HEPES-buffered saline (HeBS) (6.5 ml) over 5 seconds, while vortexing. This DNA/CaCl<sub>2</sub>-HeBS mixture was further vortexed for 20 seconds and then left to sit at room temperature for another 90 seconds before being gently poured onto the cells at the plate edge, being careful not to disturb the cell monolayer. This procedure was repeated until all plates had been through this process. Plates were incubated at 37°C, 5% CO<sub>2</sub> in air for 8 hours. After this incubation, the medium was replaced with 170 ml of Opti-pro serum free medium (Invitrogen, Carlsbad, CA, USA) per plate, being careful not to disturb cells. After a 40 hour incubation at 37°C, 5% CO<sub>2</sub> in air, all 3400 ml of supernatant was harvested from the 20 plates. Supernatant was filtered through a 0.45  $\mu\text{m}$  hollow fibre cartridge (CFP-4-E-4MA, Amersham Biosciences Corporation Piscataway, NJ, USA) at room temperature using the QuixStand™ bench top system (Amersham Biosciences Corporation, Piscataway, NJ, USA). The filtrate was concentrated to 150 ml with a 750 kDA cut-off hollow fibre ultrafiltration cartridge (UFP-750-E-4x2MA; Amersham Biosciences Corporation, Piscataway, NJ, USA) using the QuixStand™ benchtop system at room temperature. The retentate was passed through a 0.8  $\mu\text{m}$  syringe filter unit (Millex-AA, Millipore,

Carrigtwohill, Co. Cork, Ireland) before ultracentrifugation at 50 000 g for 90 minutes (using a SW32 Ti rotor in a Beckman ultracentrifuge; Beckman Coulter Inc, Fullerton, CA, USA) at 4°C. The lentiviral pellet was gently resuspended in 3 ml ophthalmic balanced salt solution (BSS) (Cytosol, Ophthalmics, Lenoir, NC, USA) and filtered through 0.45 µm filter (Minisart, Sartorius AG, Goettingen, Germany). The purified, concentrated lentiviral vector preparation was distributed into 27 µl aliquots and stored at -80°C until required.

### **2.5.b. Medium scale lentiviral vector preparations**

To produce approximately 500 µl of purified concentrated lentiviral stock, HEK-293T cells were seeded at  $3.75 \times 10^5$  cells/ml in 105 ml DMEM (5% FCS) on 5 x 245 mm<sup>2</sup> plates and incubated for 20-24 hours at 37°C, 5% CO<sub>2</sub> in air. Transfection was performed by calcium phosphate precipitation as described in Section 2.4.a., and incubated for 40 hours at 37°C, 5% CO<sub>2</sub> in air. Supernatant (850 ml) was harvested and filtered through a 0.45 µm Polydisc™ TF filter device (Whatman, Kent, England, UK) at room temperature. Filtrate was concentrated to approximately 50 ml volume using the 750 kDa hollow fibre cartridge (UFP-750-E-4X2MA) at room temperature. Retentate was passed through a series of filters of pore size 5 µm, 1.2 µm and 0.8 µm (Millex-AA, Millipore, Carrigtwohill, Cork, Ireland) to further filter the lentiviral solution, which was ultracentrifuged at 50 000 g for 90 minutes (using a SW32 Ti rotor in a Beckman ultracentrifuge; Beckman Coulter Inc, Fullerton, CA, USA) at 4°C. The lentiviral pellet was gently resuspended in 500 µl ophthalmic BSS. The purified, concentrated lentiviral vector preparation was put through a 0.45 µm filter and 27 µl aliquots were distributed and stored at -80°C.

### **2.5.c. Detection of replication-competent lentivirus**

Detection of replication-competent viral particles in concentrated lentiviral vector preparations was performed by quantifying the level of p24 (HIV-1 Gag protein) in the culture medium of HEK-293T cells transduced with lentivirus. If no replication-competent lentiviral particles were present, then the level of p24 dropped over several days after the initial transduction. HEK-293T cells were seeded at  $5 \times 10^5$  cells per well in DMEM (10%) in a 12 well plate. Cells were left for 4 hours at 37°C, 5% CO<sub>2</sub> to adhere to the plastic, and once attached, the medium was replaced with 1 ml per well of DMEM (10% FCS) supplemented with 4 µg/ml polybrene (Sigma, St Louis, MO, USA) and 50 µg/ml gentamicin (Sigma). Lentiviral vector (1 µl) was added to triplicate wells and three wells were left untransduced as controls. Cells were incubated at 37°C, 5% CO<sub>2</sub> in air. After 24 hours, the medium was replaced with fresh 1 ml DMEM (10% FCS) with 50 µg/ml gentamicin (Sigma, St Louis, MO, USA). Cells were split 1:10 every three days and 1 ml of supernatant was collected on days 6 and 12 and stored at -80°C. Culture supernatants collected on day 6 and 12 from the transduced and untransduced HEK-293T cells were tested in a commercially available ELISA for the HIV p24 protein (PerkinElmer, Boston, MA, USA). A lentiviral vector preparation was judged to be free of replication-competent lentiviral particles if p24 levels declined to levels comparable to untransduced controls after 12 days of culture, indicating the absence of significant virus replication in the culture.

### **2.5.d. Titration of lentiviral vector preparations**

A549 cells (CCL-185, American Type Culture Collection) were seeded at  $2.5 \times 10^5$  cells/well in DMEM (10% FCS) in a 24 well plate. Cells were left to attach to plastic for 3 hours at 37°C, 5% CO<sub>2</sub> in air. Once attached, the medium was replaced with 0.5



ml per well of DMEM (10% FCS) supplemented with 4 µg/ml polybrene and 50 µg/ml gentamicin. Two different doses of lentiviral vector were added to triplicate wells: a high dose (0.5 µl) and low dose (0.1 µl), and three wells were left untransduced as controls. Cells were incubated at 37°C, 5% CO<sub>2</sub> in air. After 24 hours, the medium was replaced with fresh 0.5 ml DMEM (10% FCS) with 50 µg/ml gentamicin. Cells were split 1:4 every 48 hours, were harvested after 5 days and cell culture continued for a total of 4 weeks, when a second cell harvest was performed. Titration of lentiviral vectors was performed by reporter gene (eYFP) quantification using flow cytometry (Section 2.5.d.1.) or by proviral DNA integration using real-time PCR (qPCR) (Section 2.5.d.2.).

#### ***2.5.d.1. Reporter gene (eYFP) titration of lentiviral vector preparations***

Flow cytometry was used to determine the viral titre of lentiviral vectors that expressed eYFP. Cells were harvested by washing in 0.5 ml PBS and then trypsinised in 200 µl Trypsin-EDTA (Appendix 1). Detached cells were transferred to a 5 ml FACS tube (Falcon®, Becton Dickinson Labware, Franklin Lakes, NJ, USA) containing 1% FCS in PBS. Tubes were centrifuged at 800 g for 5 minutes and supernatant was aspirated. PBS (1 ml) was added to tubes which were centrifuged at 800 g for 5 minutes and supernatant was aspirated. FACS fixative (100 µl) (Appendix 1) was added to each tube. EYFP fluorescence was analysed from transduced cells using the FACScan and results were analysed using the Cell-Quest software v3.01f. Untransduced cells were used as a background control. The corrected percentage of eYFP positive cells in the lentivirus-transduced sample was calculated as the percentage of eYFP positive cells in the transduced cells minus the average percentage of positives in the untransduced control cells. The viral titre was determined by multiplying the corrected percentage of positive cells by the number

of cells plated and corrected for the amount of virus added. The calculation of viral titre using flow cytometric analysis is shown below.

$$\begin{aligned} & \text{A549 eYFP viral titre in transducing units (TU)/ml} \\ & = ((2.5 \times 10^5 \text{ cells} \times (\text{transduced \% gated} - \text{untransduced \% gated}) / 100 \times \\ & 1000) / \mu\text{l of lentivirus added per well.} \end{aligned}$$

#### ***2.5.d.2. Titration of lentiviral vector preparations by quantifying proviral integration***

The proviral integration qPCR viral titre assay was used to titrate lentiviral vectors in the absence of eYFP. This assay detects the beginning of the gag sequence in the lentiviral vector (as seen in Figure 3.9). Cells were washed in 0.5 ml PBS and then trypsinised using 200  $\mu\text{l}$  Trypsin-EDTA (Appendix 1). Once cells had detached, they were transferred to a 10 ml tube (Sarstedt Australia Pty Ltd-Technology Park, Adelaide, SA, Australia) containing 2.5 ml 1% FCS in PBS. Cells were centrifuged at 800 g for 5 minutes and the supernatant was aspirated. PBS (3 ml) was added to cells which were centrifuged again at 800 g for 5 minutes and the supernatant was aspirated. Genomic DNA (gDNA) was isolated from cells using the Wizard® SV Genomic DNA Purification System (Promega Corporation, Madison, WI, USA) as per the manufacturer's instructions. GDNA was stored at  $-80^{\circ}\text{C}$  until required. Primers were designed to detect the gag sequence and human transferrin (housekeeper gene) (Table 2.5). Each qPCR reaction contained 20  $\mu\text{M}$  of forward and reverse primers and 10  $\mu\text{l}$  Quantitect™ SYBR Green PCR master mix containing hot start Taq DNA polymerase, SYBR Green I, dNTPs and PCR buffer (5 mM  $\text{MgCl}_2$ , Tris-Cl, KCl,  $(\text{NH}_4)_2\text{SO}_4$ , pH 8.7) (Qiagen, Hilden, Germany). Each assay included standards (gDNA isolated from A549 cells which contained 1 copy of the

viral genome per cell) and no template controls in triplicate for each gene. QPCR was performed using a Rotor-Gene™ 6000 real time thermal cycler (Corbett Life Science, Mortlake, NSW, Australia) under the following conditions: 50°C for 2 minutes, 95°C for 10 minutes followed by 40 cycles of 95°C for 15 seconds and 60°C for 1 minute. The fluorescence of each reaction was read at the end of each cycle. The data was analysed using the Rotor-Gene™ 6000 Series Software 1.7 (Corbett Life Science, Mortlake, NSW, Australia). The threshold bar was placed in the linear part of the plot and the Ct for each sample was determined. The calculations used to determine the viral titre using qPCR can be seen below.

$$\Delta Ct = Ct \text{ gag} - Ct \text{ transferrin (housekeeper gene)}$$

$$\Delta\Delta Ct = \Delta Ct \text{ of sample} - \text{average } \Delta Ct \text{ of standard}$$

$$\text{Copy number per cell} = 1/2^{\Delta\Delta Ct}$$

$$\text{Titre} = (\text{copy number per cell} \times \text{number of cells initially plated} \times 1000) / \text{volume assayed} (\mu\text{l})$$

## 2.6 ADENOVIRAL VECTOR PREPARATION

### 2.6.a. Adenoviral vector production

Dr Claire Jessup (Department of Ophthalmology, Flinders University, Bedford Park, SA) constructed fHSSOX38scFv in pAdtrackCMV (Table 2.3), which was used to make a replication-deficient E1-, E3- deleted serotype 5 adenovirus encoding anti-rat CD4 scFv with a fHSS and polyhistidine tag under cytomegalovirus immediate early promoter (CMV) control. This construct also encoded enhanced green fluorescence protein (eGFP) which was controlled under a separate CMV promoter.<sup>220</sup> Ms Lauren Mortimer (Department of Ophthalmology, Flinders University, Bedford Park, SA) performed all adenoviral vector production and purification in this project, using methods based on those previously described.<sup>221-222</sup>

Three rounds of twenty flasks (75 cm<sup>2</sup>) were infected with 2 ml of passage 3 crude adenoviral lysate (0.5 ml passage 3 in 39.5 ml DMEM (5% FCS) into 20 flasks). Cells were harvested when most were displaying cytopathic effects (CPE), usually between 1-5 days. Cells were scraped from each flask using a rubber policeman and centrifuged at 600 g for 5 minutes. The supernatant was poured off and cells were resuspended in a total of 3 ml of the supernatant that had been poured off immediately prior.

Adenovirus was released from the cell suspension by 5 rounds of freeze thawing. This was performed by pooling cells into a 50 ml tube, snap freezing for 30 seconds and thawing in a 37°C water bath for 3 minutes, with vigorous vortexing for 10 seconds after 2 minutes and again once cells had thawed. The adenoviral lysate was stored at -80°C until required.

The crude adenoviral lysate was purified using the ViraBind™ Adenovirus Purification Kit (Cell Biolabs Inc, San Diego, CA, USA) as per the manufacturer's instructions. Briefly, viral lysates were thawed and all three rounds were pooled and made up to 20 ml with fresh DMEM (5% FCS). Viral lysate was centrifuged at 3000 g for 10 minutes at room temperature. The viral lysate was passed through a glass fibre prefilter (Millipore, Carrigtwohill, Cork, Ireland) assembled on top of a 0.22 µm stericup unit (Millipore, Carrigtwohill, Co. Cork, Ireland), attached to a vacuum source. Benzonase (50 µl at 25 U/µl; Novagen; EMD Chemicals Inc; Merck KGaA, Darmstadt, Germany) was mixed with lysate and incubated at 37°C for 30 minutes. The ViraBind™ adenovirus purification filter was washed with 5 ml 1 x wash buffer by gravity flow. The flow-through was passed over the filter again, with gentle pressure applied to the syringe. The filter was washed with 10 ml 1 x wash buffer

and repeated twice for a total of three times. Adenovirus was eluted with 2 ml 1 x elution buffer. Purified adenovirus was dialysed using a 2 ml Slide-A-Lyzer® dialysis cassette (10 kDa membrane; Thermo Scientific; Pierce Biotechnology, Rockford, IL, USA) against 5 changes of 500 ml endotoxin low HeBS (Appendix 1), at 4°C over 18-24 hours. Purified adenovirus was filter sterilised using a 0.22 µm, 13 mm disposable low protein binding filter (Millipore, Carrigtwohill, Cork, Ireland) and stored at -80°C in 55 µl aliquots until required.

### 2.6.b. Titration of adenoviral vector preparations

The titre of adenoviral vector preparations was determined using the tissue culture infectious dose method (TCID<sub>50</sub>) which has been previously described.<sup>220-221,223</sup> HEK-293A cells (10<sup>4</sup> cells/well) were plated in 96 well flat-bottomed plates (Nunc, Roskilde, Denmark). Ten fold dilutions of adenovirus in DMEM (2% FCS) were added into wells with 100 µl added per well, and 10 wells per dilution. Plates were incubated at 37°C and 5% CO<sub>2</sub> in air for 10 days. Wells were scored for eGFP expression. The test was deemed valid if all of the wells containing the most concentrated adenovirus dilution were positive and all of the wells containing the least concentrated adenovirus dilution were negative. A well was scored positive even if there was only one isolated patch or a few cells that showed eGFP expression. Adenoviral titres were calculated using the equation below (based on Poisson distribution) and expressed in plaque forming units (pfu)/ml.

$$\text{Adenoviral titre* (pfu/ml)} = 10^{s+0.8}$$

s = sum of percentages of positive wells per virus dilution

\*Duplicates should be within 0.7 log of each other.<sup>223</sup>

## **2.7 ANIMAL AND TISSUE METHODS**

### **2.7.a. Conventional histology**

Tissue samples were fixed in buffered formalin (Appendix 1) for at least 24 hours prior to processing. Tissue samples were dehydrated in 70% ethanol for 1 hour, 90% ethanol for 1 hour and 100 % ethanol (3 x 30 minute washes). Tissue was placed in chloroform for 18 hours then melted wax (Paraplast tissue embedding medium, TycoHealthcare Group, Mansfield MA, USA) for 45 minutes at 37°C. Tissue samples were transferred to fresh melted wax under vacuum at 37°C and this was repeated once more before tissue samples were embedded in wax blocks. Sections (5 µm) were cut at the microtome (Lieca RM2/35, Leica Microsystems, Gladesville, NSW, Australia) and mounted onto chrome-alum subbed microscope slides (Appendix 1). Slides were cleared in xylene (2 x 4 minutes) and hydrated in 100% ethanol (2 x 2 minutes), 90% ethanol (2 minutes) and 70% ethanol (2 minutes) before being rinsed in DDH<sub>2</sub>O. Slides were stained in haematoxylin (Appendix 1) for 10 minutes and rinsed in tap water for 1 minute. Sections were dipped in lithium carbonate solution and rinsed in de-ionised water before being stained with eosin (Appendix 1) for 2 minutes and washed in tap water for 1 minute. Sections were dehydrated in 100% ethanol (three brief washes), cleared in xylene (2 x 2 minutes) and mounted in DePex mounting medium (BDH Laboratory Supplies, Poole, UK).

### **2.7.b. Nuclear staining of tissues**

All nuclear staining of tissues was performed using Hoechst 33258 dye (Sigma, St Louis, MO, USA) diluted to 10 µg/ml in BSS immediately prior to use. Staining was performed at room temperature in the dark.

### **2.7.b.1. Nuclear staining of corneal flatmounts**

Corneas were fixed in ice cold buffered formalin for 10 minutes and rinsed twice in PBS prior to staining. Hoechst 33258 (10 µg/ml at 100 µl) was added to corneas for 30 minutes at room temperature in the dark, followed by two washes in PBS. Corneas were flatmounted endothelium up, in Bartels Buffered Glycerol Mounting Medium (Trinity Biotech PLC, Bray, Wicklow, Ireland) onto chrome-alum subbed microscope slides. Four small incisions were made at the scleral edge to lay the cornea flat on the slide. Weight was applied to the coverslip overnight to flatten corneas. Cell nuclei were observed using a fluorescence microscope.

### **2.7.b.2. Nuclear staining of whole globes**

Whole globes were pricked at scleral/corneal border and placed in ice cold buffered formalin for 20 minutes. The cornea, iris and retina were stained separately with Hoechst 33258 (100 µl at 10 µg/ml) for 30 minutes at room temperature in the dark and washed twice in PBS and flatmounted onto chrome-alum subbed microscope slides in Bartels Buffered Glycerol Mounting Medium. Incisions were made in corneal and retinal flatmounts to flatten the preparations. Cell nuclei were observed using fluorescence microscopy.

### **2.7.c. Fluorescence microscopy of rat tissues**

Flatmounted tissue was examined at the fluorescence microscope (BX50, Olympus Optical Co., Japan) using a digital camera (CoolSNAP high resolution cooled CCD, 1.0X tube) and image analysis software (AnalySIS® FIVE, Software Imaging System; Olympus Soft Imaging Solutions GmbH, Münster, Germany). Fields were examined under blue light (for detection of eYFP and eGFP positive cells) and UV light (for detection of Hoechst 33258-stained nuclei). Viral transduction efficiency

into corneal cells was calculated from five central fields (each 0.15 mm<sup>2</sup>) and expressed as the percentage of eYFP or eGFP positive cells divided by total the number of endothelial cells. Filter cube specifications for the BX50 fluorescence microscope can be found in Table 2.7.

#### **2.7.d. Transduction of rat tissues with viral vectors**

##### ***2.7.d.1. Ex vivo transduction of the rat cornea with viral vectors***

HEPES-buffered RPMI (Appendix 1) was used for all corneal organ culture and, unless otherwise stated, media were supplemented with penicillin (100 IU/ml), streptomycin (100 µg/ml) and L-glutamine (2 µM) (all from Gibco GRL, Gaithersburg, MD, USA). L-glutamine was replenished every 14 days.

The donor rat was euthanised by inhalation anaesthetic overdose (active constituent: isoflurane 1 ml/ml, Veterinary Companies of Australia Pty Ltd, Kings Park, NSW, Australia). Globes were removed and decontaminated in 10% w/v povidine-iodine (Faulding Pharmaceuticals, Salisbury, SA) for 2 minutes. Globes were rinsed twice in ophthalmic BSS. Under aseptic conditions and using a dissecting microscope, corneas were dissected using Vannas scissors with a 1-2 mm scleral rim. The iris was detached from the cornea by running fine smooth-tipped forceps around the scleral rim, while the holding the scleral edge with toothed forceps. Corneas were placed in HEPES-buffered RPMI (2% FCS) before being transferred to a round-bottom 96 well plate (Nunc, Roskilde, Denmark), endothelium up. HEPES-buffered RPMI (2% FCS) (100 µl) containing either a lentiviral vector ( $2.5 \times 10^7$  TU/cornea) or an adenoviral vector ( $2 \times 10^7$  pfu/ml) was added dropwise to the cornea and incubated for 3 hours at 37°C, 5% CO<sub>2</sub> in air. Corneas to be used for transplantation were washed twice in HEPES-buffered RPMI (without serum or L-glutamine) and rinsed



in ophthalmic BSS  $\leq 10$  minutes prior to transplantation into a recipient rat. Corneas that were used only for culture, as well as rims from corneas used for transplantation, were placed in 2 ml HEPES-buffered RPMI (10% FCS) supplemented with 2.5  $\mu\text{g/ml}$  amphotericin B (Amphostat, Thermo Electron, Melbourne, Vic, Australia) in a 24 well plate. Corneas were cultured for up to 10 days at 37°C, 5% CO<sub>2</sub> in air, with a medium change every 48-72 hours.

#### ***2.7.d.2. Anterior chamber injection of virus into the rat eye***

Rats were placed in an isoflurane nose cone (2.5-3% oxygen). The left eye was taped to prevent drying. A drop of Ophthetic© local anaesthetic (ophthaine; Allergen Australia Pty Ltd, French Forest, NSW, Australia) was applied to the right eye for 1 minute and a drop of Mydriacyl© (10 mg/ml tropicamide; Abbott Laboratories, North Chicago, IL, USA) was added to dilute the pupil. A 4.0 silk suture (No. S405; Dynek Pty Ltd, London, UK) was threaded through the conjunctiva at 12 o'clock and 6 o'clock and artery forceps were attached to proptose the eye. A drop of Neosynephrine© (Abbott Laboratories, North Chicago, IL, USA) was added for 1 minute to further dilate the pupil and was rinsed away thoroughly with ophthalmic BSS. A detached 31G non-coring needle (Hamilton Co., Reno, Nevada, USA) was used to make a full thickness paracentesis at 12 o'clock, being careful to avoid the iris and lens. Conjunctival sutures were removed to release pressure in the eye. A 36G non-coring needle attached to a 10  $\mu\text{l}$  syringe (Hamilton Co., Reno, Nevada, USA) was used to slowly inject 5  $\mu\text{l}$  of virus into the anterior chamber at 6 o'clock, avoiding the iris and lens. Once the virus had been injected, the needle was left in the anterior chamber for 30 seconds before removing. Chloromycetin (1%; Park Davies, NSW, Australia) was applied to the eye which was sutured closed using 10-0 nylon sutures (No. 9005G; Ethicon Inc, Somerville, NJ, USA) for 24 hours.

### **2.7.d.3. Intranodal injection of virus into the rat**

Rats were placed in an isoflurane nose cone (2.5-3% oxygen). The fur underneath the chin was clipped and the area was decontaminated with 10% w/v povidone-iodine. An incision was made under the chin using a scalpel to expose the cervical (superficial cervical and facial) lymph nodes (Figure 2.1). A 31G non-coring needle attached to a 10 µl syringe was used to slowly inject 5 µl of virus into each of the exposed cervical lymph nodes (usually 4-6 nodes). The needle was left in place for 30 seconds before removing carefully. The wound was closed with 4-5 disposable tissue staples (Royal 35W disposable skin stapler; United States Surgical Corporation, Norwalk, ST, USA).

### **2.7.e. Rat orthotopic corneal transplantation**

Mrs Kirsty Kirk (Department of Ophthalmology, Flinders University, Bedford Park, SA, Australia) performed all orthotopic rat corneal grafts. Recipient rats were adult male Fischer 344 (F344) (RT<sup>lv1</sup>). Allograft corneal donors were adult male Wistar Furth (WF) (RT<sup>lu</sup>) and isografts corneal donors were adult male F344 rats. The methods used for rat orthotopic corneal transplantation were based on those previously described.<sup>18</sup> Only the right eye of each recipient rat was used for transplantation. As described in Section 2.7.d.1., corneas that had been treated with virus were washed twice in HEPES-buffered RPMI (without serum or L-glutamine) and placed in ophthalmic BSS for  $\leq$  10 minutes prior to transplantation. The donor cornea was placed endothelium up (to prevent endothelial damage) on a sterile Teflon block. A 3.1 mm trephine was used to punch the central corneal button and Vannas scissors were used to complete the dissection. The donor button was kept moist in ophthalmic BSS while the recipient eye was being prepared. The recipient

rat was anaesthetised with isoflurane inhalation anaesthetic delivered with a nose cone (2.5-3% in oxygen). The left eye was taped to prevent drying. A drop of Ophthetic© local anaesthetic was applied to the right eye for 1 minute and a drop of Mydriacyl© (10 mg/ml tropicamide) was added to dilute the pupil. A 4.0 silk suture (No. S405) was threaded through the conjunctiva at 12 o'clock and 6 o'clock and artery forceps were attached to proptose the eye. A drop of Neosynephrine© was added for 1 minute to further dilate the pupil and was rinsed thoroughly with ophthalmic balanced salt solution. A 2.9 mm trephine (to slightly undersize the graft bed) was used to cut a partial thickness disc on the recipient cornea. A diamond knife was used to complete the initial full thickness incision. The dissection was completed using Vannas scissors and the recipient button was removed. The donor button was transferred endothelium down to the recipient bed and eight interrupted sutures (10-0 nylon) were used to hold the graft in place.

#### **2.7.f. Post-operative assessment of corneal grafts**

Rats were examined daily under the operating microscope and grafted eyes were scored for clarity, corneal neovascularisation and inflammation on a 0-4 numerical scale with 0.1 increments. Corneal graft clarity was used to determine graft failure. Grafts were deemed transplant failures if they had clarity scores  $\geq 2.0$  (graft obscuring observation of iris vessels). Corneal grafts that did not reach a clarity score of  $\leq 1.5$  by day 7 were classified as technical failures. Other reasons for technical failure included the development of cataract or severe intraocular bleeding. The technical failure rate was 4% for all corneal grafts performed in this study. Failure of corneal allografts that had previously been clear were regarded as rejected. After rejection or after 60 days (for isografts or long-surviving allografts), rats were euthanised by isoflurane overdose. Eyes were removed and processed for

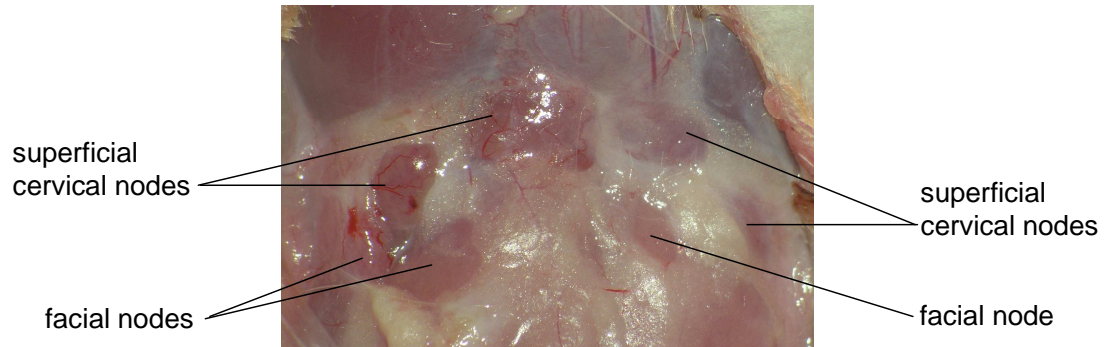


**Figure 2.1: The superficial cervical and facial lymph nodes in the rat.**

Named as reported by Tilney.<sup>105</sup>

conventional histology (Section 2.7.a.) or corneas were snap frozen in liquid nitrogen and stored at  $-80^{\circ}\text{C}$  for RNA extraction (Section 2.2.k.3).

### **2.7.g. Collection of rat blood by tail tipping**

Rats were placed on an electric heating pad (A.E.M. Co. Pty. Ltd., Sydney, NSW, Australia) and anaesthetised using isoflurane inhalation anaesthetic delivered with a nose cone (2.5-3% in oxygen). A scalpel was used to cut 10 mm off the end of the tail, and plastic-clad heparinised microhaematocrit tubes (Becton Dickinson, Franklin Lakes, NJ, USA) were used to collect approximately 500  $\mu\text{l}$  of blood into a lithium heparin tube (12.5 IU per tube; Termumo Medical Corporation, Elkton, MD, USA) containing 500  $\mu\text{l}$  of PBS-azide-heparin (10 units/ml). Heparinised blood samples were immediately mixed by inversion and centrifuged at 2500 g for 5 minutes. Plasma was collected and transferred to a 1.5 ml tube and centrifuged again at 2500 g for 5 minutes. Plasma was transferred to a fresh 1.5 ml tube, 1  $\mu\text{l}$  sodium azide (4M) was added and plasma samples were stored at  $4^{\circ}\text{C}$  until required. Pelleted cells were resuspended in 300  $\mu\text{l}$  of PBS-azide and 50  $\mu\text{l}$  aliquots of cells were transferred to 10 ml FACS tubes. Detection of anti-rat CD4 scFv in plasma and PBL was performed using flow cytometry (Section 2.4.g.1.).

### **2.7.h. Lymphadenectomy of cervical lymph nodes**

Rats were placed in an isoflurane nose cone (2.5-3% in oxygen). The fur underneath the chin was clipped and the area was decontaminated with 10% w/v povidone-iodine. An incision was made under the chin using a scalpel to expose the cervical lymph nodes (Figure 2.1). Bilateral lymphadenectomy of the exposed cervical lymph nodes (superficial cervical and facial lymph nodes, between 4-6 lymph nodes) was

performed using sterile instruments, including forceps and a pair of sharp scissors. The wound was closed with 4-5 disposable tissue staples.

## **2.8 STATISTICAL ANALYSIS**

### **2.8.a. Statistical analysis of transgene expression**

To identify statistical differences in transgene expression from cells transduced or transfected with virus or plasmid respectively, an unpaired Student T-test was performed using Microsoft Office Excel 2003 (Microsoft Corporation, Redmond, WA, USA). P values  $<0.05$  were considered significant.

### **2.8.b. Statistical analysis of corneal graft survival and inflammation**

#### **data**

Corneal graft survival and inflammation data were analysed using non-parametric statistical analysis. For comparisons between three or more groups, a Kruskal-Wallis test (corrected for ties) was performed, and to further identify which groups were statistically different from one another, pair-wise Mann Whitney-U tests (corrected for ties) using Bonferroni adjustment were performed. For comparisons between two groups, Mann Whitney U tests (correct for ties) were performed. Non-parametric statistical analysis was performed using SPSS statistical software (SPSS Inc., Chicago, IL, USA). P values  $<0.05$  were considered significant.

**CHAPTER 3: CONSTRUCTION AND CHARACTERISATION OF  
LENTIVIRAL VECTORS**

### 3.1 ABSTRACT

Aims: To construct and characterise single-gene and dual-gene lentiviral vectors carrying therapeutic transgenes and reporter genes. In addition, the methods used to titrate lentiviral vector preparations were optimised. Methods: Dual-gene vectors were constructed by inserting the F2A self-processing sequence between two transgenes. This allowed for expression of two transgenes within a single open reading frame (ORF). Single-gene vectors were also constructed. The transgenes cloned into the single-gene and dual-gene vectors included eYFP, anti-rat CD4 scFv and EK5. The expression of the transgenes cloned into the dual-gene vectors was compared to the expression from single-gene counterparts by transfecting and transducing mammalian cell lines with these vectors *in vitro*. Moreover, the methods used to titrate eYFP and non-eYFP expressing lentiviral vectors were optimised. Results: Lentiviral vector titration by eYFP quantification (using flow cytometry) produced similar titres after 5 days and 4 weeks of culture, suggesting that 5 days of culture was adequate for reliable titration using this method. However, lentiviral titration by quantifying proviral integration in A549 cells using qPCR was greatly improved when the transduced A549 cells were cultured for 4 weeks compared to 5 days, suggesting that 4 weeks of culture is necessary for reliable titration using this method. The characterisation of transgene expression from three separate dual-gene vectors (each containing the F2A sequence), showed reduced expression when a transgene was positioned downstream of F2A (ranging from 2-20 fold lower), compared to when the same transgene was situated upstream of F2A in a different dual-gene construct, or when compared to the expression from a single-gene construct. Conclusions: Proviral integration is a reliable functional titration method that can be used to titrate lentiviral vectors that do not carrying a reporter gene, as



long as the transduced cells are cultured for 4 weeks prior to quantification of proviral integration. Moreover, although there is reduced expression of a protein when it is positioned downstream of 2A in a dual-gene vector compared to a single-gene counterpart, expression of the downstream protein might still be adequate for its intended function. In relation to the pHIV-CD4scFV\_F2A\_eYFP vector, the downstream protein (eYFP) was not expressed at high enough levels to be used to determine transduction efficiency, to perform vector titration using flow cytometry or to track transduced cells *in vivo*. However, expression of the upstream protein (anti-rat CD4 scFv) showed similar expression levels when compared to the single-gene vector (pHIV-CD4scFv\_F2A) and was judged to be suitable for *in vivo* work on regional immunosuppression.

## **3.2 INTRODUCTION**

### **3.2.a. Gene transfer to the eye**

Gene transfer has the potential to provide long term expression of a transgene after a single intervention. There have been many reports of successful gene transfer to the anterior segment of the eye in animals including mice,<sup>112,156</sup> rats,<sup>221</sup> rabbits,<sup>37</sup> sheep<sup>50,224</sup> and non-human primates.<sup>225</sup>

### **3.2.b. Lentiviral vectors for gene transfer**

Lentiviral vectors have little immunogenicity<sup>170</sup> and their ability to provide stable integration of a transgene into chromosomal DNA enables long-term expression. Lentiviral vectors are also able to transduce both mitotic and post-mitotic cell types<sup>226</sup> which is extremely useful as the human corneal endothelium (a potential target for prolonging corneal graft survival) is post-mitotic.<sup>227</sup>

Anson and colleagues have developed a VSV-G-pseudotyped lentiviral vector, which is based upon HIV-1 and is self-inactivating.<sup>195-197</sup> Anson's lentiviral vector has codon-optimised reading frames and is constructed using multiple plasmids, which enables safe and efficient production of large-scale quantities. Parker and colleagues have shown successful transduction of rat, sheep and human corneas *in vitro*, with long term gene expression in a rat model of corneal transplantation using the Anson lentiviral vector.<sup>198</sup> For these reasons, Anson's lentiviral vector was selected for use in this project.

### **3.2.c. CD4 as a target for T cell activation**

The most common mechanism involved in corneal graft rejection is a DTH response, mediated by CD4+ T cells.<sup>46</sup> As part of this process, antigen presentation between an APC and a CD4+ T cell triggers an immune insult on the graft, which can lead to rejection. CD4 was selected as the molecule to be targeted in this project, because it is critical to the process of T cell sensitisation and is expressed on the surface of T cells. Systemic delivery of a whole antibody against CD4 has already been shown to prolong survival of corneal grafts in rats.<sup>154</sup>

### **3.2.d. ScFv as a potential treatment to the cornea**

Genetic engineering has allowed for the isolation of the genes encoding the variable heavy and variable light domains of antibody binding sites and their covalent linkage into a scFv (Figure 1.5). ScFvs are approximately 28 kDa, which is significantly smaller than a whole antibody (IgG is 146 kDa).<sup>228</sup> ScFvs do not contain the inflammatory Fc region, which is present in a whole antibody. For these reasons a

scFv targeting the T cell molecule CD4 was selected as a tool to block T cell sensitisation.

### **3.2.e. The Foot and Mouth Disease Virus (FMDV) 2A self-processing sequence**

The Foot and Mouth Disease Virus (FMDV) 2A sequence is a short (18 amino acids) self-processing sequence, which cleaves at its C-terminus through a ribosomal ‘skip’ mechanism.<sup>229</sup> The self-processing activity of the 2A sequence has been exploited in many multi-gene transfer vectors including retroviral,<sup>230-237</sup> AAV,<sup>238-240</sup> oncolytic adenoviral<sup>241</sup> and lentiviral vectors.<sup>242-243</sup> The FMDV 2A self-processing sequence was selected for use in this study because of its small size, and its reported ability to produce equimolar expression of multiple genes within a single ORF.<sup>237-239,244</sup>

### **3.2.f. Specific aims**

The specific experimental aims of the work described in this chapter were:

- (1) to construct single-gene lentiviral vectors;
- (2) to construct dual-gene lentiviral vectors using the 2A self-processing sequence;
- (3) to compare the different methods of lentiviral titration;
- (4) to assess the effects of long term lentiviral vector storage and freeze thawing;
- (5) to quantify transgene expression *in vitro* in cell lines transfected or transduced with single-gene and dual-gene plasmids or lentiviral vectors respectively.

### 3.3 RESULTS

#### 3.3.a. Construction of lentiviral plasmids

The plasmids that were constructed by others that were used in this project are listed below. Additional information about these plasmids can be found in Table 2.3 and vector maps can be found in Appendix 2.

- pBS-CD55-F2A-CD59 was a kind donation from Professor Peter Cowan, St Vincent's Hospital, Melbourne, Victoria, Australia.
- pHIV-eYFP was a kind donation from Associate Professor Donald Anson, Women's and Children's Hospital, Adelaide, South Australia, Australia.
- pBLAST41-hEndoKring5 is a commercially available expression vector purchased from InvivoGen, San Diego, CA, USA.
- pHIV-EK5 was cloned by Ms Lauren Mortimer, Dept of Ophthalmology, Flinders University, Adelaide, South Australia, Australia.

The plasmids constructed as part of this thesis are listed below. The construction of pHIV-CD4scFv can be found in Appendix 3 and the construction of the other plasmids will be described in this chapter.

- pHIV-CD4scFv
- pHIV-CD4scFv\_F2A\_eYFP
- pHIV-eYFP\_F2A\_CD4scFv
- pHIV-CD4scFv\_F2A
- pHIV-CD4scFv\_F2A\_EK5

### **3.3.a.1. Construction of pHIV-CD4scFv\_F2A\_eYFP**

A dual-gene plasmid carrying anti-rat CD4 scFv and eYFP was constructed using the FMDV 2A sequence (19 amino acids, including the 2B proline at the C-terminus of 2A) with a furin cleavage site (arginine, alanine, lysine, arginine) immediately upstream of 2A (F2A). Fang and colleagues have shown that the addition of a furin cleavage site upstream of 2A was able to successfully remove the 2A amino acids attached to the C-terminus of the protein upstream of 2A during post-translational modification in the Golgi apparatus.<sup>238</sup>

SOE-PCR was performed to assemble the anti-rat CD4 scFv\_F2A fragment using the methods described in Section 2.2.j. and a diagrammatic representation is shown in Figure 3.1. Firstly, the anti-rat CD4 scFv without its stop codon and the F2A self-processing sequence were amplified from pHIV-CD4scFv (Table 2.3, Appendix 3) and pBS-CD55-F2A-CD59 (Table 2.3; Appendix 2) respectively (Figure 3.2). These PCR products were joined together using SOE-PCR (Figure 3.2). The anti-rat CD4 scFv\_F2A SOE-PCR product was ligated into the pHIV-eYFP plasmid (Table 2.3; Appendix 2) between the SV40 promoter and eYFP at the ClaI site and electroporated into DH5 $\alpha$  electrocompetent *E. coli* (Figure 3.3). A PCR screen was performed on 22 colonies and 14 were detected as containing the anti-rat CD4 scFv\_F2A insertion in the pHIV-eYFP plasmid (Figure 3.4). Colony 4.11 was randomly selected for sequence analysis and was found to have the anti-rat CD4 scFv\_F2A insertion in the correct orientation and in the correct reading frame (Appendix 4). The pHIV-CD4scFv\_F2A\_eYFP plasmid (Figure 3.5) was used for lentiviral vector production.

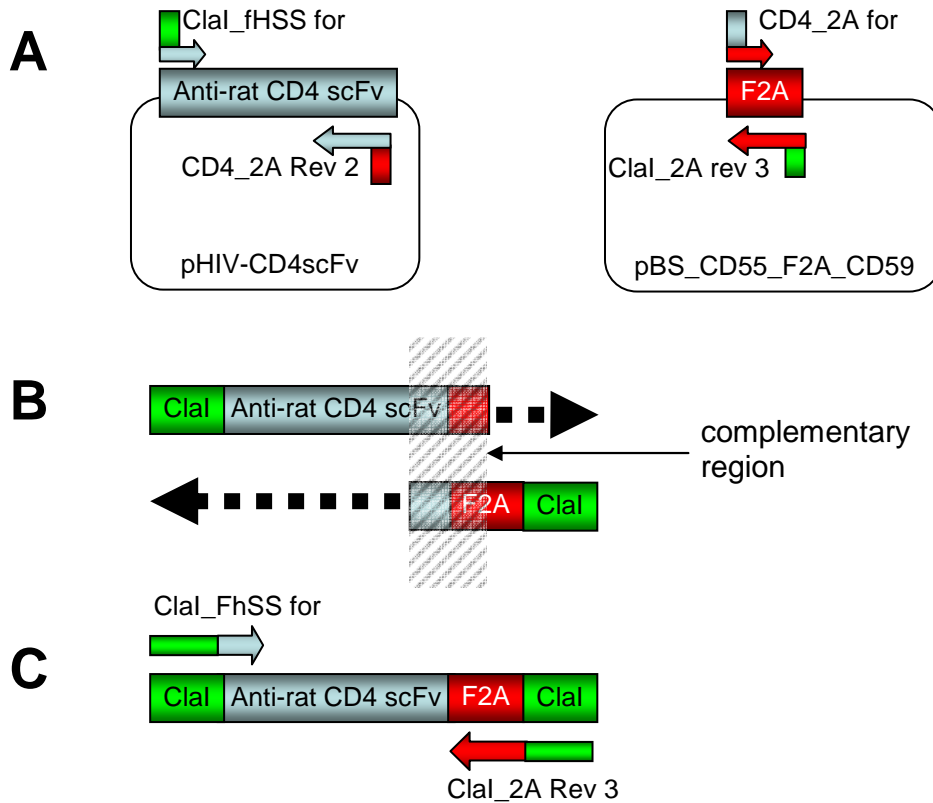


**Figure 3.1: Diagrammatic representation of the assembly of the anti-rat CD4 scFv\_F2A fragment using splice-overlap extension (SOE-PCR). (A)** Anti-rat CD4 scFv without its stop codon and F2A were amplified from pHIV-CD4scFv and pBS-CD55-F2A-CD59, respectively. The ClaI\_fHSS for primer was designed to add a ClaI site 5' of anti-rat scFv. The ClaI\_2A rev 3 primer was designed to add a ClaI site 3' of the F2A sequence (refer to Table 2.5 for primer sequences). **(B)** The first three SOE-PCR cycles were performed with the products from (A) without the addition of primers. This allowed for the two templates to anneal at their complementary region (highlighted in grey-striped area). The strands were completed using a DNA polymerase with proof-reading activity (represented by dashed arrows). **(C)** The external primers ClaI\_fHSS for and ClaI\_2A rev 3 were added to the reaction to amplify the full length double stranded PCR product for the remaining 35 cycles. Primers are indicated as short, filled arrows alongside their binding region.

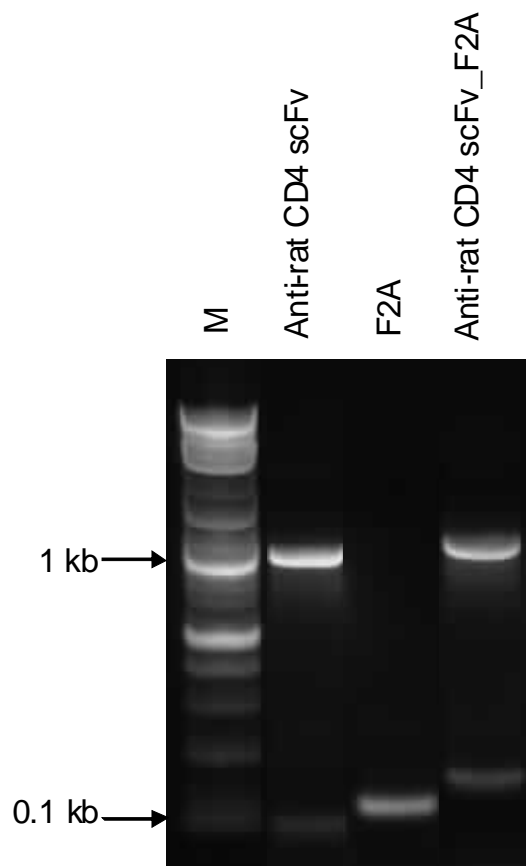


**Figure 3.2: An agarose gel showing the anti-rat CD4 scFv PCR product (0.9 kb bp), the F2A PCR product (0.1 kb) and the anti-rat CD4 scFv\_F2A SOE-PCR product (1 kb).** Non specific bands are present in the anti-rat CD4 scFv (<0.1 kb) and anti-rat CD4 scFv\_F2A (0.15 kb) lanes, but at lower abundance than the expected species. The lane marked M contained the 2-log DNA ladder.

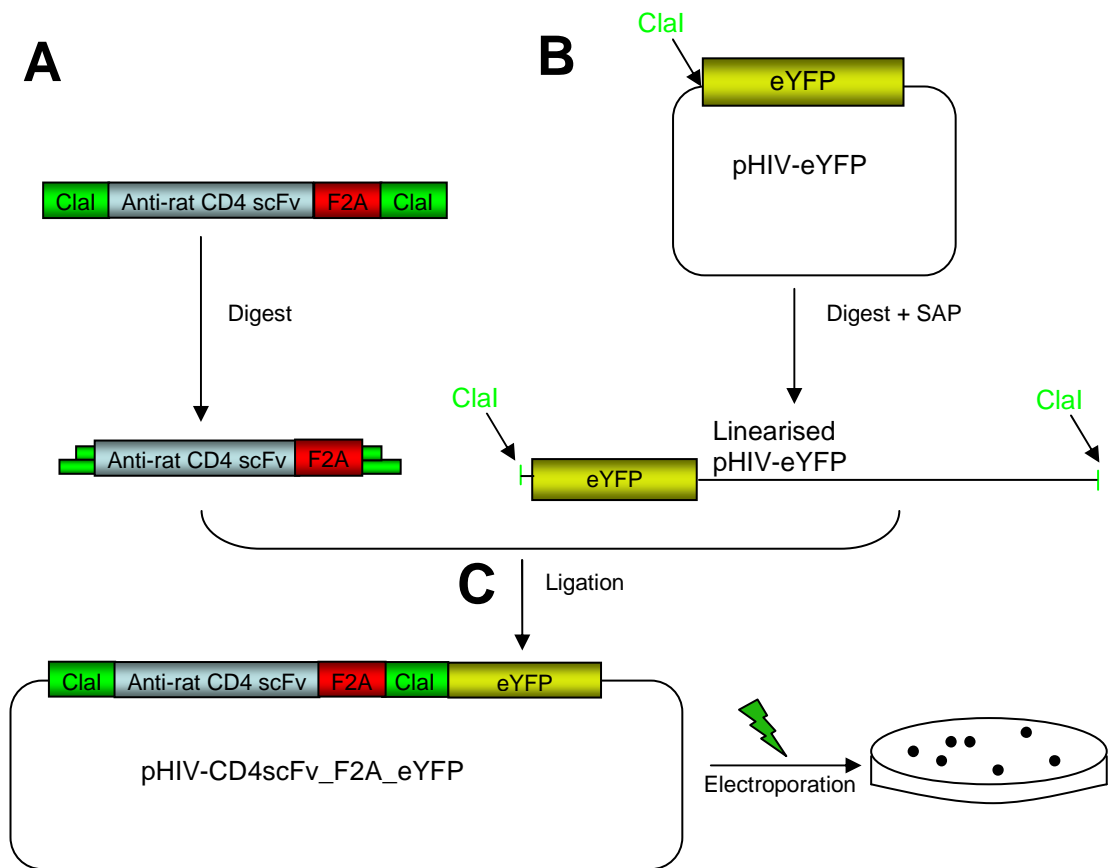


**Figure 3.3: Diagrammatic representation of the construction of pHIV-CD4scFv\_F2A\_eYFP. (A)** The anti-rat CD4 scFv\_F2A SOE-PCR product was digested with ClaI. **(B)** pHIV-eYFP was digested with ClaI and then treated with Shrimp Alkaline Phosphatase (SAP) which de-phosphorylated the ends of the plasmid to prevent self re-ligation. **(C)** The SOE-PCR product was ligated into the plasmid to create pHIV-CD4scFv\_F2A\_eYFP which was electroporated into DH5 $\alpha$  electrocompetent *E. coli*.



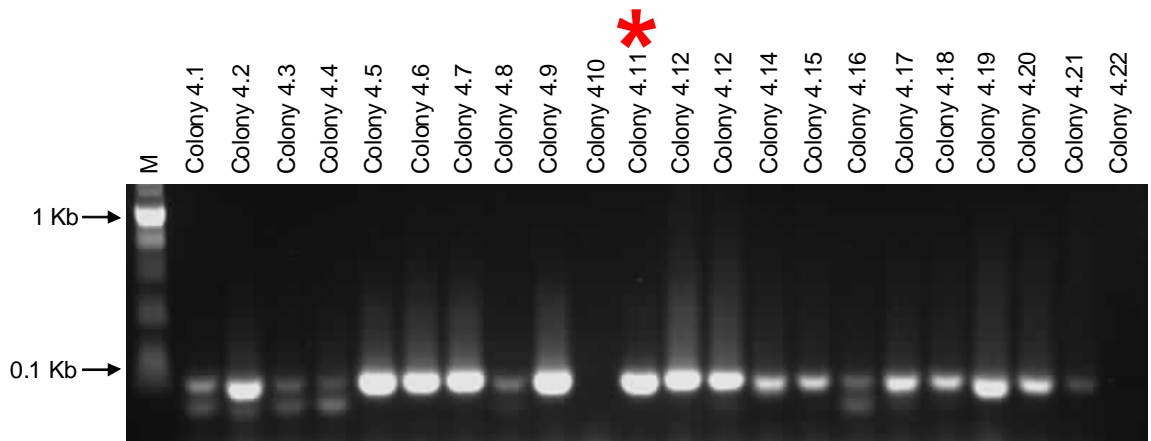


**Figure 3.4: A PCR screen revealed 14 from 22 colonies contained the anti-rat CD4 scFv\_F2A insert.** The primers used in the PCR screen were CD4 2A for and CD4 2A rev 2 (refer to Table 2.5 for primer sequences). The expected product size was 0.1 kb. Colony 4.11 (\*) was randomly selected for sequence analysis from the colonies that amplified the correct size product.

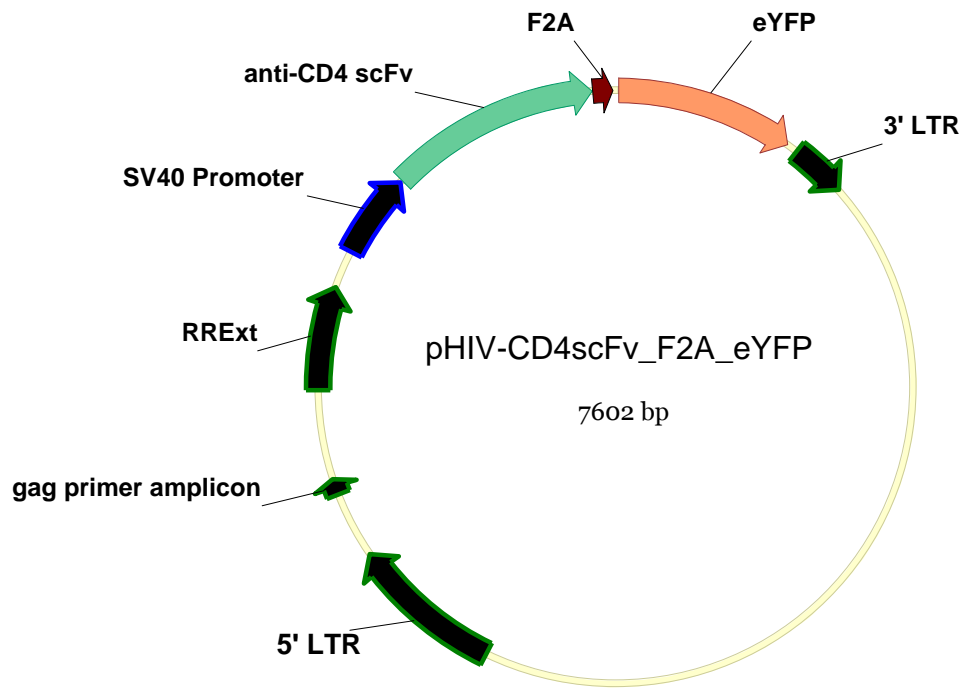


**Figure 3.5: pHIV-CD4scFv\_F2A\_eYFP vector map.** Sequences of interest are marked with arrows. Expression of anti-rat CD4 scFv (anti-CD4 scFv), the F2A self-processing sequence and eYFP were all controlled by the internal SV40 promoter. The 5' and 3' long terminal repeats (LTRs), the extended rev response element (RRExt) and the gag primer amplicon are also highlighted.

### **3.3.a.2. Construction of pHIV-eYFP\_F2A\_CD4scFv**

A dual-gene plasmid, pHIV-eYFP\_F2A\_CD4scFv, carrying the same transgenes as pHIV-CD4scFv\_F2A\_eYFP, but in the reverse order (eYFP followed by anti-rat CD4 scFv), with the F2A sequence in between, was constructed. For the construction of pHIV-eYFP\_F2A\_CD4scFv, the experimental design was prepared by me and laboratory assistance was provided by Mr Yazad Irani, Ophthalmology, Flinders University, Adelaide, South Australia.

SOE-PCR was used to assemble the eYFP\_F2A fragment using the methods described in Section 2.2.j. The eYFP sequence without its stop codon was amplified from pHIV-eYFP using primers that attached a ClaI restriction site at its 5' end. The F2A sequence was amplified from pBS\_CD55\_F2A\_CD59 using primers that attached a ClaI site to its 3' end. The eYFP\_F2A SOE-PCR product was ligated into the pHIV-CD4scFv plasmid at the ClaI site and electroporated into DH5 $\alpha$  electrocompetent E. coli.

A PCR screen on 9 colonies revealed 4 with a single insertion of the eYFP\_F2A fragment in the correct orientation (Figure 3.6). Colony 3 was randomly selected for sequence analysis, which revealed an identical match to the predicted sequence of eYFP\_F2A (Appendix 4). The pHIV-eYFP\_F2A\_CD4scFv plasmid (Figure 3.7) was used in lentiviral vector production.

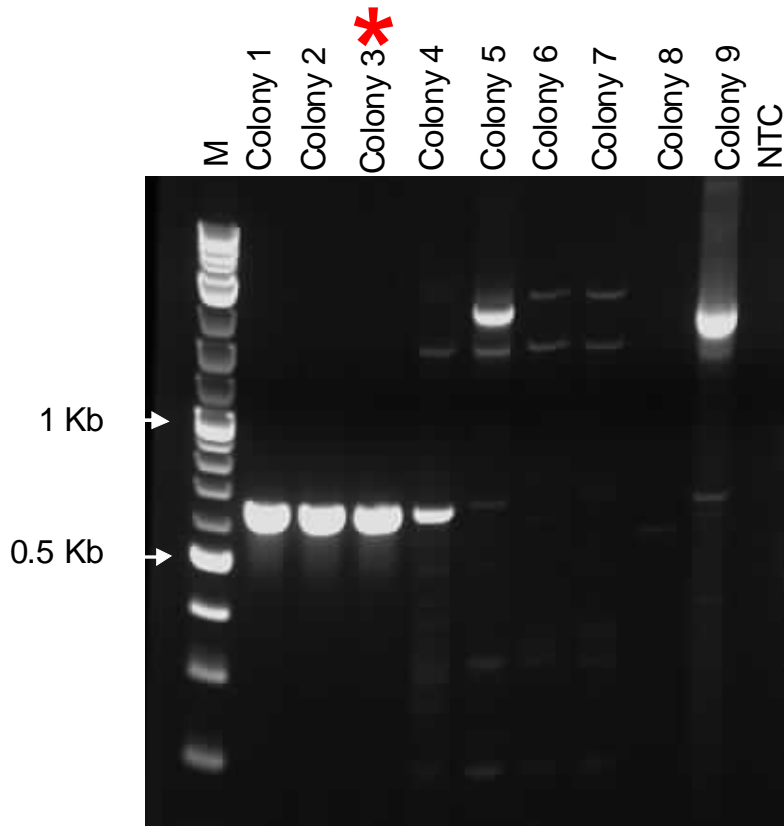


**Figure 3.6: A PCR was performed on selected colonies to screen for those containing a single eYFP\_F2A fragment in the correct orientation within the pHIV-CD4scFv plasmid.** The primers used for the PCR screen were pHIVSV for2 (within the SV40 promoter) and eYFP rev2 (within the insert) (refer to Table 2.5 for primer sequences). The expected product size was 0.6 kb. The lane marked M contained the 2-log ladder. NTC = no template control (water). Colony 3 (\*) was randomly selected for sequence analysis from the 4 colonies that amplified the correct size product. The PCR screen was performed by Mr Yazad Irani, Ophthalmology, Flinders University, Adelaide, South Australia, Australia.

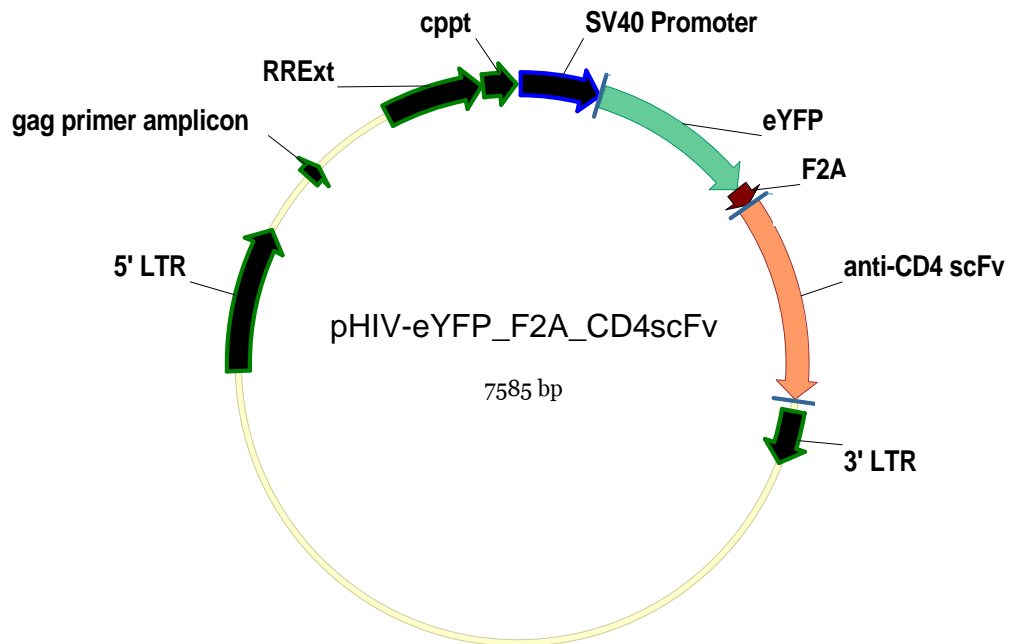


**Figure 3.7: pHIV-eYFP\_F2A\_CD4scFv vector map.** Sequences of interest are marked with arrows. The expression of eYFP, the F2A self-processing sequence and anti-rat CD4 scFv (anti-CD4 scFv) were all controlled by the internal SV40 promoter. The 5' and 3' long terminal repeats (LTRs), the central polypurine tract (cppt), the extended rev response element (RRExt) and the gag primer amplicon are also highlighted.

### **3.3.a.3 Construction of pHIV-CD4scFv\_F2A**

A single-gene anti-rat CD4scFv lentiviral plasmid (pHIV-CD4scFv) was constructed (Appendix 3). However, expression of the anti-rat CD4 scFv was very low from this construct when it was used to transfect HEK-293A cells (data not shown). The dual-gene pHIV-CD4scFv\_F2A\_eYFP plasmid produced strong expression of anti-rat CD4 scFv when transfected into HEK-293A cells (Figure 3.19), so an alternative single-gene plasmid was developed from this construct, as a control vector for further experiments.

The new single-gene anti-rat CD4 scFv plasmid was constructed by removing the eYFP sequence from pHIV-CD4scFv\_F2A\_eYFP by restriction digestion with XmaI and NdeI, leaving anti-rat CD4 scFv and F2A (Figure 3.8). The incompatible cohesive ends of XmaI and NdeI were filled using the Klenow fragment of DNA polymerase I to create blunt ends. The blunt ends were ligated together to form the pHIV-CD4scFv\_F2A construct which was electroporated into DH5 $\alpha$  electrocompetent *E. coli*. Cleavage of the furin cleavage site after translation (in the Golgi apparatus) will result in the removal of the remaining F2A residues attached to the C-terminus of the anti-rat CD4 scFv, so they were not removed from the plasmid. In addition, the anti-rat CD4 scFv gene in the pHIV-CD4scFv\_F2A construct does not encode a stop codon, thus the transcript will stay attached to the ribosome during translation.

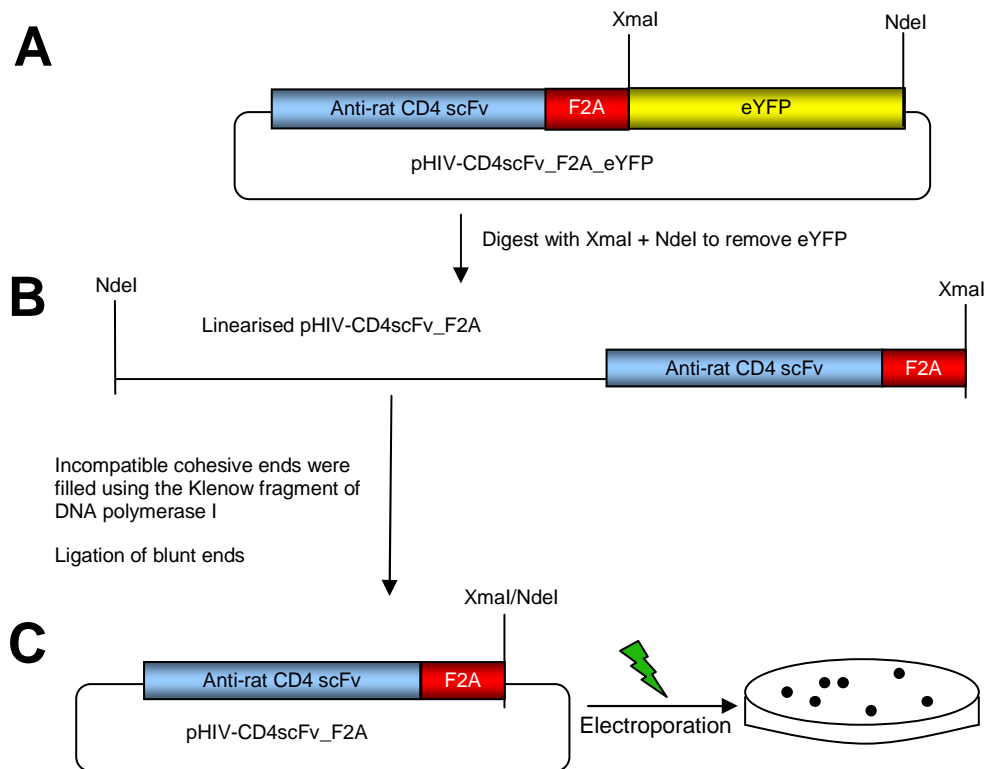


**Figure 3.8: Diagrammatic representation of the construction of pHIV-CD4scFv\_F2A.** **(A)** The pHIV-CD4scFv\_F2A\_eYFP plasmid was digested with XmaI and NdeI restriction enzymes to remove eYFP. **(B)** The incompatible cohesive ends of XmaI and NdeI were filled using the Klenow fragment of DNA polymerase I and were ligated together. **(C)** The pHIV-CD4scFv\_F2A plasmid was electroporated into DH5 $\alpha$  electrocompetent *E. coli*.

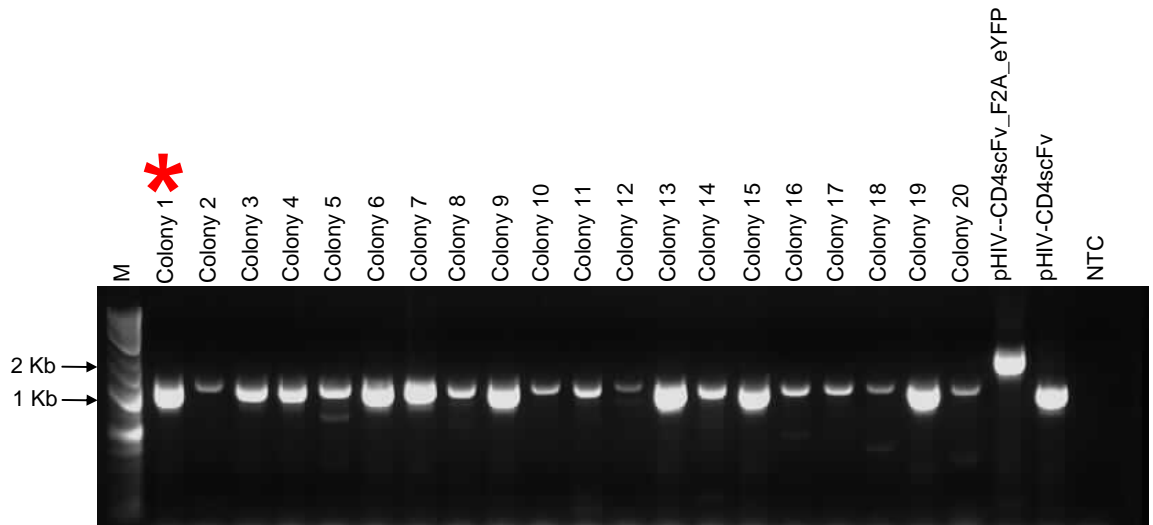
A PCR screen on potential pHIV-CD4scFv\_F2A colonies revealed all 20 colonies lacked eYFP (Figure 3.9). Colony 1 was selected for sequence analysis, which confirmed the removal of eYFP from the vector (Appendix 4). The pHIV-CD4scfv\_F2A construct (Figure 3.10) was used in lentiviral vector production.

#### **3.3.a.4 Construction of pHIV-CD4scFv\_F2A\_EK5**

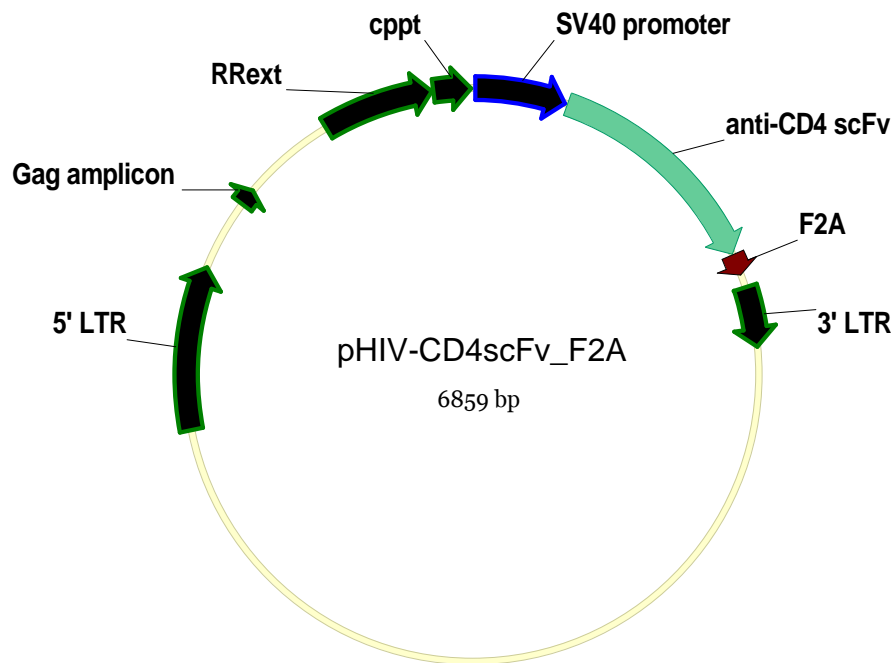
A dual-gene plasmid encoding anti-rat CD4 scFv and EK5 with an F2A self processing sequence situated in between the two transgenes was constructed. A diagrammatic representation outlining the construction of pHIV-CD4scFv\_F2A\_EK5 is shown in Figure 3.11. The pHIV-CD4scFv\_F2A\_eYFP plasmid was digested with the XmaI and NdeI restriction enzymes to remove the eYFP sequence. However, the EK5 gene contains an XmaI site within its sequence, so, using PCR techniques, an AgeI site (with the same cohesive ends as XmaI) was added onto the 5' end of the EK5 PCR product (which was amplified from pBLAST41-hEndokrangle5; Table 2.3; Appendix 2) and an NdeI site was added to the 3' end. EK5 was ligated into the digested plasmid and the pHIV-CD4scFv\_F2A\_EK5 construct was electroporated into DH5 $\alpha$  electrocompetent *E. coli*.

A PCR screen on potential pHIV-CD4scFv\_F2A\_EK5 colonies revealed 16 of 20 colonies had successful insertion of EK5 (Figure 3.12). Colony 12 was selected for sequence analysis, which confirmed successful ligation of the pHIV-CD4scFv\_F2A plasmid and EK5 (Appendix 4). The pHIV-CD4scfv\_F2A\_EK5 construct (Figure 3.13) was used in lentiviral vector production.



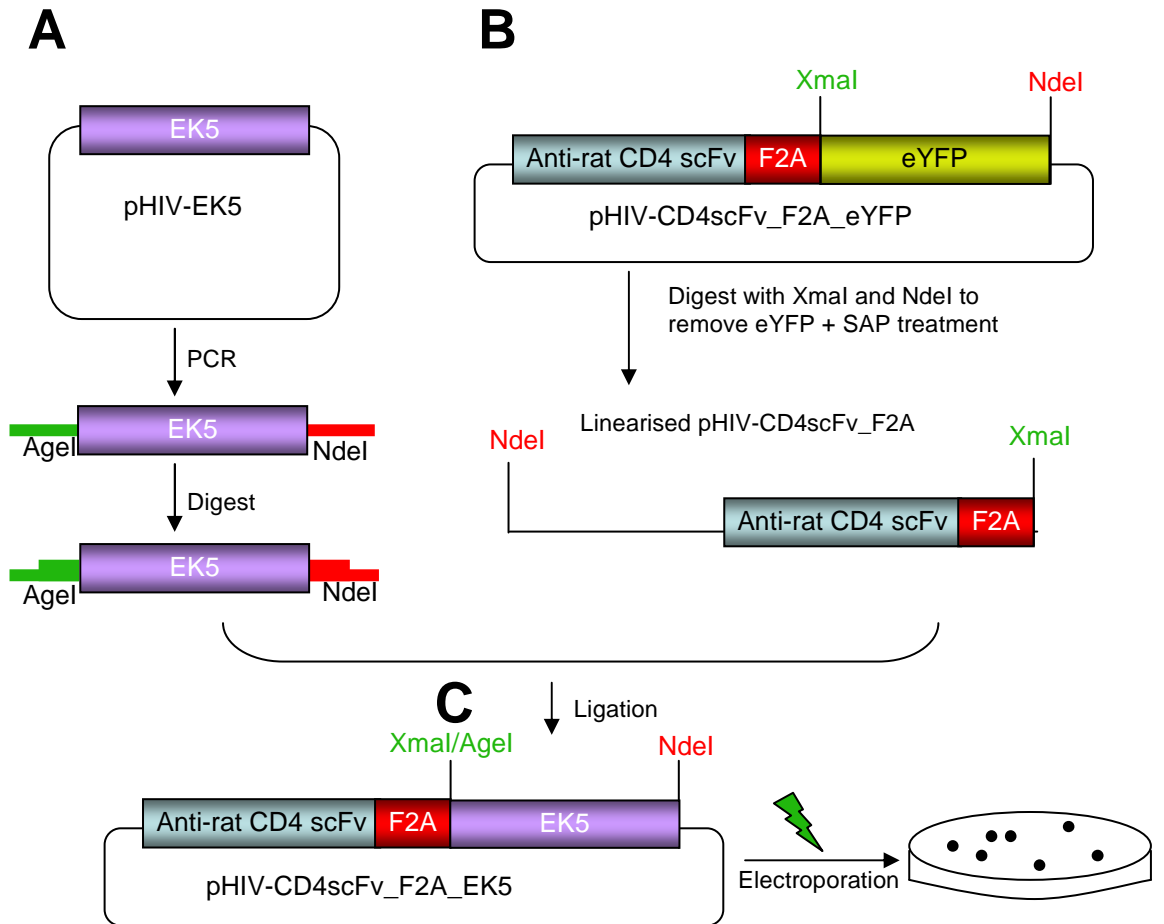


**Figure 3.9: A PCR was performed on 20 colonies to screen for those that had successful removal of eYFP, to create the pHIV-CD4scFv\_F2A construct.** The primers used for the PCR screen were pHIV1SV for2 and C+D NdeIn rev (refer to Table 2.5 for primer sequences). The expected product size was 1 kb. The control templates in the PCR screen were pHIV-CD4scFv\_F2A\_eYFP which amplified a 1.8 kb product (that contained anti-rat CD4 scFv, F2A and eYFP) and pHIV-CD4scFv which amplified a 0.9 kb product (that consisted of the anti-rat CD4 scFv sequence without F2A). The lane marked M contained the 2-log ladder. NTC = no template control (water). Colony 1 (\*) was randomly selected for sequence analysis from the colonies that amplified the correct size product.



**Figure 3.10: pHIV-CD4scFv\_F2A vector map:** Sequences of interest are marked with arrows. Expression of anti-rat CD4 scFv (anti-CD4 scFv) and F2A were controlled by the internal SV40 promoter. The 5' and 3' long terminal repeats (LTRs), the central polypurine tract (cppt), the extended rev response element (RRExt) and the gag primer amplicon are also highlighted. Note: F2A residues attached to the C-terminal end of anti-rat CD4 scFv will be removed during post-translational modification in the Golgi by cleavage at the furin site.

**Figure 3.11: Diagrammatic representation of the construction of pHIV-CD4scFv\_F2A\_EK5. (A)** Endostatin::kringle-5 (EK5) was amplified from the pHIV-EK5 plasmid. The forward primer (AgeI EK5 for; refer to Table 2.5 for the primer sequence) was designed to add an AgeI restriction site to the 5' end of the PCR product and the reverse primer (NdeI EK5 rev; refer to Table 2.5 for the primer sequence) was designed to add an NdeI restriction site to the 3' end of the PCR product and these restriction sites were digested. **(B)** The pHIV-CD4scFv\_F2A\_eYFP plasmid was digested with XmaI and NdeI restriction enzymes to remove eYFP. The digested plasmid was treated with Shrimp Alkaline Phosphatase (SAP) to prevent rejoining of the plasmid without an insert. **(C)** The AgeI and XmaI sites from the PCR product and the plasmid respectively, had compatible cohesive ends and were ligated together along with the NdeI sites on the PCR product and the plasmid. The pHIV-CD4scFv\_F2A\_EK5 plasmid was electroporated into DH5 $\alpha$  electrocompetent *E. coli*.



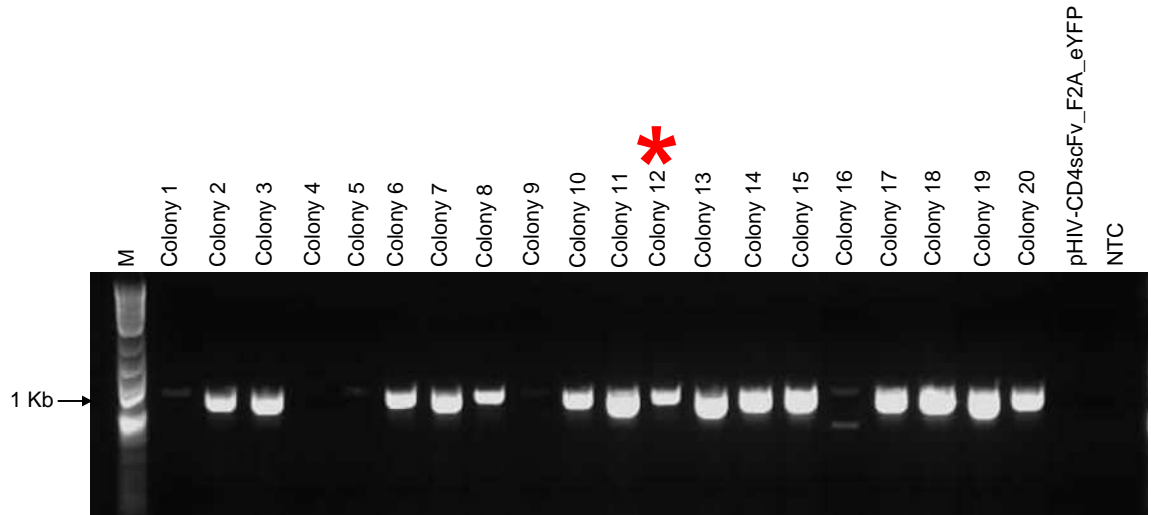


**Figure 3.12: A PCR was performed on 20 colonies to screen for the EK5 insertion, to create pHIV-CD4scFv\_F2A\_EK5.** The primers used for the PCR screen were EK5 for2 and C+D NdeIn rev (refer to Table 2.5 for primer sequences). The expected product size was 0.7 kb. The negative control template (pHIV-CD4scFv\_F2A\_eYFP) amplified nothing. The lane marked M contained the 2-log ladder. NTC = no template control (water). Colony 12 (\*) was randomly selected for sequence analysis from the colonies that amplified the correct size product.

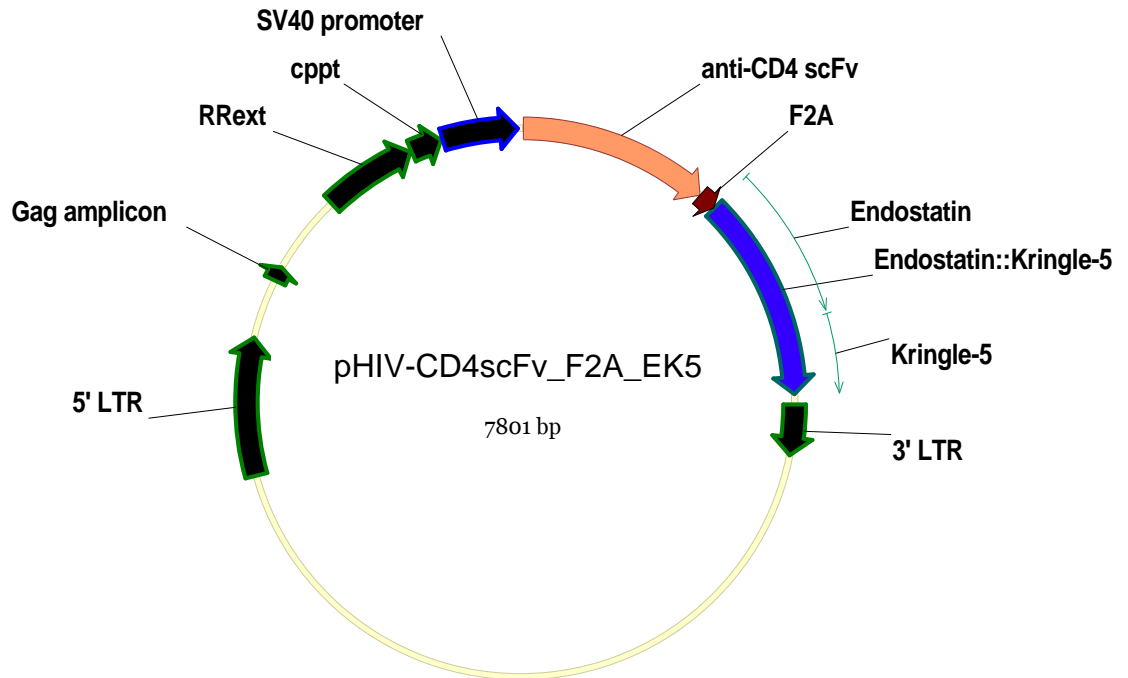


**Figure 3.13: pHIV-CD4scFv\_F2A\_EK5 vector map:** Sequences of interest are highlighted. Expression of the anti-rat CD4 scFv (anti-CD4 scFv), F2A and the endostatin::kringle-5 fusion protein were driven by the internal SV40 promoter. The 5' and 3' long terminal repeats (LTRs), the central polypurine tract (cppt), the extended rev response element (RRExt) and the gag primer amplicon are also highlighted.

### 3.3.b. Analysis of lentiviral vector titration

#### 3.3.b.1. Lentiviral titration by quantifying reporter gene (eYFP)

##### *expression*

The established method used in our laboratory to titrate eYFP-expressing lentiviral vectors involved the transduction of A549 cells with a small amount of a lentiviral vector (0.1 and 0.5  $\mu$ l), culture of the cells for 5 days and quantification of the number of eYFP-expressing cells using flow cytometry. The number of lentiviral particles was expressed in TU/ml. A detailed method can be found in Section 2.5.d.1.

An experiment was performed to determine whether extending the period of time that the transduced A549 cells were in culture, would have an effect on eYFP expression from these cells, and subsequently, whether this would affect the calculated titre. To test this, a preparation of the lentiviral vector LV-eYFP was used to transduce A549 cells. The transduced cells were then cultured for either 5 days or 4 weeks. The lentiviral titres calculated after 5 days and 4 weeks were very similar to each other, (Table 3.1), indicating that 5 days in culture was sufficient to produce a reliable titre using this method.

#### **Table 3.1: Titration of LV-eYFP by reporter gene (eYFP) quantification on**

**A549 cells.** Mean values are shown with standard deviation, n=3.

5 days ( $10^9$ TU/ml)	4 weeks ( $10^9$ TU/ml)
$2.43 \pm 0.45$	$2.41 \pm 0.24$

### **3.3.b.2. Titration of lentiviral vectors by quantifying proviral integration**

Previously, the standard method used in our laboratory for titration of lentiviral vectors that do not express a reporter gene, involved the transduction of A549 cells with a small amount of a lentiviral vector (0.1 and 0.5  $\mu$ l) and culture of these cells for 5 days. The genomic DNA (gDNA) was then harvested from these cells and qPCR using primers specific for the gag sequence was performed to quantify integration of proviral DNA into the transduced cells (Section 2.5.d.2.). However, this method of titration produced titres that were inconsistent, hard to replicate and were not comparable to the titres obtained from reporter gene quantification.

Considering this, it was hypothesised that extending the period of time that the transduced cells were in culture before quantifying proviral integration, might result in more consistent titres. To test this, three lentiviral vectors were titrated by quantifying proviral integration after 5 days and 4 weeks in culture (Table 3.2). For all three lentiviral vector preparations, the calculated viral titres were higher after 5 days, than they were after 4 weeks and there was no similarity in the fold difference between the 5 day and 4 week titres amongst the three lentiviral vector preparations (Table.3.2). The number of calculated copies/cell varied greatly amongst all three lentiviral vector preparations after 5 days, with one lentiviral vector calculated as having greater than 100 copies/cell (Table 3.2). However, by 4 weeks, the calculated copies/cell was less than 4 for all three lentiviral vector preparations and the 4 week titres were comparable to each other and were in a similar range to the viral titres calculated by reporter gene (eYFP) quantification (Table 3.1).



**Table 3.2: Proviral integration titration of lentiviral vectors on A549 cells.** Mean values are shown with standard deviation, n=6.

Lentiviral vector	5 days		4 weeks		5 weeks	
	10 <sup>9</sup> TU/ml	copies/cell	10 <sup>9</sup> TU/ml	copies/cell	10 <sup>9</sup> TU/ml	copies/cell
LV-CD4scFv	35.3 ± 10.3	46.1 ± 38.46	3.46 ± 0.88	3.88 ± 2.61	n/a	n/a
LV-CD4scFv_F2A_eYFP	90.6 ± 23.7	112.28 ± 93.32	1.25 ± 0.17	1.46 ± 1.04	n/a	n/a
LV-eYFP	187 ± 198	39.17 ± 45.58	2.38 ± 0.67	0.58 ± 0.31	1.71 ± 0.59	0.66 ± 0.17

n/a, not applicable

Furthermore, when one of these lentiviral vectors was cultured for an extra week (5 weeks in total), the viral titre ( $1.71 \times 10^9$  TU/ml) was similar to the titre calculated after 4 weeks ( $2.38 \times 10^9$  TU/ml) (Table 3.2). These results suggested that 4 weeks in culture was long enough to produce stable and consistent titres by quantifying proviral integration.

### 3.2.b.3. Comparison of titre methods

Next, I wanted to directly compare the proviral integration method of titration to the reporter gene quantification method of titration. Titration was performed by quantifying eYFP expression (using flow cytometry) and proviral integration (using qPCR on gDNA) on the same transduced A549 cells after 5 days and 4 week in culture (Table 3.3). After 5 days in culture, titration using the proviral integration method produced a viral titre much greater than that produced by eYFP quantification. However, after 4 weeks of culture, the proviral integration titre was comparable to the eYFP quantification viral titre.

**Table 3.3: Titration of LV-eYFP using the proviral integration (qPCR) and reporter gene (eYFP) quantification methods on the same A949 cells.** Mean values are shown with standard deviation,  $n \geq 3$ .

eYFP ( $10^9$ TU/ml)	5 days		eYFP ( $10^9$ TU/ml)	4 weeks	
	qPCR ( $10^9$ TU/ml)	qPCR (copies/cell)		qPCR ( $10^9$ TU/ml)	qPCR (copies/cell)
$2.43 \pm 0.45$	$187 \pm 198$	$39.17 \pm 45.58$	$2.41 \pm 0.24$	$2.38 \pm 0.67$	$0.58 \pm 0.31$

#### **3.3.b.4. Long-term storage of a lentiviral vector at -80°C**

The effect of long-term storage of lentiviral vectors at -80°C was tested. A lentiviral vector (LV-eYFP) was titrated initially after its production in September 2006 on A549 cells after 5 days of culture using flow cytometry. The same viral batch was titrated once again, 21 months after the initial titration (June 2008), using the same method as before and a 10 fold decrease in lentiviral particles was observed (Table 3.4). So, thereafter lentiviral preparations that were used 6 months after production were re-titrated prior to use.

**Table 3.4: Reporter gene (eYFP) titration of LV-eYFP after 21 months in storage on A549 cells.** Mean values are shown with standard deviation, n=3.

Date of titration	10 <sup>9</sup> TU/ml
Sep-06	1.33 ± 0.34
Oct-08	0.18 ± 0.06

#### **3.3.b.5. Titration of previously thawed then refrozen lentiviral vector preparations**

To determine whether freeze-thawing would reduce the activity of lentiviral vectors, two aliquots of the same non-eYFP-expressing lentiviral vector (LV-CD4scFv), were titrated on A549 cells after 4 weeks in culture, using qPCR (Table 3.5). One aliquot had been thawed and refrozen previously and the other was a fresh aliquot of the same virus. There was no difference in the number of lentiviral particles calculated in the aliquot which had been previously thawed and refrozen compared to the fresh aliquot, indicating that a single freeze-thaw had not reduced the activity of the virus.

**Table 3.5: Proviral integration titration of fresh and previously thawed then refrozen LV-CD4scFv aliquots on A549 cells after 4 weeks in culture.** Mean values are shown with standard deviation, n=6.

Sample	10 <sup>9</sup> TU/ml	copies/cell
Fresh	3.46 ± 0.88	3.88 ± 2.62
Previously thawed then refrozen	3.28 ± 1.54	3.47 ± 2.13

### 3.3.c. Transgene expression from single-gene and dual-gene vectors

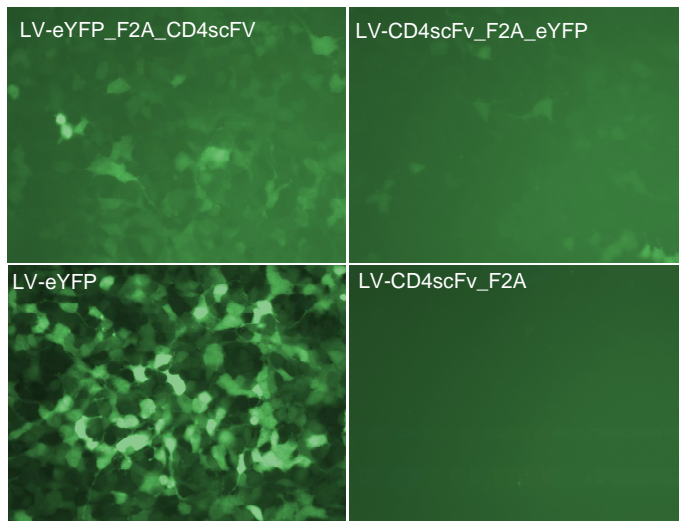
#### 3.3.c.1. Expression of proteins targeted to different cellular compartments

##### 3.3.c.1.a EYFP expression from single-gene and dual-gene vectors

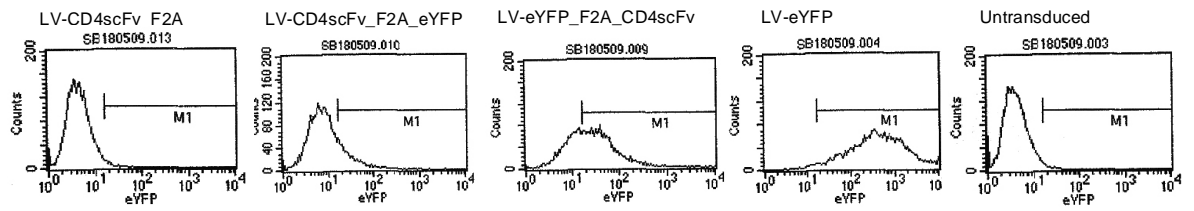
Experiments were performed to characterise the expression of eYFP from dual-gene constructs carrying the F2A sequence, LV-CD4scFv\_F2A-eYFP and LV-eYFP\_F2A\_CD4scFv, compared to expression from a single-gene construct (LV-eYFP). HEK-293A cells were transduced with lentiviral vectors at an MOI of 5 for 24 hours, and the cells were cultured for 5 days. Six biological replicates were performed for each vector in a 6 well plate. Fluorescence microscopy was used to visualise eYFP expression of the transduced cells (Figure 3.18A) and flow cytometry was used to quantify the number of cells expressing intracellular eYFP (Figure 3.18B and Figure 3.18C). When comparing the expression of eYFP from the two dual-gene vectors, eYFP expression was approximately 2 fold higher in cells transduced with the vector which had eYFP positioned upstream of F2A (LV-eYFP\_F2A\_CD4scFv), compared to expression of eYFP from cells transduced with the vector which had eYFP positioned downstream of F2A (LV-CD4scFv\_F2A\_eYFP) (p=0.005). Also, eYFP expression

**Figure 3.18: EYFP expression from HEK-293A cells transduced with lentiviral vectors.** HEK-293A cells were transduced with lentiviral vectors at an MOI of 5 for 24 hours, and cultured for 5 days. **(A)** Representative fluorescence images of eYFP positive cells were taken using a 20x objective lens. **(B)** Flow cytometry was used to quantify the number of eYFP-positive cells from each well and representative histograms are shown (n=6). **(C)** The eYFP-flow cytometric data was quantified. The biological replicates were averaged (mean), (n = 6). Error bars represent one standard deviation from the mean. \* = Statistically lower eYFP expression from cells transduced with LV-CD4scFv\_F2A\_eYFP compared to cells that were transduced with LV-eYFP\_F2A\_CD4scFv (p=0.005), and compared to expression from cells transfected with LV-eYFP (p=0.005) (unpaired Student T-test). \*\* = Statistically lower eYFP expression compared to expression from LV-eYFP (p<0.005) (unpaired Student T-test).

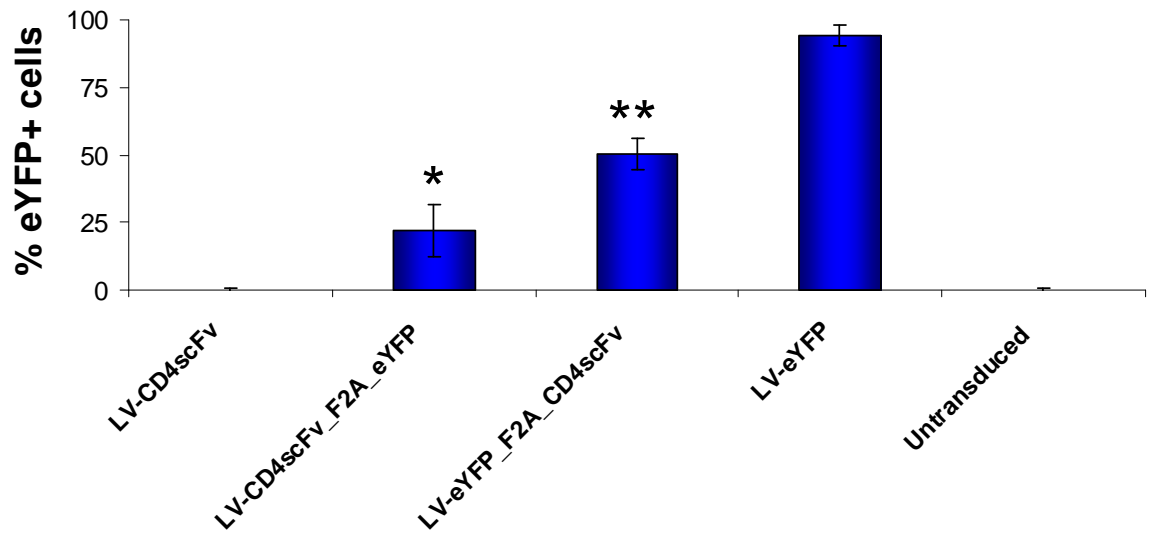
**A**



**B**



**C**



was 2 fold higher from cells transduced with the single-gene eYFP vector (LV-eYFP) compared to expression from LV-eYFP\_F2A\_CD4scFv ( $p=0.005$ ) and almost 4 fold higher when compared to expression from LV-CD4scFv\_F2A\_eYFP ( $p<0.005$ ).

In summary, eYFP expression was significantly lower from each dual-gene vector compared to expression from the single-gene vector. Also, eYFP expression was lowest when positioned downstream of F2A in a dual-gene vector.

### *3.3.c.1.b. Anti-rat CD4 scFv expression from single-gene and dual-gene vectors*

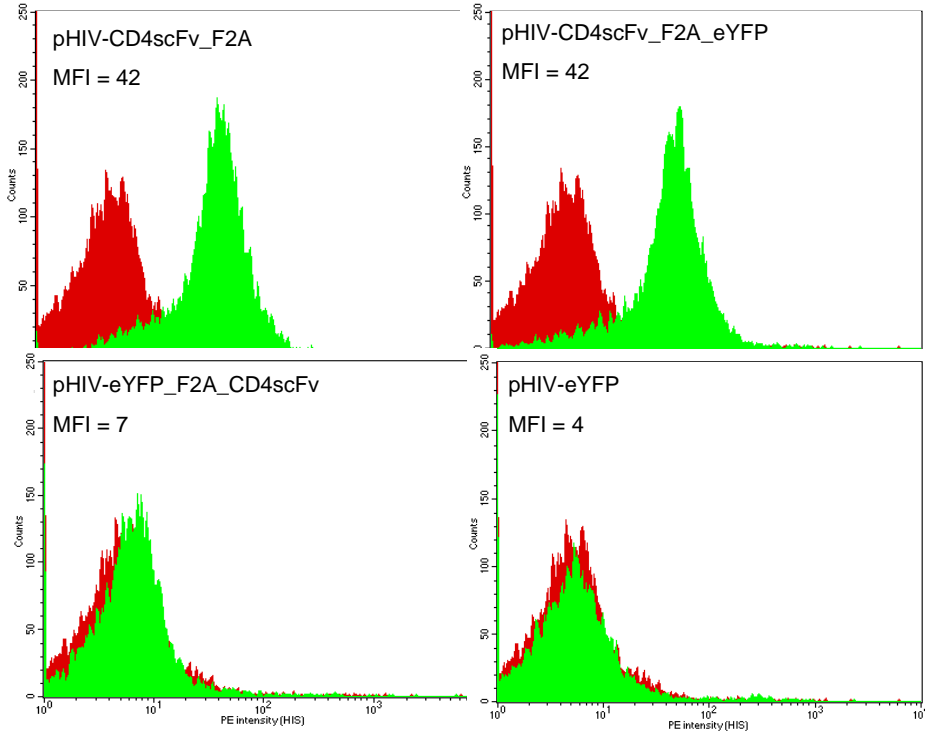
Next, expression of anti-rat CD4 scFv from the dual-gene constructs containing the F2A sequence, pHIV-CD4scFv\_F2A\_eYFP and pHIV-eYFP\_F2A\_CD4scFv was compared to expression from a single-gene construct (pHIV-CD4scFv\_F2A). HEK-293A cells were transfected with the plasmid constructs for 16 hours and then cultured for 5 days, and five biological replicates were performed for each construct in a 6 well plate. Secretion of anti-rat CD4 scFv into the culture supernatant was detected by flow cytometry on rat thymocytes (which express CD4 highly on their cell surface) (Figure 3.19A). A serial dilution of bacterially-produced anti-rat CD4 scFv was used to quantify the amount of scFv present in each supernatant (Figure 3.19B). Comparable levels of anti-rat CD4 scFv expression were detected in cells transfected with the single-gene anti-rat CD4 scFv vector (pHIV-CD4scFv\_F2A) compared to expression from the dual-gene vector, in which the anti-rat CD4 scFv was situated upstream of F2A (pHIV-CD4scFv\_F2A\_eYFP) ( $p>0.05$ ). However expression of the anti-rat CD4 scFv

**Figure 3.19: Anti-rat CD4 scFv detection in culture supernatant of HEK-292A cells after plasmid transfection.** Flow cytometry on rat thymocytes was performed to detect the anti-rat CD4 scFv via the histidine tag. **(A)** Representative histograms (green) show the expression of anti-rat CD4 scFv from transfected cells. The mean fluorescence intensity (MFI) is labelled on each histogram. The untransfected cell supernatant (which is negative for anti-rat CD4 scFv), is represented on each panel in red. **(B)** Anti-rat CD4 scFv expression was quantified from a standard curve prepared from serial dilutions of bacterially produced anti-rat CD4 scFv. The biological samples were averaged (mean), (n = 5). Error bars represent one standard deviation from the mean. \* = Statistically lower expression of anti-rat CD4 scFv from cells transfected with pHIV-eYFP\_F2A\_CD4scFv compared to expression from cells transfected with pHIV-CD4scFV\_F2A\_eYFP (p=0.012) and compared to expression from cells transfected with pHIV-CD4scFv\_F2A (p=0.007) (unpaired Student T-tests).

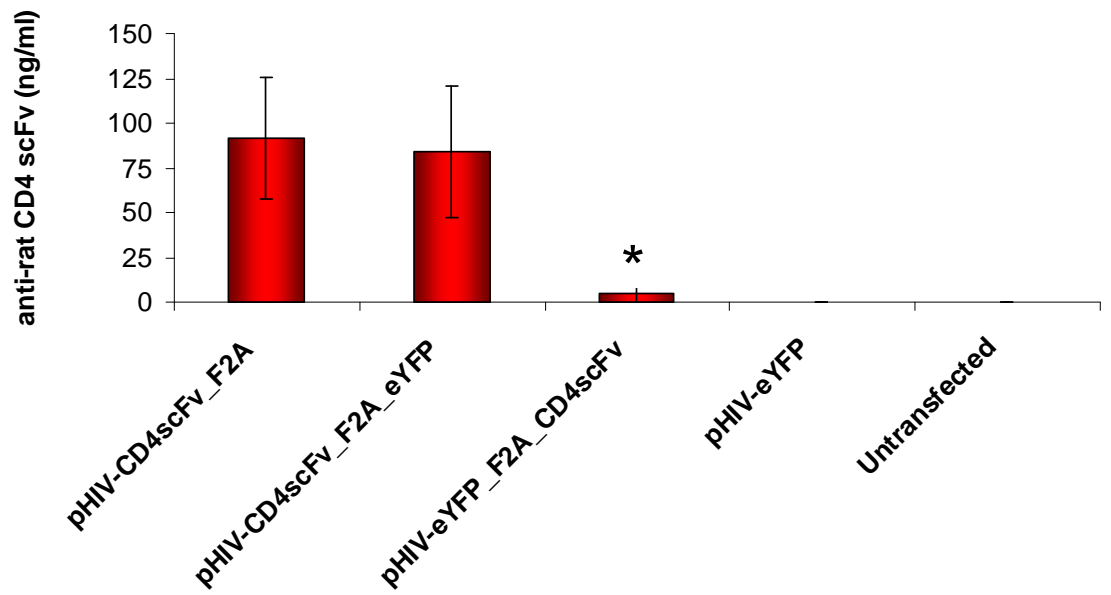
.



**A**



**B**



from the dual-gene construct in which the anti-rat CD4 scFv was situated downstream of the F2A sequence (pHIV-eYFP\_F2A\_CD4scFv), was 20 fold lower when compared to expression of the anti-rat CD4 scFv from the dual-gene vector which had the anti-rat CD4 scFv situated upstream of 2A (pHIV-CD4scFv\_F2A\_eYFP) ( $p=0.012$ ). Anti-rat CD4 scFv expression was also 20 fold lower from cells transfected with pHIV-eYFP\_F2A\_CD4scFv, compared to expression of the anti-rat CD4 scFv from cells transfected with the single-gene vector (pHIV-CD4scFv\_F2A) ( $p=0.007$ ).

In summary, anti-rat CD4 scFv expression was lowest when the anti-rat CD4 scFv was positioned downstream of F2A in a dual-gene vector. However, when anti-rat CD4 scFv was positioned upstream of F2A, anti-rat CD4 scFv expression was comparable to the expression from the single-gene anti-rat CD4 scFv vector.

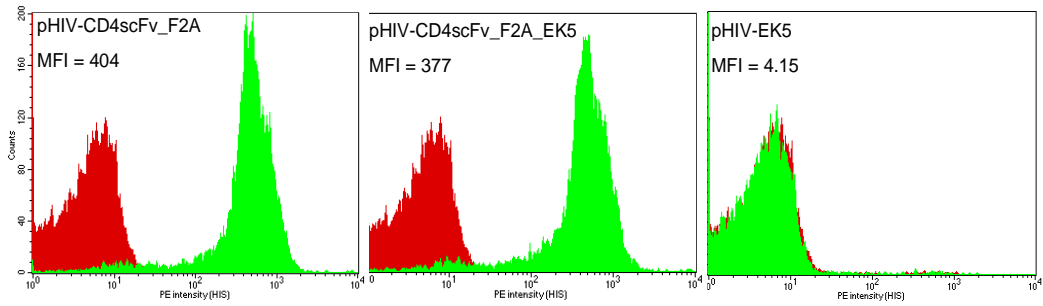
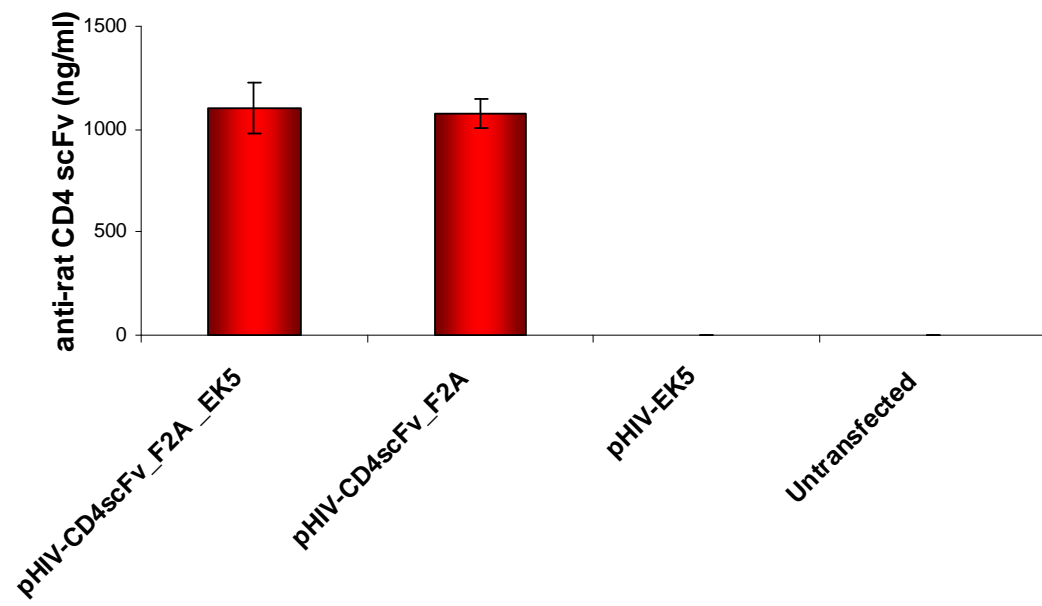
### ***3.3.c.2. Expression of proteins targeted to different cellular compartments***

It was postulated that the reduced detection of the protein downstream of F2A may have been due to “slip-streaming”,<sup>242,245</sup> which occurs when both proteins within a dual-gene 2A construct are translocated through the exocytic pathway, even when the protein upstream contains a leader sequence and the protein downstream does not (i.e., the anti-rat CD4 scFv had a secretory leader sequence and was targeted for secretion, whilst eYFP lacked a leader sequence and remained cytoplasmic). Therefore, the next experiment was performed to determine whether a dual-gene vector carrying two proteins targeted for secretion, (the anti-rat CD4 scFv and EK5), would express similar levels of the protein situated downstream of F2A (EK5), compared to a single-gene EK5 construct, because both anti-rat CD4 scFv and EK5

would be targeted to the same cellular compartment. To test this, CHO cells were transfected with plasmid constructs for 16 hours and then cultured for 5 days. Each plasmid was used to transfect triplicate wells in a 6 well plate. Secretion of anti-rat CD4 scFv into the culture supernatant was detected by flow cytometry on rat thymocytes and a serial dilution of bacterially-produced anti-rat CD4 scFv was used to quantify the amount of scFv present in each supernatant (Figure 3.20). Secretion of EK5 into the culture supernatant was quantified by ELISA (Figure 3.21). Anti-rat CD4 scFv was situated upstream of the F2A sequence in the pHIV-CD4scFv\_F2A\_EK5 vector, and expression of the anti-rat CD4scFv from cells transfected with this construct produced similar levels of anti-rat CD4 scFv compared to the expression from cells transfected with the single-gene anti-rat CD4 scFv vector (pHIV-CD4scFv\_F2A) ( $p > 0.05$ ) (Figure 3.20). EK5 was located downstream of the F2A sequence in the pHIV-CD4scFv\_F2A\_EK5 vector, and expression of EK5 from cells transfected with this construct was approximately 10 fold lower than expression from cells transfected with the single-gene EK5 construct (pHIV-EK5) ( $p = 0.00001$ ) (Figure 3.21).

These results reveal that regardless of whether the proteins either side of the F2A sequence are targeted to the same or different cellular compartments, expression of the protein downstream of F2A appears to be reduced when compared to expression of the same protein from a single-gene construct.

**Figure 3.20: Anti-rat CD4 scFv detection in the culture supernatant of CHO cells transfected with plasmid constructs.** CHO cells were transfected with plasmid constructs for 16 hours and cultured for 5 days. Flow cytometry on rat thymocytes was performed to detect the anti-rat CD4 scFv via the histidine tag. **(A)** Representative histograms (green) show the expression of anti-rat CD4 scFv from transfected cells. The mean fluorescence intensity (MFI) is labelled on each histogram. The untransfected cell supernatant (which is negative for anti-rat CD4 scFv), is represented on each panel in red. **(B)** Anti-rat CD4 scFv expression was quantified from a standard curve prepared from serial dilutions of bacterially produced anti-rat CD4 scFv and triplicates were averaged (mean). Error bars represent one standard deviation from the mean, n=3.  $p > 0.05$ , (unpaired Student T-test).

**A****B**

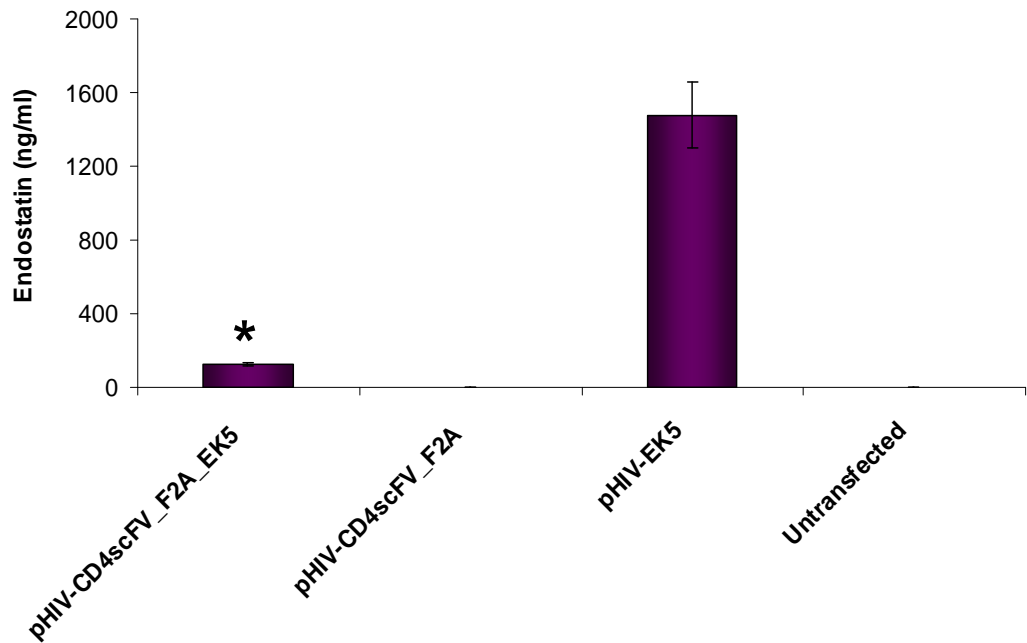


**Figure 3.21: Endostatin::Kringle-5 (EK5) detection in culture supernatant of CHO cells transfected with plasmid constructs.** CHO cells were transfected with plasmid constructs for 16 hours and cultured for 5 days. Secretion of EK5 within the culture supernatant was quantified using a commercially available ELISA kit (R&D Systems, Minneapolis, MN, USA) designed to detect human endostatin. Error bars represent one standard deviation from the mean, n=3. \* = statistically lower expression of EK5 compared to expression from pHIV-EK5, p=0.00001 (unpaired Student T-test).

### 3.4: SUMMARY AND DISCUSSION

#### 3.4.a. Summary

In this chapter, I described the construction and titration of single-gene and dual-gene lentiviral vectors. Transgene expression from these vectors was characterised *in vitro* on adherent cells lines. Functional titration of lentiviral vectors on A549 cells by reporter gene (eYFP) detection yielded comparable titres after 5 days and 4 weeks in culture. When titration was performed by quantifying proviral integration, the 5 day titre produced much higher titres when compared to the eYFP titres, however, after 4 weeks in culture, the proviral integration titres dropped to comparable levels to the eYFP titres. Long term storage of lentiviral vectors at -80°C produced a one-log drop in activity. However, a single freeze-thaw did not affect the activity of a lentiviral vector.

The expression of eYFP from LV-CD4scFv\_F2A\_eYFP and LV-eYFP\_F2A\_CD4scFv was significantly lower, 2 fold and 4 fold respectively, compared to expression of eYFP from the single-gene vector (LV-eYFP). EYFP expression was also 2 fold higher when expressed from the dual-gene construct where it was positioned upstream of F2A (LV-eYFP\_F2A\_CD4scFv) compared to when it was positioned downstream of F2A (LV-CD4scFv\_F2A\_eYFP).

It was proposed that the reduced expression of eYFP may have been due to “slip-streaming”, which occurs when both proteins within a dual-gene 2A construct are translocated through the exocytic pathway. This can occur when the protein upstream contains a leader sequence and the protein downstream does not. However, the

expression of two proteins (each with secretory leader sequences) from a dual-gene construct (pHIV-CD4scFv\_F2A\_EK5), showed 10 fold lower expression of the protein positioned downstream of F2A (EK5), when compared to expression from a single-gene vector (pHIV-EK5). Therefore, the reduced detection of the protein downstream of F2A within a dual-gene vector was unlikely to have been caused by “slip-streaming”.

The expression of anti-rat CD4 scFv from the pHIV-CD4scFv\_F2A\_eYFP construct was comparable to expression from the single-gene counterpart (pHIV-CD4scFv\_F2A). However, expression of anti-rat CD4 scFv from pHIV-eYFP\_F2A\_CD4scFv was 20 fold lower compared to the expression from a single-gene vector (pHIV-CD4scFv\_F2A). Therefore, the *in vivo* experiments described in the following chapter were performed using the pHIV-CD4scFv\_F2A\_eYFP construct, because it produced strong expression of the therapeutic transgene (anti-rat CD4 scFv), even though the expression of eYFP from this vector was too low to be used to determine transduction efficiency, to perform eYFP quantification for vector titration or to track transduced cells *in vivo*.

### **3.4.b. Titration of lentiviral vector preparations**

There are several methods currently used to titre lentiviral preparations (Table 3.6) and most can be categorised into two main groups: non-functional and functional titration methods.<sup>246</sup> Non-functional titration is performed directly on the lentiviral vector preparations, whereas functional titration requires transduction of a cell line followed by quantification of transgene expression.



**Table 3.6: The methods used to titrate lentiviral vectors**

Method of titration	Non-functional/ Functional	References
Quantification of RNA in viral supernatant	Non-functional	250 265 270 259 264 256 254 261
Quantification of gag (p24) in viral supernatant	Non-functional	271 251 254 261
Quantification of reporter protein expression	Functional	252 255 264 251 256 257 261 254
Drug resistance	Functional	260
Quantification of mRNA expression of a transgene	Functional	263 256 266 254 247
Quantification of integrated proviral DNA	Functional	253 267 268 248 262 264 256 249

Non-functional titration methods include the quantification of viral RNA<sup>250,256,259,261,264-265,270</sup> or p24 protein<sup>251,254,261,271</sup> within lentiviral vector preparations. While non-functional titration methods produce rapid results, they grossly overestimate functional titre due to the presence of defective interfering particles and inhibitors of transduction within the viral preparations.<sup>256,264</sup> It has also been shown that only between 0.1-1% of a typical viral particles present in a viral preparation are actually infectious.<sup>265</sup>

Functional titration methods traditionally involve the transduction of a cell line with a lentiviral vector followed by quantification of a reporter gene by flow cytometry,<sup>251-252,255-257,261,264</sup>  $\beta$ -galactosidase staining<sup>257</sup> or drug resistance.<sup>260</sup> Functional titres are highly reliable and produce consistent titres.

The development of lentiviral vectors carrying therapeutic transgenes rather than reporter genes has created a need for functional titration methods that do not rely on reporter gene expression or drug resistance. For these lentiviral vectors, mRNA expression of a transgene can be quantified using qRT-PCR. This titration method has been proven to be a reliable alternative when a reporter gene is not present, producing viral titres comparable to those yielded by reporter gene quantification using flow cytometry.<sup>254,256</sup>

Functional titration of lentiviral vectors that do not express a reporter gene can also be determined by calculating the number of integrated proviral particles per cell.<sup>256,264</sup> I demonstrated that after 5 days in culture, proviral integration titres were much higher than eYFP flow cytometric titres on the same viral preparation (Table

3.3). The high copies per cell calculated after 5 days in culture are most likely due to carry-over of plasmid DNA from the transfection process. Anson revealed that treatment of viral preparations with nucleases did not remove contaminating DNA (Anson, personal communication). A possible explanation may be that the DNA used in the transfection is bound with the calcium phosphate co-precipitate, which is protects the DNA from nuclease attack. On the other hand, Sastry *et al.* showed that <0.01% of contaminating DNA in lentiviral preparations is transferred to cells during transduction.<sup>264</sup> The variation in plasmid contamination between studies may be due to differences in the cell lines used for virus production and titration, the transduction conditions, and the amount of contaminating DNA present in the viral preparation.

Other studies have also reported higher titres from quantification of proviral integration compared to quantification of reporter gene (GFP) expression on the same viral preparation after less than a week in culture<sup>256,264</sup> and after 2 weeks in culture.<sup>264</sup> The conclusions made by these authors were that the reporter gene titres were lower than the proviral integration titres due to the lack of GFP expression by some of the integrated lentiviral particles and/or that a significant proportion of the viral vectors integrated into areas of the genome that were not amenable to gene transcription.<sup>256,264</sup> However, in this chapter, proviral titration on cells that had been in culture for 4 weeks produced viral titres comparable to the reporter gene (eYFP) titres (Table 3.3). Also, the copies per cell dropped from 39 after 5 days in culture to <1 after 4 weeks in culture (Table 3.3).

Functional titration methods rely on the transduction of a viral vector into cells *in vitro*. Several variables need to be carefully monitored in order to produce consistent

results. Zhang and co-workers studied the effects of controlling parameters when transducing cell lines with lentiviral vectors.<sup>272</sup> They demonstrated that factors such as the volume of viral inoculum used, the number and type of cells being transduced, and the susceptibility and viability of these cells, were all variables that affected the transduction of the target cells.<sup>272</sup> They also found that the exposure time to the viral vector and the vector half-life were other parameters that must be kept consistent in order to produce comparable transduction conditions between experiments.<sup>272</sup>

A number of groups have compared different lentiviral vector titration methods (Table 3.7). Delenda and Gaillard published a comprehensive review of the literature on qPCR methods of titration, such as RNA quantification in viral preparations, mRNA transgene expression and proviral integration and came to the conclusion, that proviral integration is the most accurate method of titration using qPCR.<sup>246</sup>

The findings from this chapter strongly suggest that when the transduced cells are cultured for 4 weeks, prior to testing, proviral integration is a reliable functional titration method, and produces titres that are comparable to titres obtained by reporter gene quantification.

**Table 3.7: Studies that have compared two or more methods of lentiviral titration**

Viral components assayed	Reference	Conclusions
RNA in viral supernatant + reporter protein expression	264	Quantification of RNA in viral supernatant overestimates functional titre due to presence of defective lentiviral particles.
RNA in viral supernatant + reporter protein expression	256	Quantification of RNA in viral supernatant overestimates functional titre due to presence of defective lentiviral particles.
RNA in viral supernatant + reporter protein expression	261	The novel hybridisation assay developed to quantify RNA in viral supernatant produced consist titres, but they were not comparable with the reporter protein expression titres.
RNA in viral supernatant + reporter protein expression	254	Cannot predict functional titre by quantifying the RNA in viral supernatant because functional titre is dependent on vector construct and the cell type transduced.
mRNA transgene expression + reporter protein expression	256	mRNA transgene expression showed a strong correlation with reporter protein expression.
mRNA transgene expression + reporter protein expression	254	Quantifying the mRNA transgene expression is a good alternative for non-fluorescent transgenes.
Proviral integration + reporter protein expression	264	GFP titres were consistently 1-log lower than proviral integration titres.
Proviral integration + reporter protein expression	256	Titres calculated by reporter protein expression were 20 fold lower than proviral integration.
p24 in viral supernatant + reporter protein expression	261	Titres calculated from p24 quantification in viral supernatant were higher than titres calculated from reporter protein expression
p24 in viral supernatant + reporter protein expression	254	Cannot predict functional titre by quantifying the p24 protein in viral supernatant because functional titre is dependent on vector construct and the cell type transduced.
p24 in viral supernatant + RNA in viral supernatant	261	Titration of p24 in viral supernatant quantified the total number of viral particles (both empty and packaged with RNA genomes) and subsequently calculated higher titres than titres that quantified the RNA in viral supernatant
Proviral integration + mRNA transgene expression	256	Proviral integration produced higher titres than those that quantified mRNA transgene expression

### 3.4.c. Multigenic expression using the 2A self-processing sequence

Picornaviruses are positive strand RNA viruses that encode all their proteins in a single ORF in the form of a 225 kDa polyprotein.<sup>273</sup> In some genera of the picornavirus family, including the enterovirus and rhinovirus, primary cleavage of the P1 capsid protein precursor and the replicative domains of the polyprotein are cleaved by a virus-encoded proteinase (2A<sup>pro</sup>) which is ~17 kDa. However, aphthoviruses, such as the FMDV, encode a relatively small 2A self-processing sequence (18 amino acids) which undergoes self-processing in between the 2A C-terminal glycine and the 2B N-terminal proline residue in an enzyme-independent manner.<sup>274-276</sup> FMDV 2A-like sequences with self-cleavage activity have been identified in other organisms, including other picornaviruses, Type C rotaviruses, insect viruses, parasitic protists and a bacterium.<sup>277</sup> The cleavage of 2A and 2A-like sequences occurs in only eukaryotic ribosomes and not in prokaryotic ribosomes.<sup>278</sup>

The mechanism of 2A self-processing has been identified as a translational 'skipping' of peptide bond formation between the 2A glycine and the 2B proline residues at the ribosome.<sup>229,279</sup> In its native state, 2A/2B cleavage is complete, however, many studies have shown incomplete cleavage in an artificial setting ranging from 5-20% accumulation of uncleaved polyprotein products.<sup>229,240-242,275,277-278</sup> Cleavage of 2A can be enhanced by the addition of the FMDV 1D sequence upstream of 2A.<sup>229,242,277-278</sup> The addition of 5 1D amino acids reduced the accumulation of uncleaved material and the addition of 14 1D amino acids resulted in complete cleavage.<sup>277</sup> The addition of 39 1D amino acids has been shown to result in complete cleavage in an artificial setting. However, the additional residues attached to the upstream protein interfered with its function.<sup>241</sup> These results indicate

that the upstream protein structure within the ribosomal exit tunnel plays a role in the processing of 2A.

To reduce and/or eliminate interference of the 2A residues that remain attached to the C-terminus of the upstream protein, some groups have added a 3 amino acid spacer (glycine, serine, glycine) between 2A and the upstream protein<sup>232,241</sup> and others have added a furin cleavage site which causes the removal of the attached 2A residues by furin cleavage in the Golgi apparatus.<sup>238-239</sup> The dual-gene vectors constructed as part of the work described in this chapter, consisted of the first transgene followed by the F2A sequence, which consisted of a furin cleavage site located immediately upstream of 5 FMDV 1D residues, 18 FMDV 2A residues and the FMDV 2B proline residue. The second transgene was positioned downstream of the F2A sequence (Figure 3.22).

I discovered that a dual-gene vector carrying an upstream transgene with a secretory sequence (anti-rat CD4 scFv) and a downstream transgene without a signal sequence (eYFP) showed reduced expression of the downstream transgene after transduction into HEK-293A cells, when compared to a single-gene eYFP vector (Figure 3.18). Also, a dual-gene vector carrying the same transgenes in the reverse order was used to transfect HEK-293A cells. In this vector the upstream transgene (eYFP) lacked a signal sequence and the downstream transgene contained the secretory sequence (anti-rat CD4 scFv). Once again there was lower expression of the downstream transgene (this time it was anti-rat CD4 scFv), compared to expression from a single-gene vector (Figure 3.19).

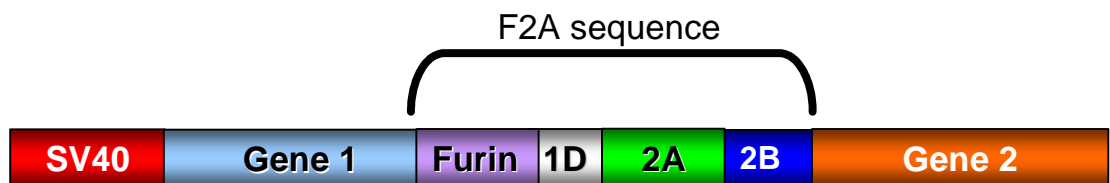


**Figure 3.22: Schematic of the dual-gene open reading frame (ORF) used in this study.** The first gene was positioned upstream of the F2A sequence. The F2A sequence consisted of a furin cleavage site which was upstream of 5 FMDV 1D residues, followed by 18 FMDV 2A residues and the FMDV 2B proline residue. The second gene was positioned downstream of the F2A sequence. Expression was controlled by the internal SV40 promoter.



It was also noted that both anti-rat CD4 scFv and eYFP expression was lower when positioned downstream of 2A compared to when they were situated upstream of 2A (Figures 3.18 and 3.19). It was postulated that a ‘slipstreaming’ effect was the cause of lower expression of the downstream protein. ‘Slipstreaming’ occurs when the protein upstream of 2A (carrying a signal sequence), and the protein downstream of 2A (lacking a signal sequence), are both translocated through the exocytic pathway.<sup>242,245</sup> To test whether ‘slipstreaming’ was causing lower detection of the downstream protein, an additional vector was constructed, pHIV-CD4scFv\_F2A\_EK5, which contained the anti-rat CD4 scFv and EK5, both of which carry secretory signals and should therefore be targeted for secretion into the culture supernatant after transfection. Expression of the transgene downstream of F2A, EK5, was approximately 10 fold lower compared to the expression of EK5 from a single-gene vector (Figure 3.21). On the other hand, expression of the transgene upstream of F2A (anti-rat CD4 scFv) was comparable to the expression of anti-rat CD4 scFv from the single-gene vector (Figure 3.20). These results suggest that it was not the ‘slipstreaming’ effect which was causing lower detection of proteins positioned downstream of F2A.

Furthermore, eYFP expression was lower when positioned upstream of 2A in a dual-gene vector, compared to expression from a single-gene construct. However, anti-rat CD4 scFv expression was comparable from a dual-gene vector when positioned upstream of 2A compared to expression from a single-gene construct. A possible explanation for the differences in expression of anti-rat CD4 scFv and eYFP when situated upstream of F2A could be that not all polyproteins undergo self-cleavage at the 2A sequence during translation.<sup>229,279</sup> If this were the case, then folding of the

upstream protein might be affected and the eYFP protein might be more sensitive to misfolding than the anti-rat CD4 scFv, and subsequently might therefore not be detectable under blue light.

Multiple studies have reported equimolar ratios of proteins upstream and downstream of the 2A self-processing sequence.<sup>238-239,244</sup> However, there also have been reports of an imbalance of protein expression when using 2A to express two transgenes within a single ORF, with the protein upstream of 2A being expressed at higher levels than the protein downstream of 2A.<sup>229,241,279</sup> The molar excess of the upstream protein was the initial inspiration for the 2A ribosomal ‘skip’ mechanism hypothesis.<sup>229,279</sup> The hypothesis stated that molar excess of the protein upstream of 2A may be caused when the translational ‘pause’ occurs at the ribosome. In this ribosome ‘skip’ model there are three proposed outcomes. The first outcome results in no ‘skip’ between the 2A glycine and 2B proline, producing an uncleaved polyprotein. The second outcome results in a ‘pause’ and a break in the peptide bond between the 2A glycine and the 2B proline, followed by resumption of translation of the downstream protein after the 2B proline. The third outcome results in termination of translation at the 2A glycine/2B proline bond. This model accounts for the imbalance in the downstream and upstream 2A proteins as well as the small amount of uncleaved product.<sup>229,279</sup> Funston *et al.* also reported a molar excess of the protein upstream in a dual-gene construct containing a FMDV 2A, but not in a dual-gene construct encoding a porcine teschovirus 2A-like sequence.<sup>241</sup>

In summary of my own data, regardless of whether the upstream or downstream protein contains a secretory signal sequence, there is consistently lower expression

(between 2 and 20 fold) of the downstream protein compared to a single-gene vector carrying the same transgene, or when the same transgene is located upstream of 2A in the reverse-order construct. The molar imbalance described above may explain these findings. One possible explanation for the molar excess observed in some studies and not others, may be that the upstream protein is influencing the 'skip' mechanism (the importance of the sequence upstream of 2A has already been discussed). Another explanation may be that some authors are assuming equimolar expression of both transgenes, when this may not in fact be the case.

Other methods that have been used to express multiple transgenes from a single construct include the use of internal ribosome entry sites (IRES),<sup>231,280-282</sup> internal promoters<sup>231</sup> and bidirectional promoters.<sup>242</sup> The expression of multiple genes from vectors containing either 2A or IRES sequences has been directly compared. The first gene produced similar expression levels from both 2A and IRES constructs, however expression of the second gene was higher from 2A constructs.<sup>240,242-243</sup> Also, a 2A dual-gene vector produced higher expression of both genes when compared to a dual-gene vector using internal promoters.<sup>231</sup>

Amendola *et al.* have developed a dual-gene construct using a bidirectional promoter consisting of a minimal core promoter from elements of human cytomegalovirus joined upstream and in opposite orientation to an efficient promoter, phosphoglycerate kinase (PGK). These bidirectional constructs produced more efficient expression of both gene products than 2A or IRES constructs and both transgenes were expressed at levels comparable to single-gene counterparts *in vitro*, *ex vivo* and *in vivo*.<sup>242</sup>

Multi-gene transfer vectors have been used for a variety of functions, such as the expression of a therapeutic gene coupled to a reporter gene for simple detection of transduction efficiency and vector titration<sup>233,236</sup> or to track the location of gene delivery *in vivo*.<sup>240,242</sup> Dual-gene vectors have been used to confer a proliferative potential upon transduced cells<sup>235</sup> and to express various subunits of a large molecule.<sup>237-239,244,283</sup>

The results described in this chapter suggest that there is reduced expression of the transgene situated downstream of 2A. However others have shown that expression of the downstream transgene is still higher using 2A compared to dual-gene vectors carrying internal promoters or IRES. The use of bidirectional promoters appears to be a more efficient method of dual-gene expression; however for expression of three or more transgenes within a single construct, 2A appears to be the best choice currently. Quad-gene 2A vectors have already been developed using 2A sequences from different viruses.<sup>237</sup>

In summary, even though there is reduced expression of a protein when it is positioned downstream of 2A in a dual-gene vector compared to a single-gene counterpart vector, expression of the downstream protein might still be adequate for its intended function. Further testing should be performed to determine the level of expression required for a particular protein to produce a desired outcome. In the *in vivo* experiments described in the following chapter, the pHIV-CD4scFv\_F2A\_eYFP construct was used because it produced strong expression of the therapeutic transgene (anti-rat CD4 scFv), even though the expression of eYFP from this vector

was too low to be used to determine transduction efficiency, to perform eYFP quantification for vector titration or to track transduced cells *in vivo*.

**CHAPTER 4: EXPRESSION OF ANTI-RAT CD4 SCFV AT  
POTENTIAL SITES OF ANTIGEN PRESENTATION**

## 4.1 ABSTRACT

Aim: To investigate the anatomic site of antigen presentation during corneal transplantation in the rat. To achieve this, an anti-rat CD4 scFv was delivered in a lentiviral vector (LV-CD4scFv\_F2A\_eYFP) to sites of interest, including the donor corneal endothelium, the anterior segment of the eye and the cervical lymph nodes.

Methods: Transduction of the donor corneal endothelium with LV-CD4scFv\_F2A\_eYFP was performed immediately prior to corneal transplantation by *ex vivo* transduction. Transduction of both the donor and recipient corneal endothelium 5 days prior to grafting was achieved by anterior chamber injection of the lentiviral vector. LV-CD4scFv\_F2A\_eYFP was injected into the cervical lymph nodes of recipient rats 2 days prior to corneal transplantation. A group of rats underwent *bilateral* lymphadenectomy of the cervical lymph nodes 7 days prior to corneal transplantation. Corneal allografts were scored daily for signs of rejection, inflammation and neovascularisation. Expression of the anti-rat CD4 scFv from transduced tissues was detected using flow cytometry and PCR. Results: Significant prolongation of corneal allograft survival was experienced by rats that received *ex vivo* transduction of the donor corneas with LV-CD4scFv\_F2A\_eYFP immediately prior to corneal transplantation. However, delivery of the lentiviral vector 5 days prior to corneal transplantation by anterior chamber injection into both the donor and recipient, did not prolong corneal allograft survival. Intranodal injection of LV-CD4scFv\_F2A\_eYFP did not affect the survival of the corneal allografts and neither did *bilateral* lymphadenectomy of the cervical lymph nodes 7 days prior to corneal transplantation. Conclusions: Neither expression of the anti-rat CD4 scFv in the cervical lymph nodes nor the removal of these nodes was able to prolong corneal allograft survival in rats, suggesting that antigen presentation can occur elsewhere,

even though extensive evidence from other studies has highlighted the critical role these lymph nodes play in corneal allograft rejection in mice. Expression of the anti-rat CD4 scFv from the donor corneal endothelium *was* able to prolong corneal allograft survival. These results suggest antigen presentation does occur within the anterior segment of the eye as expression of the anti-rat CD4 scFv from the donor corneal endothelium was able to modulate antigen presentation. However, because all corneal allografts did eventually reject, suggests that rejection was merely delayed and that antigen presentation could also occur elsewhere in the body. Potential sites include the conjunctiva-associated lymphoid tissue (CALT), the cervical lymph nodes or other secondary lymphoid organs.

## **4.2 INTRODUCTION**

### **4.2.a. Corneal graft rejection**

In Australia, human corneal grafts experience high survival rates of >90% at one year post surgery.<sup>13</sup> However, the survival rate drops considerably within ten years post surgery, with a ten-year Kaplan Meier corneal graft survival of 60%.<sup>13</sup> In addition, there have only been modest improvements to the survival rates of corneal allografts over the last 20 years, mainly because the approach for preventing and treating corneal graft rejection has not changed significantly over this period.<sup>13</sup> For these reasons, it is evident that a novel therapy for the prevention of corneal graft rejection is necessary.

### **4.2.b. Regional immunosuppression**

A novel approach to prevent corneal allograft rejection could be to use a regional immunosuppressive strategy. This might be achieved by delivering an antibody



fragment to the actual site where the immune response is being generated. Regional immunosuppression has the potential to have a more potent effect, be more cost effective and may further reduce any potential side effects compared to systemic delivery of an antibody fragment. Regional immunosuppression can only be performed if the site of antigen presentation has been identified. Currently, this is uncertain. As discussed in Section 1.6.d.2., the cervical lymph nodes have been reported to be essential for corneal allograft rejection in mice.<sup>120</sup> Their role in rat corneal allograft rejection is not currently known, however the work of Tilney<sup>105</sup> and the McMenamin group,<sup>106-107</sup> has provided insight into the drainage of ocular antigen in the rat, which appears to follow a similar pattern to that seen in the mouse (into the cervical lymph nodes).<sup>106-107</sup>

Another potential site of antigen presentation could be within the ocular tissue. Infiltrating T cells, NK cells and APCs have been identified within the rat and human cornea at the time of rejection.<sup>34-35</sup> Moreover, Rosenbaum and colleagues have reported the interaction of stationary APCs with mobile T cells within the iris,<sup>92</sup> and Dullforce and colleagues have reported that uveal tract APCs do not appear to migrate after antigen uptake.<sup>91</sup> For these reasons it is believed that antigen presentation might be occurring within the cornea or the uveal tract.

In summary, the potential sites of antigen presentation in response to corneal transplantation might be within the cervical lymph nodes, or in the ocular environment, including the cornea, or the anterior segment of the eye. The work described in this chapter aimed to identify which of these sites (if any) were involved

in antigen presentation in response to corneal transplantation in the rat, by expressing an anti-rat CD4 scFv in these tissues.

#### **4.2.c. Anti-rat CD4 scFv as an immunosuppressive agent**

The anti-rat CD4 scFv is a suitable immunosuppressive agent to investigate the site of antigen presentation in response to corneal transplantation for several reasons. CD4 is abundantly expressed on T cells and because CD4 is essential for antigen presentation,<sup>38</sup> inhibiting its function will prevent T cell activation and prolong corneal allograft survival (Table 1.1). In addition, by inhibiting the function of CD4 with the local expression of an anti-rat CD4 scFv, the actual site of antigen presentation can be identified, because CD4 is expressed on T cells and not on migratory or stationary APCs.

An anti-rat CD4 scFv has been shown to inhibit alloproliferation in a mixed lymphocyte reaction (MLR).<sup>221</sup> However, when the anti-rat CD4 scFv was delivered to the corneal endothelium of donor corneas using an adenoviral vector immediately prior to corneal transplantation in rats, there was no prolongation of allograft survival.<sup>221</sup> Further, when the donor corneas were transduced with the adenoviral vector carrying the anti-rat CD4 scFv three days prior to corneal transplantation (by anterior chamber injection into the donor rat, so that the scFv was being expressed at the time of grafting), there was still no prolongation of corneal allograft survival.<sup>221</sup> Adenoviral expression of the anti-rat CD4 scFv peaked 4-5 days after transduction and by day 8-14 very little anti-rat CD4 scFv was detected.<sup>221</sup> Thus sustained expression of the anti-rat CD4 scFv may be required for prolonged corneal allograft survival, or alternatively, antigen presentation may not occur within the eye, but

rather in the cervical lymph nodes or other secondary lymphoid organs. Another explanation could be that the immunogenicity of the adenoviral vector might have counteracted the immunosuppressive ability of the anti-rat CD4 scFv.

It is hypothesised that sustained expression of the anti-rat CD4 scFv at the site of antigen presentation using a viral vector with minimal immunogenicity (such as a lentiviral vector), will prevent antigen presentation and T cell activation and subsequently prolong corneal allograft survival.

#### **4.2.d. Specific aims**

The experimental aims of the work described in this chapter were to investigate the site of antigen presentation in response to corneal transplantation in the rat. To identify the actual site of antigen presentation, an anti-rat CD4 scFv was expressed at potential sites, including the donor corneal endothelium and the cervical lymph nodes of the recipient. Successful inhibition of antigen presentation was assessed by comparing the survival of the corneal allografts in rats treated with the anti-rat CD4 scFv, to the survival of unmodified corneal allografts. A lentiviral vector was selected for gene transfer of the anti-rat CD4 scFv to target tissues because (1) lentiviral vectors produce long term stable transgene expression in transduced cells<sup>179,226</sup> and (2) lentiviral vectors have low immunogenicity in ocular tissue.<sup>170</sup>

## 4.3 RESULTS

### 4.3.a Lentiviral transduction of the corneal endothelium

#### 4.3.a.1. *Optimisation of lentiviral transduction time for corneal transplantation*

Initial experiments were performed to optimise the incubation time required for a donor rat cornea to be efficiently transduced with a lentiviral vector, without compromising the quality of the cornea for transplantation. Rat corneas were transduced with a lentiviral vector carrying the reporter gene eYFP (LV-eYFP) at a MOI of 400, for either 3 or 24 hours and cultured for 5 days *in vitro*. Corneal flatmounts were stained with the nuclear dye, Hoechst 33258, and visualised under UV light at the fluorescence microscope, where the different layers of the cornea could be seen distinctly, including the epithelium, the stroma and the endothelium (Figure 4.1). Endothelial cell densities were calculated by counting the cell nuclei in 5 central fields (each 0.15 mm<sup>2</sup>). Unmodified corneas had a mean endothelial cell density of 2103 ± 445 mm<sup>2</sup> (n=3). EYFP expression was visualised at the fluorescence microscope under blue light (Figure 4.2) and the percentage of eYFP positive endothelial cells was determined by counting the number of eYFP positive endothelial cells divided by the endothelial density. The percentage of eYFP positive cells expressed from a transduced cornea represented the transduction efficiency of a given lentiviral vector.

There was no significant difference in the mean number of eYFP positive endothelial cells expressed in corneas transduced for 24 hours (45% ± 30) compared to 3 hours (49% ± 13) ( $p > 0.05$ ) (Figure 4.3). The mean endothelial cell density for corneas transduced for 24 hours was 1653 ± 204 mm<sup>2</sup> which was not significantly different

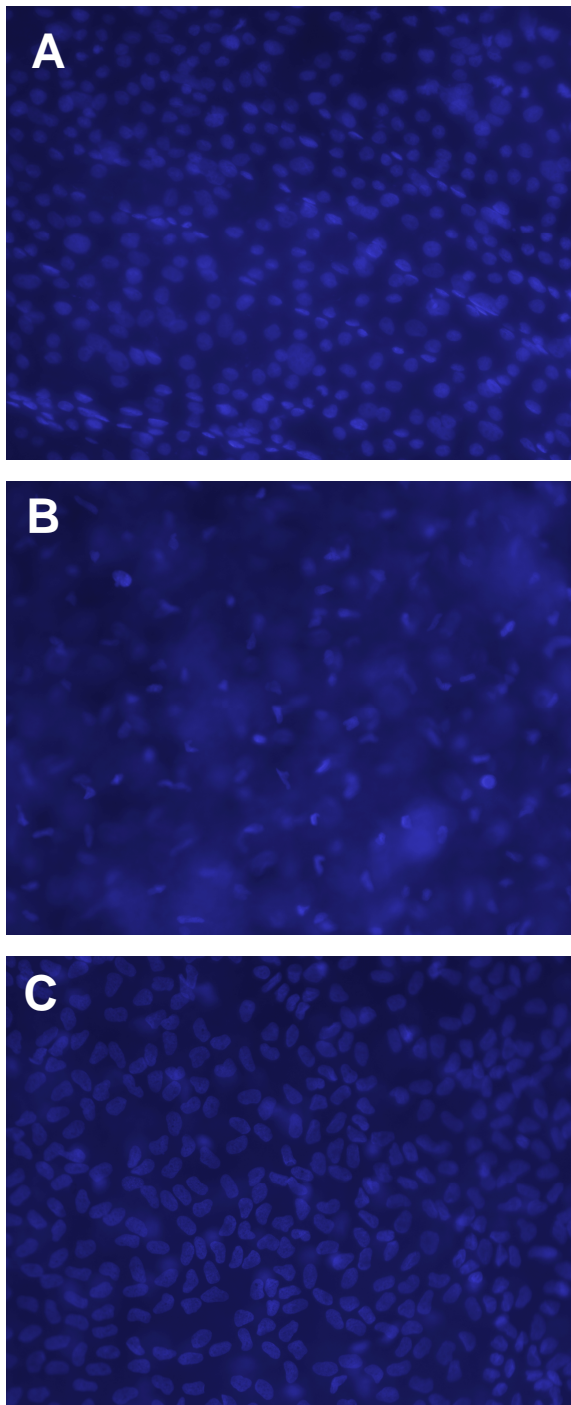


**Figure 4.1: Hoechst 33258 staining of a transduced rat cornea.** Cell nuclei were detected in various layers of the corneal flatmounts including **(A)** the epithelium **(B)** the stroma and **(C)** the endothelial monolayer. Original magnification of all panels: 20X.

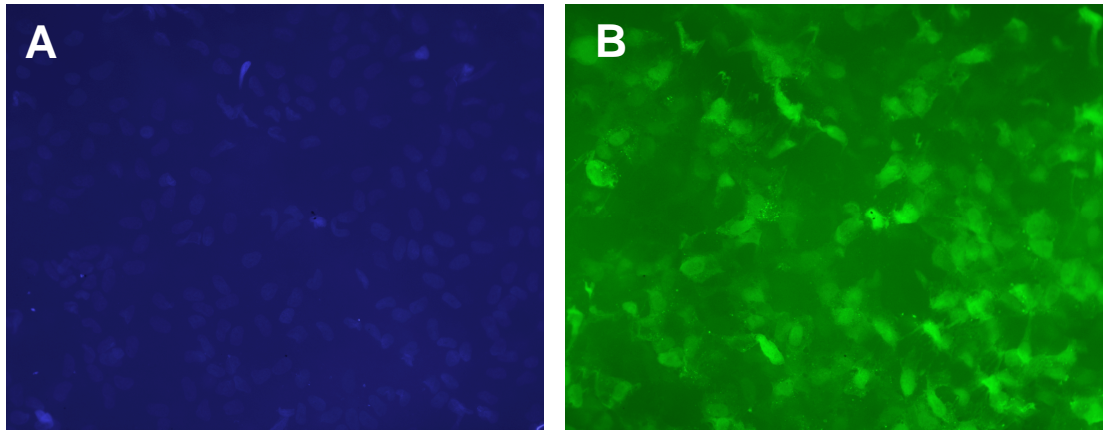


**Figure 4.2: Representative eYFP expression from the rat corneal endothelium after a 3 hour transduction with LV-eYFP.** Rat corneas were transduced with LV-eYFP at an MOI of 400 for 3 hours and cultured for 5 days. Corneal flatmounts were stained with the nuclear dye, Hoechst 33258. Fluorescence images were taken of **(A)** the cell nuclei (under UV light) and of **(B)** the eYFP expression (under blue light), within the same field. Original magnification of all panels: 20X.

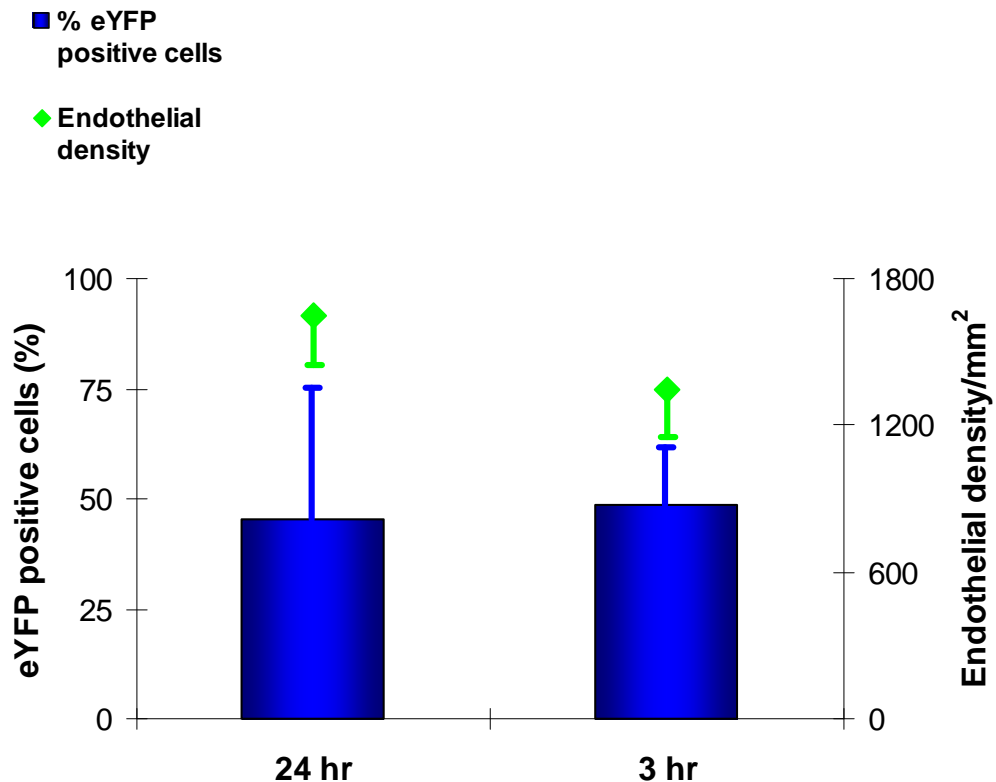


**Figure 4.3: Quantification of eYFP expression from rat corneas after a 24 or 3 hour transduction with LV-eYFP.** Rat corneas were transduced with LV-eYFP at an MOI of 400, for either 24 hours or 3 hours and cultured for 5 days. Rat corneas were stained with the nuclear dye, Hoechst 33258, flatmounted and fluorescence images were taken. The endothelial cell density was calculated by counting the number of endothelial nuclei stained with Hoechst 33258 in 5 central fields (each 0.15 mm<sup>2</sup>). The percentage of eYFP positive cells was determined by counting the number of eYFP positive cells divided by the endothelial density in each field. Error bars represent one standard deviation from the mean, n = 3 corneas. p>0.05, (unpaired Student T-test).

to the mean endothelial cell density of corneas transduced for 3 hours, which was  $1346 \pm 189 \text{ mm}^2$  ( $p > 0.05$ ) (Figure 4.3). When comparing the mean endothelial cell density of unmodified corneas to corneas transduced with lentivirus, (for either 24 or 3 hours), there was also no significant difference ( $p > 0.05$ ).

Thus in summary, a 3 hour transduction was as efficient as the 24 hour transduction, as it produced a comparable percentage of eYFP-expressing endothelial cells. In addition, the corneas appeared to be in a condition suitable for transplantation (with no oedema) after the 3 hour, but not after the 24 hour transduction. Subsequent experiments were performed using a 3 hour transduction with a lentiviral vector.

#### **4.3.a.2. Expression of anti-rat CD4 scFv from rat corneas transduced with lentiviral and adenoviral vectors**

A previous study showed that when the rat corneal endothelium was transduced with an adenoviral vector, strong expression of an anti-rat CD4 scFv was achieved for 4-5 days.<sup>221</sup> However, expression was transient and by days 8-14, very little anti-rat CD4 scFv was expressed from the transduced corneas. In addition, allografts that were transduced *ex vivo* with the adenoviral vector carrying the anti-rat CD4 scFv did not experience prolonged corneal allograft survival.<sup>221</sup> In another study, a rat corneal isograft showed reporter gene expression 60 days post lentiviral transduction, indicating long-term, stable transgene expression.<sup>198</sup>

An experiment was performed to compare the expression of the anti-rat CD4 scFv after transduction of the rat corneal endothelium with either a lentiviral vector (LV-CD4scFv\_F2A\_eYFP) at an MOI of 400, or an adenoviral vector



(Adv-CD4scFv) at an MOI of 320. Rat corneas were transduced with the viral vectors for 3 hours and cultured for 11 days. The culture supernatant was collected and replaced every three days and secretion of the anti-rat CD4 scFv into the culture supernatant was detected using flow cytometry on rat thymocytes (as CD4 is expressed highly on the surface of rat thymocytes) (Figure 4.4).

Significantly higher levels of the anti-rat CD4 scFv were detected in the culture supernatant of rat corneas transduced with the adenoviral vector, compared to the lentiviral vector from days 2-8 ( $p < 0.05$ ), with a 10 fold difference seen at day 5 (Figure 4.4). By day 11 post transduction, the difference in anti-rat CD4 scFv expression was not significant between the rat corneas transduced with either the adenoviral or the lentiviral vector ( $p > 0.05$ ) (Figure 4.4). Anti-rat CD4 scFv expression was detected from adenoviral-transduced corneas 2 days after transduction, whilst lentiviral-transduced corneas did not express detectable levels of anti-rat CD4 scFv until day 5 post transduction. Untransduced corneas did not produce detectable expression of the anti-rat CD4 scFv (as expected) (Figure 4.4). These results reveal a more rapid and stronger expression of the anti-rat CD4 scFv from rat corneas transduced with the adenoviral vector compared to the rat corneas transduced with the lentiviral vector.

#### **4.3.a.3. Ex vivo transduction of rat corneas prior to transplantation**

##### **4.3.a.3.a LV-eYFP corneal isograft**

A previous study reported long term transgene expression in rats after transduction of the donor corneal endothelium with a lentiviral vector.<sup>198</sup> To replicate this and to confirm functionality of the LV-eYFP vector, a single donor cornea was transduced

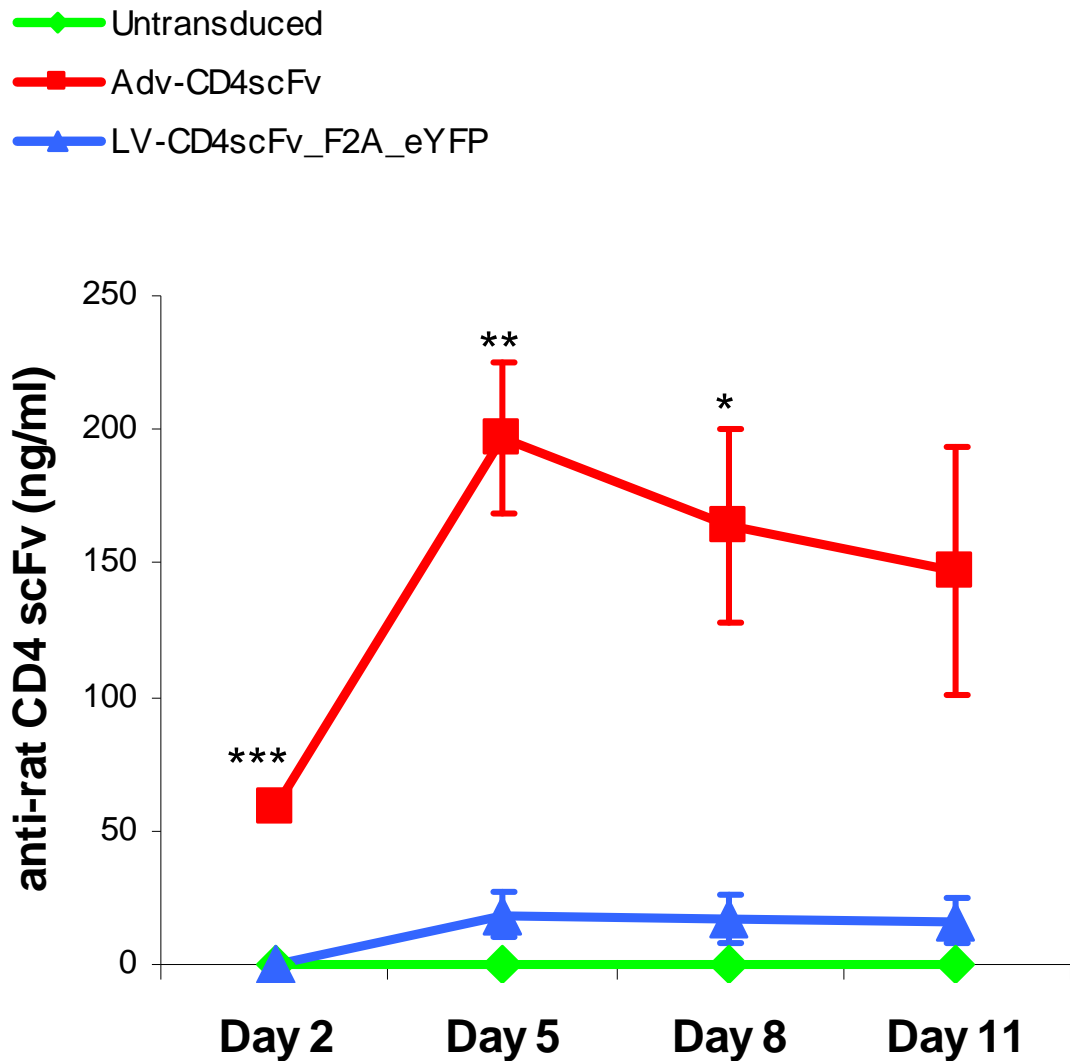


**Figure 4.4: Anti-rat CD4 scFv expression from rat corneas transduced with LV-CD4scFv\_F2A\_eYFP and Adv-CD4scFv.** Rat corneas were transduced with lentiviral (MOI of 400) and adenoviral (MOI of 320) vectors for 3 hours and cultured for 11 days. Culture supernatant was collected and replaced every 3 days from day 2. Flow cytometry on rat thymocytes using culture supernatants was performed to detect anti-rat CD4 scFv via the histidine tag. Error bars represent one standard deviation from the mean, n=3 corneas. \*\*\* represents  $p < 0.0005$ , \*\* represents  $p < 0.01$  and \* represents  $p < 0.05$ , (unpaired Student t-test).

with LV-eYFP prior to transplantation as an isograft. The corneal isograft remained clear for the duration of the experiment (60 days). After 60 days, the LV-eYFP-transduced corneal isograft was flatmounted and Hoechst 33258 stained (Figure 4.5). Images were taken in 5 central fields to visualise both Hoechst 33258-stained nuclei and eYFP expression. Five percent of the endothelial monolayer was seen to express eYFP after 60 days and the endothelium appeared healthy with a cell density of 2699 cell/mm<sup>2</sup> (n=1).

#### *4.3.a.3.b. Transduction of the donor corneal endothelium with viral vectors carrying the anti-rat CD4 scFv*

Donor corneas were transduced *ex vivo* with a lentiviral vector carrying the anti-rat CD4 scFv (LV-CD4scFv\_F2A\_eYFP) at an MOI of 400, for three hours, immediately prior to corneal transplantation of allografts. The control groups for this experiment included unmodified allografts, allografts transduced with LV-eYFP at an MOI of 400, and allografts transduced with Adv-CD4scFv at an MOI of 320 (which previously was shown not to be able to prolong corneal allograft survival).<sup>221</sup>

To detect successful transduction of the donor corneas using the lentiviral and adenoviral vectors carrying the anti-rat CD4 scFv, the remaining donor corneal tissue left over after surgery (the donor corneal rims), were cultured for 5 days and flow cytometry on rat thymocytes was used to detect anti-rat CD4 scFv (via the histidine tag) in the culture supernatants. Anti-rat CD4 scFv expression was detected in every donor corneal rim that was cultured, indicating that the donor corneas had been successfully transduced with both adenoviral and lentiviral vectors (Figure 4.6).

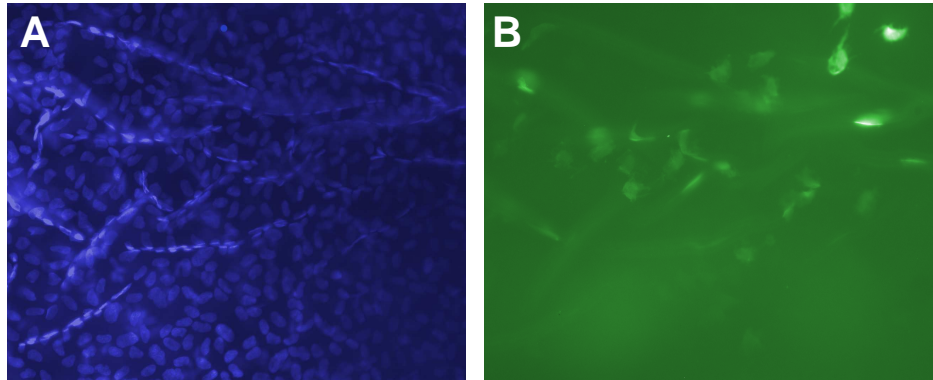


**Figure 4.5: An isograft transduced with LV-eYFP shows eYFP expression after 60 days.** The donor cornea was transduced with LV-eYFP prior to transplantation. After 60 days, the cornea was flatmounted and the endothelial cell nuclei were stained with Hoechst 33258. **(A)** A representative image of the Hoechst 33258-stained endothelial nuclei, visualised under UV light. **(B)** A representative image of eYFP expressing-endothelial cells visualised under blue light. Original magnification of all panels: 20X.

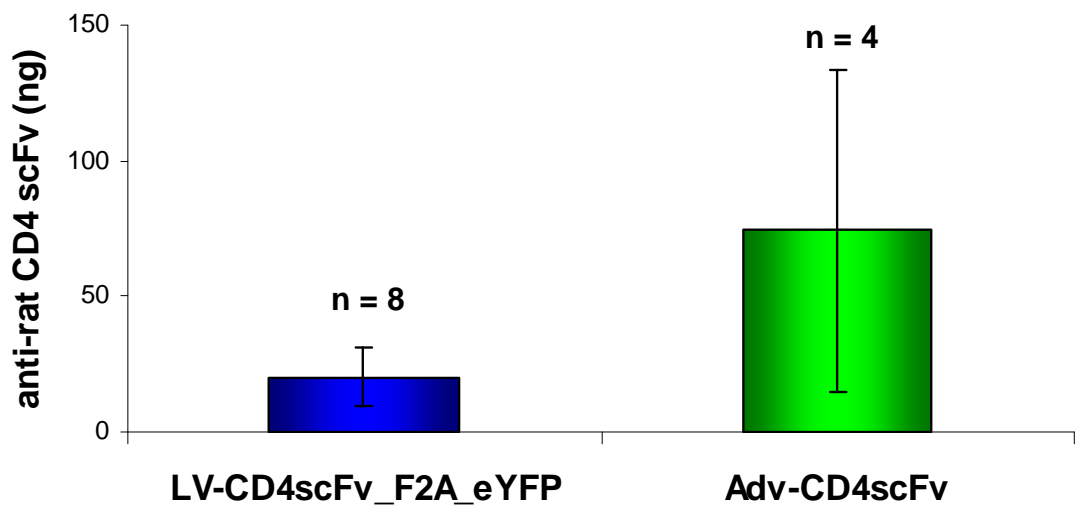


**Figure 4.6: Anti-rat CD4 scFv expression from donor corneal rims transduced with either LV-CD4scFv\_F2A\_eYFP or Adv-CD4scFv.** Flow cytometry on rat thymocytes was performed to detect anti-rat CD4 scFv (via the histidine tag) in the culture supernatant of transduced donor corneal rims after 5 days in culture. Expression of anti-rat CD4 scFv was detected in all donor rims in this experiment. Error bars represent one standard deviation from the mean. The number of corneal rims in each group is marked on the graph. There was no significant difference in anti-rat CD4 scFv expression between the two groups,  $p > 0.05$  (unpaired Student t-test).

Prolonged survival was observed in allografts that were transduced with LV-CD4scFv\_F2A\_eYFP with a median day of rejection of 22 days, compared to allografts transduced with Adv-CD4scFv which had a median day of rejection of 17 days ( $p=0.018$ ) (Table 4.1). Prolonged survival was also observed from corneal allografts transduced with LV-CD4scFv\_F2A\_eYFP when compared to the unmodified allografts and allografts that were transduced with LV-eYFP (both had a median day of rejection of 17 days) ( $p=0.004$ ) (Table 4.1). All of the corneal allografts transduced with LV-CD4sFv\_F2A\_eYFP did eventually reject. Ocular inflammation was also assessed daily on a 0-4 numerical scale with 0.1 increments. Ocular inflammation was similar amongst all groups from days 1-10 post transplantation, however, at day 15, LV-CD4scFv\_F2A\_eYFP-transduced allografts showed significantly less inflammation than allografts transduced with Adv-CD4scFv ( $p<0.005$ ), or allografts transduced with LV-eYFP ( $p<0.01$ ) (Table 4.2). The median day of blood vessel infiltration into the grafted tissue was comparable amongst all groups (Table 4.1).

#### **4.3.a.4. Anterior chamber injection of lentiviral vectors**

##### **4.2.a.4.a. Anterior chamber injection of LV-eYFP**

Data presented in Figure 4.4 revealed a 5 day lag in anti-rat CD4 scFv expression from corneas transduced with the lentiviral vector. Since there was a moderate prolongation of graft survival observed when donor corneas were transduced *ex vivo* with a lentiviral vector carrying the anti-rat CD4 scFv (Table 4.1), the next set of experiments were performed so that corneal transplantation was performed when donor corneas were actively expressing the anti-rat CD4 scFv, i.e. 5 days after transduction.

**Table 4.1: Summary of rat corneal allograft survival after *ex vivo* transduction with viral vectors prior to transplantation**

Treatment	Graft	n	Median day of vessel infiltration into graft	Day of rejection	Median day of rejection
Unmodified	allograft	10	10	11, 12, 14, 15, 16, 18, 19, 19, 20, >60 <sup>^</sup>	17
LV-eYFP	allograft	10	10	10, 11, 14, 15, 16, 18, 19, 19, 27, 30	17
LV-CD4scFv_F2A_eYFP	allograft	8	10	17, 20, 20, 21, 22, 25, 27, 38	22*
Adv-CD4scFv	allograft	8	11	13, 13, 14, 16, 17, 18, 21, 22	17

n = number of animals used in analysis

<sup>^</sup> = graft did not reject

\* = statistically significant compared with Adv-CD4scFv (p=0.018, Mann Whitney U test, corrected for ties) and compared to the unmodified and LV-eYFP allografts, p=0.004, (Kruskal-Wallis, corrected for ties with Bonferroni adjustment)

**Table 4.2: Summary of the ocular inflammation in allografts after *ex vivo* transduction with viral vectors prior to corneal transplantation.**

Inflammation was scored daily on a 0-4 numerical scale with 0.1 increments. This table summarises the median inflammation scores at days 1, 5, 10 and 15 post transplantation for each group.

Treatment	n	Median inflammation scores			
		Day 1	Day 5	Day 10	Day 15
Unmodified	10	0.5	0.6	0.4	0.1
LV-eYFP	10	0.8	0.9	0.2	0.5
LV-CD4scFv_F2A_eYFP	8	0.65	0.75	0.3	0.05*
Adv-CD4scFv	8	0.7	0.7	0.15	0.9

\* = statistically different compared to the Adv-CD4scFv group ( $p < 0.005$ ), and the LV-eYFP group ( $p = 0.01$ ), at day 15 post transplantation (Mann Whitney U tests, corrected for ties).



Because rat corneas are not in a condition suitable for transplantation after 5 days in culture, to achieve active expression at the time of grafting, anterior chamber injections were performed.

Initial experiments involved the injection of LV-eYFP ( $5 \times 10^6$  TU/injection) into the anterior chamber of 15 rats. Eyes were harvested 5 days after injection, fixed in buffered formalin and the cornea, iris and retina were stained with the nuclear stain Hoechst 33258, and the tissues were flatmounted. Fluorescence microscopy was used to detect eYFP-expressing cells within the flatmounts and their corresponding cell nuclei within the same field.

eYFP was expressed in the cornea, iris and retina after initial anterior chamber injection of LV-eYFP (Table 4.3; Figure 4.7). Varying degrees of traumatic damage occurred in some rats after anterior chamber injection, with 4 of 15 rats developing cataracts (Table 4.3).

**Table 4.3: eYFP expression from rat eyes 5 days after receiving an anterior chamber (AC) injection of LV-eYFP ( $5 \times 10^6$  TU/injection).**

Total number of AC injections	eYFP+ corneas	eYFP+ irides	eYFP+ retinae	No. of cataracts
15	11/15	7/15	4/15	4/15

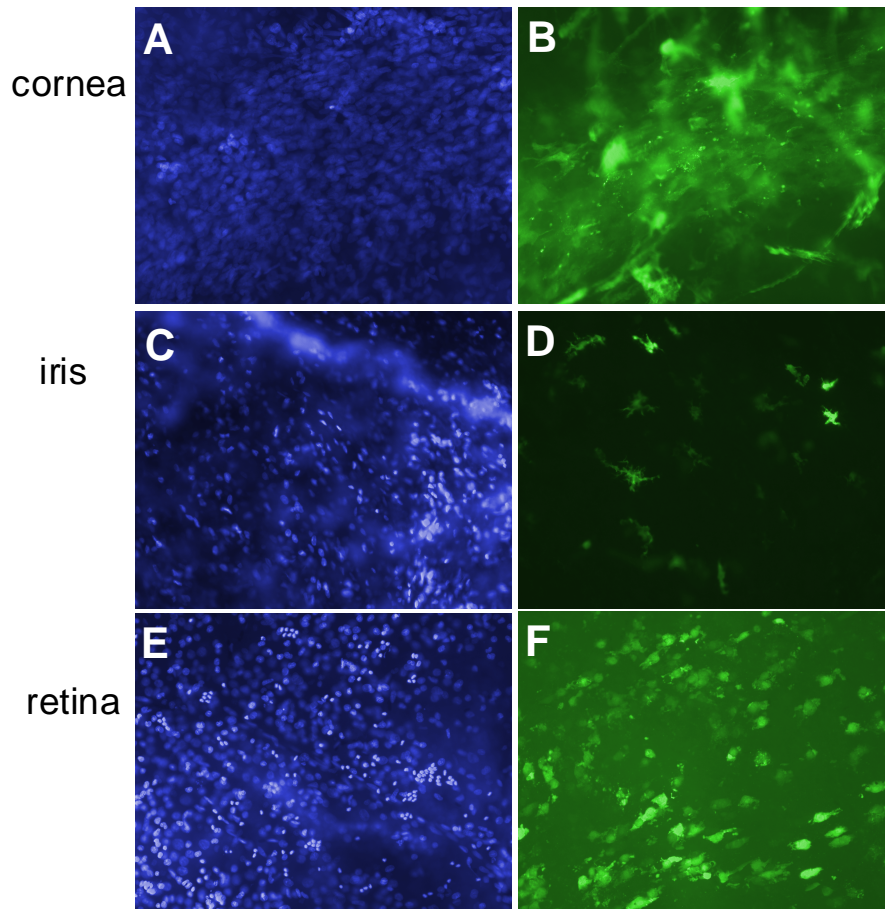


**Figure 4.7: Detection of eYFP-expressing cells within the eye after anterior chamber injection of LV-eYFP ( $5 \times 10^6$  TU/injection).** Five days post injection, eyes were harvested and fixed in buffered formalin. The cornea, iris and retina were Hoechst 33258 stained, flatmounted and images were taken using the fluorescence microscope to visualise Hoechst 33258 stained cell nuclei (under UV light) and eYFP expression (under blue light), within the same field. Panels **A**, **C** and **E** show Hoechst 33258 stained cell nuclei. Panels **B**, **D** and **F** show eYFP-expressing cells. Original magnification of all panels: 20X.

EYFP-expression was observed in 11 of the 15 corneas after anterior chamber injection of LV-eYFP (Table 4.3). However, transduced cells were not uniformly spread throughout the cornea. EYFP-expressing cells within the cornea were mainly observed around the injection and paracentesis sites, with bright eYFP-expression observed within the central area of the cornea. These cells were a combination of endothelial cells and cells with the morphology of APCs (Figure 4.7B). Fainter eYFP-positive cells (in both the endothelium and the stroma) were observed within the peripheral region of the cornea (data not shown). Almost half the total number of eyes that received an anterior chamber injection of LV-eYFP had detectable eYFP expression within the iris (Table 4.3). The eYFP-expressing cells had the morphology of APCs and were uniformly dispersed throughout the iris (Figure 4.7D). Expression of eYFP in the retina was patchy (Figure 4.7F) and was only detected in 4 of the 15 rats that received anterior chamber injection of LV-eYFP (Table 4.3). The eYFP-expressing cells within the retina are likely to be retinal ganglion cells. To determine the actual phenotype of the eYFP-expressing cells with APC morphology, future experiments will involve immunophenotyping using anti-leucocyte mAbs.

#### *4.3.a.4.b. Anterior chamber injection of a lentiviral vector carrying the anti-rat CD4 scFv prior to corneal transplantation*

Preliminary experiments revealed that it was possible to transduce the cells within the cornea, iris and retina with a lentiviral vector after anterior chamber injection. The next step was to determine whether injecting a lentiviral vector carrying the anti-rat CD4 scFv ( $5 \times 10^6$  TU/injection), into both the donor and recipient anterior

chambers, 5 days prior to corneal transplantation, would modulate corneal allograft survival.

All recipient rats that received anterior chamber injections of LV-eYFP developed some degree of lens damage; 4 exhibited minor damage and 4 developed cataracts. The cataracts were only mild and these rats maintained deep anterior chambers with no lens swelling observed and were subsequently used in the allografting experiment. All of the recipient rats that received anterior chamber injections of LV-CD4scFv\_F2A\_eYFP showed minor lens damage from the injections, however no cataracts formed, which might have been a reflection of improved technique as time went by.

Allografts performed in rats that received anterior chamber injection of LV-CD4scFv\_F2A\_eYFP, had a median day of rejection of 13 days, which was comparable to the survival of rats that received anterior chamber injection of LV-eYFP, which had a median day of rejection of 11 days ( $p>0.05$ ) (Table 4.4). There was no significant difference in graft survival between the two anterior chamber injected-allograft groups, compared to the unmodified allografts, which had a median day of rejection of 17 days ( $p>0.05$ ) (Table 4.4). The median day of vessel infiltration into the donor tissue was similar amongst all groups (Table 4.4).

Inflammation scores at day 1 and 5 after grafting were higher in the recipients that received anterior chamber injection of LV-eYFP compared to recipients that received anterior chamber injection of LV-CD4scFv\_F2A\_eYFP ( $p<0.01$ ) (Table 4.5), indicating that the anti-rat CD4 scFv might have inhibited inflammation

**Table 4.4: Summary of rat corneal allograft survival data after anterior chamber injection of lentiviral vectors in both donor and recipient eyes.**

Treatment	Graft	n	Median day of vessel infiltration into graft	Day of rejection	Median day of rejection
Unmodified	allograft	10	10	11, 12, 14, 15, 16, 18, 19, 19, 20, >60 <sup>^</sup>	17
LV-eYFP	allograft	7	11	9, 10, 11, 11, 14, 15, 22	11
LV-CD4scFv_F2A_eYFP	allograft	7	10	11, 12, 12, 13, 14, 22, 33	13

n = number of animals used in analysis

<sup>^</sup> = graft did not reject

p > 0.05 (Kruskal-Wallis, corrected for ties)

**Table 4.5: Summary of the ocular inflammation in allografts after anterior chamber injection of lentiviral vectors prior to corneal transplantation.** Inflammation was scored daily on a 0-4 numerical scale with 0.1 increments. This table summarises the median inflammation scores at days 1, 5, 10 and 15, post transplantation for each group.

Anterior chamber injection	Median inflammation scores				
	n	Day 1	Day 5	Day 10	Day 15
Unmodified	10	0.5	0.6	0.4	0.1
LV-eYFP	7	1.15*	1*	1	0.6
LV-CD4scFv_F2A_eYFP	7	0.3	0.4	0.2	0.1

\* = statistically significant difference compared to the anterior chamber injection of LV-CD4scFv\_F2A\_eYFP at days 1 and 5 ( $p < 0.01$ , Mann Whitney U test, corrected for ties).

triggered either by the trauma of the injection or transplantation. Another possibility could be that the eYFP transgene was immunogenic. Following rejection, the cornea (both the donor button and recipient bed), iris and retina from rats that received anterior chamber injection of LV-eYFP, were flatmounted and residual transduction was assessed (Table 4.6). All donor corneal buttons contained eYFP-positive cells and 2 of 7 recipient corneal beds showed eYFP-positive cells. Two types of eYFP-expressing cells were observed (similar to what was shown in Figure 4.7), in both the donor corneal buttons and the recipient corneal beds: eYFP-positive endothelial cells, and eYFP-positive cells that resembled APCs within the stroma (Figure 4.8).

**Table 4.6: eYFP expression in rats with rejected grafts after anterior chamber injection of LV-eYFP.**

No. of grafts performed	No. of grafts expressing eYFP in donor tissue	No. of rats with eYFP expression in recipient bed	No. of rats with eYFP expression in the iris	No. of rats with eYFP expression in the retina
7	7/7	2/7	4/7	1/7

After rejection, PCR analysis revealed expression of the anti-rat CD4 scFv mRNA from 5 out of 7 corneas that had received anterior chamber injection of LV-CD4scFv\_F2A\_eYFP (Figure 4.9), indicating successful transduction of cells within the corneal tissue in these animals. Some corneas only amplified a very faint band using the anti-rat CD4 scFv primers, indicating that only low levels of anti-rat CD4 scFv were detected in these corneas at the time of rejection. All corneas amplified the correct size product when using primers to amplify ARBP (the housekeeping gene). It is important to note that it was not technically feasible to distinguish between the donor corneal tissue and the recipient bed in the PCR.

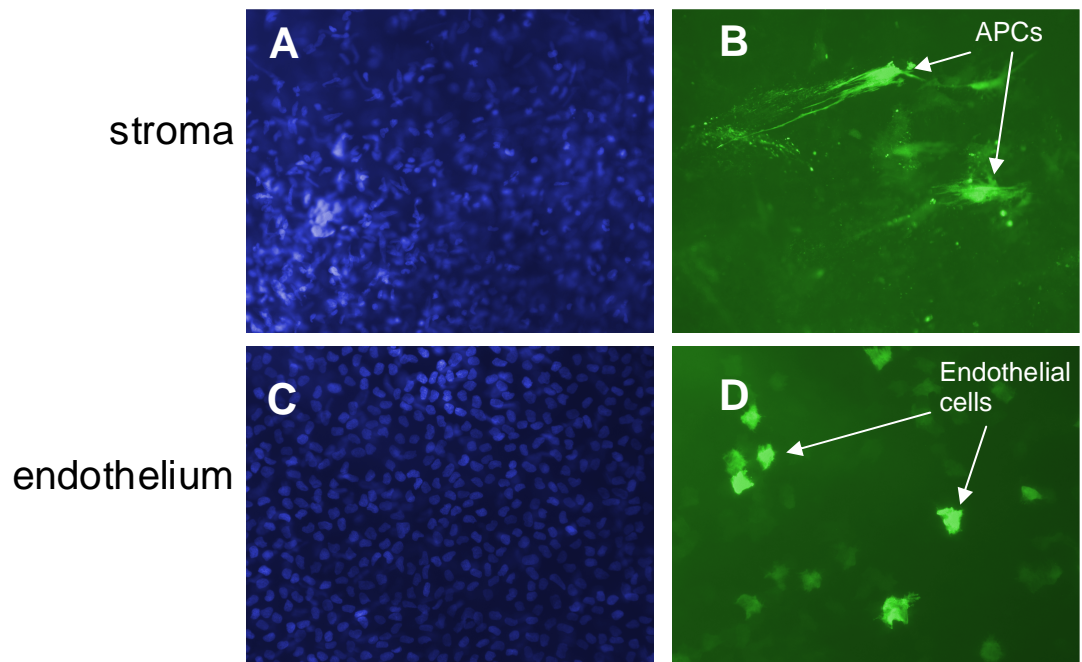


**Figure 4.8: Representative images showing the different types of cells transduced with LV-eYFP within both the donor corneal button and the recipient corneal bed after rejection.** Fluorescence images were taken of Hoechst 33258 stained cell nuclei (under UV light) in the same field as eYFP-expressing cells (under blue light). Panels **A** and **C** show Hoechst 33258 stained cell nuclei. Panels **B** and **D** show eYFP-expressing cells. Panels (A) and (B) are images taken from within the peripheral stroma of a recipient bed. Panels (C) and (D) are images taken of the endothelium of a donor button. Original magnification of all panels: 20X.



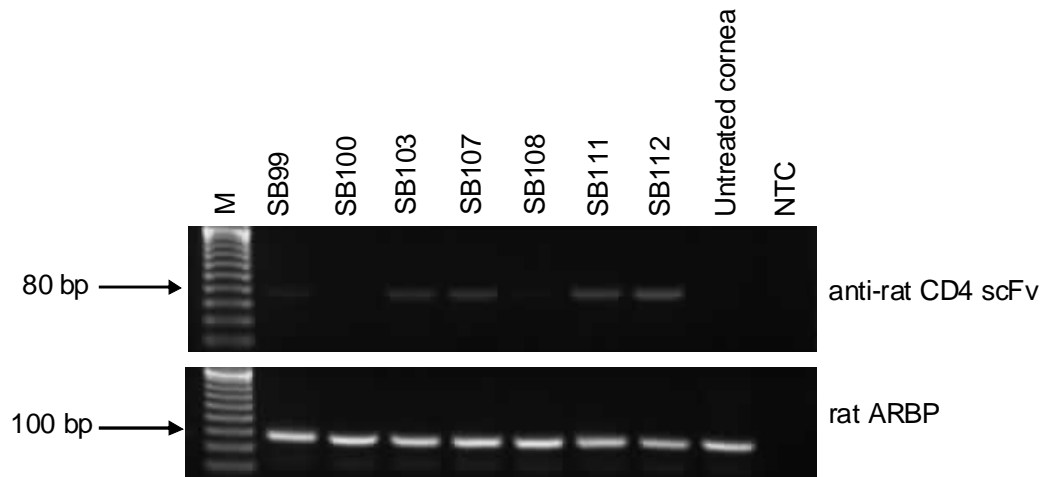


**Figure 4.9: Anti-rat CD4 scFv mRNA expression from rejected corneas from rats that received anterior chamber injections of LV-CD4scFv\_F2A\_eYFP.** Primers specific for anti-rat CD4 scFv and the housekeeper rat ARBP (refer to Table 2.5 for primer sequences) were used in separate reactions. Anti-rat CD4 scFv cDNA was amplified in 5 from 7 treated corneas, with nothing amplifying from the untreated cornea cDNA or in the no template control (NTC; water). Rat ARBP (housekeeper) amplified in all cDNA-containing reactions (as expected). The lane marked M contained the 20 bp ladder.

### 4.3.b. Lentiviral transduction of the cervical lymph nodes

Local immunosuppression by expression of the anti-rat CD4 scFv from the donor corneal endothelium after *ex vivo* lentiviral transduction, resulted in a moderate prolongation of allograft survival, but eventually all allografts did reject (Table 4.1). Some studies have shown lymphatic drainage from the eye to the cervical lymph nodes in rodents (section 1.6.d.)<sup>26,106-107,111</sup> The next set of experiments involved expressing the anti-rat CD4 scFv, using a lentiviral vector, within the cervical (superficial and facial) lymph nodes in the rat (Figure 2.1) (named as reported by Tilney),<sup>105</sup> prior to corneal transplantation.

Preliminary experiments involved the injection of LV-CD4scFv\_F2A\_eYFP ( $5 \times 10^6$  TU/injection) into the cervical lymph nodes (between 4-6 lymph nodes) in 3 rats. Expression of the anti-rat CD4 scFv was determined by qRT-PCR after 2, 5, and 14 days post injection from each individual lymph node. Similar levels of anti-rat CD4 scFv expression were measured at days 2 and 5 post injection, however, by day 14 no anti-rat CD4 scFv was detected (Figure 4.10).

Anti-rat CD4 scFv mRNA was detected 2 days after intranodal injection (Figure 4.10), therefore it was decided that corneal transplantation would be performed 2 days after intranodal injection of a lentiviral vector ( $5 \times 10^6$  TU/injection). Allograft survival in rats that received intranodal injection of LV-CD4scFv\_F2A\_eYFP showed comparable graft survival to allografts in rats that had received an intranodal injection of LV-eYFP, with a median day of rejection of 18 and 17 days respectively ( $p > 0.05$ ) (Table 4.7). The survival of corneal allografts in rats that had received intranodal injection of either LV-CD4scFv\_F2A\_eYFP or LV-eYFP was also

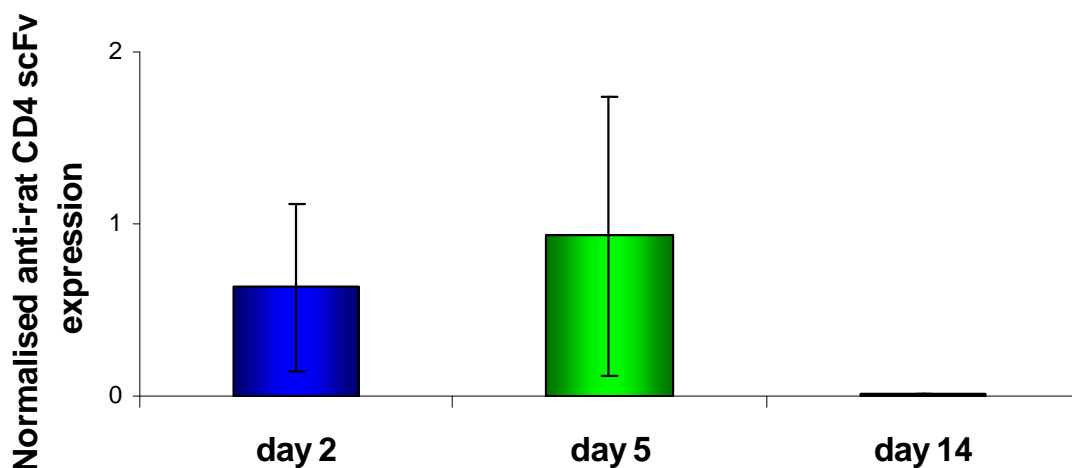


**Figure 4.10: Anti-rat CD4 scFv expression in the cervical lymph nodes, after injection of LV-CD4scFv\_F2A\_eYFP ( $5 \times 10^6$  TU/injection).** Three rats were injected with LV-CD4scFv\_F2A\_eYFP into four-six lymph nodes. At each time point (days 2, 5 and 14 post injection), a single rat was euthanised, all injected lymph nodes were collected, RNA was extracted and anti-rat CD4 scFv mRNA was detected by qRT-PCR in each individual lymph node. Anti-rat CD4 scFv expression was normalised to the housekeepers ARBP and HPRT (refer to Table 2.5 for primer sequence). Error bars represent one standard deviation from the mean of the biological replicates (the different lymph nodes from a single rat).  $n \geq 4$  lymph nodes from a single rat.

**Table 4.7: Summary of the survival of corneal allografts in rats that had received injections of lentiviral vectors 2 days prior to transplantation into the cervical lymph nodes.**

Treatment	Graft	n	Median day of vessel infiltration into graft	Day of rejection	Median day of rejection
Unmodified	allograft	10	10	11, 12, 14, 15, 16, 18, 19, 19, 20, >60 <sup>^</sup>	17
LV-eYFP	allograft	10	10	15, 16, 17, 17, 20, 21, 24	17
LV-CD4scFv_F2A_eYFP	allograft	8	10	12, 15, 16, 17, 19, 19, 20, 23	18

n = number of animals used in analysis

<sup>^</sup> = graft did not reject

p>0.05 (Kruskal-Wallis, corrected for ties)

comparable to the survival of corneal allografts in the unmodified animals, with a median day of rejection of 17 days ( $p>0.05$ ) (Table 4.7). The day of vessel infiltration into the donor cornea was similar amongst all groups (Table 4.7). There was also no difference in inflammation at any time point post transplantation between groups ( $p>0.05$ ) (Table 4.8).

To detect circulating anti-rat CD4 scFv, blood was collected from recipients once a week after grafting until rejection. PBL were isolated, and flow cytometry was performed to detect anti-rat CD4 scFv bound to circulating leucocytes. To detect soluble anti-rat CD4 scFv, flow cytometry using rat plasma was performed against rat thymocytes. No cell bound (Figure 4.11) or soluble (Figure 4.12) anti-rat CD4 scFv was detected within the circulation of any recipient rat at any time point.

It is important to note that there is background fluorescence present in the phycoerythrin (PE) channel of the flow cytometer, even when the anti-histidine antibody is not used (Figure 4.11). This is most likely non-specific binding of the mouse anti-biotin antibody. Positive anti-histidine binding on CD3<sup>+</sup> T cells was detected over this background, when rat PBL was incubated with the anti-rat CD4 whole antibody (OX35) (Figure 4.11D).

#### **4.3.c. Bilateral lymphadenectomy of the cervical lymph nodes**

A previous study has shown that removal of the cervical lymph nodes prior to corneal transplantation resulted in indefinite corneal allograft survival in all mice.<sup>120</sup>

To determine whether the cervical lymph nodes were essential for the rejection of

**Table 4.8: Summary of the ocular inflammation in allografts after intranodal injection of lentiviral vectors into the cervical lymph nodes prior to corneal transplantation.** Inflammation was scored daily on a 0-4 numerical scale with 0.1 increments. This table summarises the median inflammation scores at days 1, 5, 10 and 15, post transplantation for each group.

Intranodal injection	Median inflammation scores				
	n	Day 1	Day 5	Day 10	Day 15
Unmodified	10	0.5	0.6	0.4	0.1
LV-eYFP	10	0.6	0.7	0.1	0
LV-CD4scFv_F2A_eYFP	8	0.6	0.4	0.2	0.1

$p > 0.05$  at each time point between all groups (Kruskal-Wallis, corrected for ties).

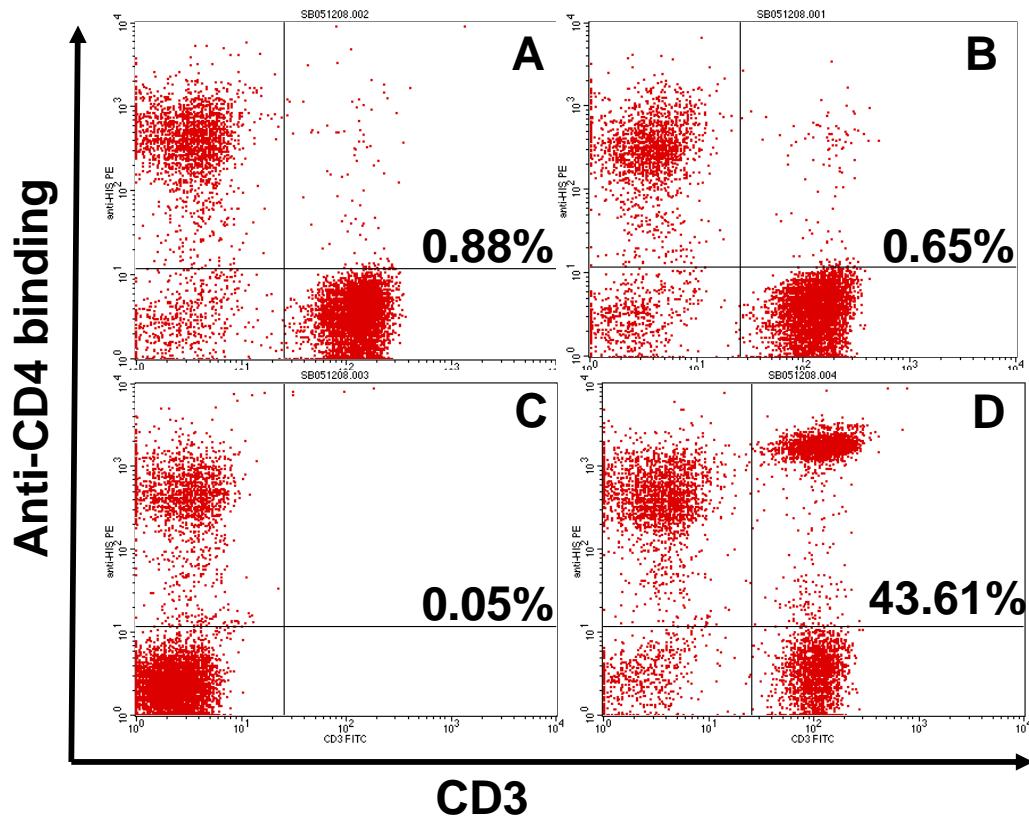


**Figure 4.11: Representative histograms revealing the absence of cell bound anti-rat CD4 scFv in rats that received intranodal injection of LV-CD4scFv\_F2A\_eYFP into the cervical lymph nodes.** Peripheral blood lymphocytes (PBL) were isolated from rats weekly after intranodal injection and flow cytometry was performed to detect the presence of cell-bound anti-rat CD4 scFv via the histidine tag. PBL were incubated with an antibody against histidine (visualised by phycoerythrin (PE)-fluorescence) and an antibody against CD3 (an antigen abundant on most T cells) conjugated to FITC. **(A)** PBL incubated with the anti-histidine antibody and anti-CD3 FITC. No cell bound anti-rat CD4 scFv was detected. **(B)** PBL incubated with the CD3 FITC alone. **(C)** PBL incubated with anti-histidine alone. **(D)** Positive control: PBL incubated with an anti-rat CD4 whole antibody (OX35). A population of CD3<sup>+</sup> T cells with bound anti-rat CD4 scFv was detected. Representative histograms are of rat SB46 PBL collected 3 weeks after intranodal injection of LV-CD4scFv\_F2A\_eYFP.

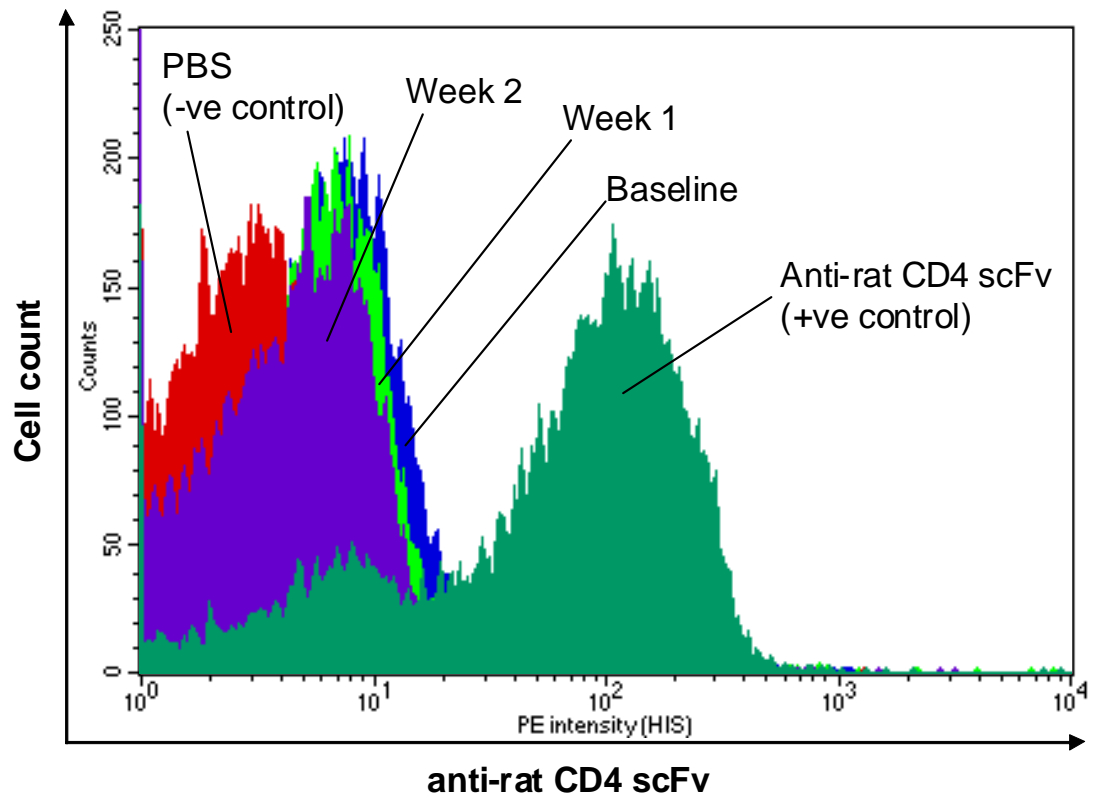


**Figure 4.12: Representative histogram revealing the absence of soluble anti-rat CD4 scFv in the circulation of rats that received injection of LV-CD4scFv\_F2A\_eYFP into the cervical lymph nodes.** Blood was collected from each rat immediately prior to corneal transplantation (baseline) and weekly there after until rejection. Plasma was collected from blood samples and flow cytometry on rat thymocytes was performed to detect soluble anti-rat CD4 scFv. The positive control was bacterially-produced anti-rat CD4 scFv incubated with the rat thymocytes. Histograms are of rat SB46 plasma data (i.e. from one representative rat).



corneal allografts in our WF into F344 rat model of corneal transplantation, 4-6 *contralateral* and *ipsilateral* cervical lymph nodes were removed 7 days before corneal transplantation.

Rats that underwent *bilateral* lymphadenectomy exhibited a median day of rejection of 15 days, which was comparable to the median day of rejection of the unmodified controls, which was 17 days (Table 4.9). This suggests that the cervical lymph nodes are not essential for corneal allograft rejection in our rat model. There was also no difference in blood vessel infiltration into the donor tissue (Table 4.9). The degree of ocular inflammation in the grafted eyes (Table 4.10) in rats that underwent the *bilateral* lymphadenectomy was significantly less at day 10 post transplantation, compared to unmodified controls ( $p=0.008$ ), suggesting that trafficking of infiltrating leucocytes to the eye may have been reduced.

## 4.4 SUMMARY AND DISCUSSION

### 4.4.a. Summary

The experiments presented in this chapter describe the outcomes of expressing an anti-rat CD4 scFv (using a lentiviral vector) in the corneal endothelium, the anterior segment of the eye, and the cervical lymph nodes, prior to corneal transplantation in the rat. *Ex vivo* transduction of donor corneas with LV-CD4scFv\_F2A\_eYFP significantly prolonged corneal allograft survival compared to controls ( $p=0.004$ ). In contrast, *ex vivo* transduction of donor corneas with Adv-CD4scFv did not prolong corneal allograft survival compared to unmodified allografts ( $p>0.05$ ). Inflammation was significantly lower in allografts transduced with LV-CD4scFv\_F2A\_eYFP

**Table 4.9: Summary of corneal allograft survival data from rats that underwent bilateral lymphadenectomy of the cervical lymph nodes.**

Treatment	Graft	n	Median day of vessel infiltration into graft	Day of rejection	Median day of rejection
Unmodified	allograft	10	10	11, 12, 14, 15, 16, 18, 19, 19, 20, >60 <sup>^</sup>	17
Removal of lymph nodes	allograft	8	11	12, 14, 14, 14, 15, 18, 21, 27	15

n = number of animals used in analysis

<sup>^</sup> = graft did not reject

p>0.05 (Mann-Whitney U test, corrected for ties)

**Table 4.10: Summary of the ocular inflammation in allografts after bilateral lymphadenectomy of the cervical lymph nodes prior to corneal transplantation.** Inflammation was scored daily on a 0-4 numerical scale with 0.1 increments. This table summarises the median inflammation scores at days 1, 5, 10 and 15, post transplantation for each group.

Treatment	Median inflammation scores			
	Day 1	Day 5	Day 10	Day 15
Unmodified	0.5	0.6	0.4	0.1
Removal of lymph nodes	0.6	0.35	0*	1.5

\* = statistically significant difference (p=0.008, Mann-Whitney U test, corrected for ties)

compared to allografts transduced with Adv-CD4scFv and allografts transduced with LV-eYFP. Anterior chamber injection of a lentiviral vector into recipient and donor eyes was able to transduce cells within the cornea, iris and retina, but delivery of the anti-rat CD4 scFv into the anterior segment using this method, did not prolong corneal allograft survival ( $p>0.05$ ). However, significantly reduced ocular inflammation was observed in rats after anterior chamber injection with LV-CD4scFv\_F2A\_eYFP compared rats that received anterior chamber injection of LV-eYFP, 1-5 days post transplantation ( $p<0.01$ ). Injection of LV-CD4scFv\_F2A\_eYFP into the cervical lymph nodes did not prolong corneal allograft survival and neither did *bilateral* lymphadenectomy of these nodes prior to corneal transplantation ( $p>0.05$ ). However, 10 days after transplantation, ocular inflammation was lower in allografts performed in rats that underwent bilateral lymphadenectomy of the cervical lymph nodes, compared to unmodified controls ( $p=0.008$ ).

#### **4.4.b. Immunosuppression produced by the corneal endothelium**

The results presented in this chapter indicate that a modest but significant prolongation of corneal allograft survival can be achieved after *ex vivo* transduction of the donor corneal endothelium with a lentiviral vector carrying an anti-rat CD4 scFv immediately prior to corneal transplantation, compared to unmodified allografts and allografts that were transduced with LV-eYFP ( $p=0.004$ ) (Table 4.1). Despite expression of the anti-rat CD4 scFv being approximately 10 fold higher from adenoviral-transduced corneas compared to lentiviral-transduced corneas after 5 days in culture (Figure 4.4), donor corneas transduced with a lentiviral vector carrying the anti-rat CD4 scFv showed prolonged allograft survival compared with donor corneas transduced with an adenoviral vector carrying the anti-rat CD4 scFv ( $p=0.018$ )

(Table 4.1). Allografts transduced with a lentiviral vector carrying the anti-rat CD4 scFv showed significantly lower levels of inflammation 15 days post transplantation, compared to allografts transduced with an adenoviral vector carrying the anti-rat CD4 scFv and allografts transduced with LV-eYFP ( $p \leq 0.01$ ) (Table 4.2). Similar to what has been reported previously,<sup>221</sup> *ex vivo* transduction of the donor corneal endothelium with an adenoviral vector carrying an anti-rat CD4 scFv did not prolong corneal allograft survival compared to unmodified allografts ( $p > 0.05$ ) (Table 4.1). These results suggest that the immunogenicity of the adenoviral vector might be offsetting the immunosuppressive abilities of the anti-rat CD4 scFv, and preventing the modulation of corneal allograft survival. On the other hand, these results reveal that sustained expression of an antibody fragment targeting a T cell from the donor corneal endothelium (even at low levels), can prolong corneal allograft survival, when expressed from a lentiviral vector.

It is conceivable that if stronger expression of the anti-rat CD4 scFv could be achieved from the donor corneal endothelium, then a more pronounced prolongation of allograft survival might be experienced. Transgene expression from all lentiviral vectors used in this study was controlled by the constitutive SV40 promoter. The use of a stronger constitutive promoter such as cytomegalovirus (CMV) (Clarke, personal communication) could increase expression of the anti-rat CD4 scFv and a greater prolongation of corneal allograft survival might thereby be achieved.

The results described in this chapter suggest that expression of anti-rat CD4 scFv from the donor corneal endothelium is able to modulate T cell sensitisation and subsequently delay allograft rejection. Whether the anti-rat CD4 scFv is remaining

within the ocular tissue or draining to other areas of the body remains unclear. The fact that all of the corneal allografts did eventually reject indicates that sensitisation and the generation of an effector cell response did occur, but with delayed kinetics.

Rosenbaum and colleagues have described the migration of T cells into the anterior chamber after intravitreal injection of antigen in mice.<sup>92</sup> T cells were seen in close proximity of the resident APCs within the iris, suggesting that T cell sensitisation may occur within the eye before sequestration to the secondary lymphoid tissues such as the cervical lymph nodes,<sup>106-107,110-111</sup> the mesenteric lymph nodes,<sup>106-107</sup> or even within CALT, which is induced in response to cornea transplantation in the rat.<sup>81</sup>

APCs within the eye have been well documented, with APCs detected in the cornea,<sup>69-70,72-73,84</sup> and the uveal tract.<sup>75-77,87-88,284</sup> Whether ocular APCs are involved in the generation or the suppression of an immune response remains unclear. There is evidence to suggest that ocular APCs are involved in immune deviation responses within the eye (ACAID).<sup>89,134-136</sup> Whilst the data presented in this chapter suggests that antigen presentation may be occurring within the anterior segment, as low levels of the immunosuppressive anti-rat CD4 scFv expressed from the donor corneal endothelium was able to prolong corneal allograft survival. This implies that ocular APCs might be activating the CD4+ T cells within the anterior segment which can lead to a DTH response and corneal allograft rejection. It is possible that ocular APCs are involved in both the generation and suppression of an immune response, depending on what cytokines are present within the ocular tissues and within the aqueous humour at the time of antigen exposure.

#### 4.4.c. Immunosuppression within the anterior segment

Expression of the anti-rat CD4 scFv from corneas after lentiviral transduction was detected 5 days post transduction (Figure 4.4). It was consequently hypothesised that if transplantation of the donor cornea were performed when expression of the anti-rat CD4 scFv was already occurring, then this may further prolong allograft survival, compared to when the donor cornea was transduced immediately prior to corneal transplantation. It was also hypothesised that if the surrounding tissues within the anterior chamber (such as the iris) were expressing the anti-rat CD4 scFv at the time of transplantation, then this might further suppress T cell sensitisation to donor alloantigen.

To achieve this, anterior chamber injection of a lentiviral vector carrying the anti-rat CD4 scFv was injected into both the donor and recipient anterior chamber 5 days prior to corneal transplantation. The survival of these corneal allografts was not significantly different to the survival of the controls (Table 4.4). Ocular inflammation was significantly higher in recipients that received anterior chamber injection of LV-eYFP, compared to recipients that received anterior chamber injection of the lentiviral vector carrying the anti-rat CD4 scFv, within the first 5 days post transplantation ( $p < 0.01$ ) (Table 4.5). A possible explanation for the increased ocular inflammation after anterior chamber injection of LV-eYFP could be that the eYFP protein is immunogenic. In support of this theory, Table 4.2 reveals that allografts transduced *ex vivo* with LV-eYFP also showed increased ocular inflammation compared to allografts transduced with LV-CD4scFv\_F2A\_eYFP.

There are several possible explanations for why anterior chamber injection of a lentiviral vector carrying the anti-rat CD4 scFv did not modulate corneal allograft survival. Firstly, the transduction efficiency might have been too low to produce levels of the anti-rat CD4 scFv sufficient for a therapeutic effect. *Ex vivo* transduction of LV-eYFP showed uniform expression of eYFP throughout the corneal endothelium (Figure 4.2).<sup>198</sup> However, after anterior chamber injection of LV-eYFP, eYFP-expression from transduced cells was very bright near the injection site and the paracentesis (in both the endothelium and the stroma) (Figure 4.7), but the number of eYFP-positive cells was sparse in the other areas of the cornea, and the expression of eYFP from these cells was low, making transduction efficiency difficult to calculate. Also, the number of lentiviral particles injected into the anterior chamber ( $5 \times 10^6$  TU/injection) was 5 times less than the number of viral particles used in the *ex vivo* transductions to the corneal endothelium with a lentiviral vector ( $2.5 \times 10^7$  TU/cornea). The limiting factor for the number of lentiviral particles injected into the anterior chamber was volume (with the maximum volume injected being 5  $\mu$ l). Improvements in lentiviral vector processing and concentration could permit for an increased number of viral particles injected into the anterior chamber, and this might improve the transduction efficiency when using this method.

Furthermore, transduced cells were detected in the retina of some rats after anterior chamber injection with LV-eYFP, indicating that the lentiviral vector spread outside the anterior segment. This suggests, that injection of a lentiviral vector into the anterior chamber, can drain to other areas (including the retina), therefore potentially reducing the number of cells within the anterior segment transduced by this method.



In addition, inflammatory signals have been shown to promote the upregulation of MHC class II expression in resident immature APCs within the corneas of mice.<sup>68</sup> The results described in this chapter showed that after anterior chamber injection of LV-eYFP, eYFP-expressing cells with a dendriform morphology were observed within the central region of the corneal stroma (Figures 4.7 and 4.8). The expression of MHC class II on these APCs might have been upregulated in response to the trauma of the anterior chamber injection, and consequently, these resident corneal MHC class II<sup>+</sup> APCs might have been ready to phagocytose antigen from the donor cornea at the time of transplantation. A future experiment could involve injecting a lentiviral vector carrying the anti-rat CD4 scFv only into the anterior chamber of the donor rat, and grafting into an unmodified recipient. However, if there are MHC class II<sup>+</sup> APCs within the donor cornea, these cells could potentially present antigen to recipient T cells via the direct pathway and could lead to corneal graft rejection.<sup>26</sup>

In summary, anterior chamber injection of a lentiviral vector carrying an anti-rat CD4 scFv was not able to prolong corneal allograft survival. The possible reasons for this might be that (1) the transduction efficiency was too low to produce therapeutic levels of the anti-rat CD4 scFv after anterior chamber injection of the lentiviral vector, (2) the lentiviral vector drained outside the anterior segment after anterior chamber injection, and this might have reduced the number of cells transduced within cornea and the iris or (3) the APCs in the cornea might have been expressing high levels of MHC class II after the trauma caused by the anterior chamber injection, and were thus able to take-up and process donor antigen immediately after grafting.

#### 4.4.d. Immunosuppression within the cervical lymph nodes

The main pathway for aqueous outflow from the anterior segment of the eye is reportedly through the Schlemm's canal into the circulation and to the spleen.<sup>286</sup> However, recent studies have revealed that ocular antigen from the anterior segment can leave the eye through an unconventional pathway, which drains through the ciliary body into the suprachoroidal space, the conjunctiva and into the *ipsilateral* cervical lymph nodes (uveoscleral drainage).<sup>106-107,110</sup> In the mouse, an antigen-specific increase in the number of activated T cells within the *ipsilateral* cervical lymph nodes occurred within 3-6 days of antigen exposure in the eye.<sup>100,109</sup> These activated T cells expressed IL-2, suggesting the development of a Th1 response.<sup>109</sup>

In this study, an anti-rat CD4 scFv was delivered to the *ipsilateral* and *contralateral* cervical lymph nodes prior to corneal transplantation in the rat, with the intention of inhibiting sensitisation to the corneal allograft. However, injection of a lentiviral vector carrying the anti-rat CD4 scFv into the cervical lymph nodes 2 days before transplantation did not prolong corneal allograft survival compared to controls ( $p > 0.05$ ) (Table 4.7). Transduction of the cells within the lymph nodes was successful, however, expression of the anti-rat CD4 scFv was transient, and sufficient scFv may not have been expressed within the cervical lymph nodes at the time when T cell sensitisation was occurring. It was considered that the transient expression of the anti-rat CD4 scFv might have been due to migration of the transduced cells into the circulation. However, no soluble or cell bound anti-rat CD4 scFv was detected in the blood of any recipient at any time point (Figures 4.11 and 4.12). Another explanation for the transient expression of anti-rat CD4 scFv after intranodal injection, was that the transduced cells had died, as bone-marrow derived

DCs located within the peripheral lymph nodes have a turnover of approximately 10 days.<sup>287</sup>

Antigen-bearing APCs have been observed within the *ipsilateral* cervical lymph nodes as early as 6 hours after corneal transplantation, and were still detected 3 days after transplantation in mice.<sup>26,100</sup> If the migration of antigen-bearing APCs to the draining lymph nodes in our rat model of corneal transplantation was similar to that observed in mice,<sup>26,100</sup> then the anti-rat CD4 scFv should have been expressed at the same time the antigen-bearing APCs were present in the *ipsilateral* cervical lymph nodes. Therefore, it seems unlikely that the transient expression of anti-rat CD4 scFv was the main contributing factor for the failure to prolong corneal allograft survival.

Another plausible explanation for why intranodal injection of a lentiviral vector carrying the anti-rat CD4 scFv into the cervical lymph nodes did not prolong corneal allograft survival, may be that antigen presentation was occurring elsewhere, such as in the anterior segment of the eye, or in other secondary lymphoid tissues including the mesenteric lymph nodes,<sup>106-107</sup> or in the CALT.<sup>81</sup> In support of this possibility, rats that underwent *bilateral* lymphadenectomy of the cervical lymph nodes prior to corneal transplantation did not show prolonged corneal allograft survival compared with controls ( $p>0.05$ ) (Table 4.9). However, inflammation was reduced in these allografts 10 days after transplantation, compared to unmodified controls ( $p=0.008$ ) (Table 4.10), suggesting that trafficking of infiltrating leucocytes to the eye might have been reduced.

The corneal allograft survival data from this study is at variance with those obtained from some studies in mice, in which prolonged allograft survival after removal of the cervical lymph nodes *was* observed.<sup>118-121</sup> Yamagami *et al.* showed indefinite survival of all allografts after *bilateral* removal of the cervical lymph nodes when corneal transplantation was performed into normal recipient corneal beds in mice,<sup>120</sup> and significant prolongation of graft survival was achieved when grafting into vascularised beds.<sup>121</sup> In these studies, the onset of DTH was delayed<sup>121</sup> or inhibited.<sup>120</sup> Plskova and colleagues discovered that in mice, an immune response to a corneal allograft was generated within a specific superficial cervical lymph node (referred to as the submandibular lymph node).<sup>118</sup> This study found that both *bilateral* and *ipsilateral* removal of the superficial cervical lymph nodes significantly prolonged corneal allograft survival, and the authors concluded that corneal allograft acceptance after bilateral lymphadenectomy was due to immunological ignorance rather than tolerance, as the site at which antigen presentation may occur was removed (i.e. the draining superficial cervical lymph nodes).<sup>119</sup>

The difference in corneal allograft survival after bilateral lymphadenectomy of the cervical lymph nodes, between the different studies, could be due to the different strengths of the immunological barriers between the inbred strain combinations used in each study. The murine model described by Yamagami *et al.* grafted C57BL/6 donor corneas into BALB/c recipients.<sup>120-121</sup> This is a weak immunological barrier in which approximately 50% of untreated corneal allografts do not undergo rejection.<sup>120</sup> The large proportion of corneal allografts that experience indefinite survival using the C57BL/6 to BALB/c murine model has been well documented by others,<sup>25,47</sup> and the high acceptance rate of unmodified allografts in this murine model might be the

reason why such successful corneal allograft survival was achieved after the removal of the cervical lymph nodes.

In contrast, in the rat model of corneal transplantation described in this chapter, only 10% of unmodified allografts remained clear after 60 days, which represents a strong immunological barrier (Table 4.1). No prolongation of corneal allograft survival occurred in rats after bilateral lymphadenectomy of the cervical lymph nodes. Furthermore, in a C3H to BALB/c mouse model of corneal transplantation, which represents a strong immunological barrier in which all unmodified corneal allografts did reject, bilateral lymphadenectomy of the cervical lymph nodes prior to corneal transplantation did not significantly prolong the survival of corneal allografts compared to untreated mice.<sup>111</sup> The evidence suggests that the strength of the immunological barrier between the donor and recipient strains might influence allograft survival after bilateral lymphadenectomy of the cervical lymph nodes.

In summary, when using inbred rodent strains, a weak immunological barrier between the donor and recipient can lead to higher acceptance of corneal allografts. The rat model described in this thesis is a strong immunological barrier, and is likely to reflect the rejection process seen in an outbred species such as humans.

#### **4.4.e. Regional immunosuppression for corneal transplantation in the rat**

The results presented in this chapter suggest that regional immunosuppression using an anti-CD4 antibody fragment is possible when expressed from the donor corneal endothelium. However, all corneal allografts did reject with delayed kinetics,

suggesting that antigen presentation may occur at a site other than the anterior segment of the eye. It is possible that antigen presentation during corneal transplantation is occurring at multiple sites, including within the anterior chamber of the eye as well as in the secondary lymphoid tissues such as the cervical lymph nodes,<sup>106-107</sup> the mesenteric lymph nodes<sup>106-107</sup> or CALT.<sup>81</sup> An immunosuppressive strategy that targets multiple sites of antigen presentation simultaneously might be more effective at inhibiting antigen presentation in response to corneal alloantigens and may result in indefinite survival of corneal allografts.

#### **4.4.f. Splenectomy prior to corneal transplantation**

It is well established that the spleen is critical for the induction of ACAID.<sup>89</sup> Thus, future experiments could involve the removal of the spleen prior to corneal transplantation. If the spleen is playing a critical role in the presentation of corneal antigens, then its removal will result in prolonged corneal graft survival.

## **CHAPTER 5: FINAL DISCUSSION**

This project investigated the potential of regional immunosuppression for corneal transplantation by using an integrative lentiviral vector to deliver an immunosuppressive transgene to various anatomic locations within the rat. The following sections will discuss the major findings of this project.

## 5.1 SUMMARY OF THE MAJOR FINDINGS FROM THIS THESIS

In this project dual-gene vectors were designed to contain an immunosuppressive transgene (anti-rat CD4 scFv) and a reporter gene (eYFP) using the F2A self-processing sequence. These vectors had the potential to modulate an immune response (through the expression of anti-rat CD4 scFv) whilst expression of the reporter gene eYFP had the potential to permit simple titration of the lentiviral vector, quantification of transduction efficiency and tracking of transduced cells *in vivo*. I first examined the levels of transgenic proteins expressed from dual-gene vectors carrying the F2A self-processing sequence. Transgenes situated downstream of the F2A sequence expressed from dual-gene vectors produced significantly lower levels of protein (between 2 and 20 fold lower) when compared to expression of the same protein from a single-gene vector. This occurred in three individual dual-gene vectors. Expression was also significantly lower when a transgene was positioned downstream of F2A compared to when the same transgene was positioned upstream of F2A in a different dual-gene construct.

A major aim of this project was to determine the anatomic site of antigen presentation in response to corneal transplantation in the rat. Modest, but significant prolongation of corneal allograft survival was observed after *ex vivo* transduction of donor corneas with a lentiviral vector carrying an anti-rat CD4 scFv. However, when



the lentiviral vector carrying the anti-rat CD4 scFv was injected into the anterior chamber in both recipient and donor rats 5 days prior to corneal transplantation, no prolongation of graft survival was observed. Intranodal injection of the lentiviral vector carrying an anti-rat CD4 scFv into the cervical lymph nodes 2 days prior to corneal allografting did not prolong graft survival. Moreover, when the cervical lymph nodes were removed from recipient rats 7 days before corneal allografting, graft survival was not prolonged. These results indicated that the cervical lymph nodes were not essential for corneal allograft rejection in the WF into F344 rat strain combination. However, expression of an anti-rat CD4 scFv from the donor corneal endothelium was able to inhibit sensitisation and prolong corneal allograft survival, suggesting that antigen presentation might occur locally.

In this final chapter I will discuss how multi-gene vectors using the 2A self-processing sequence can be used to develop novel strategies to prevent immunological rejection of corneal allografts. This chapter will also explain how the findings discussed in this thesis add to the knowledge of antigen presentation during corneal transplantation in rodents.

## **5.2 MULTI-GENE EXPRESSION USING THE 2A SELF-PROCESSING SEQUENCE**

### **5.2.a. Expression of multiple transgenes from a single lentiviral construct**

Until recently, the expression of multiple transgenes from a single construct could only be achieved using individual promoters to control the expression of each transgene. However, when using integrative vectors such as lentivirus, this can cause

variations between the sites of integration of each of the transgenes and the number of copies integrated into the genome,<sup>288</sup> which can lead to further issues, including transgene separation after successive generations and a lack of coordination of transcriptional activity of the transgenes.

The development of IRES greatly improved the delivery of multiple transgenes from a single construct. IRES are able to direct ribosomes to initiate translation at internal sites within the mRNA and have been used extensively to express multiple transgene from a single vector.<sup>289</sup> However, IRES are large (approximately 500 bp) and produce much lower expression of the second ORF.<sup>242</sup>

The 2A self-processing sequence derived from the FMDV has enabled the expression of multiple transgenes within a single ORF by the insertion of the 2A sequence between transgenes.<sup>275</sup> The FMDV 2A self-processing sequence is a short (18 amino acid) region that is hypothesised to undergo a unique processing event during translation at the ribosome. This processing is believed to involve translational “skipping” of the peptide bond formation between the 2A glycine and the 2B proline residues.<sup>279</sup> A number of studies have reported equimolar ratios of the proteins situated upstream and downstream of 2A within multi-gene constructs.<sup>234,237-239,244</sup>

Amendola and colleagues have recently developed a dual-gene vector using a bidirectional promoter consisting of a minimal core promoter element of the human CMV joined upstream and in reverse orientation to an efficient promoter PGK.<sup>242</sup> Strong expression of both the upstream and downstream proteins has been shown when using a bidirectional vector *in vitro* and *in vivo*.<sup>242</sup> In fact, these bidirectional

constructs produced more efficient expression of both transgenes than 2A-containing dual-gene vectors in at least one study.<sup>242</sup>

In summary, the use of the 2A self-processing sequence has improved the expression of multiple transgenes from a single construct, with reports of equimolar expression of both the upstream and downstream proteins.<sup>234,237-239,244</sup> However, the results described in this thesis reveal significantly lower expression of the transgene downstream of the 2A sequence compared to expression of the same transgene when positioned upstream of 2A. The next section will discuss this finding in more detail.

### **5.2.b. Stoichiometry of upstream and downstream proteins expressed from 2A vectors**

The original model proposed by Ryan and colleagues to elucidate the process of 2A self-processing during translation at the ribosomes was based on the imbalance between the expression of proteins situated downstream and upstream of 2A when using cell-free translation systems (rabbit reticulocyte lysates).<sup>229,279</sup> Several studies have since reported equimolar expression of the upstream and downstream proteins from mammalian cells and animals.<sup>234,237-239,244</sup>

The results reported in this thesis revealed significantly lower expression (between 2 and 20 fold) of a transgene when positioned downstream of 2A compared to when the same transgene was positioned upstream of 2A in dual-gene constructs. Furthermore, using three separate dual-gene constructs, the expression of the downstream transgene was considerably lower when compared to the expression of the same transgene from a single-gene vector.

Critical assessment of the studies that reported equimolar expression of the upstream and downstream proteins when using the 2A self-processing sequence revealed that some of these studies did not report quantitative data to validate their claims,<sup>238-239,244</sup> and these studies did not directly compare the expression of the proteins from the dual-gene vectors to the expression from single-gene constructs.<sup>238-239,244</sup> For these reasons, it is possible that an accurate assessment of expression efficiency was not made for the proteins expressed from the 2A-containing dual-gene vectors used in these studies.<sup>238-239,244</sup>

Using multiple 2A sequences, Szymczak *et al.* constructed multi-gene vectors containing two to four transgenes per vector.<sup>237</sup> In this study equimolar ratios of proteins were reported from multi-gene vectors using western blot analysis.<sup>237</sup> However, the authors did not compare the expression of each protein from the multi-gene vectors to the expression of the same protein from a single-gene vector,<sup>237</sup> therefore expression efficiency from the multi-gene vectors could not be accurately assessed.

Lorens *et al.* reported similar expression of proteins from a dual-gene vector compared to expression from single-gene constructs.<sup>234</sup> However, based on the data provided in the paper, it is difficult to reach this conclusion. According to my interpretation, the protein situated upstream of 2A appeared to show lower expression compared to expression from a single-gene counterpart vector.<sup>234</sup> Furthermore, although the authors stated that they produced comparable levels of the protein downstream of 2A using a dual-gene vector compared to a single-gene vector, no data was presented to back up this claim.<sup>234</sup>

At least two studies have compared transgenic protein expression from multi-gene 2A-containing vectors to the expression of the same protein from single-gene constructs.<sup>242-243</sup> Chinnasamy *et al.* constructed dual-gene and tri-gene vectors using various combinations of 2A and IRES.<sup>243</sup> Transgene expression from the multi-gene constructs was compared to the expression from single-gene vectors. The authors reported between 2.2-2.5 fold lower expression of proteins when they were positioned downstream of 2A in either dual-gene or tri-gene vectors, when compared to expression from a single-gene construct.<sup>243</sup> In a separate study, Amendola and colleagues also compared expression of the downstream protein from a dual-gene 2A-containing construct to the expression from a single-gene vector. The authors reported significantly lower expression of the protein situated downstream of 2A compared to expression from a single-gene vector.<sup>242</sup> Thus the results reported by Chinnasamy *et al.*<sup>243</sup> and Amendola *et al.*<sup>242</sup> are similar to the findings described in this thesis, which show lower expression of a protein positioned downstream of 2A compared to expression from a single-gene vector.

In summary, the findings described in this thesis showed that when using the 2A self-processing sequence to construct multi-gene vectors, the protein situated downstream of 2A consistently expressed at a significantly lower level when compared to the expression of the same protein situated upstream of 2A, or when the same protein was expressed from a single-gene vector. However, the fact that there have been so many successful reports of multi-gene transfer using the 2A self-processing sequence suggests that in many instances, equimolar expression might not be required for the intended biological outcome to be achieved.

### **5.2.c. The use of the 2A self-processing sequence to prevent corneal allograft rejection**

The 2A self-processing sequence has been used for many biotechnological applications, recently reviewed by de Felipe and colleagues.<sup>288</sup> The reason for the development of the dual-gene 2A-containing vectors described in this thesis was to couple the expression of a therapeutic transgene (anti-rat CD4 scFv) with a reporter gene (eYFP). However, because the expression of eYFP was extremely low when positioned downstream of the 2A sequence in a dual-gene vector, lentiviral vector titration, quantification of transduction efficiency or the tracking of transduced cells *in vivo*, by way of eYFP expression was not possible. For these reasons the dual-gene vectors constructed as part of this study were not used for their intended purpose. Nevertheless, many other studies have reported the successful use of 2A for their intended purposes,<sup>288</sup> suggesting that reduced expression of the downstream protein still might be at functional levels.

In light of this, multi-gene vectors using the 2A self-processing sequence might be useful in the context of preventing corneal allograft rejection in the future. Irreversible immunological corneal allograft rejection occurs through the erosion of ocular immune privilege, which is achieved through several independent but not mutually exclusive mechanisms, including inflammation, neovascularisation, T cell activation and the generation of a DTH response.

Disrupting one of these mechanisms, (as was performed in this study), can prolong corneal allograft survival. However, in most instances graft acceptance is not universal and rejection is only delayed in some animals, which do eventually

undergo corneal allograft rejection. The reasons for this might be that blocking only one arm of the rejection process is not enough to prevent failure of the corneal allograft. Therefore, blocking multiple mechanisms of rejection might have the potential to have a more powerful impact on the survival of a corneal allograft.

It is possible that a multi-gene vector containing transgenes that can prevent each process known to be involved in the immunological failure of a corneal allograft, could prevent rejection. A recent review by Parker *et al.* has summarised the transgenes which have been able to prolong corneal allograft survival in animal models when used individually as gene therapy.<sup>168</sup> These transgenes include immunosuppressive molecules targeting antigen presentation and early T cell activation (CTLA-Ig), immunomodulatory molecules that can modulate the effector immune response (IL-10, IL-4) and anti-angiogenic molecules that can prevent neovascularisation of the cornea (sflt-1 and EK5). It is proposed that a multi-gene construct (using the 2A self-processing sequence) that contains transgenes targeting each potential mechanism of corneal allograft rejection could be a successful strategy to prevent corneal allograft rejection.

### **5.3 ANTIGEN PRESENTATION DURING CORNEAL TRANSPLANTATION**

#### **5.3.a. Antigen travels from the eye to the secondary lymphoid organs in soluble form**

There is evidence to show that in rodents, antigen delivered to the eye via topical application, injection into the anterior and posterior chamber, or shed from a corneal allograft can travel to the secondary lymphoid tissues either through the circulation<sup>106-107,111-112</sup> or through lymphatic drainage,<sup>26,91,100,106-107,110-112</sup> where

antigen-specific T cell priming and expansion can occur.<sup>109</sup> Hoffman and colleagues have shown that 16% of the aqueous outflow drains to the cervical lymph nodes in mice, whilst the remaining aqueous outflow drains into the circulation.<sup>110</sup> A detailed discussion on lymphatic drainage from the eye to the cervical lymph nodes can be found in Section 1.6.d.2.

The form (soluble or cell-bound) in which antigen leaves the eye and arrives at the secondary lymphoid tissues such as the cervical lymph nodes (a potential site of antigen presentation), can determine the process of T cell sensitisation (either via the direct or indirect pathway), and is an important factor to be considered when investigating the site of antigen presentation in relation to corneal transplantation. In this section I will discuss how in rodents (in most instances), antigen drains from the eye in soluble and not cell-bound form to the secondary lymphoid tissues (Table 5.1).

Camelo *et al.* investigated the pathways of antigen drainage from the eye in rats and discovered that antigen injected into the anterior chamber mimicked the drainage of antigen injected into the subconjunctival space.<sup>106</sup> The majority of antigen drained to the ipsilateral cervical lymph nodes and a small quantity of antigen reached the spleen and the mesenteric lymph nodes. Bilateral ocular injection of different coloured antigen showed dual uptake of the fluorescent antigen by resident APCs within the cervical lymph nodes, indicating that antigen drained in soluble form from the anterior segment of the eye.<sup>106</sup>



**Table 5.1: Evidence for antigen drainage to the secondary lymphoid organs in soluble form**

Species	Type of Ag	Method of delivery	Findings	Reference
Rat	CB-Dx	Bilateral injection of CB-Dx into the AC	Bilateral injection of different coloured antigen into the AC showed dual uptake of the fluorescent Ag by resident APCs within the CLN	106
Mouse	Fluorescent OVA + fluorescent latex beads	Injection of fluorescent OVA or fluorescent latex beads into the AC	Soluble Ag was detected in the CLN and the spleen after AC injection. Phagocytosis by uveal tract APCs was observed after Ag inj into AC, however these Ag-loaded cells did not appear to migrate.	91
Mouse	C5' and eGFP DNA plasmids	DNA plasmids were applied to donor cornea as droplets after mild epithelial abrasion prior to grafting	Donor MHC class II+ APCs were identified in the central cornea. However, donor MHC class II+ APCs did not migrate to the CLNs. Instead, Ag-loaded recipient APCs were detected in the CLN and in the spleen.	100

---

CB-Dx, cascade blue dextran, 70 kDa; OVA, Ovalbumin peptide; AC, anterior chamber; CLN, cervical lymph nodes; Ag, antigen

Dullforce and co-workers have monitored antigen uptake by uveal tract APCs after the injection of fluorescent antigen into the anterior chamber using intravital time-lapse videomicroscopy in mice.<sup>91</sup> This study reported phagocytosis of the fluorescent antigen by uveal tract APCs.<sup>91</sup> However, the fluorescently-labelled APCs within the anterior segment failed to move during multiple observation times,<sup>91</sup> suggesting that antigen-loaded APCs within the uveal tract do not migrate after antigen uptake. The authors of this study also identified soluble antigen within the cervical lymph nodes 6 hours after antigen exposure, however there was no sign of cell-bound antigen in these nodes.<sup>91</sup>

In mice, Kuffova *et al.* identified a donor MHC class II+ APC population within corneal allografts and showed no evidence that these donor APCs draining to the cervical lymph nodes at any time point after grafting.<sup>100</sup> Instead, donor-derived antigen was associated with *recipient* APCs within the cervical lymph nodes within 6 hours of grafting, and antigen-specific T cell activation and expansion was subsequently detected within these nodes and peaked between 4-6 days after transplantation.<sup>100</sup>

It should be noted here, that a study by Liu and co-workers identified MHC class II+ *donor* APCs in the cervical lymph nodes in mice within 6 hours after corneal transplantation, and the trafficking of the donor APCs increased when allografts were performed in high-risk corneal beds (which had been prevascularised prior to corneal transplantation).<sup>26</sup> However, these donor APCs had reduced allostimulatory function compared to splenic APCs in MLR experiments.<sup>26</sup> The fact that the donor APCs had reduced allostimulatory function suggests that soluble donor antigen may have

drained to the cervical lymph nodes, and that recipient APCs may have been involved in indirect allorecognition and corneal graft rejection. It is unclear why migration of donor APCs to the cervical lymph nodes was detected by Liu *et al.*<sup>26</sup> and not by Kuffova *et al.*<sup>100</sup> as both studies used the C57BL/6 into BALB/c murine strain combination.

In summary, based on the findings discussed in this section, I suggest that in rodents, under most circumstances, antigen delivered to the anterior segment of the eye drains to the secondary lymphoid organs in soluble rather than cell-bound form.

### **5.3.b. Evidence for antigen presentation within the anterior segment of the eye**

The results described in this thesis revealed a modest (5 days), but significant ( $p=0.004$ ) prolongation of corneal allograft survival in rats when an antibody fragment targeting CD4 (a molecule expressed on T cells which is known to be essential for antigen presentation), was expressed from the donor corneal endothelium. These data suggest that antigen presentation *can* occur within the anterior segment of the eye and can be inhibited by the expression of the anti-CD4 antibody fragment. However, all allografts did eventually reject, implying that the rejection process was merely delayed. In a separate experiment, when the cervical lymph nodes were removed from recipient rats prior to corneal transplantation, corneal allograft survival was comparable to rats that were unmodified, indicating that antigen presentation can occur at a site *besides* the draining cervical lymph nodes.

To support the hypothesis that antigen presentation can occur within the anterior segment of the eye, a recent study by Rosenbaum and colleagues reported the interaction of a migrating T cell with an antigen-loaded APC within the iris.<sup>92</sup> This study used videomicroscopy to visualise the interaction of a T cell with an antigen-loaded APC within the irides of murine eyes after intravitreal injection of fluorescent antigen (OVA) and lipopolysaccharide (to induce inflammation within the eye).<sup>92</sup> T cells lingered when adjacent to antigen-loaded APCs, suggesting that they were physically interacting. This T cell “interaction” was observed with most T cells within the iris during a single observation period (mean 99 min).<sup>92</sup> This study is the first to report the interaction of a T cell with an antigen-loaded APC within the anterior segment, and provides evidence that antigen presentation might occur at this site.

To further support the hypothesis that antigen presentation can occur within the anterior segment of the eye, Kuffova and colleagues have reported infiltration of macrophages, DCs and neutrophils into a corneal graft within 24 hours after transplantation and T cells within 2 days after transplantation, in both isografts and allografts.<sup>33</sup> The fact that this cellular infiltration occurred in both allografts and isografts suggests it was initiated by an innate immune response triggered by the trauma of surgery.<sup>33</sup> It is possible that within the infiltrating T cell population were naïve antigen-specific CD4<sup>+</sup> T cells, that could potentially interact with either antigen-loaded recipient APCs within the anterior segment or mature MHC class II<sup>+</sup> donor APCs from within the donor cornea.






In summary, the studies described in this section suggest that antigen presentation can occur within the anterior segment of the eye. Based on these findings, I propose a model of how and where antigen presentation occurs in rodents following orthotopic corneal transplantation, which will be discussed in the next section.

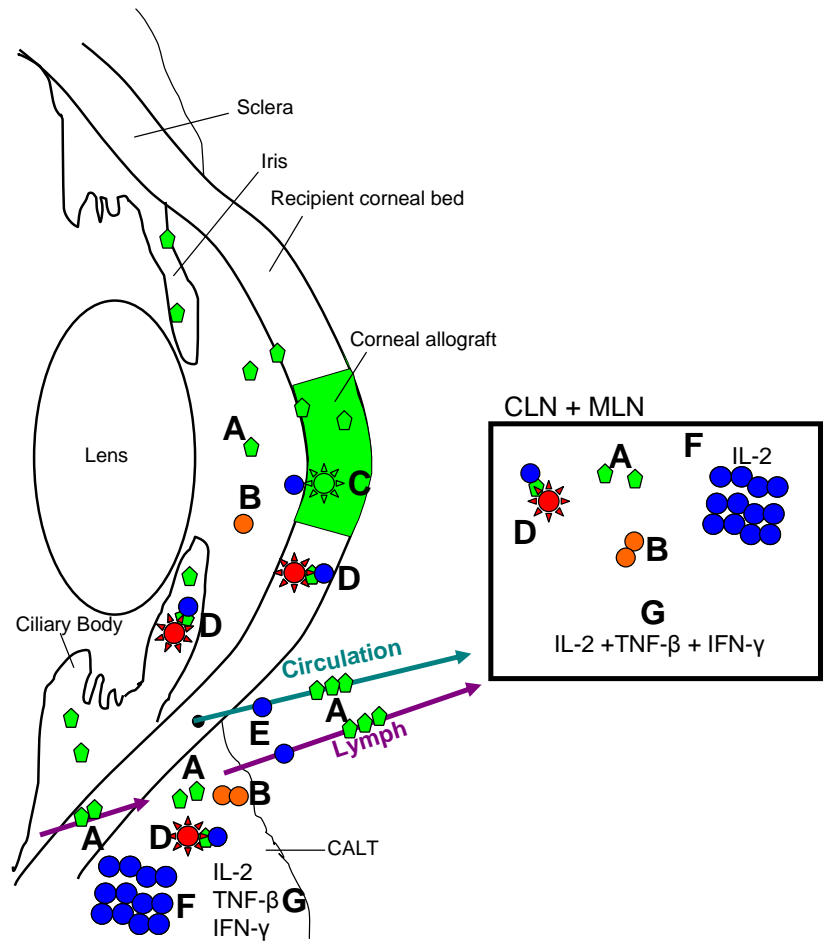
### **5.3.c. A proposed model of antigen presentation during corneal transplantation in rodents**

A diagrammatic representation of the proposed model of antigen presentation during corneal transplantation in rodents is shown in Figure 5.1. It is proposed that the immune response against the donor corneal allograft is initiated by an innate inflammatory response brought on by the trauma of surgery.<sup>33</sup> This innate response causes the infiltration of inflammatory cells to the graft including macrophages, DCs and neutrophils within 24 hours of transplantation.<sup>33</sup> These inflammatory cells release proinflammatory cytokines such as IL-1, IFN- $\gamma$  and TNF- $\alpha$ ,<sup>31</sup> which start an assault on the corneal allograft.

The first arm of this model proposes that proinflammatory cytokines trigger the infiltration of T cells to the site of inflammation (i.e. the corneal allograft).<sup>33</sup> Amongst this population of infiltrating T cells is a sub-population of naïve CD4+ T cells with specificity for donor-derived antigen.<sup>290</sup> Once at the site of inflammation,

**Figure 5.1: Diagrammatic representation of the proposed model of antigen presentation during corneal transplantation in rodents. (A)** The innate inflammatory response against the corneal allograft releases donor-derived antigens in soluble form, which either remain within the anterior segment of the eye, or drain to the secondary lymphoid tissue through the lymph to CALT and the cervical lymph nodes (CLN), or through Schlemm's canal and into the circulation to the spleen (involved in deviant immune responses) and mesenteric lymph nodes (MLN). **(B)** The inflammatory response also stimulates the infiltration of naïve T cells to the corneal allograft and naïve CD4<sup>+</sup> T cells recirculate through to the secondary lymphoid tissue. **(C)** Direct processing takes place within the anterior segment and the donor APCs activate the antigen-specific CD4<sup>+</sup> T cells. **(D)** Recipient APCs within the anterior segment and the secondary lymphoid tissue phagocytose and process antigen and present processed peptide to naïve CD4<sup>+</sup> T cells, causing their activation via indirect processing. **(E)** Activated T cells from the anterior segment are sequestered to the secondary lymphoid tissue via the lymph and the circulation. **(F)** Clonal expansion of the activated CD4<sup>+</sup> T cells occurs within the secondary lymphoid tissue and **(G)** a DTH response against the corneal allograft is generated and can lead to rejection.

-  Recipient APC
-  Donor APC
-  Naïve T cells
-  Activated T cells
-  Soluble antigen



indirect processing through the interaction between a naïve CD4<sup>+</sup> T cell with specificity for donor-derived antigen associated with a recipient APC, occurs within the anterior segment,<sup>92</sup> thus activating antigen-specific CD4<sup>+</sup> T cells.

Moreover, the inflammatory cytokines also stimulate the up-regulation of MHC class II and costimulatory molecules such as CD40, CD80 and CD86 on donor APCs.<sup>26</sup> The migrating naïve CD4<sup>+</sup> T cells with specificity for donor-derived MHC epitopes interact with the donor APCs and antigen presentation takes place via the direct pathway.

T cells activated via both the indirect and the direct pathways are sequestered to the secondary lymphoid tissue including CALT<sup>81</sup> and the cervical lymph nodes<sup>100,109</sup> through the lymph and the circulation. Within the cervical lymph nodes and other secondary lymphoid tissues, a DTH response is generated through the release of Th1 cytokines<sup>100,109</sup> (such as IL-2 and IFN- $\gamma$ ) which can lead to corneal allograft rejection.<sup>100</sup> Activated CD4<sup>+</sup> T cells can also amplify the CD8<sup>+</sup> T cell response,<sup>291</sup> which can subsequently aid in the rejection of the corneal allograft.<sup>292</sup>

The second arm of the proposed model hypothesises that soluble donor-derived antigen within the aqueous humour leaves the anterior segment and travels to the secondary lymphoid tissues using two separate routes; via the uveoscleral pathway to CALT<sup>81</sup> and the cervical lymph nodes<sup>26,91,100,106-107,109-112</sup> (Section 1.6.d.2) or via Schlemm's canal into the circulation and thus to the spleen<sup>106-107,111-112</sup> and the mesenteric lymph nodes,<sup>106-107</sup> where it is taken up and processed by recipient APCs.<sup>100</sup> Naïve CD4<sup>+</sup> T cells within the secondary lymphoid tissues are



subsequently activated by antigen-loaded recipient APCs via the indirect pathway of antigen presentation.<sup>100</sup> A DTH response is then generated through the release of Th1 cytokines (such as IL-2 and IFN- $\gamma$ )<sup>100,109</sup> and the activation of CD8+ T cells can also occur through help from the activated CD4+ T cells.<sup>291-292</sup> These immune responses can consequently lead to corneal allograft rejection.<sup>100,292</sup>

This proposed model hypothesises that the direct pathway of antigen presentation occurs primarily within the anterior segment of the eye, rather than in the secondary lymphoid tissues. It should be noted that there is between 100-fold to 1000-fold more CD4+ T cells that can recognise foreign MHC on donor APCs for direct processing, compared to CD4+ T cells with specificity for a specific foreign-peptide complexed with recipient MHC for indirect processing.<sup>293</sup> The direct pathway of antigen presentation is much stronger than the indirect pathway at mounting an immune response against alloantigen. Moreover, in rodent models of renal and cardiac transplants, the number of alloreactive T cells specific for donor APCs decreases with time.<sup>102</sup> This suggests that the direct pathway of antigen presentation may be most critical for sensitisation shortly after transplantation and that sensitisation through the indirect pathway may occur at a later stage after transplantation. This proposed model hypothesises that the most potent immune response against the corneal allograft is likely to occur within the anterior segment shortly after transplantation via the direct pathway and the indirect processing appears to take place at a later stage after transplantation and can occur within the anterior segment or within the secondary lymphoid tissues.

In summary, this model proposes that two independent branches of the immune response work concurrently to survey and eliminate foreign antigen within the anterior segment of the eye. The premise is that CD4<sup>+</sup> T cells can be activated within (1) the anterior segment of the eye by antigen presentation via both indirect and direct pathways, and (2) within the secondary lymphoid tissue via the indirect pathway of antigen presentation after drainage of soluble donor-derived antigen through the lymph and the blood to these tissues. It is hypothesised that disrupting one arm of the antigen presentation process has the potential to delay the course of corneal allograft rejection. However, to abolish all antigen presentation during corneal transplantation, disruption of both arms of the antigen presentation process must take place to achieve universal corneal allograft acceptance.

#### **5.3.d. Inhibition of antigen presentation with anti-CD4 antibodies and antibody fragments in rodents**

Experiments described in this thesis showed that expression of an anti-CD4 antibody fragment from the donor corneal endothelium *was* able to significantly prolong the median day of rejection by 5 days in rats, indicating that antigen presentation within the anterior segment of the eye was suppressed. However, rejection did occur in all recipients, also suggesting that antigen presentation can occur elsewhere. If antigen shed from a corneal allograft were to travel to the secondary lymphoid tissues in soluble form, whilst also remaining locally within the anterior segment of the eye, then expression of the anti-CD4 antibody fragment from the donor corneal endothelium is likely to suppress only the immune response within the anterior segment and is unlikely to modulate antigen presentation in the distant tissues. Consequently, only one branch of the antigen presentation process would be

inhibited, and sensitisation and DTH would occur within the secondary lymphoid tissues, which could then lead to corneal allograft rejection. This may be the reason why expression of the anti-CD4 antibody fragment from the donor corneal endothelium was only able to delay corneal allograft rejection in my experiments.

It is possible that the anti-rat CD4 scFv expressed from the donor corneal endothelium may travel to the secondary lymphoid tissues, in a similar way as soluble antigen does when it is delivered to the anterior chamber.<sup>91,106-107</sup> However, if a small amount of scFv were able to reach the secondary lymphoid tissues, it is likely to be cleared rapidly from the tissues,<sup>163</sup> and is unlikely to have an impact on antigen presentation.

Previous studies in mice and rats have revealed that systemic delivery of anti-CD4 mAbs have been able to significantly delay corneal allograft rejection after transplantation into healthy recipient corneal beds.<sup>151,153-154</sup> Using strong immunological strain combinations where no unmodified allografts survived indefinitely, a proportion of recipients that received the systemic delivery of the anti-CD4 mAbs survived indefinitely in all studies, suggesting that antigen presentation had been suppressed in these recipients. Although indefinite survival was reported in some rats in each study, there were also reports of corneal allograft rejection in each study. When applying my proposed model of antigen presentation during corneal transplantation to explain these findings, it is likely that systemic delivery of the anti-CD4 mAbs would reach most secondary lymphoid organs through the vasculature and the lymphatics. Therefore, the indirect pathway of antigen presentation within these tissues was possibly suppressed and inhibited. However, the systemic delivery

of the anti-CD4 mAb might not have been able to reach the anterior segment of the eye and antigen presentation via either the indirect or direct pathway might have occurred locally. If this were the case, it would explain why rejection was not completely suppressed in all animals but rather simply delayed.

Vitova and colleagues reported prolonged survival of corneal allografts after systemic delivery of an anti-CD4 mAb in mice that had prevascularised corneal beds prior to transplantation. However, rejection did eventually occur in all allografts.<sup>152</sup> This study shows that in a high-risk setting systemic delivery of the anti-CD4 mAb was not able to abolish T cell sensitisation, but might have been able to inhibit at least the one arm of the process (i.e. antigen presentation within the secondary lymphoid organs).

In summary, I hypothesise that in the rat, expression of an anti-rat CD4 scFv from the donor corneal endothelium using a lentiviral vector, coupled with the systemic delivery of an anti-CD4 mAb (which will be retained within tissue for longer than a scFv), will inhibit sensitisation within the anterior segment and within the secondary lymphoid organs. This immunosuppressive strategy has the potential to completely eliminate sensitisation of alloantigens and might therefore lead to complete acceptance of all corneal allografts indefinitely.

### **5.3.e. The outcome of corneal allograft survival after bilateral lymphadenectomy of the cervical lymph nodes in rodents**

Bilateral lymphadenectomy of the cervical lymph nodes prior to corneal transplantation has proven to be a successful strategy to prolong corneal allograft

survival in some studies (Table 5.2).<sup>118-121</sup> Yamagami *et al.* reported indefinite survival in all mice that received allografts into normal recipient corneal beds,<sup>120</sup> whilst Plskova reported prolonged survival in a similar study.<sup>118</sup> Bilateral lymphadenectomy of the cervical lymph nodes was also able to prolong corneal allograft survival in recipients with prevascularised corneal beds<sup>119,121</sup> but not in presensitised mice.<sup>119</sup> These studies suggest that the cervical lymph nodes are a site of ocular antigen drainage, as their removal delays<sup>121</sup> and even prevents<sup>120</sup> the onset of DTH to alloantigen.

However, in my experiments bilateral lymphadenectomy of the cervical lymph nodes prior to corneal transplantation *did not* prolong corneal allograft survival in the WF into F344 rat strain combination. A study by Schulte *et al.* also showed that mice that underwent bilateral cervical lymphadenectomy prior to corneal transplantation *did not* experience prolonged corneal allograft survival.<sup>111</sup>

A possible explanation for the differences between the different studies may be because antigen presentation *does not* occur within the eye when using the C57BL/6 into BALB/c strain combination (used by Yamagami and colleagues) and this might be why this study showed indefinite survival of all corneal allografts after the bilateral removal of the cervical lymph nodes.<sup>120</sup>

If antigen presentation did not occur within the eye when using the C57BL/6 into BALB/C strain combination, this would account for the prolonged survival of the corneal allografts when the cervical lymph nodes were removed,<sup>120</sup> because these nodes would be the main site of antigen presentation in these recipients. To support

**Table 5.2: Corneal allograft survival outcome after bilateral lymphadenectomy of the cervical lymph nodes**

Species	Donor strain	Recipient strain	Corneal bed	Corneal allograft survival	Survival of unmodified allografts	Additional information	Reference
Rat	WF	F344	Healthy	Not prolonged	10%	-	Table 4.9
Mouse	C3H	BALB/c	Healthy	Not prolonged	0%	Increased aqueous outflow found in the blood, liver and spleen	111
Mouse	C57BL/6	BALB/c	Healthy	Prolonged*	50%	C57BL/6 donor is able to induce ACAID	120
Mouse	C57BL/6	BALB/c	Vascularised	Prolonged	0%	C57BL/6 donor is able to induce ACAID	121
Mouse	C57BL/10	BALB/c	Healthy	Prolonged	0%	-	118
Mouse	C57BL/10	BALB/c	Vascularised	Prolonged	0%	-	119
Mouse	C57BL/10	BALB/c	Presensitised with corneal allograft	Not prolonged	0%	-	119
Mouse	C57BL/10 (H-2b)	BALB/c (H-2d)	Presensitised with skin graft	Not prolonged	0%	-	119

\* = Indefinite survival of all corneal allografts; ACAID, anterior chamber-associated immune deviation

Note: All rodent strain combinations had MHC and multiple minor histocompatibility mismatches

this hypothesis, the removal of the cervical lymph nodes appeared to have the greatest impact on sensitisation and subsequent corneal allograft survival in the C57BL/6 into BALB/C mouse model,<sup>120</sup> when compared to other rodent strain combinations (Table 5.2). Plskova and colleagues also reported prolonged corneal allograft survival after bilateral removal of the cervical lymph nodes in a different murine strain combination (C57BL/10 into BALB/c mice),<sup>118-119</sup> however indefinite survival in all corneal allografts was not reported in these studies.<sup>118-119</sup> It could be speculated that the C57BL/10 into BALB/c strain combination might have *reduced* ability for antigen presentation within the anterior segment, but not to the same extent as the C57BL/6 into BALB/c strain combination, which might explain how corneal allograft survival was prolonged in the Plskova *et al.* studies.<sup>118-119</sup>

The C57BL/6 into BALB/C strain combination is known to produce between 50-60% indefinite survival of unmodified allografts (Table 5.2).<sup>25,47,120-121</sup> To further support the hypothesis that antigen presentation does not occur within the eye when using the C57BL/6 into BALB/C strain combination, Yamada and co-workers revealed that the C57BL/6 into BALB/C strain combination more readily induces ACAID compared to other murine strain combinations.<sup>25</sup>

In summary, I suggest that the strength of the immunological barrier between the recipient and the donor when using inbred rodent strains can determine the anatomic site at which antigen presentation occurs during corneal graft rejection, and can subsequently affect the outcome of corneal allograft survival after bilateral lymphadenectomy of the cervical lymph nodes. Since humans are an outbred species it is likely that the immune response that occurs in humans is more similar to the

immune response that occurs when using a strong immunological barrier, such as the WF into F344 rat strain combination, compared to the immune response that occurs when using a weaker immunological barrier such as the C57BL/6 into BALB/C murine strain combination. Therefore, the results obtained when using a strong immunological barrier may be more reflective of the human immune response during corneal transplantation.

#### **5.3.f. Regional immunosuppression for human corneal transplantation**

This project aimed to identify the anatomic site where antigen presentation occurred in response to corneal transplantation for the purpose of identifying the most suitable location for a regional immunosuppressive therapy to prevent corneal allograft rejection. The findings described in this thesis showed that in the rat, moderate success was achieved when the donor corneal endothelium was transduced with a lentiviral vector carrying an anti-CD4 antibody fragment prior to corneal transplantation. These recipients experienced modest prolongation of corneal allograft survival compared to controls. However, all corneal allografts did eventually reject, suggesting that the immune response was merely delayed, and that sensitisation to the corneal allograft occurred at a site other than within the anterior segment of the eye.

Several studies have identified the cervical lymph nodes as another potential site of antigen presentation during corneal transplantation in rodents,<sup>26,100,111-112,118-121,123,292</sup> and the systemic delivery of anti-CD4 mAbs has also been able to prolong corneal allograft survival.<sup>151-154</sup> In humans, systemic delivery of CAMPATH-1H, (a



humanised mAb against CD52), reduced ocular inflammation in patients including those with corneal grafts, with no adverse side effects observed.<sup>150</sup>

I propose that in order to abolish sensitisation to corneal allografts in humans, a regional and systemic immunosuppressive strategy is required. This could involve regional immunosuppression by transducing the donor corneal endothelium prior to transplantation with a lentiviral vector carrying an anti-CD4 antibody fragment, in addition to systemic delivery of an anti-CD4 mAb (which will be retained within the tissue for longer than a scFv) to the recipient. This strategy would be adjunctive to the topical administration of glucocorticosteroids. This strategy has the potential to inhibit antigen presentation and early T cell activation at all potential anatomic sites. Expression of the anti-CD4 antibody fragment from the donor corneal endothelium may inhibit sensitisation within the anterior segment of the eye and systemic delivery of the anti-CD4 mAb may reach the secondary lymphoid organs via the circulation and the lymphatics where sensitisation may also be inhibited. In summary, this regional and systemic immunosuppressive strategy has the potential to completely eliminate the generation of an immune response to a corneal allograft and could potentially prevent corneal allograft rejection.

## **APPENDIX 1: BUFFERS AND SOLUTIONS**

**A1.1 Chrome-alum-subbed microscope slides**

Prepare 0.05%  $\text{Cr}(\text{SO}_4)_2 \cdot 12\text{H}_2\text{O}$  w/v in  $\text{DDH}_2\text{O}$ . Submerge glass microscope slides for 5 min. Allow to dry.

**A1.2 DEPC- $\text{H}_2\text{O}$** 

1 ml diethylpyrocarbonate (DEPC)

Up to 1L  $\text{DDH}_2\text{O}$

**A1.3 DMEM (high glucose)**

1 sachet DMEM powdered medium (Multicel™ # 50-114-PA,  
ThermoElectron, Melbourne, Australia)

3.7 g  $\text{NaHCO}_3$

3 g D-glucose (anhydrous)

**A1.4 Eosin stain**

Stock: 1 g eosin Y

20 ml  $\text{DDH}_2\text{O}$

80 ml 95% ethanol

Add 25 ml eosin stock to 75 ml ethanol (80%). Immediately prior to use add 0.5 ml glacial acetic acid.

**A1.5 FACS fixative**

10 g	D-glucose
13 ml	formaldehyde
625 µl	4M sodium azide
Up to 500 ml PBS	

Adjust pH to 7.3. Protect from light and store at 4°C.

**A1.6 GelRed™ agarose plates**

1 g	agarose
100 ml	DDH <sub>2</sub> O

Combine and melt in the microwave. Add 10 µl GelRed™ (10 000X; Biotium Inc, Hayward, CA, USA) and swirl to mix. Pour into gel tank with comb placed at top of tank to set wells. Allow gel to set before loading DNA into wells.

**A1.7 Haematoxylin solution**

125 g	haematoxylin powder
75 ml	glycerol
0.25 ml	sodium iodate
12.5 g	aluminium potassium sulphate
0.5 ml	glacial acetic acid
2-4 ml	absolute ethanol
175 ml DDH <sub>2</sub> O	

Stir alum in 100 ml water over gentle heat until it forms a paste and then add remaining H<sub>2</sub>O. Dissolve in ethanol. Cool and add haematoxylin powder. In fume hood, add sodium iodate, acid and glycerol. Store at RT for at least 24 hours. Filter through Whatmans No 1 (Whatman, Maldstone, UK) prior to use.

**A1.8 HEPES-buffered RPMI medium**

1 sachet	RPMI 1640 medium (Gibco™ #23400-021, with L glutamine, 25 mM HEPES buffer, no NaHCO <sub>3</sub> ; Invitrogen, Vic)
2.0 g	NaHCO <sub>3</sub>
up to 1L	DDH <sub>2</sub> O

**A1.9 HEPES-buffered Saline**

HEPES	2.39 g
MgCl	0.406 g
Sucrose	20 g
NaCl	6.65 g
NaOH (10 M)	0.8 ml
Up to 1L	Water for irrigation (Baxter)

Adjust pH to 8.0

**A1.10 LB medium**

10 g	Bactoc Tryptone (Becton, Dickinson and Company, Sparks, MD, USA)
5 g	Bacto™ Yeast extract (Becton, Dickinson and Company)
Up to 1L	DDH <sub>2</sub> O

Adjust pH to 7.0 with NaOH and autoclave.

**A1.11 LB agar plates**

1.5 g            Bacto™ Agar (Becton, Dickinson and Company)

100 ml        LB

Combine and autoclave. Allow to cool until bottle can be held. Add appropriate antibiotic and pour into Petri dishes. Allow plates to set and dry before sealing and storing at 4°C. Leftover agar can be stored at RT and melted in microwave prior to use.

**A1.12 Low salt LB medium**

5 g            Bacto™ Tryptone (Becton, Dickinson and Company)

2.5 g            Bacto™ Yeast extract (Becton, Dickinson and Company)

2.5 g            NaCl

Adjust pH to 7.0 with NaOH and autoclave.

**A1.13 PBS (10x)**

28.55 g        Na<sub>2</sub>HPO<sub>4</sub>·2H<sub>2</sub>O

(or 22.85 g)    Na<sub>2</sub>HPO<sub>4</sub>)

6.26 g        NaH<sub>2</sub>PO<sub>4</sub>·2H<sub>2</sub>O

70 g            NaCl

up to 1 L      DDH<sub>2</sub>O

Autoclave.

**A1.14 PBS-azide**

4 M sodium azide stock

10X PBS stock

DDH<sub>2</sub>O

**A1.15 RBC lysis solution (10X)**

16.52 g            NH<sub>4</sub>Cl

2 g                KHCO<sub>3</sub>

0.074 g           EDTA

Make up to 200 ml with water for irrigation; adjust pH to between 7.3-7.5 with 1 M NaOH and autoclave.

**A1.16 SOC medium**

2 g                Bacto™ Tryptone (Becton, Dickinson and Company)

0.5 g              Bacto™ Yeast extract (Becton, Dickinson and Company)

0.06 g            NaCl

0.08 g            KCl

0.25 g            MgSO<sub>4</sub>·7H<sub>2</sub>O

up to 100 ml    DDH<sub>2</sub>O

Adjust pH to 7.0 and autoclave. Add 2 ml sterile glucose (1 M) and 1 ml sterile MgCl<sub>2</sub> (1 M).

**A1.17 Sodium azide 4M stock**

26 g              NaN<sub>3</sub>

up to 100 ml    DDH<sub>2</sub>O

**A1.18 TBE (10x)**

108 g	Tris base
55 g	Boric acid
40 ml	0.5 M EDTA pH 8

Dissolve in 1L DDH<sub>2</sub>O and autoclave. Dilute in DDH<sub>2</sub>O prior to use.

**A1.19 Trypan blue stock**

1 g	Trypan Blue
Up to 100 ml	DDH <sub>2</sub> O

Filter through Whatman No 1 paper and store at 4°C. Use at 1:10 in PBS.

**A1.20 Trypsin-EDTA**

0.5 g	trypsin (1:250)
0.2 g	EDTA
100 ml	PBS (10X)
Up to 1 L	DDH <sub>2</sub> O

Filter sterilise (0.2 µm) and store at -20°C in 20 ml aliquots. Store at 4°C during use.



## **APPENDIX 2: VECTOR MAPS**

### A2.1: pBS-CD55-F2A-CD59 vector map

Refer to Chapter 2, Table 2.3 for more details.

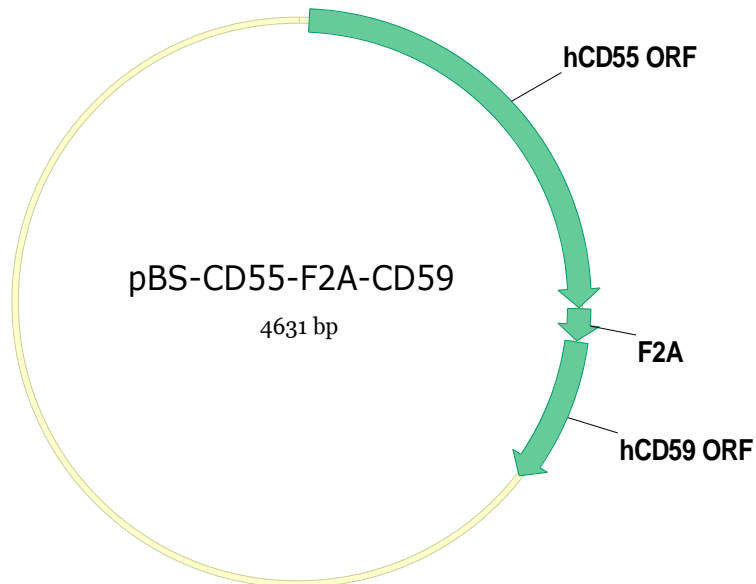


**Figure A2.1: pBS-CD55-F2A-CD59 vector map:** Sequences of interest are marked with arrows including the human CD55 open reading frame (ORF) (hCD55 ORF), the FMDV 2A self-processing sequence (F2A) and the human CD59 ORF (hCD59 ORF).

## A2.2: pHIV-eYFP vector map

Refer to Chapter 2, Table 2.3 for more details.

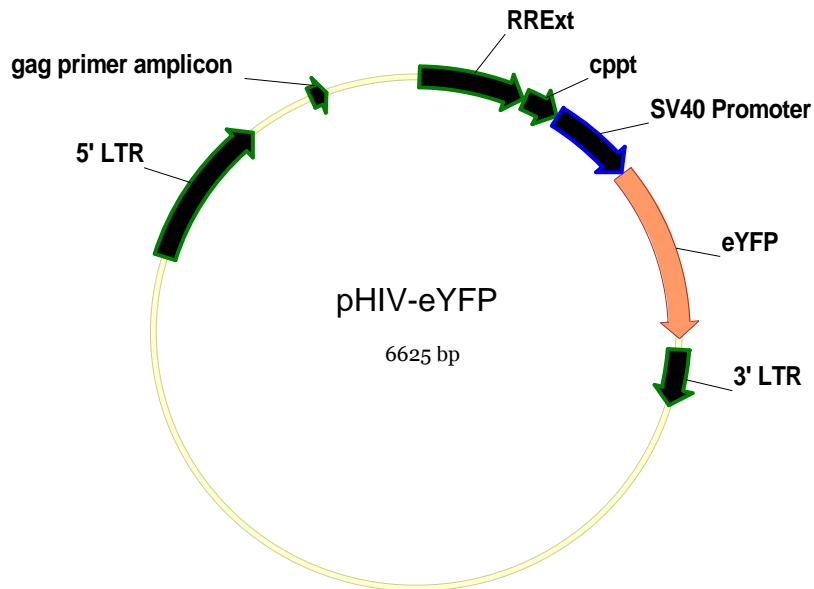


**Figure A2.2: pHIV-eYFP vector map:** Sequences of interest are marked with arrows. The internal SV40 promoter controls expression of eYFP. The 5' and 3' long terminal repeats (LTRs), the central polypurine tract (cppt), the extended rev response element (RRExt) and the gag primer amplicon are also highlighted.

### A2.3 fHSSOX38scFv in pAdtrackCMV vector map

Refer to Chapter 2, Table 2.3 for more details.

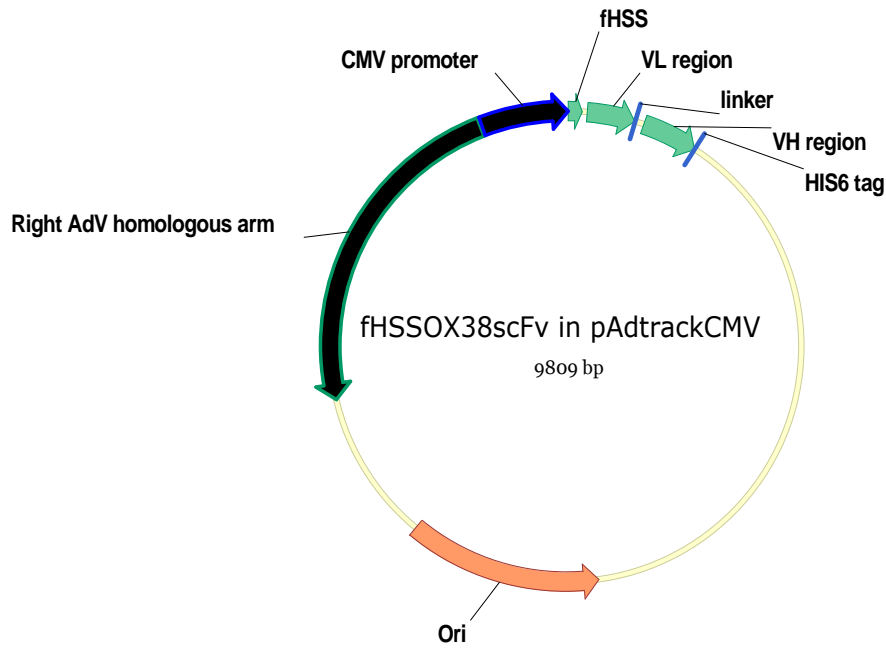


**Figure A2.3: fHSSOX38scFv in pAdtrackCMV vector map:** Sequences of interest are shown with arrows. The anti-rat CD4 scFv gene consists of a variable light (VL) domain and a variable heavy (VH) domain joined together with a 20 amino acid linker sequence. The anti-rat CD4 scFv gene had a factor H secretory sequence (fHSS) at its amino terminus and a 6 histidine tag (HIS6) at its carboxyl terminus. The origin of replication and the Right AdV homologous arm are also highlighted.

## A2.4 pHIV-EK5 vector map

Refer to Chapter 2, Table 2.3 for more details.

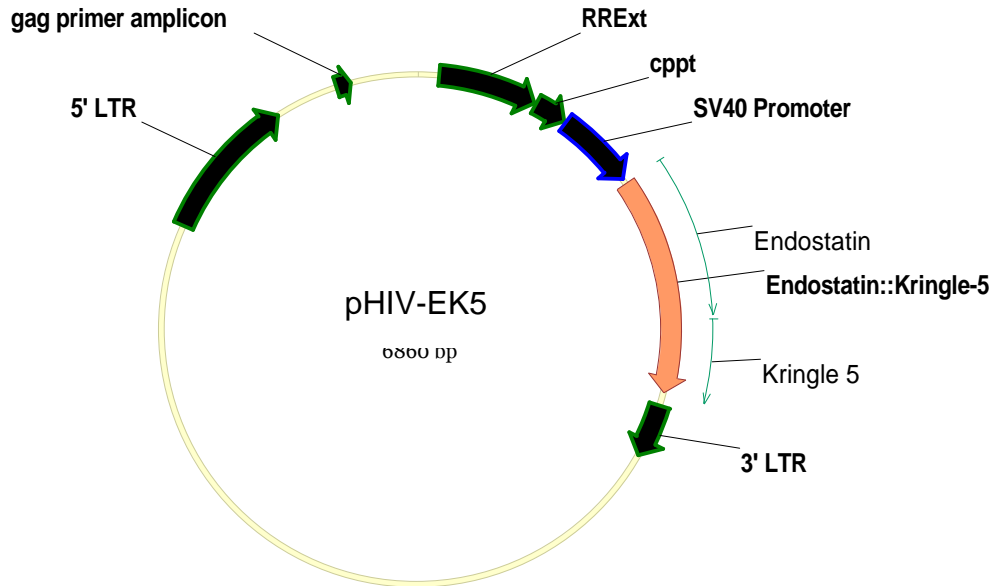


**Figure A2.4: pHIV-EK5 vector map:** Sequences of interest are shown with arrows. The internal SV40 promoter drove expression of Endostatin::Kringle-5. The 5' and 3' long terminal repeats (LTRs), the central polypurine tract (cppt), the extended rev response element (RRExt) and the gag primer amplicon are also highlighted.

### A2.5 pBLAST41-hEndoKring5 vector map

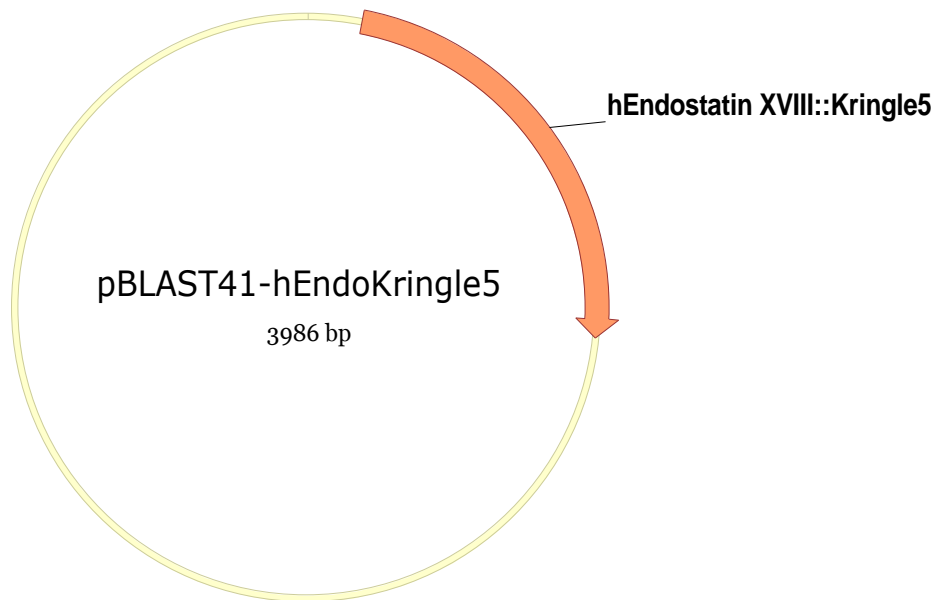


**Figure A2.5: pBLAST41-hEndoKring5 vector map:** This commercially available expression vector contains the hEndostatinXVIII::Kring5 fusion protein (InvivoGen, San Diego, CA, USA).

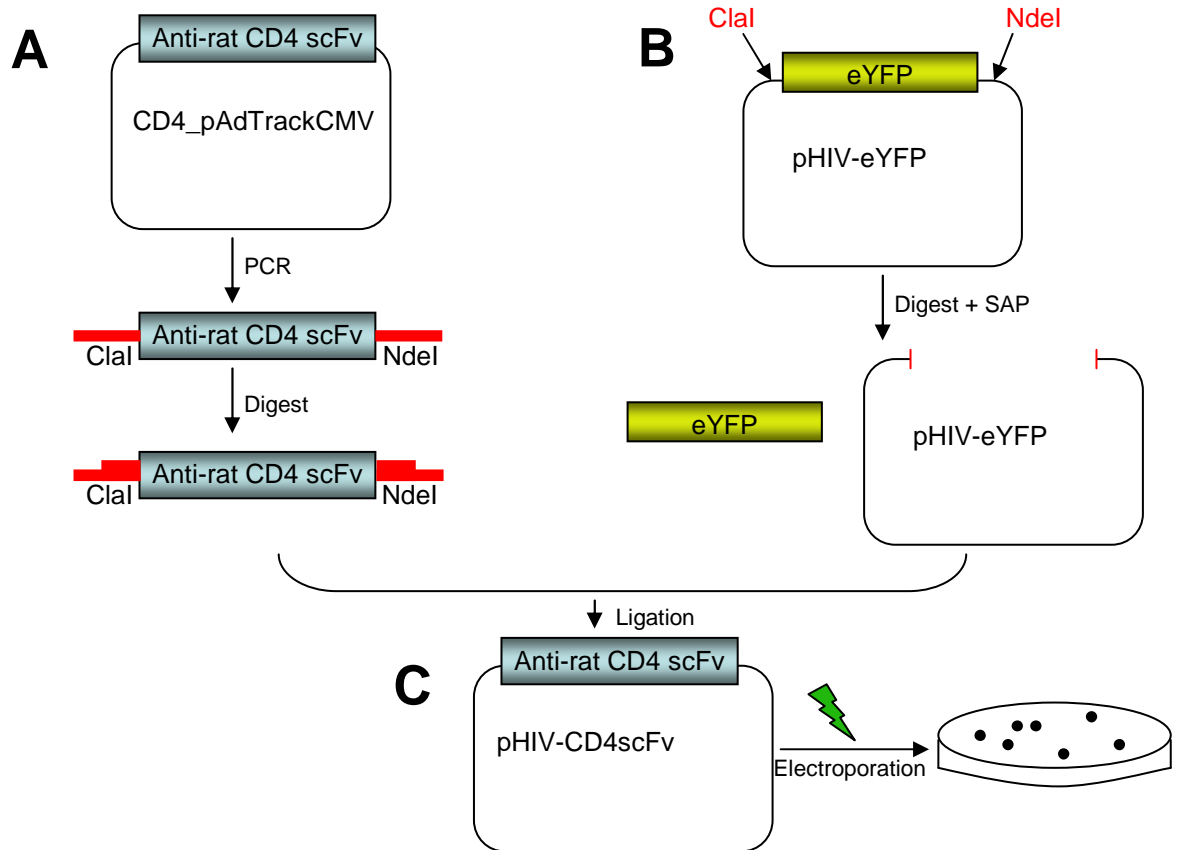
## **APPENDIX 3: CONSTRUCTION OF pHIV-CD4scFv**

The anti-rat CD4 scFv sequence was amplified from fHSSOX38scFv in pAdtrackCMV (Table 2.3; Appendix 2) using primers that added a ClaI restriction site to the 5' end of the PCR product and an NdeI restriction site to the 3' end of the PCR product (Figure A3.1). The anti-rat CD4 scFv sequence was ligated into the pHIV-eYFP plasmid (Appendix 2) using the ClaI and NdeI restriction sites and electroporated into DH5 $\alpha$  electrocompetent *E. coli* (Figure A3.1).

A PCR was performed on the plasmid DNA from potential pHIV-CD4scFv clones and all eight clones were seen to contain the anti-rat CD4 scFv insert (Figure A3.2). Clone 7 was randomly selected for sequence analysis and was found match the predicted sequence for anti-rat CD4 scFv in the correct orientation within the plasmid (Figure A3.3). The pHIV-CD4scFv plasmid (Figure A3.4) was used to construct the pHIV-CD4scFv\_F2A\_eYFP plasmid (Section 3.3.a.1.), the pHIV-eYFP\_F2A\_CD4scFv plasmid (Section 3.3.a.2.) and was used for lentiviral vector production.



**Figure A3.1: Diagrammatic representation of the construction of pHIV-CD4scFv.** **(A)** Anti-rat CD4 scFv was amplified from the fHSSOX38scFv in pAdtrackCMV plasmid. The forward primer (ClaI fHSS for; refer to Table 2.5 for the primer sequence) was designed to add a ClaI restriction site to the 5' end of the PCR product and the reverse primer (NdeI scFv rev; refer to Table 2.5 for the primer sequence) was designed to add an NdeI restriction site to the 3' end of the PCR product and these restriction sites were digested. **(B)** The eYFP sequence was removed from the pHIV-SV40-eYFP plasmid by digestion with ClaI and NdeI restriction enzymes. The digested plasmid was treated with Shrimp Alkaline Phosphatase (SAP) which de-phosphorylated the ends of the plasmid to prevent them from self re-ligation. **(C)** The ClaI/NdeI digested anti-rat CD4 scFv PCR product and the ClaI/NdeI digested pHIV-SV40 linearised plasmid were ligated together and electroporated into DH5 $\alpha$  electrocompetent *E. coli*.



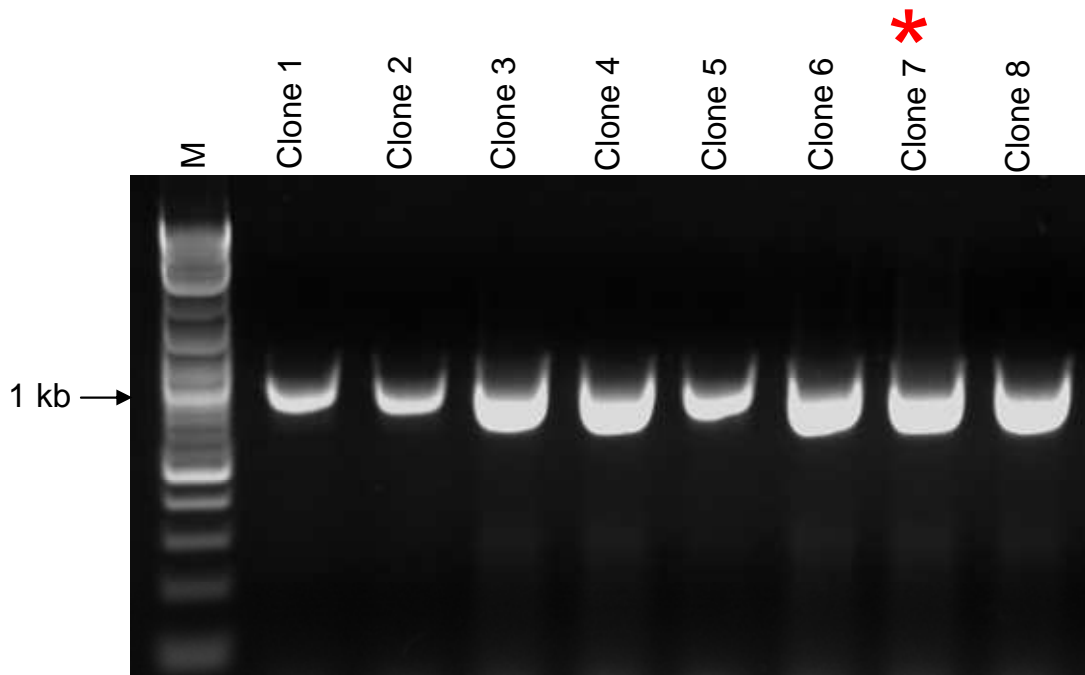


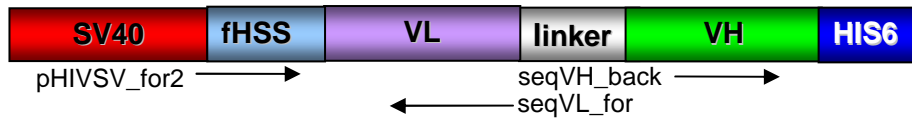
**Figure A3.2: Detection of the anti rat CD4 scFv insert (0.9 kb) in pHIV-CD4scFv clones.** Anti-rat CD4 scFv amplified in all plasmid DNA extracts from potential pHIV-SV40-CD4scFv constructs using ClaI fHSS for and NdeI scFv rev2 primers (refer to Table 2.5 for primer sequences). Clone 7 (\*) was randomly selected for sequence analysis. Lane M contained 2 log DNA ladder.

**Figure A2.3: Clone 7 sequencing results show insertion of anti-rat CD4 scFv into the pHIV-SV40 plasmid in the correct orientation. (A)**

Sequencing reactions were performed using three primers (as seen in diagram; refer to Table 2.5 for primer sequences) to determine the exact sequence of the anti-rat CD4 scFv insert. **(B)** Alignment of the predicted sequence against the actual sequence of the anti-rat CD4 scFv insert in clone 7 is shown. Numbers represent base pair count and coding regions of interest are coloured. | represents exact nucleotide matches. VL, variable light; VH, variable heavy.s

.

**A**



**B**

	fHSS	
predicted	1 CGATCAAAAAATGAGACTTCTAGCAAAGATTATTTGCCTTATGTTATGGG	50
pHIV-SV40-CD4scFv_clone_7	1 CGATCAAAAAATGAGACTTCTAGCAAAGATTATTTGCCTTATGTTATGGG	50
predicted	51 CTATTTGTGTAGCAGAAGATTGCTCGAGGCCAGCCGGCCATGGCGGAC	100
pHIV-SV40-CD4scFv_clone_7	51 CTATTTGTGTAGCAGAAGATTGCTCGAGGCCAGCCGGCCATGGCGGAC	100
predicted	101 TACAAAGACATTGTGCTCACTCAGTCTCCAGCCACCCTGTCTGTGACTCC	150
pHIV-SV40-CD4scFv_clone_7	101 TACAAAGACATTGTGCTCACTCAGTCTCCAGCCACCCTGTCTGTGACTCC	150
predicted	151 AGGAGATAGCGTCAGTCTTTCCTGCAGGGCCAGCCGAANTATTAGCAACA	200
pHIV-SV40-CD4scFv_clone_7	151 AGGAGATAGCGTCAGTCTTTCCTGCAGGGCCAGCCGAANTATTAGCAACA	200
predicted	201 ACCTACACTGGTATCAACAAAAATCACATGAGTCTCCAAGGCTTCTCATC	250
pHIV-SV40-CD4scFv_clone_7	201 ACCTACACTGGTATCAACAAAAATCACATGAGTCTCCAAGGCTTCTCATC	250
predicted	251 AAGTATGCTTCCAGTCCATCTCTGGGATCCCTCCAGGTTCCAGNGGCAG	300
pHIV-SV40-CD4scFv_clone_7	251 AAGTATGCTTCCAGTCCATCTCTGGGATCCCTCCAGGTTCCAGNGGCAG	300
predicted	301 TGGATCAGGGACAGATTTCACTCTCAGTATCAACAGTGTGGAGACTGAAG	350
pHIV-SV40-CD4scFv_clone_7	301 NGGATCAGGGACAGATTTCACTCTCAGTATCAACAGTGTGGAGACTGAAG	350
predicted	351 ATTTTGAATGTATTCTGTCAACAGAGTAACAGCTGGCCGTACACGTTT	400
pHIV-SV40-CD4scFv_clone_7	351 ATTTTGAATGTATTCTGTCAACAGAGTAACAGCTGGCCGTACACGTTT	400
predicted	401 GGAGGGGGACCAAGCTGGAAATAAACCGTGGTGGTGGTCTGGTGG	450
pHIV-SV40-CD4scFv_clone_7	401 GGAGGGGGACCAAGCTGGAAATAAACCGTGGTGGTGGTCTGGTGG	450
predicted	451 TGGTGGTCTGGCGGCGCGCTCCGGTGGTGGTGGATCCGAAGTGAAG	500
pHIV-SV40-CD4scFv_clone_7	451 TGGTGGTCTGGCGGCGCGCTCCGGTGGTGGTGGATCCGAAGTGAAG	500
predicted	501 TTGAGGAGTCTGGCCCTGGGATATTGAAGCCCTCAGACCCCTCAGTCTG	550
pHIV-SV40-CD4scFv_clone_7	501 TTGAGGAGTCTGGCCCTGGGATATTGAAGCCCTCAGACCCCTCAGTCTG	550
predicted	551 ACTTGTCTTCTCTGGGTTTCACTGAGCACTTCTGGTATGGGTGATAG	600
pHIV-SV40-CD4scFv_clone_7	551 ACTTGTCTTCTCTGGGTTTCACTGAGCACTTCTGGTATGGGTGATAG	600
predicted	601 CTGGATTTCGTAGCCCTCAGGGAAGGGTCTGGAGTGGCTGGCACACATTT	650
pHIV-SV40-CD4scFv_clone_7	601 CTGGATTTCGTAGCCCTCAGGGAAGGGTCTGGAGTGGCTGGCACACATTT	650
predicted	651 GGTGGGATGATGATAAGTACTATAACCCATCCCTGAAGAGCCAGCTCACA	700
pHIV-SV40-CD4scFv_clone_7	651 GGTGGGATGATGATAAGTACTATAACCCATCCCTGAAGAGCCAGCTCACA	700
predicted	701 ATCTCCAAGGATACCTCCAGAAACCAGGTATTCTCAAGATCACCAGTGT	750
pHIV-SV40-CD4scFv_clone_7	701 ATCTCCAAGGATACCTCCAGAAACCAGGTATTCTCAAGATCACCAGTGT	750
predicted	751 GGACACTGCAGATACTGCCACTTACTACTGTGCTCGAAATTATGATTACG	800
pHIV-SV40-CD4scFv_clone_7	751 GGACACTGCAGATACTGCCACTTACTACTGTGCTCGAAATTATGATTACG	800
predicted	801 ACGGGTACTTCGATGCTGGGGCGCAGGGACCTCAGTCACCGTCTCCTCG	850
pHIV-SV40-CD4scFv_clone_7	801 ACGGGTACTTCGATGCTGGGGCGCAGGGACCTCAGTCACCGTCTCCTCG	850
predicted	851 GCCTCGGGGGCCGATCACCATCATCACCATCATTAGCATATG	892
pHIV-SV40-CD4scFv_clone_7	851 GCCTCGGGGGCCGATCACCATCATCACCATCATTAGCATATG	892

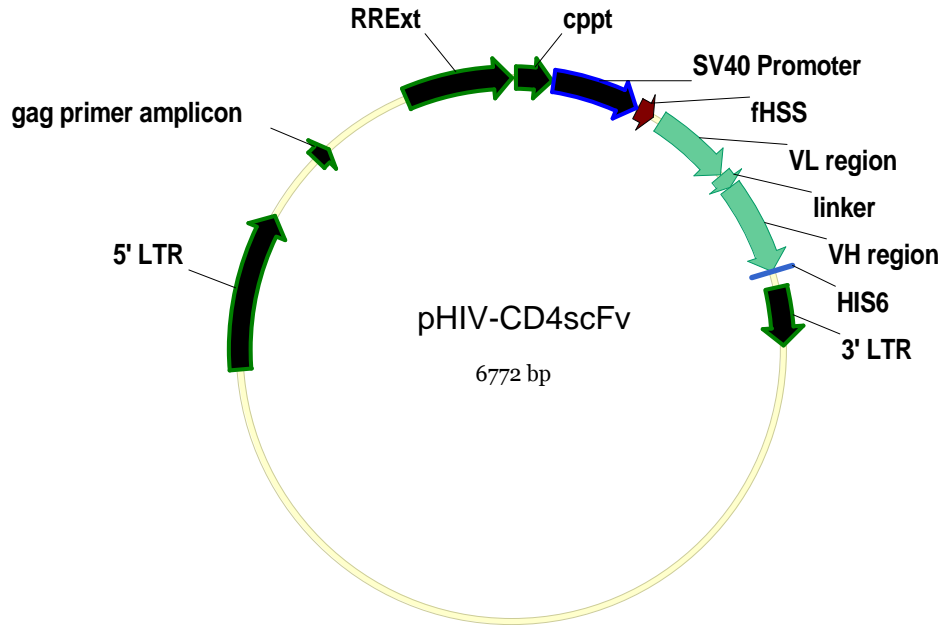


**Figure A2.4: pHIV-CD4scFv vector map.** Sequences of interest are shown with arrows. The anti-rat CD4 scFv gene consists of a variable light (VL) domain and a variable heavy (VL) domain joined together with a 20 amino acid linker sequence. The anti-rat CD4 scFv has a factor H secretory sequence (fHSS) at its amino terminus and a 6 histidine tag (HIS6) at its carboxyl terminus. The internal SV40 promoter controls the expression of anti-rat CD4 scFv. The 5' and 3' long terminal repeats (LTRs), the central polypurine tract (cppt), the extended rev response element (RRExt) and the gag primer amplicon are also highlighted.

## **APPENDIX 4: SEQUENCE ANALYSIS**

**Figure A4.1: Colony 4.11 sequencing results show insertion of the anti-rat CD4scFv\_F2A SOE-PCR product into the pHIV-SV40 plasmid at the *Cla*I restriction site. (A)** Sequencing reactions were performed using three primers (as seen on the diagram; refer to Table 2.5 for primer sequences) to determine the exact sequence of the SOE-PCR product. **(B)** Alignment of the predicted sequence against the actual sequence of colony 4.11 is shown. Refer to Section 3.3.a.1. for the construction of pHIV-CD4scFv\_F2A\_eYFP. Numbers represent base pair count and coding regions of interest are colour coded. Exact nucleotide matches are represented by \*.



A4.1 Sequence analysis of pHIV-CD4scFv\_F2A\_eYFP

**A**



**B**

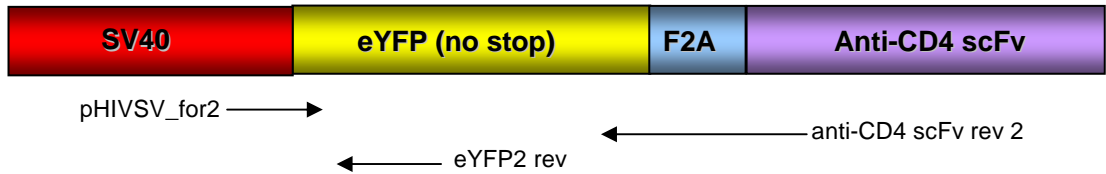
	C1aI	fHSS	
predicted HIV-SV-CD4_F2A_eYFP_colony_4.11	<b>CGATCAAAAAATGAGACTTCTAGCAAAGATTATTGCTTATGTTATGGG</b>		50
	CGATCAAAAAATGAGACTTCTAGCAAAGATTATTGCTTATGTTATGGG		50
	*****		
predicted HIV-SV-CD4_F2A_eYFP_colony_4.11	CTATTTGTGTAGCAGAAGATTGCCTCGAGGCCAGCCGGCCATGGCGGAC		100
	CTATTTGTGTAGCAGAAGATTGCCTCGAGGCCAGCCGGCCATGGCGGAC		100
	*****		
	<b>anti-rat CD4 scFv</b>		
predicted HIV-SV-CD4_F2A_eYFP_colony_4.11	TACAAAGACATTTGTGCTCACTCAGTCTCCAGCCACCCTGTCTGTGACTCC		150
	TACAAAGACATTTGTGCTCACTCAGTCTCCAGCCACCCTGTCTGTGACTCC		150
	*****		
predicted HIV-SV-CD4_F2A_eYFP_colony_4.11	AGGAGATAGCGTCAGTCTTTCCTGCAGGCCAGCCGAANTATTAGCAACA		200
	AGGAGATAGCGTCAGTCTTTCCTGCAGGCCAGCCGAANTATTAGCAACA		200
	*****		
predicted HIV-SV-CD4_F2A_eYFP_colony_4.11	ACCTACACTGGTATCAACAAAAATCACATGAGTCTCCAAGGCTTCTCATC		250
	ACCTACACTGGTATCAACAAAAATCACATGAGTCTCCAAGGCTTCTCATC		250
	*****		
predicted HIV-SV-CD4_F2A_eYFP_colony_4.11	AAGTATGCTTCCCAGTCCATCTCTGGGATCCCCTCCAGGTTCAAGGCGAG		300
	AAGTATGCTTCCCAGTCCATCTCTGGGATCCCCTCCAGGTTCAAGGCGAG		300
	*****		
predicted HIV-SV-CD4_F2A_eYFP_colony_4.11	TGGATCAGGGACAGATTTCACTCTCAGTATCAACAGTGTGGAGACTGAAG		350
	TGGATCAGGGACAGATTTCACTCTCAGTATCAACAGTGTGGAGACTGAAG		350
	*****		
predicted HIV-SV-CD4_F2A_eYFP_colony_4.11	ATTTTGAATGTATTTCTGTCAACAGAGTAACAGCTGGCCGTACACGTTTC		400
	ATTTTGAATGTATTTCTGTCAACAGAGTAACAGCTGGCCGTACACGTTTC		400
	*****		
predicted HIV-SV-CD4_F2A_eYFP_colony_4.11	GGAGGGGGACCAAGCTGGAATAAAACGTGGTGGTGGTGTCTGTGGTGG		450
	GGAGGGGGACCAAGCTGGAATAAAACGTGGTGGTGGTGGTGTCTGTGGTGG		450
	*****		
predicted HIV-SV-CD4_F2A_eYFP_clone_4.11	TGGTGGTTCGCGCGCGCGGCTCCGGTGGTGGTGGATCCGAAGTGAAGC		500
	TGGTGGTTCGCGCGCGCGGCTCCGGTGGTGGTGGATCCGAAGTGAAGC		500
	*****		
predicted HIV-SV-CD4_F2A_eYFP_colony_4.11	TTGAGGAGTCTGGCCCTGGGATATTGAAGCCCTCACAGACCCTCAGTCTG		550
	TTGAGGAGTCTGGCCCTGGGATATTGAAGCCCTCACAGACCCTCAGTCTG		550
	*****		
predicted HIV-SV-CD4_F2A_eYFP_colony_4.11	ACTTGTCTTCTCTGGGTTTTCCTGAGCACTTCTGGTATGGGTGATAGG		600
	ACTTGTCTTCTCTGGGTTTTCCTGAGCACTTCTGGTATGGGTGATAGG		600
	*****		
predicted HIV-SV-CD4_F2A_eYFP_colony_4.11	CTGGATTCCTCAGCCTTCAGGAAGGGTCTGGAGTGGCTGGCACACATTT		650
	CTGGATTCCTCAGCCTTCAGGAAGGGTCTGGAGTGGCTGGCACACATTT		650
	*****		
predicted HIV-SV-CD4_F2A_eYFP_colony_4.11	GGTGGGATGATGATAAGTACTATAACCCATCCCTGAAGAGCCAGCTCACA		700
	GGTGGGATGATGATAAGTACTATAACCCATCCCTGAAGAGCCAGCTCACA		700
	*****		
predicted HIV-SV-CD4_F2A_eYFP_colony_4.11	ATCTCCAAGGATACCTCCAGAAACCAGGTATTCTCAAGATCACCAGTGT		750
	ATCTCCAAGGATACCTCCAGAAACCAGGTATTCTCAAGATCACCAGTGT		750
	*****		
predicted HIV-SV-CD4_F2A_eYFP_colony_4.11	GGACACTGCAGATACTGCCACTTACTACTGTGCTCGAAATATGATTACG		800
	GGACACTGCAGATACTGCCACTTACTACTGTGCTCGAAATATGATTACG		800
	*****		
predicted HIV-SV-CD4_F2A_eYFP_colony_4.11	ACGGTACTTCGATGCTGGGGCGCAGGGACCTCAGTCACCCTCTCCTCG		850
	ACGGTACTTCGATGCTGGGGCGCAGGGACCTCAGTCACCCTCTCCTCG		850
	*****		
predicted HIV-SV-CD4_F2A_eYFP_colony_4.11	GCCTCGGGGGCCGATCACCATCATCACCATATTCTAGAGCCAAACGCGC	<b>F2A</b>	900
	GCCTCGGGGGCCGATCACCATCATCACCATATTCTAGAGCCAAACGCGC		900
	*****		
predicted HIV-SV-CD4_F2A_eYFP_colony_4.11	TCCCGTGAAGCAGACCCTGAACCTTGACCTTCTGAAACTTGCCGGCGAGC		950
	TCCCGTGAAGCAGACCCTGAACCTTGACCTTCTGAAACTTGCCGGCGAGC		950
	*****		
predicted HIV-SV-CD4_F2A_eYFP_colony_4.11	TCGAGTCCAACCTGGCCCGGACATCGATA	<b>C1aI</b>	982
	TCGAGTCCAACCTGGCCCGGACATCGATA		982
	*****		

**Figure A4.2: Colony 3 sequencing results show insertion of eYFP\_F2A SOE-PCR product into the pHIV-CD4scFv plasmid at the Clal restriction site. (A)** Sequencing reactions were performed using three primers (as seen on the diagram; refer to Table 2.5 for primer sequences). **(B)** Alignment of the predicted sequence against the actual sequence of colony 3 is shown. Refer to Section 3.3.a.2 for the construction of pHIV-eYFP\_F2A\_CD4scFv. Coding regions of interest are colour coded. Exact nucleotide matches are represented by \*

.

### A4.2 Sequence analysis of pHIV-eYFP\_F2A\_CD4scFv

**A**



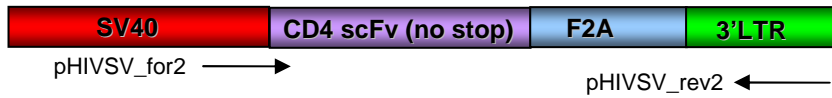
**B**

	Clal	eYFP
predicted eYFP_F2A	ATCGAT	GCCACCATGGTGAGCAAGGGCGAGGAGCTGTTACCGGGGTGGTGCCCATCCTG
		ATCGATGCCACCATGGTGAGCAAGGGCGAGGAGCTGTTACCGGGGTGGTGCCCATCCTG
		*****
predicted eYFP_F2A		GTCGAGCTGGACGGCGACGTAACCGGCCACAAGTTCAGCGTGTCCGGCGAGGGCGAGGGC
		GTCGAGCTGGACGGCGACGTAACCGGCCACAAGTTCAGCGTGTCCGGCGAGGGCGAGGGC
		*****
predicted eYFP_F2A		GATGCCACCTACGGCAAGCTGACCTGAAGTTCATCTGCACCACCGCAAGCTGCCCGTG
		GATGCCACCTACGGCAAGCTGACCTGAAGTTCATCTGCACCACCGCAAGCTGCCCGTG
		*****
predicted eYFP_F2A		CCCTGGCCACCCTCGTGACCACCTTCGGCTACGGCCTGCAGTGCTTCGCCCGCTACCCC
		CCCTGGCCACCCTCGTGACCACCTTCGGCTACGGCCTGCAGTGCTTCGCCCGCTACCCC
		*****
predicted eYFP_F2A		GACCACATGAAGCAGCAGACTTCTCAAGTCCGCCATGCCCGAAGGCTACGTCCAGGAG
		GACCACATGAAGCAGCAGACTTCTCAAGTCCGCCATGCCCGAAGGCTACGTCCAGGAG
		*****
predicted eYFP_F2A		CGCACCATCTTCTTCAAGGACGACGGCAACTACAAGACCCGCGCCGAGGTGAAGTTCGAG
		CGCACCATCTTCTTCAAGGACGACGGCAACTACAAGACCCGCGCCGAGGTGAAGTTCGAG
		*****
predicted eYFP_F2A		GGCGACACCTGGTGAACCGCATCGAGCTGAAGGGCATCGACTTCAAGGAGGACGGCAAC
		GGCGACACCTGGTGAACCGCATCGAGCTGAAGGGCATCGACTTCAAGGAGGACGGCAAC
		*****
predicted eYFP_F2A		ATCCTGGGGCACAAGCTGGAGTACAACACTACAACAGCCACAACGTCTATATCATGGCCGAC
		ATCCTGGGGCACAAGCTGGAGTACAACACTACAACAGCCACAACGTCTATATCATGGCCGAC
		*****
predicted eYFP_F2A		AAGCAGAAGAACGGCATCAAGGTGAACTTCAAGATCCGCCACAACATCGAGGACGGCAGC
		AAGCAGAAGAACGGCATCAAGGTGAACTTCAAGATCCGCCACAACATCGAGGACGGCAGC
		*****
predicted eYFP_F2A		GTGCAGCTCGCCGACCACTACCAGCAGAACACCCCATCGGCGACGGCCCCGTGCTGCTG
		GTGCAGCTCGCCGACCACTACCAGCAGAACACCCCATCGGCGACGGCCCCGTGCTGCTG
		*****
predicted eYFP_F2A		CCCGACAACCACTACCTGAGCTACCAGTCCGCCCTGAGCAAAGACCCCAACGAGAAGCGC
		CCCGACAACCACTACCTGAGCTACCAGTCCGCCCTGAGCAAAGACCCCAACGAGAAGCGC
		*****
predicted eYFP_F2A		GATCACATGGTCTGCTGGAGTTCGTGACCGCCGCGGGATCACTCTCGGCATGGACGAG
		GATCACATGGTCTGCTGGAGTTCGTGACCGCCGCGGGATCACTCTCGGCATGGACGAG
		*****
		<b>F2A</b>
predicted eYFP_F2A		CTGTACAAGAGAGCCAAACGCGCTCCCGTGAAGCAGACCCCTGAACTTGACCTTCTGAAA
		CTGTACAAGAGAGCCAAACGCGCTCCCGTGAAGCAGACCCCTGAACTTGACCTTCTGAAA
		*****
		<b>Clal</b>
predicted eYFP_F2A	CTTGCCGGCGACGTCGAGTCCAACCCTGGCCCCATCGAT	
	CTTGCCGGCGACGTCGAGTCCAACCCTGGCCCCATCGAT	
	*****	

**Figure A4.3: Colony 1 sequencing results show removal of eYFP, to create the pHIV-CD4scFv\_F2A construct. (A)** Sequencing reactions were performed using two primers (as seen on the diagram; refer to Table 2.5 for primer sequences). **(B)** Alignment of the predicted sequence against the actual sequence of colony 1 is shown. It is important to note that there is no stop codon after the anti-rat CD4 scFv gene or the F2A sequence therefore translation will continue on. Refer to Section 3.3.a.3. for the construction of pHIV-CD4scFv\_F2A. Coding regions of interest are colour coded. Exact nucleotide matches are represented by \*.

### A4.3 Sequence analysis of pHIV-CD4scFv\_F2A

**A**



**B**

```

predicted          F2A
F2A_3' LTR        AGAGCCAAACGCGCTCCCGTGAAGCAGACCCTGAACTTTGACCTTCTGAAACTTGCCGGC
                  AGAGCCAAACGCGCTCCCGTGAAGCAGACCCTGAACTTTGACCTTCTGAAACTTGCCGGC
                  *****
                  Partial XmaI  Partial NdeI   3'LTR
predicted          GACGTCGAGTCCAACCCTGGCCCGGTATGCTATGGATCTTAGCCACTTTTAAAGAAA
F2A_3' LTR        GACGTCGAGTCCAACCCTGGCCCGGTATGCTATGGATCTTAGCCACTTTTAAAGAAA
                  *****

predicted          AGGGGGACTGGAAGGGCTAATTCACTCCCAACAAAGACAAGATCTGCTTTTGCCTGTAC
F2A_3' LTR        AAAGGGGGACTGGAAGGGCTAATTCACTCCCAACAAAGACAAGATCTGCTTTTGCCTAC
                  *****

predicted          TGGGTCTCTCTGGTTAGACCAGATCTGAGCCTGGGAGCTCTCTGGCTAGCTAGGAAACC
F2A_3' LTR        TGTGGGTCTCTCTGGTTAGACCAGATCTGAGCCTGGGAGCTCTCTGGCTAGCTAGGAAACC
                  *****

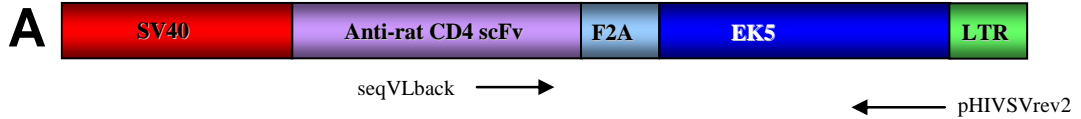
predicted          ACTGCTTAAGCCTCAATAAAGCTTGCCCTTGAGTGCTTTAAGTAGTATGTGCCCGTCTGTT
F2A_3' LTR        ACACTGCTTAAGCCTCAATAAAGCTTGCCCTTGAGTGCTTTAAGTAGTATGTGCCCGTCTT
                  *****

predicted          GTGTGACTCTGGTAACTAGAGATCCCTCAGACCCTTTTAGTCAGTGTGGAAAATCTCTAG
F2A_3' LTR        GTGTGACTCTGGTAACTAGAGATCCCTCAGACCCTTTTAGTCAGTGTGGAAAATCTCTAG
                  *****

predicted          CA
F2A_3' LTR        CA
                  **
    
```

**Figure A4.4: Colony 12 sequencing results show insertion of the Endostatin:Kringle-5 fusion protein (EK5) into the pHIV-CD4scFv\_F2A plasmid at the XmaI and NdeI restriction sites. (A)** Sequencing reactions were performed using two primers (as seen on the diagram; refer to Table 2.5 for primer sequences) to determine the exact sequence of the EK5 insert. **(B)** Alignment of the predicted sequence against the actual sequence of Colony 12 is shown. Coding regions of interest are colour coded. Exact nucleotide matches are represented by \*.

### A4.4 Sequence analysis of pHIV-CD4scFv\_F2A\_EK5



<b>B</b>	Agel/XmaI merged	EK5
predicted pHIV-SV40-CD4scFv_F2A_EK5	----- <b>CCCCGGT</b> ATGTACAGGATGCAACTCCTGTCTGCATTGCACTA ACCCTGGCCCCGGTATGTACAGGATGCAACTCCTGTCTGCATTGCACTA *****	
predicted pHIV-SV40-CD4scFv_F2A_EK5	<b>AGTCTTGC</b> ACTTGTACAGAA <b>TTCGGCC</b> ACAGCCACC <b>CGGACTTCCAGCC</b> AGTCTTGCACCTGTCCAGAA <b>TTCGGCC</b> ACAGCCACC <b>CGGACTTCCAGCC</b> *****	
predicted pHIV-SV40-CD4scFv_F2A_EK5	<b>GGTGTCC</b> ACCTGGTTGCGCTCAACAGCC <b>CCCTGT</b> CAGGGCGGCATGCGGG GGTGTCCACCTGGTTGCGCTCAACAGCC <b>CCCTGT</b> CAGGGCGGCATGCGGG *****	
predicted pHIV-SV40-CD4scFv_F2A_EK5	<b>GCATCCG</b> GGGGCCGACTTCCAGT <b>GCTTCC</b> AGCAGGCGCGGGCCGTGGGG GCATCCGCGGGCCGACTTCCAGT <b>GCTTCC</b> AGCAGGCGCGGGCCGTGGGG *****	
predicted pHIV-SV40-CD4scFv_F2A_EK5	<b>CTGGCGG</b> CACCTTCCGCGCTTCTCTCGC <b>CTGC</b> AGGACCTGTA CTGGCGGACCTTCCGCGCTTCTCTCGC <b>CTGC</b> AGGACCTGTA *****	
predicted pHIV-SV40-CD4scFv_F2A_EK5	<b>CAGCATCG</b> TGCGCGT <b>GCCGAC</b> CGCGCAGCC <b>GTGCC</b> ATCGTCAACCTCA CAGCATCGTGC <b>CGTGC</b> CGCAGCC <b>GTGCC</b> ATCGTCAACCTCA *****	
predicted pHIV-SV40-CD4scFv_F2A_EK5	<b>AGGACG</b> AGCTGCTGTTCCAGCTGGGAG <b>GCTG</b> TCTCAGGCTCTGAG AGGACGAGCTGCTGTTCCAGCTGGGAG <b>GCTG</b> TCTCAGGCTCTGAG *****	
predicted pHIV-SV40-CD4scFv_F2A_EK5	<b>GGTCCG</b> CTGAAGCCCGGGC <b>CACGC</b> ATCTTCTC <b>CTTT</b> GACGGCAAGGACG GGTCCGCTGAAGCCCGGGC <b>CACGC</b> ATCTTCTC <b>CTTT</b> GACGGCAAGGACG *****	
predicted pHIV-SV40-CD4scFv_F2A_EK5	<b>TCCTG</b> AGGCACCCACCTGGCC <b>CCAGA</b> AGCGTGTGGC <b>ATGG</b> CTCGGAC TCCTGAGGCACCCACCTGGCC <b>CCAGA</b> AGCGTGTGGC <b>ATGG</b> CTCGGAC *****	
predicted pHIV-SV40-CD4scFv_F2A_EK5	<b>CCCAAC</b> GGGCGCAGGCTGACCGAG <b>CTACT</b> GTGAGAC <b>GTGG</b> CGGACGGA CCCAACGGGCGCAGGCTGACCGAG <b>CTACT</b> GTGAGAC <b>GTGG</b> CGGACGGA *****	
predicted pHIV-SV40-CD4scFv_F2A_EK5	<b>GGCTCC</b> CTCGGCCACGGCCAGG <b>CCCTC</b> CTCGCTGCTGGGGG <b>CGAG</b> GCTCC GGCTCCCTCGGCCACGGCCAGG <b>CCCTC</b> CTCGCTGCTGGGGG <b>CGAG</b> GCTCC *****	
predicted pHIV-SV40-CD4scFv_F2A_EK5	<b>TGGGC</b> AGAGTGCCCGAGCTGCC <b>ATCAC</b> GCCTACATCGTCTG <b>CAATT</b> TGGGCAGAGTGCCCGAGCTGCC <b>ATCAC</b> GCCTACATCGTCTG <b>CAATT</b> *****	
predicted pHIV-SV40-CD4scFv_F2A_EK5	<b>GAGAAC</b> AGCTTCATGACTGC <b>CTCCA</b> AGGTACCAGGAGTAGGTACGA <b>ATT</b> GAGAACAGCTTCATGACTGC <b>CTCCA</b> AGGTACCAGGAGTAGGTACGA <b>ATT</b> *****	
predicted pHIV-SV40-CD4scFv_F2A_EK5	<b>GCCTG</b> TTGCTCCTGCTTCCAGATGTAGAG <b>ACTC</b> CTCCGAAGAA <b>AGACT</b> GTA GCCTGTTGCTCCTGCTTCCAGATGTAGAG <b>ACTC</b> CTCCGAAGAA <b>AGACT</b> GTA *****	
predicted pHIV-SV40-CD4scFv_F2A_EK5	<b>TGTTT</b> GGAAATGGAAAGGATACCGAGG <b>CAAG</b> AGGGCGACCA <b>CTGTT</b> ACT TGTTTGGAAATGGAAAGGATACCGAGG <b>CAAG</b> AGGGCGACCA <b>CTGTT</b> ACT *****	
predicted pHIV-SV40-CD4scFv_F2A_EK5	<b>GGGAC</b> CCCATGCCAGGACTGGG <b>CTGCC</b> AGGAGCC <b>CATAG</b> ACACAGCAT GGGACCCCATGCCAGGACTGGG <b>CTGCC</b> AGGAGCC <b>CATAG</b> ACACAGCAT *****	
predicted pHIV-SV40-CD4scFv_F2A_EK5	<b>TTTCA</b> CTCCAGAGCAAATCCAGGGCGGG <b>CTG</b> GAAAAAA <b>TTACT</b> GCC TTTCACTCCAGAGCAAATCCAGGGCGGG <b>CTG</b> GAAAAAA <b>TTACT</b> GCC *****	
predicted pHIV-SV40-CD4scFv_F2A_EK5	<b>GTAACC</b> CTGATGGTGATGTAGGTG <b>CTCC</b> TGGTGCTACACGACAA <b>TCCA</b> GTAACCCTGATGGTGATGTAGGTG <b>CTCC</b> TGGTGCTACACGACAA <b>TCCA</b> *****	
predicted pHIV-SV40-CD4scFv_F2A_EK5	<b>AGAAA</b> ACTTTACGACTACTGTGATG <b>CCCT</b> CAGTGTGCGG <b>CCCTT</b> CATT AGAAAACTTTACGACTACTGTGATG <b>CCCT</b> CAGTGTGCGG <b>CCCTT</b> CATT *****	
predicted pHIV-SV40-CD4scFv_F2A_EK5	<b>TGATT</b> AGCATATG TGATTAGCATATG *****	NdeI

**REFERENCES**

- 1 Joyce, N. C. Proliferative capacity of the corneal endothelium. *Prog Retin Eye Res* **22**, 359-389 (2003).
- 2 Murphy, C., Alvarado, J., Juster, R. & Maglio, M. Prenatal and postnatal cellularity of the human corneal endothelium. A quantitative histologic study. *Invest Ophthalmol Vis Sci* **25**, 312-322 (1984).
- 3 Kaufman, H. E. & Katz, J. I. Pathology of the corneal endothelium. *Invest Ophthalmol Vis Sci* **16**, 265-268 (1977).
- 4 Joyce, N. C., Joyce, S. J., Powell, S. M. & Meklir, B. EGF and PGE<sub>2</sub>: effects on corneal endothelial cell migration and monolayer spreading during wound repair in vitro. *Curr Eye Res* **14**, 601-609 (1995).
- 5 Joyce, N. C., Meklir, B. & Neufeld, A. H. In vitro pharmacologic separation of corneal endothelial migration and spreading responses. *Invest Ophthalmol Vis Sci* **31**, 1816-1826 (1990).
- 6 Schilling-Schon, A., Pleyer, U., Hartmann, C. & Rieck, P. W. The role of endogenous growth factors to support corneal endothelial migration after wounding in vitro. *Exp Eye Res* **71**, 583-589 (2000).
- 7 Senoo, T. & Joyce, N. C. Cell cycle kinetics in corneal endothelium from old and young donors. *Invest Ophthalmol Vis Sci* **41**, 660-667 (2000).
- 8 Chen, K. H., Harris, D. L. & Joyce, N. C. TGF-beta<sub>2</sub> in aqueous humor suppresses S-phase entry in cultured corneal endothelial cells. *Invest Ophthalmol Vis Sci* **40**, 2513-2519 (1999).
- 9 Joyce, N. C. & Zieske, J. D. Transforming growth factor-beta receptor expression in human cornea. *Invest Ophthalmol Vis Sci* **38**, 1922-1928 (1997).
- 10 Yanoff, M. & Cameron, J. D. Human cornea organ cultures: epithelial-endothelial interactions. *Invest Ophthalmol Vis Sci* **16**, 269-273 (1977).
- 11 Whitcher, J. P., Srinivasan, M. & Upadhyay, M. P. Corneal blindness: a global perspective. *Bull World Health Organ* **79**, 214-221 (2001).
- 12 Zirm, E. Eine erfolgreiche totale Keratoplastik. *Graefes Arch Clin Exp Ophthalmol* **64**, 580-592 (1906).
- 13 Williams, K. A., Lowe, M. T., Bartlett, C. M., Kelly, L. & Coster, D. J. *The Australian corneal graft registry 2007 report*. (Flinders University Press 2007, 2007).



- 14 Coster, D. J. & Williams, K. A. The impact of corneal allograft rejection on the long-term outcome of corneal transplantation. *Am J Ophthalmol* **140**, 1112-1122 (2005).
- 15 Kapturczak, M. H., Meier-Kriesche, H. U. & Kaplan, B. Pharmacology of calcineurin antagonists. *Transplant Proc* **36**, 25S-32S (2004).
- 16 Opelz, G., Wujciak, T., Dohler, B., Scherer, S. & Mytilineos, J. HLA compatibility and organ transplant survival. Collaborative Transplant Study. *Rev Immunogenet* **1**, 334-342 (1999).
- 17 She, S. C., Steahly, L. P. & Moticka, E. J. A method for performing full-thickness, orthotopic, penetrating keratoplasty in the mouse. *Ophthalmic Surg* **21**, 781-785 (1990).
- 18 Williams, K. A. & Coster, D. J. Penetrating corneal transplantation in the inbred rat: a new model. *Invest Ophthalmol Vis Sci* **26**, 23-30 (1985).
- 19 Hunter, P. A., Garner, A., Wilhelmus, K. R., Rice, N. S. & Jones, B. R. Corneal graft rejection: a new rabbit model and cyclosporin-A. *Br J Ophthalmol* **66**, 292-302 (1982).
- 20 Bahn, C. F., Meyer, R. F., MacCallum, D. K., Lillie, J. H., Lovett, E. J., Sugar, A. & Martonyi, C. L. Penetrating keratoplasty in the cat. A clinically applicable model. *Ophthalmology* **89**, 687-699 (1982).
- 21 Williams, K. A., Standfield, S. D., Mills, R. A., Takano, T., Larkin, D. F., Krishnan, R., Russ, G. R. & Coster, D. J. A new model of orthotopic penetrating corneal transplantation in the sheep: graft survival, phenotypes of graft-infiltrating cells and local cytokine production. *Aust N Z J Ophthalmol* **27**, 127-135 (1999).
- 22 Li, C., Xu, J. T., Kong, F. S. & Li, J. L. Experimental studies on penetrating heterokeratoplasty with human corneal grafts in monkey eyes. *Cornea* **11**, 66-72 (1992).
- 23 Katami, M. Is a corneal transplantation immunologically privileged from graft rejection? *Ann Acad Med Singapore* **20**, 433-438 (1991).
- 24 Sano, Y., Ksander, B. R. & Streilein, J. W. Minor H, rather than MHC, alloantigens offer the greater barrier to successful orthotopic corneal transplantation in mice. *Transpl Immunol* **4**, 53-56 (1996).
- 25 Yamada, J. & Streilein, J. W. Fate of orthotopic corneal allografts in C57BL/6 mice. *Transpl Immunol* **6**, 161-168 (1998).
- 26 Liu, Y., Hamrah, P., Zhang, Q., Taylor, A. W. & Dana, M. R. Draining lymph nodes of corneal transplant hosts exhibit evidence for donor major histocompatibility complex (MHC) class II-positive dendritic cells derived from MHC class II-negative grafts. *J Exp Med* **195**, 259-268 (2002).

- 27 Van Horn, D. L., Sendele, D. D., Seideman, S. & Bucu, P. J. Regenerative capacity of the corneal endothelium in rabbit and cat. *Invest Ophthalmol Vis Sci* **16**, 597-613 (1977).
- 28 Tuft, S. J., Williams, K. A. & Coster, D. J. Endothelial repair in the rat cornea. *Invest Ophthalmol Vis Sci* **27**, 1199-1204 (1986).
- 29 Matsubara, M. & Tanishima, T. Wound-healing of corneal endothelium in monkey: an autoradiographic study. *Jpn J Ophthalmol* **27**, 444-450 (1983).
- 30 Niederkorn, J. Y. See no evil, hear no evil, do no evil: the lessons of immune privilege. *Nat Immunol* **7**, 354-359 (2006).
- 31 Zhu, S., Dekaris, I., Duncker, G. & Dana, M. R. Early expression of proinflammatory cytokines interleukin-1 and tumor necrosis factor-alpha after corneal transplantation. *J Interferon Cytokine Res* **19**, 661-669 (1999).
- 32 Cursiefen, C., Cao, J., Chen, L., Liu, Y., Maruyama, K., Jackson, D., Kruse, F. E., Wiegand, S. J., Dana, M. R. & Streilein, J. W. Inhibition of hemangiogenesis and lymphangiogenesis after normal-risk corneal transplantation by neutralizing VEGF promotes graft survival. *Invest Ophthalmol Vis Sci* **45**, 2666-2673 (2004).
- 33 Kuffova, L., Lumsden, L., Vesela, V., Taylor, J. A., Filipiec, M., Holan, V., Dick, A. D. & Forrester, J. V. Kinetics of leukocyte and myeloid cell traffic in the murine corneal allograft response. *Transplantation* **72**, 1292-1298 (2001).
- 34 Larkin, D. F., Alexander, R. A. & Cree, I. A. Infiltrating inflammatory cell phenotypes and apoptosis in rejected human corneal allografts. *Eye (Lond)* **11** ( Pt 1), 68-74 (1997).
- 35 Larkin, D. F., Calder, V. L. & Lightman, S. L. Identification and characterization of cells infiltrating the graft and aqueous humour in rat corneal allograft rejection. *Clin Exp Immunol* **107**, 381-391 (1997).
- 36 Lai, Y. K., Shen, W. Y., Brankov, M., Lai, C. M., Constable, I. J. & Rakoczy, P. E. Potential long-term inhibition of ocular neovascularisation by recombinant adeno-associated virus-mediated secretion gene therapy. *Gene Ther* **9**, 804-813 (2002).
- 37 Murthy, R. C., McFarland, T. J., Yoken, J., Chen, S., Barone, C., Burke, D., Zhang, Y., Appukuttan, B. & Stout, J. T. Corneal transduction to inhibit angiogenesis and graft failure. *Invest Ophthalmol Vis Sci* **44**, 1837-1842 (2003).
- 38 Konig, R., Huang, L. Y. & Germain, R. N. MHC class II interaction with CD4 mediated by a region analogous to the MHC class I binding site for CD8. *Nature* **356**, 796-798 (1992).
- 39 Salter, R. D., Benjamin, R. J., Wesley, P. K., Buxton, S. E., Garrett, T. P., Clayberger, C., Krensky, A. M., Norment, A. M., Littman, D. R. & Parham,

- P. A binding site for the T-cell co-receptor CD8 on the alpha 3 domain of HLA-A2. *Nature* **345**, 41-46 (1990).
- 40 Norment, A. M., Salter, R. D., Parham, P., Engelhard, V. H. & Littman, D. R. Cell-cell adhesion mediated by CD8 and MHC class I molecules. *Nature* **336**, 79-81 (1988).
- 41 Marrack, P., McDuffie, M., Born, W., Blackman, M., Hannum, C. & Kappler, J. The T cell receptor: its repertoire and role in thymocyte development. *Adv Exp Med Biol* **213**, 1-12 (1987).
- 42 Bretscher, P. The two-signal model of lymphocyte activation twenty-one years later. *Immunol Today* **13**, 74-76 (1992).
- 43 Linsley, P. S., Brady, W., Grosmaire, L., Aruffo, A., Damle, N. K. & Ledbetter, J. A. Binding of the B cell activation antigen B7 to CD28 costimulates T cell proliferation and interleukin 2 mRNA accumulation. *J Exp Med* **173**, 721-730 (1991).
- 44 Larsen, C. P., Elwood, E. T., Alexander, D. Z., Ritchie, S. C., Hendrix, R., Tucker-Burden, C., Cho, H. R., Aruffo, A., Hollenbaugh, D., Linsley, P. S., Winn, K. J. & Pearson, T. C. Long-term acceptance of skin and cardiac allografts after blocking CD40 and CD28 pathways. *Nature* **381**, 434-438 (1996).
- 45 Mosmann, T. R. & Coffman, R. L. TH1 and TH2 cells: different patterns of lymphokine secretion lead to different functional properties. *Annu Rev Immunol* **7**, 145-173 (1989).
- 46 Joo, C. K., Pepose, J. S. & Stuart, P. M. T-cell mediated responses in a murine model of orthotopic corneal transplantation. *Invest Ophthalmol Vis Sci* **36**, 1530-1540 (1995).
- 47 Sonoda, Y., Sano, Y., Ksander, B. & Streilein, J. W. Characterization of cell-mediated immune responses elicited by orthotopic corneal allografts in mice. *Invest Ophthalmol Vis Sci* **36**, 427-434 (1995).
- 48 Hargrave, S. L., Mayhew, E., Hegde, S. & Niederkorn, J. Are corneal cells susceptible to antibody-mediated killing in corneal allograft rejection? *Transpl Immunol* **11**, 79-89 (2003).
- 49 Pleyer, U. & Schlickeiser, S. The taming of the shrew? The immunology of corneal transplantation. *Acta Ophthalmol* **87**, 488-497 (2009).
- 50 Klebe, S., Sykes, P. J., Coster, D. J., Krishnan, R. & Williams, K. A. Prolongation of sheep corneal allograft survival by ex vivo transfer of the gene encoding interleukin-10. *Transplantation* **71**, 1214-1220 (2001).
- 51 Gong, N., Pleyer, U., Volk, H. D. & Ritter, T. Effects of local and systemic viral interleukin-10 gene transfer on corneal allograft survival. *Gene Ther* **14**, 484-490 (2007).

- 52 Hargrave, S. L., Hay, C., Mellon, J., Mayhew, E. & Niederkorn, J. Y. Fate of MHC-matched corneal allografts in Th1-deficient hosts. *Invest Ophthalmol Vis Sci* **45**, 1188-1193 (2004).
- 53 Aggarwal, S., Ghilardi, N., Xie, M. H., de Sauvage, F. J. & Gurney, A. L. Interleukin-23 promotes a distinct CD4 T cell activation state characterized by the production of interleukin-17. *J Biol Chem* **278**, 1910-1914 (2003).
- 54 Cua, D. J., Sherlock, J., Chen, Y., Murphy, C. A., Joyce, B., Seymour, B., Lucian, L., To, W., Kwan, S., Churakova, T., Zurawski, S., Wiekowski, M., Lira, S. A., Gorman, D., Kastelein, R. A. & Sedgwick, J. D. Interleukin-23 rather than interleukin-12 is the critical cytokine for autoimmune inflammation of the brain. *Nature* **421**, 744-748 (2003).
- 55 Langrish, C. L., Chen, Y., Blumenschein, W. M., Mattson, J., Basham, B., Sedgwick, J. D., McClanahan, T., Kastelein, R. A. & Cua, D. J. IL-23 drives a pathogenic T cell population that induces autoimmune inflammation. *J Exp Med* **201**, 233-240 (2005).
- 56 Loong, C. C., Hsieh, H. G., Lui, W. Y., Chen, A. & Lin, C. Y. Evidence for the early involvement of interleukin 17 in human and experimental renal allograft rejection. *J Pathol* **197**, 322-332 (2002).
- 57 Min, S. I., Ha, J., Park, C. G., Won, J. K., Park, Y. J., Min, S. K. & Kim, S. J. Sequential evolution of IL-17 responses in the early period of allograft rejection. *Exp Mol Med* **41**, 707-716 (2009).
- 58 Chen, H., Wang, W., Xie, H., Xu, X., Wu, J., Jiang, Z., Zhang, M., Zhou, L. & Zheng, S. A pathogenic role of IL-17 at the early stage of corneal allograft rejection. *Transpl Immunol* **21**, 155-161 (2009).
- 59 Hamrah, P. & Dana, M. R. Corneal antigen-presenting cells. *Chem Immunol Allergy* **92**, 58-70 (2007).
- 60 Lanzavecchia, A. & Sallusto, F. The instructive role of dendritic cells on T cell responses: lineages, plasticity and kinetics. *Curr Opin Immunol* **13**, 291-298 (2001).
- 61 Liu, Y. J., Kanzler, H., Soumelis, V. & Gilliet, M. Dendritic cell lineage, plasticity and cross-regulation. *Nat Immunol* **2**, 585-589 (2001).
- 62 Austyn, J. M. New insights into the mobilization and phagocytic activity of dendritic cells. *J Exp Med* **183**, 1287-1292 (1996).
- 63 Larsen, C. P., Ritchie, S. C., Hendrix, R., Linsley, P. S., Hathcock, K. S., Hodes, R. J., Lowry, R. P. & Pearson, T. C. Regulation of immunostimulatory function and costimulatory molecule (B7-1 and B7-2) expression on murine dendritic cells. *J Immunol* **152**, 5208-5219 (1994).
- 64 Cella, M., Sallusto, F. & Lanzavecchia, A. Origin, maturation and antigen presenting function of dendritic cells. *Curr Opin Immunol* **9**, 10-16 (1997).

- 65 Mellman, I. & Steinman, R. M. Dendritic cells: specialized and regulated antigen processing machines. *Cell* **106**, 255-258 (2001).
- 66 Banchereau, J., Briere, F., Caux, C., Davoust, J., Lebecque, S., Liu, Y. J., Pulendran, B. & Palucka, K. Immunobiology of dendritic cells. *Annu Rev Immunol* **18**, 767-811 (2000).
- 67 Banchereau, J. & Steinman, R. M. Dendritic cells and the control of immunity. *Nature* **392**, 245-252 (1998).
- 68 Hamrah, P., Liu, Y., Zhang, Q. & Dana, M. R. Alterations in corneal stromal dendritic cell phenotype and distribution in inflammation. *Arch Ophthalmol* **121**, 1132-1140 (2003).
- 69 Hamrah, P., Liu, Y., Zhang, Q. & Dana, M. R. The corneal stroma is endowed with a significant number of resident dendritic cells. *Invest Ophthalmol Vis Sci* **44**, 581-589 (2003).
- 70 Hamrah, P., Zhang, Q., Liu, Y. & Dana, M. R. Novel characterization of MHC class II-negative population of resident corneal Langerhans cell-type dendritic cells. *Invest Ophthalmol Vis Sci* **43**, 639-646 (2002).
- 71 Nakamura, T., Ishikawa, F., Sonoda, K. H., Hisatomi, T., Qiao, H., Yamada, J., Fukata, M., Ishibashi, T., Harada, M. & Kinoshita, S. Characterization and distribution of bone marrow-derived cells in mouse cornea. *Invest Ophthalmol Vis Sci* **46**, 497-503 (2005).
- 72 Yamagami, S., Ebihara, N., Usui, T., Yokoo, S. & Amano, S. Bone marrow-derived cells in normal human corneal stroma. *Arch Ophthalmol* **124**, 62-69 (2006).
- 73 Yamagami, S., Yokoo, S., Usui, T., Yamagami, H., Amano, S. & Ebihara, N. Distinct populations of dendritic cells in the normal human donor corneal epithelium. *Invest Ophthalmol Vis Sci* **46**, 4489-4494 (2005).
- 74 Zhivov, A., Stave, J., Vollmar, B. & Guthoff, R. In vivo confocal microscopic evaluation of Langerhans cell density and distribution in the normal human corneal epithelium. *Graefes Arch Clin Exp Ophthalmol* **243**, 1056-1061 (2005).
- 75 Knisely, T. L., Anderson, T. M., Sherwood, M. E., Flotte, T. J., Albert, D. M. & Granstein, R. D. Morphologic and ultrastructural examination of I-A+ cells in the murine iris. *Invest Ophthalmol Vis Sci* **32**, 2423-2431 (1991).
- 76 McMenemy, P. G., Crewe, J., Morrison, S. & Holt, P. G. Immunomorphologic studies of macrophages and MHC class II-positive dendritic cells in the iris and ciliary body of the rat, mouse, and human eye. *Invest Ophthalmol Vis Sci* **35**, 3234-3250 (1994).
- 77 McMenemy, P. G. & Holthouse, I. Immunohistochemical characterization of dendritic cells and macrophages in the aqueous outflow pathways of the rat eye. *Exp Eye Res* **55**, 315-324 (1992).

- 78 McMenamin, P. G., Holthouse, I. & Holt, P. G. Class II major histocompatibility complex (Ia) antigen-bearing dendritic cells within the iris and ciliary body of the rat eye: distribution, phenotype and relation to retinal microglia. *Immunology* **77**, 385-393 (1992).
- 79 Steptoe, R. J., Holt, P. G. & McMenamin, P. G. Origin and steady-state turnover of major histocompatibility complex class II-positive dendritic cells and resident-tissue macrophages in the iris of the rat eye. *J Neuroimmunol* **68**, 67-76 (1996).
- 80 McMenamin, P. G., Kezic, J. & Camelo, S. Characterisation of rat corneal cells that take up soluble antigen: an in vivo and in vitro study. *Exp Eye Res* **83**, 1268-1280 (2006).
- 81 Banerjee, S., Figueiredo, F. C., Easty, D. L., Dick, A. D. & Nicholls, S. M. Development of organised conjunctival leucocyte aggregates after corneal transplantation in rats. *Br J Ophthalmol* **87**, 1515-1522 (2003).
- 82 van Rooijen, N., Wijburg, O. L., van den Dobbelsteen, G. P. & Sanders, A. Macrophages in host defense mechanisms. *Curr Top Microbiol Immunol* **210**, 159-165 (1996).
- 83 Steptoe, R. J., McMenamin, P. G. & Holt, P. G. Resident tissue macrophages within the normal rat iris lack immunosuppressive activity and are effective antigen-presenting cells. *Ocul Immunol Inflamm* **8**, 177-187 (2000).
- 84 Brissette-Storkus, C. S., Reynolds, S. M., Lepisto, A. J. & Hendricks, R. L. Identification of a novel macrophage population in the normal mouse corneal stroma. *Invest Ophthalmol Vis Sci* **43**, 2264-2271 (2002).
- 85 Camelo, S., Voon, A. S., Bunt, S. & McMenamin, P. G. Local retention of soluble antigen by potential antigen-presenting cells in the anterior segment of the eye. *Invest Ophthalmol Vis Sci* **44**, 5212-5219 (2003).
- 86 McMenamin, P. G. Dendritic cells and macrophages in the uveal tract of the normal mouse eye. *Br J Ophthalmol* **83**, 598-604 (1999).
- 87 Li, X., Shen, S., Urso, D., Kalique, S., Park, S. H., Sharafieh, R., O'Rourke, J. & Cone, R. E. Phenotypic and immunoregulatory characteristics of monocytic iris cells. *Immunology* **117**, 566-575 (2006).
- 88 Williamson, J. S., Bradley, D. & Streilein, J. W. Immunoregulatory properties of bone marrow-derived cells in the iris and ciliary body. *Immunology* **67**, 96-102 (1989).
- 89 Streilein, J. W. & Niederkorn, J. Y. Induction of anterior chamber-associated immune deviation requires an intact, functional spleen. *J Exp Med* **153**, 1058-1067 (1981).
- 90 Becker, M. D., Planck, S. R., Crespo, S., Garman, K., Fleischman, R. J., Dullforce, P., Seitz, G. W., Martin, T. M., Parker, D. C. & Rosenbaum, J. T. Immunohistology of antigen-presenting cells in vivo: a novel method for

- serial observation of fluorescently labeled cells. *Invest Ophthalmol Vis Sci* **44**, 2004-2009 (2003).
- 91 Dullforce, P. A., Garman, K. L., Seitz, G. W., Fleischmann, R. J., Crespo, S. M., Planck, S. R., Parker, D. C. & Rosenbaum, J. T. APCs in the anterior uveal tract do not migrate to draining lymph nodes. *J Immunol* **172**, 6701-6708 (2004).
- 92 Rosenbaum, J. T., Ronick, M. B., Song, X., Choi, D. & Planck, S. R. T cell-antigen-presenting cell interactions visualized in vivo in a model of antigen-specific inflammation. *Clin Immunol* **126**, 270-276 (2008).
- 93 Gillette, T. E., Chandler, J. W. & Greiner, J. V. Langerhans cells of the ocular surface. *Ophthalmology* **89**, 700-711 (1982).
- 94 Seto, S. K., Gillette, T. E. & Chandler, J. W. HLA-DR+/T6- Langerhans cells of the human cornea. *Invest Ophthalmol Vis Sci* **28**, 1719-1722 (1987).
- 95 Chinnery, H. R., Humphries, T., Clare, A., Dixon, A. E., Howes, K., Moran, C. B., Scott, D., Zakrzewski, M., Pearlman, E. & McMenamin, P. G. Turnover of bone marrow-derived cells in the irradiated mouse cornea. *Immunology* **125**, 541-548 (2008).
- 96 Cursiefen, C., Chen, L., Borges, L. P., Jackson, D., Cao, J., Radziejewski, C., D'Amore, P. A., Dana, M. R., Wiegand, S. J. & Streilein, J. W. VEGF-A stimulates lymphangiogenesis and hemangiogenesis in inflammatory neovascularization via macrophage recruitment. *J Clin Invest* **113**, 1040-1050 (2004).
- 97 Karpanen, T., Wirzenius, M., Makinen, T., Veikkola, T., Haisma, H. J., Achen, M. G., Stacker, S. A., Pytowski, B., Yla-Herttuala, S. & Alitalo, K. Lymphangiogenic growth factor responsiveness is modulated by postnatal lymphatic vessel maturation. *Am J Pathol* **169**, 708-718 (2006).
- 98 Maruyama, K., Ii, M., Cursiefen, C., Jackson, D. G., Keino, H., Tomita, M., Van Rooijen, N., Takenaka, H., D'Amore, P. A., Stein-Streilein, J., Losordo, D. W. & Streilein, J. W. Inflammation-induced lymphangiogenesis in the cornea arises from CD11b-positive macrophages. *J Clin Invest* **115**, 2363-2372 (2005).
- 99 Chinnery, H. R., Pearlman, E. & McMenamin, P. G. Cutting edge: Membrane nanotubes in vivo: a feature of MHC class II+ cells in the mouse cornea. *J Immunol* **180**, 5779-5783 (2008).
- 100 Kuffova, L., Netukova, M., Duncan, L., Porter, A., Stockinger, B. & Forrester, J. V. Cross presentation of antigen on MHC class II via the draining lymph node after corneal transplantation in mice. *J Immunol* **180**, 1353-1361 (2008).
- 101 Lechler, R. I. & Batchelor, J. R. Restoration of immunogenicity to passenger cell-depleted kidney allografts by the addition of donor strain dendritic cells. *J Exp Med* **155**, 31-41 (1982).

- 102 Cote, I., Rogers, N. J. & Lechler, R. I. Allorecognition. *Transfus Clin Biol* **8**, 318-323 (2001).
- 103 Boisgerault, F., Liu, Y., Anosova, N., Ehrlich, E., Dana, M. R. & Benichou, G. Role of CD4+ and CD8+ T cells in allorecognition: lessons from corneal transplantation. *J Immunol* **167**, 1891-1899 (2001).
- 104 Huq, S., Liu, Y., Benichou, G. & Dana, M. R. Relevance of the direct pathway of sensitization in corneal transplantation is dictated by the graft bed microenvironment. *J Immunol* **173**, 4464-4469 (2004).
- 105 Tilney, N. L. Patterns of lymphatic drainage in the adult laboratory rat. *J Anat* **109**, 369-383 (1971).
- 106 Camelo, S., Kezic, J., Shanley, A., Rigby, P. & McMenemy, P. G. Antigen from the anterior chamber of the eye travels in a soluble form to secondary lymphoid organs via lymphatic and vascular routes. *Invest Ophthalmol Vis Sci* **47**, 1039-1046 (2006).
- 107 Camelo, S., Shanley, A., Voon, A. S. & McMenemy, P. G. The distribution of antigen in lymphoid tissues following its injection into the anterior chamber of the rat eye. *J Immunol* **172**, 5388-5395 (2004).
- 108 Egan, R. M., Yorkey, C., Black, R., Loh, W. K., Stevens, J. L., Storzynsky, E., Lord, E. M., Frelinger, J. G. & Woodward, J. G. In vivo behavior of peptide-specific T cells during mucosal tolerance induction: antigen introduced through the mucosa of the conjunctiva elicits prolonged antigen-specific T cell priming followed by anergy. *J Immunol* **164**, 4543-4550 (2000).
- 109 Egan, R. M., Yorkey, C., Black, R., Loh, W. K., Stevens, J. L. & Woodward, J. G. Peptide-specific T cell clonal expansion in vivo following immunization in the eye, an immune-privileged site. *J Immunol* **157**, 2262-2271 (1996).
- 110 Hoffmann, F., Zhang, E. P., Mueller, A., Schulte, F., Foss, H. D., Franke, J. & Coupland, S. E. Contribution of lymphatic drainage system in corneal allograft rejection in mice. *Graefes Arch Clin Exp Ophthalmol* **239**, 850-858 (2001).
- 111 Schulte, F., Zhang, E. P., Franke, J., Ignatius, R. & Hoffmann, F. Ipsilateral submandibular lymphadenectomy does not prolong orthotopic corneal graft survival in mice. *Graefes Arch Clin Exp Ophthalmol* **242**, 152-157 (2004).
- 112 Zhang, E. P., Franke, J., Schroff, M., Junghans, C., Wittig, B. & Hoffmann, F. Ballistic CTLA4 and IL-4 gene transfer into the lower lid prolongs orthotopic corneal graft survival in mice. *Graefes Arch Clin Exp Ophthalmol* **241**, 921-926 (2003).
- 113 Hong, Y. K., Harvey, N., Noh, Y. H., Schacht, V., Hirakawa, S., Detmar, M. & Oliver, G. Prox1 is a master control gene in the program specifying lymphatic endothelial cell fate. *Dev Dyn* **225**, 351-357 (2002).



- 114 Cursiefen, C., Schlotzer-Schrehardt, U., Kuchle, M., Sorokin, L., Breiteneder-Geleff, S., Alitalo, K. & Jackson, D. Lymphatic vessels in vascularized human corneas: immunohistochemical investigation using LYVE-1 and podoplanin. *Invest Ophthalmol Vis Sci* **43**, 2127-2135 (2002).
- 115 Chen, L., Hamrah, P., Cursiefen, C., Zhang, Q., Pytowski, B., Streilein, J. W. & Dana, M. R. Vascular endothelial growth factor receptor-3 mediates induction of corneal alloimmunity. *Nat Med* **10**, 813-815 (2004).
- 116 Cursiefen, C., Maruyama, K., Jackson, D. G., Streilein, J. W. & Kruse, F. E. Time course of angiogenesis and lymphangiogenesis after brief corneal inflammation. *Cornea* **25**, 443-447 (2006).
- 117 Dietrich, T., Onderka, J., Bock, F., Kruse, F. E., Vossmeier, D., Stragies, R., Zahn, G. & Cursiefen, C. Inhibition of inflammatory lymphangiogenesis by integrin alpha5 blockade. *Am J Pathol* **171**, 361-372 (2007).
- 118 Plskova, J., Duncan, L., Holan, V., Filipec, M., Kraal, G. & Forrester, J. V. The immune response to corneal allograft requires a site-specific draining lymph node. *Transplantation* **73**, 210-215 (2002).
- 119 Plskova, J., Holan, V., Filipec, M. & Forrester, J. V. Lymph node removal enhances corneal graft survival in mice at high risk of rejection. *BMC Ophthalmol* **4**, 3 (2004).
- 120 Yamagami, S. & Dana, M. R. The critical role of lymph nodes in corneal alloimmunization and graft rejection. *Invest Ophthalmol Vis Sci* **42**, 1293-1298 (2001).
- 121 Yamagami, S., Dana, M. R. & Tsuru, T. Draining lymph nodes play an essential role in alloimmunity generated in response to high-risk corneal transplantation. *Cornea* **21**, 405-409 (2002).
- 122 Boonman, Z. F., van Mierlo, G. J., Fransen, M. F., Franken, K. L., Offringa, R., Melief, C. J., Jager, M. J. & Toes, R. E. Intraocular tumor antigen drains specifically to submandibular lymph nodes, resulting in an abortive cytotoxic T cell reaction. *J Immunol* **172**, 1567-1574 (2004).
- 123 Liu, Y., Dana, M. R., Tewari, V. & Taylor, A. W. Immune response to intragraft antigen in draining lymph nodes after corneal transplantation is mediated by interleukin-12. *J Interferon Cytokine Res* **21**, 813-819 (2001).
- 124 Medawar, P. B. Immunity to homologous grafted skin III. The fate of skin homograftes trasplanted to the brain to subcutaneous tissue, and to the anterior chamber of the eye. *Br J Exp Path* **29**, 58-69 (1948).
- 125 Cousins, S. W., McCabe, M. M., Danielpour, D. & Streilein, J. W. Identification of transforming growth factor-beta as an immunosuppressive factor in aqueous humor. *Invest Ophthalmol Vis Sci* **32**, 2201-2211 (1991).
- 126 Granstein, R. D., Staszewski, R., Knisely, T. L., Zeira, E., Nazareno, R., Latina, M. & Albert, D. M. Aqueous humor contains transforming growth

- factor-beta and a small (less than 3500 daltons) inhibitor of thymocyte proliferation. *J Immunol* **144**, 3021-3027 (1990).
- 127 Taylor, A. W., Streilein, J. W. & Cousins, S. W. Identification of alpha-melanocyte stimulating hormone as a potential immunosuppressive factor in aqueous humor. *Curr Eye Res* **11**, 1199-1206 (1992).
- 128 Taylor, A. W., Streilein, J. W. & Cousins, S. W. Immunoreactive vasoactive intestinal peptide contributes to the immunosuppressive activity of normal aqueous humor. *J Immunol* **153**, 1080-1086 (1994).
- 129 Taylor, A. W., Yee, D. G. & Streilein, J. W. Suppression of nitric oxide generated by inflammatory macrophages by calcitonin gene-related peptide in aqueous humor. *Invest Ophthalmol Vis Sci* **39**, 1372-1378 (1998).
- 130 Stuart, P. M., Griffith, T. S., Usui, N., Pepose, J., Yu, X. & Ferguson, T. A. CD95 ligand (FasL)-induced apoptosis is necessary for corneal allograft survival. *J Clin Invest* **99**, 396-402 (1997).
- 131 Yamagami, S., Kawashima, H., Tsuru, T., Yamagami, H., Kayagaki, N., Yagita, H., Okumura, K. & Gregerson, D. S. Role of Fas-Fas ligand interactions in the immunorejection of allogeneic mouse corneal transplants. *Transplantation* **64**, 1107-1111 (1997).
- 132 Lee, H. O., Herndon, J. M., Barreiro, R., Griffith, T. S. & Ferguson, T. A. TRAIL: a mechanism of tumor surveillance in an immune privileged site. *J Immunol* **169**, 4739-4744 (2002).
- 133 Wang, S., Boonman, Z. F., Li, H. C., He, Y., Jager, M. J., Toes, R. E. & Niederkorn, J. Y. Role of TRAIL and IFN-gamma in CD4+ T cell-dependent tumor rejection in the anterior chamber of the eye. *J Immunol* **171**, 2789-2796 (2003).
- 134 Katagiri, K., Zhang-Hoover, J., Mo, J. S., Stein-Streilein, J. & Streilein, J. W. Using tolerance induced via the anterior chamber of the eye to inhibit Th2-dependent pulmonary pathology. *J Immunol* **169**, 84-89 (2002).
- 135 Sonoda, K. H., Exley, M., Snapper, S., Balk, S. P. & Stein-Streilein, J. CD1-reactive natural killer T cells are required for development of systemic tolerance through an immune-privileged site. *J Exp Med* **190**, 1215-1226 (1999).
- 136 Wilbanks, G. A. & Streilein, J. W. Studies on the induction of anterior chamber-associated immune deviation (ACAID). 1. Evidence that an antigen-specific, ACAID-inducing, cell-associated signal exists in the peripheral blood. *J Immunol* **146**, 2610-2617 (1991).
- 137 Streilein, J. W., Arancibia-Caracamo, C. & Osawa, H. The role of minor histocompatibility alloantigens in penetrating keratoplasty. *Dev Ophthalmol* **36**, 74-88 (2003).

- 138 Barshes, N. R., Goodpastor, S. E. & Goss, J. A. Pharmacologic immunosuppression. *Front Biosci* **9**, 411-420 (2004).
- 139 The collaborative corneal transplantation studies (CCTS). Effectiveness of histocompatibility matching in high-risk corneal transplantation. The Collaborative Corneal Transplantation Studies Research Group. *Arch Ophthalmol* **110**, 1392-1403 (1992).
- 140 Boisjoly, H. M., Tourigny, R., Bazin, R., Laughrea, P. A., Dube, I., Chamberland, G., Bernier, J. & Roy, R. Risk factors of corneal graft failure. *Ophthalmology* **100**, 1728-1735 (1993).
- 141 Volker-Dieben, H. J., Kok-van Alphen, C. C., Lansbergen, Q. & Persijn, G. G. The effect of prospective HLA-A and -B matching on corneal graft survival. *Acta Ophthalmol (Copenh)* **60**, 203-212 (1982).
- 142 Khaireddin, R., Wachtlin, J., Hopfenmuller, W. & Hoffmann, F. HLA-A, HLA-B and HLA-DR matching reduces the rate of corneal allograft rejection. *Graefes Arch Clin Exp Ophthalmol* **241**, 1020-1028 (2003).
- 143 Vail, A., Gore, S. M., Bradley, B. A., Easty, D. L., Rogers, C. A. & Armitage, W. J. Influence of donor and histocompatibility factors on corneal graft outcome. *Transplantation* **58**, 1210-1216 (1994).
- 144 Hill, J. C. Systemic cyclosporine in high-risk keratoplasty. Short- versus long-term therapy. *Ophthalmology* **101**, 128-133 (1994).
- 145 Inoue, K., Kimura, C., Amano, S., Sato, T., Fujita, N., Kagaya, F., Kaji, Y., Tsuru, T. & Araie, M. Long-term outcome of systemic cyclosporine treatment following penetrating keratoplasty. *Jpn J Ophthalmol* **45**, 378-382 (2001).
- 146 Poon, A. C., Forbes, J. E., Dart, J. K., Subramaniam, S., Bunce, C., Madison, P., Ficker, L. A., Tuft, S. J., Gartry, D. S. & Buckley, R. J. Systemic cyclosporin A in high risk penetrating keratoplasties: a case-control study. *Br J Ophthalmol* **85**, 1464-1469 (2001).
- 147 Rumelt, S., Bersudsky, V., Blum-Hareuveni, T. & Rehany, U. Systemic cyclosporin A in high failure risk, repeated corneal transplantation. *Br J Ophthalmol* **86**, 988-992 (2002).
- 148 Sundmacher, R., Reinhard, T. & Heering, P. Six years' experience with systemic cyclosporin A prophylaxis in high-risk perforating keratoplasty patients. A retrospective study. *Ger J Ophthalmol* **1**, 432-436 (1992).
- 149 Thiel, M. A., Coster, D. J. & Williams, K. A. The potential of antibody-based immunosuppressive agents for corneal transplantation. *Immunol Cell Biol* **81**, 93-105 (2003).
- 150 Dick, A. D., Meyer, P., James, T., Forrester, J. V., Hale, G., Waldmann, H. & Isaacs, J. D. Campath-1H therapy in refractory ocular inflammatory disease. *Br J Ophthalmol* **84**, 107-109 (2000).

- 151 He, Y. G., Ross, J. & Niederkorn, J. Y. Promotion of murine orthotopic corneal allograft survival by systemic administration of anti-CD4 monoclonal antibody. *Invest Ophthalmol Vis Sci* **32**, 2723-2728 (1991).
- 152 Vitova, A., Filipec, M., Zajicova, A., Krulova, M. & Holan, V. Prevention of corneal allograft rejection in a mouse model of high risk recipients. *Br J Ophthalmol* **88**, 1338-1342 (2004).
- 153 Coupland, S. E., Krause, L., Karow, A. C., Bartlett, R. R., Lehmann, M. & Hoffmann, F. Delay in corneal allograft rejection due to anti-CD4 antibody given alone and in combination with cyclosporin A and leflunomide. *Ger J Ophthalmol* **4**, 294-301 (1995).
- 154 Ayliffe, W., Alam, Y., Bell, E. B., McLeod, D. & Hutchinson, I. V. Prolongation of rat corneal graft survival by treatment with anti-CD4 monoclonal antibody. *Br J Ophthalmol* **76**, 602-606 (1992).
- 155 Ardjomand, N., McAlister, J. C., Rogers, N. J., Tan, P. H., George, A. J. & Larkin, D. F. Modulation of costimulation by CD28 and CD154 alters the kinetics and cellular characteristics of corneal allograft rejection. *Invest Ophthalmol Vis Sci* **44**, 3899-3905 (2003).
- 156 Konig Merediz, S. A., Zhang, E. P., Wittig, B. & Hoffmann, F. Ballistic transfer of minimalistic immunologically defined expression constructs for IL4 and CTLA4 into the corneal epithelium in mice after orthotopic corneal allograft transplantation. *Graefes Arch Clin Exp Ophthalmol* **238**, 701-707 (2000).
- 157 Comer, R. M., King, W. J., Ardjomand, N., Theoharis, S., George, A. J. & Larkin, D. F. Effect of administration of CTLA4-Ig as protein or cDNA on corneal allograft survival. *Invest Ophthalmol Vis Sci* **43**, 1095-1103 (2002).
- 158 Thiel, M. A., Steiger, J. U., O'Connell, P. J., Lehnert, A. M., Coster, D. J. & Williams, K. A. Local or short-term systemic costimulatory molecule blockade prolongs rat corneal allograft survival. *Clin Experiment Ophthalmol* **33**, 176-180 (2005).
- 159 Gebhardt, B. M., Hodkin, M., Varnell, E. D. & Kaufman, H. E. Protection of corneal allografts by CTLA4-Ig. *Cornea* **18**, 314-320 (1999).
- 160 Qian, Y. & Dana, M. R. Effect of locally administered anti-CD154 (CD40 ligand) monoclonal antibody on survival of allogeneic corneal transplants. *Cornea* **21**, 592-597 (2002).
- 161 Pleyer, U., Milani, J. K., Dukes, A., Chou, J., Lutz, S., Ruckert, D., Thiel, H. J. & Mondino, B. J. Effect of topically applied anti-CD4 monoclonal antibodies on orthotopic corneal allografts in a rat model. *Invest Ophthalmol Vis Sci* **36**, 52-61 (1995).
- 162 Thiel, M. A., Coster, D. J., Standfield, S. D., Brereton, H. M., Mavrangelos, C., Zola, H., Taylor, S., Yusim, A. & Williams, K. A. Penetration of

- engineered antibody fragments into the eye. *Clin Exp Immunol* **128**, 67-74 (2002).
- 163 Brereton, H. M., Taylor, S. D., Farrall, A., Hocking, D., Thiel, M. A., Tea, M., Coster, D. J. & Williams, K. A. Influence of format on in vitro penetration of antibody fragments through porcine cornea. *Br J Ophthalmol* **89**, 1205-1209 (2005).
- 164 Rosenberg, S. A., Aebersold, P., Cornetta, K., Kasid, A., Morgan, R. A., Moen, R., Karson, E. M., Lotze, M. T., Yang, J. C., Topalian, S. L. & et al. Gene transfer into humans--immunotherapy of patients with advanced melanoma, using tumor-infiltrating lymphocytes modified by retroviral gene transduction. *N Engl J Med* **323**, 570-578 (1990).
- 165 Edelstein, M. L., Abedi, M. R. & Wixon, J. Gene therapy clinical trials worldwide to 2007--an update. *J Gene Med* **9**, 833-842 (2007).
- 166 Cotrim, A. P. & Baum, B. J. Gene therapy: some history, applications, problems, and prospects. *Toxicol Pathol* **36**, 97-103 (2008).
- 167 Pleyer, U. & Dannowski, H. Delivery of Genes via Liposomes to Corneal Endothelial Cells. *Drug News Perspect* **15**, 283-289 (2002).
- 168 Parker, D. G., Brereton, H. M., Coster, D. J. & Williams, K. A. The potential of viral vector-mediated gene transfer to prolong corneal allograft survival. *Curr Gene Ther* **9**, 33-44 (2009).
- 169 Mohan, R. R., Sharma, A., Netto, M. V., Sinha, S. & Wilson, S. E. Gene therapy in the cornea. *Prog Retin Eye Res* **24**, 537-559 (2005).
- 170 Bennett, J. Immune response following intraocular delivery of recombinant viral vectors. *Gene Ther* **10**, 977-982 (2003).
- 171 Alba, R., Bosch, A. & Chillon, M. Gutless adenovirus: last-generation adenovirus for gene therapy. *Gene Ther* **12 Suppl 1**, S18-27 (2005).
- 172 Kochanek, S., Schiedner, G. & Volpers, C. High-capacity 'gutless' adenoviral vectors. *Curr Opin Mol Ther* **3**, 454-463 (2001).
- 173 Jager, L. & Ehrhardt, A. Emerging adenoviral vectors for stable correction of genetic disorders. *Curr Gene Ther* **7**, 272-283 (2007).
- 174 Vigna, E. & Naldini, L. Lentiviral vectors: excellent tools for experimental gene transfer and promising candidates for gene therapy. *J Gene Med* **2**, 308-316 (2000).
- 175 Challa, P., Luna, C., Liton, P. B., Chamblin, B., Wakefield, J., Ramabhadran, R., Epstein, D. L. & Gonzalez, P. Lentiviral mediated gene delivery to the anterior chamber of rodent eyes. *Mol Vis* **11**, 425-430 (2005).
- 176 Lewis, P., Hensel, M. & Emerman, M. Human immunodeficiency virus infection of cells arrested in the cell cycle. *Embo J* **11**, 3053-3058 (1992).

- 177 Weinberg, J. B., Matthews, T. J., Cullen, B. R. & Malim, M. H. Productive human immunodeficiency virus type 1 (HIV-1) infection of nonproliferating human monocytes. *J Exp Med* **174**, 1477-1482 (1991).
- 178 Follenzi, A. & Naldini, L. HIV-based vectors. Preparation and use. *Methods Mol Med* **69**, 259-274 (2002).
- 179 Naldini, L., Blomer, U., Gage, F. H., Trono, D. & Verma, I. M. Efficient transfer, integration, and sustained long-term expression of the transgene in adult rat brains injected with a lentiviral vector. *Proc Natl Acad Sci U S A* **93**, 11382-11388 (1996).
- 180 Cullen, B. R. HIV-1 auxiliary proteins: making connections in a dying cell. *Cell* **93**, 685-692 (1998).
- 181 Mann, R., Mulligan, R. C. & Baltimore, D. Construction of a retrovirus packaging mutant and its use to produce helper-free defective retrovirus. *Cell* **33**, 153-159 (1983).
- 182 Miller, A. D., Miller, D. G., Garcia, J. V. & Lynch, C. M. Use of retroviral vectors for gene transfer and expression. *Methods Enzymol* **217**, 581-599 (1993).
- 183 Freed, E. O. HIV-1 gag proteins: diverse functions in the virus life cycle. *Virology* **251**, 1-15 (1998).
- 184 Freed, E. O. HIV-1 replication. *Somat Cell Mol Genet* **26**, 13-33 (2001).
- 185 Akkina, R. K., Walton, R. M., Chen, M. L., Li, Q. X., Planelles, V. & Chen, I. S. High-efficiency gene transfer into CD34+ cells with a human immunodeficiency virus type 1-based retroviral vector pseudotyped with vesicular stomatitis virus envelope glycoprotein G. *J Virol* **70**, 2581-2585 (1996).
- 186 Naldini, L. Lentiviruses as gene transfer agents for delivery to non-dividing cells. *Curr Opin Biotechnol* **9**, 457-463 (1998).
- 187 Reiser, J., Harmison, G., Kluepfel-Stahl, S., Brady, R. O., Karlsson, S. & Schubert, M. Transduction of nondividing cells using pseudotyped defective high-titer HIV type 1 particles. *Proc Natl Acad Sci U S A* **93**, 15266-15271 (1996).
- 188 Zufferey, R., Nagy, D., Mandel, R. J., Naldini, L. & Trono, D. Multiply attenuated lentiviral vector achieves efficient gene delivery in vivo. *Nat Biotechnol* **15**, 871-875 (1997).
- 189 Dull, T., Zufferey, R., Kelly, M., Mandel, R. J., Nguyen, M., Trono, D. & Naldini, L. A third-generation lentivirus vector with a conditional packaging system. *J Virol* **72**, 8463-8471 (1998).
- 190 Iwakuma, T., Cui, Y. & Chang, L. J. Self-inactivating lentiviral vectors with U3 and U5 modifications. *Virology* **261**, 120-132 (1999).

- 191 Miyoshi, H., Blomer, U., Takahashi, M., Gage, F. H. & Verma, I. M. Development of a self-inactivating lentivirus vector. *J Virol* **72**, 8150-8157 (1998).
- 192 Zufferey, R., Dull, T., Mandel, R. J., Bukovsky, A., Quiroz, D., Naldini, L. & Trono, D. Self-inactivating lentivirus vector for safe and efficient in vivo gene delivery. *J Virol* **72**, 9873-9880 (1998).
- 193 Yu, D., Chen, D., Chiu, C., Razmazma, B., Chow, Y. H. & Pang, S. Prostate-specific targeting using PSA promoter-based lentiviral vectors. *Cancer Gene Ther* **8**, 628-635 (2001).
- 194 Parker, D. G., Brereton, H. M., Klebe, S., Coster, D. J. & Williams, K. A. A steroid-inducible promoter for the cornea. *Br J Ophthalmol* **93**, 1255-1259 (2009).
- 195 Anson, D. S. & Fuller, M. Rational development of a HIV-1 gene therapy vector. *J Gene Med* **5**, 829-838 (2003).
- 196 Fuller, M. & Anson, D. S. Helper plasmids for production of HIV-1-derived vectors. *Hum Gene Ther* **12**, 2081-2093 (2001).
- 197 Koldej, R., Cmielewski, P., Stocker, A., Parsons, D. W. & Anson, D. S. Optimisation of a multipartite human immunodeficiency virus based vector system; control of virus infectivity and large-scale production. *J Gene Med* **7**, 1390-1399 (2005).
- 198 Parker, D. G., Kaufmann, C., Brereton, H. M., Anson, D. S., Francis-Staite, L., Jessup, C. F., Marshall, K., Tan, C., Koldej, R., Coster, D. J. & Williams, K. A. Lentivirus-mediated gene transfer to the rat, ovine and human cornea. *Gene Ther* **14**, 760-767 (2007).
- 199 Cavazzana-Calvo, M., Hacein-Bey, S., de Saint Basile, G., Gross, F., Yvon, E., Nusbaum, P., Selz, F., Hue, C., Certain, S., Casanova, J. L., Bousso, P., Deist, F. L. & Fischer, A. Gene therapy of human severe combined immunodeficiency (SCID)-X1 disease. *Science* **288**, 669-672 (2000).
- 200 Gaspar, H. B., Parsley, K. L., Howe, S., King, D., Gilmour, K. C., Sinclair, J., Brouns, G., Schmidt, M., Von Kalle, C., Barington, T., Jakobsen, M. A., Christensen, H. O., Al Ghonaium, A., White, H. N., Smith, J. L., Levinsky, R. J., Ali, R. R., Kinnon, C. & Thrasher, A. J. Gene therapy of X-linked severe combined immunodeficiency by use of a pseudotyped gammaretroviral vector. *Lancet* **364**, 2181-2187 (2004).
- 201 Manno, C. S., Pierce, G. F., Arruda, V. R., Glader, B., Ragni, M., Rasko, J. J., Ozelo, M. C., Hoots, K., Blatt, P., Konkle, B., Dake, M., Kaye, R., Razavi, M., Zajko, A., Zehnder, J., Rustagi, P. K., Nakai, H., Chew, A., Leonard, D., Wright, J. F., Lessard, R. R., Sommer, J. M., Tigges, M., Sabatino, D., Luk, A., Jiang, H., Mingozzi, F., Couto, L., Ertl, H. C., High, K. A. & Kay, M. A. Successful transduction of liver in hemophilia by AAV-Factor IX and

- limitations imposed by the host immune response. *Nat Med* **12**, 342-347 (2006).
- 202 Raper, S. E., Chirmule, N., Lee, F. S., Wivel, N. A., Bagg, A., Gao, G. P., Wilson, J. M. & Batshaw, M. L. Fatal systemic inflammatory response syndrome in a ornithine transcarbamylase deficient patient following adenoviral gene transfer. *Mol Genet Metab* **80**, 148-158 (2003).
- 203 Hacein-Bey-Abina, S., Garrigue, A., Wang, G. P., Soulier, J., Lim, A., Morillon, E., Clappier, E., Caccavelli, L., Delabesse, E., Beldjord, K., Asnafi, V., MacIntyre, E., Dal Cortivo, L., Radford, I., Brousse, N., Sigaux, F., Moshous, D., Hauer, J., Borkhardt, A., Belohradsky, B. H., Wintergerst, U., Velez, M. C., Leiva, L., Sorensen, R., Wulffraat, N., Blanche, S., Bushman, F. D., Fischer, A. & Cavazzana-Calvo, M. Insertional oncogenesis in 4 patients after retrovirus-mediated gene therapy of SCID-X1. *J Clin Invest* **118**, 3132-3142 (2008).
- 204 Nathan, D. G. & Orkin, S. H. Musings on genome medicine: gene therapy. *Genome Med* **1**, 38 (2009).
- 205 Bushman, F. D. Retroviral integration and human gene therapy. *J Clin Invest* **117**, 2083-2086 (2007).
- 206 Howe, S. J., Mansour, M. R., Schwarzwaelder, K., Bartholomae, C., Hubank, M., Kempfski, H., Brugman, M. H., Pike-Overzet, K., Chatters, S. J., de Ridder, D., Gilmour, K. C., Adams, S., Thornhill, S. I., Parsley, K. L., Staal, F. J., Gale, R. E., Linch, D. C., Bayford, J., Brown, L., Quaye, M., Kinnon, C., Ancliff, P., Webb, D. K., Schmidt, M., von Kalle, C., Gaspar, H. B. & Thrasher, A. J. Insertional mutagenesis combined with acquired somatic mutations causes leukemogenesis following gene therapy of SCID-X1 patients. *J Clin Invest* **118**, 3143-3150 (2008).
- 207 Kohn, D. B., Sadelain, M. & Glorioso, J. C. Occurrence of leukaemia following gene therapy of X-linked SCID. *Nat Rev Cancer* **3**, 477-488 (2003).
- 208 Li, Z., Dullmann, J., Schiedlmeier, B., Schmidt, M., von Kalle, C., Meyer, J., Forster, M., Stocking, C., Wahlers, A., Frank, O., Ostertag, W., Kuhlcke, K., Eckert, H. G., Fehse, B. & Baum, C. Murine leukemia induced by retroviral gene marking. *Science* **296**, 497 (2002).
- 209 Somia, N. & Verma, I. M. Gene therapy: trials and tribulations. *Nat Rev Genet* **1**, 91-99 (2000).
- 210 One of three successfully treated CGD patients in a Swiss-German gene therapy trial died due to his underlying disease: A position statement from the European Society of Gene Therapy (ESGT). *J Gene Med* **8**, 1435 (2006).
- 211 Evans, C. H., Ghivizzani, S. C. & Robbins, P. D. Arthritis gene therapy's first death. *Arthritis Res Ther* **10**, 110 (2008).



- 212 Bainbridge, J. W., Smith, A. J., Barker, S. S., Robbie, S., Henderson, R., Balaggan, K., Viswanathan, A., Holder, G. E., Stockman, A., Tyler, N., Petersen-Jones, S., Bhattacharya, S. S., Thrasher, A. J., Fitzke, F. W., Carter, B. J., Rubin, G. S., Moore, A. T. & Ali, R. R. Effect of gene therapy on visual function in Leber's congenital amaurosis. *N Engl J Med* **358**, 2231-2239 (2008).
- 213 Cideciyan, A. V., Aleman, T. S., Boye, S. L., Schwartz, S. B., Kaushal, S., Roman, A. J., Pang, J. J., Sumaroka, A., Windsor, E. A., Wilson, J. M., Flotte, T. R., Fishman, G. A., Heon, E., Stone, E. M., Byrne, B. J., Jacobson, S. G. & Hauswirth, W. W. Human gene therapy for RPE65 isomerase deficiency activates the retinoid cycle of vision but with slow rod kinetics. *Proc Natl Acad Sci U S A* **105**, 15112-15117 (2008).
- 214 Maguire, A. M., Simonelli, F., Pierce, E. A., Pugh, E. N., Jr., Mingozzi, F., Bennicelli, J., Banfi, S., Marshall, K. A., Testa, F., Surace, E. M., Rossi, S., Lyubarsky, A., Arruda, V. R., Konkle, B., Stone, E., Sun, J., Jacobs, J., Dell'Osso, L., Hertle, R., Ma, J. X., Redmond, T. M., Zhu, X., Hauck, B., Zeleniaia, O., Shindler, K. S., Maguire, M. G., Wright, J. F., Volpe, N. J., McDonnell, J. W., Auricchio, A., High, K. A. & Bennett, J. Safety and efficacy of gene transfer for Leber's congenital amaurosis. *N Engl J Med* **358**, 2240-2248 (2008).
- 215 Chung, D. C., Lee, V. & Maguire, A. M. Recent advances in ocular gene therapy. *Curr Opin Ophthalmol* **20**, 377-381 (2009).
- 216 in *Antibody Engineering, A Practical Approach* eds J. McCafferty, H. R. Hoogenboom, & D.J. Chiswell) 206-208 (Oxford University Press, 1996).
- 217 Meijerink, J., Mandigers, C., van de Locht, L., Tonnissen, E., Goodsaid, F. & Raemaekers, J. A novel method to compensate for different amplification efficiencies between patient DNA samples in quantitative real-time PCR. *J Mol Diagn* **3**, 55-61 (2001).
- 218 Livak, K. J. & Schmittgen, T. D. Analysis of relative gene expression data using real-time quantitative PCR and the 2<sup>-</sup>(Delta Delta C(T)) Method. *Methods* **25**, 402-408 (2001).
- 219 Vandesompele, J., De Preter, K., Pattyn, F., Poppe, B., Van Roy, N., De Paepe, A. & Speleman, F. Accurate normalization of real-time quantitative RT-PCR data by geometric averaging of multiple internal control genes. *Genome Biol* **3**, RESEARCH0034 (2002).
- 220 Jessup, C. F. *Antigen presentation during corneal allograft rejection in the rat* Doctor of Philosophy thesis, Flinders University, (2005).
- 221 Jessup, C. F., Brereton, H. M., Sykes, P. J., Thiel, M. A., Coster, D. J. & Williams, K. A. Local gene transfer to modulate rat corneal allograft rejection. *Invest Ophthalmol Vis Sci* **46**, 1675-1681 (2005).

- 222 Kanegae, Y., Makimura, M. & Saito, I. A simple and efficient method for purification of infectious recombinant adenovirus. *Jpn J Med Sci Biol* **47**, 157-166 (1994).
- 223 QBiogene, I. (ed Inc QBiogene) 39-39 (AdEasy vector system. Application manual version 1.4.).
- 224 Klebe, S., Coster, D. J., Sykes, P. J., Swinburne, S., Hallsworth, P., Scheerlinck, J. P., Krishnan, R. & Williams, K. A. Prolongation of sheep corneal allograft survival by transfer of the gene encoding ovine IL-12-p40 but not IL-4 to donor corneal endothelium. *J Immunol* **175**, 2219-2226 (2005).
- 225 Borrás, T., Gabelt, B. T., Klintworth, G. K., Peterson, J. C. & Kaufman, P. L. Non-invasive observation of repeated adenoviral GFP gene delivery to the anterior segment of the monkey eye in vivo. *J Gene Med* **3**, 437-449 (2001).
- 226 Naldini, L., Blomer, U., Gallay, P., Ory, D., Mulligan, R., Gage, F. H., Verma, I. M. & Trono, D. In vivo gene delivery and stable transduction of nondividing cells by a lentiviral vector. *Science* **272**, 263-267 (1996).
- 227 Ikebe, H., Takamatsu, T., Itoi, M. & Fujita, S. Cytofluorometric nuclear DNA determinations on human corneal endothelial cells. *Exp Eye Res* **39**, 497-504 (1984).
- 228 Hudson, P. J. Recombinant antibody fragments. *Curr Opin Biotechnol* **9**, 395-402 (1998).
- 229 Donnelly, M. L., Luke, G., Mehrotra, A., Li, X., Hughes, L. E., Gani, D. & Ryan, M. D. Analysis of the aphthovirus 2A/2B polyprotein 'cleavage' mechanism indicates not a proteolytic reaction, but a novel translational effect: a putative ribosomal 'skip'. *J Gen Virol* **82**, 1013-1025 (2001).
- 230 De Felipe, P. & Izquierdo, M. Tricistronic and tetracistronic retroviral vectors for gene transfer. *Hum Gene Ther* **11**, 1921-1931 (2000).
- 231 de Felipe, P., Martin, V., Cortes, M. L., Ryan, M. & Izquierdo, M. Use of the 2A sequence from foot-and-mouth disease virus in the generation of retroviral vectors for gene therapy. *Gene Ther* **6**, 198-208 (1999).
- 232 Holst, J., Vignali, K. M., Burton, A. R. & Vignali, D. A. Rapid analysis of T-cell selection in vivo using T cell-receptor retrogenic mice. *Nat Methods* **3**, 191-197 (2006).
- 233 Klump, H., Schiedlmeier, B., Vogt, B., Ryan, M., Ostertag, W. & Baum, C. Retroviral vector-mediated expression of HoxB4 in hematopoietic cells using a novel coexpression strategy. *Gene Ther* **8**, 811-817 (2001).
- 234 Lorens, J. B., Pearsall, D. M., Swift, S. E., Peelle, B., Armstrong, R., Demo, S. D., Ferrick, D. A., Hitoshi, Y., Payan, D. G. & Anderson, D. Stable, stoichiometric delivery of diverse protein functions. *J Biochem Biophys Methods* **58**, 101-110 (2004).

- 235 Milsom, M. D., Woolford, L. B., Margison, G. P., Humphries, R. K. & Fairbairn, L. J. Enhanced in vivo selection of bone marrow cells by retroviral-mediated coexpression of mutant O6-methylguanine-DNA-methyltransferase and HOXB4. *Mol Ther* **10**, 862-873 (2004).
- 236 Schiedlmeier, B., Klump, H., Will, E., Arman-Kalcek, G., Li, Z., Wang, Z., Rimek, A., Friel, J., Baum, C. & Ostertag, W. High-level ectopic HOXB4 expression confers a profound in vivo competitive growth advantage on human cord blood CD34+ cells, but impairs lymphomyeloid differentiation. *Blood* **101**, 1759-1768 (2003).
- 237 Szymczak, A. L., Workman, C. J., Wang, Y., Vignali, K. M., Dilioglou, S., Vanin, E. F. & Vignali, D. A. Correction of multi-gene deficiency in vivo using a single 'self-cleaving' 2A peptide-based retroviral vector. *Nat Biotechnol* **22**, 589-594 (2004).
- 238 Fang, J., Qian, J. J., Yi, S., Harding, T. C., Tu, G. H., VanRoey, M. & Jooss, K. Stable antibody expression at therapeutic levels using the 2A peptide. *Nat Biotechnol* **23**, 584-590 (2005).
- 239 Fang, J., Yi, S., Simmons, A., Tu, G. H., Nguyen, M., Harding, T. C., VanRoey, M. & Jooss, K. An antibody delivery system for regulated expression of therapeutic levels of monoclonal antibodies in vivo. *Mol Ther* **15**, 1153-1159 (2007).
- 240 Furler, S., Paterna, J. C., Weibel, M. & Bueler, H. Recombinant AAV vectors containing the foot and mouth disease virus 2A sequence confer efficient bicistronic gene expression in cultured cells and rat substantia nigra neurons. *Gene Ther* **8**, 864-873 (2001).
- 241 Funston, G. M., Kallioinen, S. E., de Felipe, P., Ryan, M. D. & Iggo, R. D. Expression of heterologous genes in oncolytic adenoviruses using picornaviral 2A sequences that trigger ribosome skipping. *J Gen Virol* **89**, 389-396 (2008).
- 242 Amendola, M., Venneri, M. A., Biffi, A., Vigna, E. & Naldini, L. Coordinate dual-gene transgenesis by lentiviral vectors carrying synthetic bidirectional promoters. *Nat Biotechnol* **23**, 108-116 (2005).
- 243 Chinnasamy, D., Milsom, M. D., Shaffer, J., Neuenfeldt, J., Shaaban, A. F., Margison, G. P., Fairbairn, L. J. & Chinnasamy, N. Multicistronic lentiviral vectors containing the FMDV 2A cleavage factor demonstrate robust expression of encoded genes at limiting MOI. *Virol J* **3**, 14 (2006).
- 244 Chaplin, P. J., Camon, E. B., Villarreal-Ramos, B., Flint, M., Ryan, M. D. & Collins, R. A. Production of interleukin-12 as a self-processing 2A polypeptide. *J Interferon Cytokine Res* **19**, 235-241 (1999).
- 245 de Felipe, P. & Ryan, M. D. Targeting of proteins derived from self-processing polyproteins containing multiple signal sequences. *Traffic* **5**, 616-626 (2004).

- 246 Delenda, C. & Gaillard, C. Real-time quantitative PCR for the design of lentiviral vector analytical assays. *Gene Ther* **12 Suppl 1**, S36-50 (2005).
- 247 Bocker, W., Rossmann, O., Docheva, D., Malterer, G., Mutschler, W. & Schieker, M. Quantitative polymerase chain reaction as a reliable method to determine functional lentiviral titer after ex vivo gene transfer in human mesenchymal stem cells. *J Gene Med* **9**, 585-595 (2007).
- 248 Butler, S. L., Hansen, M. S. & Bushman, F. D. A quantitative assay for HIV DNA integration in vivo. *Nat Med* **7**, 631-634 (2001).
- 249 Charrier, S., Stockholm, D., Seye, K., Opolon, P., Taveau, M., Gross, D. A., Bucher-Laurent, S., Delenda, C., Vainchenker, W., Danos, O. & Galy, A. A lentiviral vector encoding the human Wiskott-Aldrich syndrome protein corrects immune and cytoskeletal defects in WASP knockout mice. *Gene Ther* **12**, 597-606 (2005).
- 250 Davis, J. L., Witt, R. M., Gross, P. R., Hokanson, C. A., Jungles, S., Cohen, L. K., Danos, O. & Spratt, S. K. Retroviral particles produced from a stable human-derived packaging cell line transduce target cells with very high efficiencies. *Hum Gene Ther* **8**, 1459-1467 (1997).
- 251 D'Costa, J., Harvey-White, J., Qasba, P., Limaye, A., Kaneski, C. R., Davis-Warren, A., Brady, R. O., Bankiewicz, K. S., Major, E. O. & Arya, S. K. HIV-2 derived lentiviral vectors: gene transfer in Parkinson's and Fabry disease models in vitro. *J Med Virol* **71**, 173-182 (2003).
- 252 Farson, D., Witt, R., McGuinness, R., Dull, T., Kelly, M., Song, J., Radeke, R., Bukovsky, A., Consiglio, A. & Naldini, L. A new-generation stable inducible packaging cell line for lentiviral vectors. *Hum Gene Ther* **12**, 981-997 (2001).
- 253 Forghani, B., Hurst, J. W. & Shell, G. R. Detection of the human immunodeficiency virus genome with a biotinylated DNA probe generated by polymerase chain reaction. *Mol Cell Probes* **5**, 221-228 (1991).
- 254 Geraerts, M., Willems, S., Baekelandt, V., Debyser, Z. & Gijssbers, R. Comparison of lentiviral vector titration methods. *BMC Biotechnol* **6**, 34 (2006).
- 255 Ikeda, Y., Collins, M. K., Radcliffe, P. A., Mitrophanous, K. A. & Takeuchi, Y. Gene transduction efficiency in cells of different species by HIV and EIAV vectors. *Gene Ther* **9**, 932-938 (2002).
- 256 Lizee, G., Aerts, J. L., Gonzales, M. I., Chinnasamy, N., Morgan, R. A. & Topalian, S. L. Real-time quantitative reverse transcriptase-polymerase chain reaction as a method for determining lentiviral vector titers and measuring transgene expression. *Hum Gene Ther* **14**, 497-507 (2003).
- 257 Loewen, N., Fautsch, M. P., Teo, W. L., Bahler, C. K., Johnson, D. H. & Poeschla, E. M. Long-term, targeted genetic modification of the aqueous

- humor outflow tract coupled with noninvasive imaging of gene expression in vivo. *Invest Ophthalmol Vis Sci* **45**, 3091-3098 (2004).
- 258 Logan, A. C., Nightingale, S. J., Haas, D. L., Cho, G. J., Pepper, K. A. & Kohn, D. B. Factors influencing the titer and infectivity of lentiviral vectors. *Hum Gene Ther* **15**, 976-988 (2004).
- 259 Martin-Rendon, E., White, L. J., Olsen, A., Mitrophanous, K. A. & Mazarakis, N. D. New methods to titrate EIAV-based lentiviral vectors. *Mol Ther* **5**, 566-570 (2002).
- 260 Metharom, P., Takyar, S., Xia, H. H., Ellem, K. A., Macmillan, J., Shepherd, R. W., Wilcox, G. E. & Wei, M. Q. Novel bovine lentiviral vectors based on Jembrana disease virus. *J Gene Med* **2**, 176-185 (2000).
- 261 Nair, A., Xie, J., Joshi, S., Harden, P., Davies, J. & Hermiston, T. A rapid and efficient branched DNA hybridization assay to titer lentiviral vectors. *J Virol Methods* **153**, 269-272 (2008).
- 262 Pan, D., Gunther, R., Duan, W., Wendell, S., Kaemmerer, W., Kafri, T., Verma, I. M. & Whitley, C. B. Biodistribution and toxicity studies of VSVG-pseudotyped lentiviral vector after intravenous administration in mice with the observation of in vivo transduction of bone marrow. *Mol Ther* **6**, 19-29 (2002).
- 263 Rose, A. C., Goddard, C. A., Colledge, W. H., Cheng, S. H., Gill, D. R. & Hyde, S. C. Optimisation of real-time quantitative RT-PCR for the evaluation of non-viral mediated gene transfer to the airways. *Gene Ther* **9**, 1312-1320 (2002).
- 264 Sastry, L., Johnson, T., Hobson, M. J., Smucker, B. & Cornetta, K. Titering lentiviral vectors: comparison of DNA, RNA and marker expression methods. *Gene Ther* **9**, 1155-1162 (2002).
- 265 Scherr, M., Battmer, K., Blomer, U., Ganser, A. & Grez, M. Quantitative determination of lentiviral vector particle numbers by real-time PCR. *Biotechniques* **31**, 520, 522, 524, passim (2001).
- 266 Scherr, M., Battmer, K., Schultheis, B., Ganser, A. & Eder, M. Stable RNA interference (RNAi) as an option for anti-bcr-abl therapy. *Gene Ther* **12**, 12-21 (2005).
- 267 Trono, D. Partial reverse transcripts in virions from human immunodeficiency and murine leukemia viruses. *J Virol* **66**, 4893-4900 (1992).
- 268 Watson, A., Ranchalis, J., Travis, B., McClure, J., Sutton, W., Johnson, P. R., Hu, S. L. & Haigwood, N. L. Plasma viremia in macaques infected with simian immunodeficiency virus: plasma viral load early in infection predicts survival. *J Virol* **71**, 284-290 (1997).

- 269 White, S. M., Renda, M., Nam, N. Y., Klimatcheva, E., Zhu, Y., Fisk, J., Halterman, M., Rimel, B. J., Federoff, H., Pandya, S., Rosenblatt, J. D. & Planelles, V. Lentivirus vectors using human and simian immunodeficiency virus elements. *J Virol* **73**, 2832-2840 (1999).
- 270 Yamada, K., Olsen, J. C., Patel, M., Rao, K. W. & Walsh, C. E. Functional correction of fanconi anemia group C hematopoietic cells by the use of a novel lentiviral vector. *Mol Ther* **3**, 485-490 (2001).
- 271 Sirin, O. & Park, F. Regulating gene expression using self-inactivating lentiviral vectors containing the mifepristone-inducible system. *Gene* **323**, 67-77 (2003).
- 272 Zhang, B., Metharom, P., Jullie, H., Ellem, K. A., Cleghorn, G., West, M. J. & Wei, M. Q. The significance of controlled conditions in lentiviral vector titration and in the use of multiplicity of infection (MOI) for predicting gene transfer events. *Genet Vaccines Ther* **2**, 6 (2004).
- 273 Palmenberg, A. C. Proteolytic processing of picornaviral polyprotein. *Annu Rev Microbiol* **44**, 603-623 (1990).
- 274 Percy, N., Barclay, W. S., Garcia-Sastre, A. & Palese, P. Expression of a foreign protein by influenza A virus. *J Virol* **68**, 4486-4492 (1994).
- 275 Ryan, M. D. & Drew, J. Foot-and-mouth disease virus 2A oligopeptide mediated cleavage of an artificial polyprotein. *Embo J* **13**, 928-933 (1994).
- 276 Ryan, M. D., King, A. M. & Thomas, G. P. Cleavage of foot-and-mouth disease virus polyprotein is mediated by residues located within a 19 amino acid sequence. *J Gen Virol* **72** ( Pt 11), 2727-2732 (1991).
- 277 Donnelly, M. L., Hughes, L. E., Luke, G., Mendoza, H., ten Dam, E., Gani, D. & Ryan, M. D. The 'cleavage' activities of foot-and-mouth disease virus 2A site-directed mutants and naturally occurring '2A-like' sequences. *J Gen Virol* **82**, 1027-1041 (2001).
- 278 Donnelly, M. L., Gani, D., Flint, M., Monaghan, S. & Ryan, M. D. The cleavage activities of aphthovirus and cardiovirus 2A proteins. *J Gen Virol* **78** ( Pt 1), 13-21 (1997).
- 279 Ryan, M. D., Donnelly, M. L., Lewis, A., Mehrotra, A., Wilkie, J. & Gani, D. A model for nonstoichiometric, cotranslational protein scission in eukaryotic ribosomes. *Bioorganic Chemistry* **27**, 55-79 (1999).
- 280 Mizuguchi, H., Xu, Z., Ishii-Watabe, A., Uchida, E. & Hayakawa, T. IRES-dependent second gene expression is significantly lower than cap-dependent first gene expression in a bicistronic vector. *Mol Ther* **1**, 376-382 (2000).
- 281 Zhou, Y., Aran, J., Gottesman, M. M. & Pastan, I. Co-expression of human adenosine deaminase and multidrug resistance using a bicistronic retroviral vector. *Hum Gene Ther* **9**, 287-293 (1998).

- 282 Ngoi, S. M., Chien, A. C. & Lee, C. G. Exploiting internal ribosome entry sites in gene therapy vector design. *Curr Gene Ther* **4**, 15-31 (2004).
- 283 Palendira, U., Kamath, A. T., Feng, C. G., Martin, E., Chaplin, P. J., Triccas, J. A. & Britton, W. J. Coexpression of interleukin-12 chains by a self-splicing vector increases the protective cellular immune response of DNA and Mycobacterium bovis BCG vaccines against Mycobacterium tuberculosis. *Infect Immun* **70**, 1949-1956 (2002).
- 284 Streilein, J. W., Cousins, S. & Williamson, J. S. Ocular molecules and cells that regulate immune responses in situ. *Int Ophthalmol* **14**, 317-325 (1990).
- 285 McMenamain, P. G., Djano, J., Wealthall, R. & Griffin, B. J. Characterization of the macrophages associated with the tunica vasculosa lentis of the rat eye. *Invest Ophthalmol Vis Sci* **43**, 2076-2082 (2002).
- 286 Bill, A. & Hellsing, K. Production and drainage of aqueous humor in the cynomolgus monkey (*Macaca irus*). *Invest Ophthalmol* **4**, 920-926 (1965).
- 287 Ruedl, C., Koebel, P., Bachmann, M., Hess, M. & Karjalainen, K. Anatomical origin of dendritic cells determines their life span in peripheral lymph nodes. *J Immunol* **165**, 4910-4916 (2000).
- 288 de Felipe, P., Luke, G. A., Hughes, L. E., Gani, D., Halpin, C. & Ryan, M. D. E unum pluribus: multiple proteins from a self-processing polyprotein. *Trends Biotechnol* **24**, 68-75 (2006).
- 289 Martinez-Salas, E. Internal ribosome entry site biology and its use in expression vectors. *Curr Opin Biotechnol* **10**, 458-464 (1999).
- 290 Zerrahn, J., Held, W. & Raulet, D. H. The MHC reactivity of the T cell repertoire prior to positive and negative selection. *Cell* **88**, 627-636 (1997).
- 291 Lee, R. S., Grusby, M. J., Glimcher, L. H., Winn, H. J. & Auchincloss, H., Jr. Indirect recognition by helper cells can induce donor-specific cytotoxic T lymphocytes in vivo. *J Exp Med* **179**, 865-872 (1994).
- 292 Boisgerault, F., Liu, Y., Anosova, N., Dana, R. & Benichou, G. Differential roles of direct and indirect allorecognition pathways in the rejection of skin and corneal transplants. *Transplantation* **87**, 16-23 (2009).
- 293 Felix, N. J. & Allen, P. M. Specificity of T-cell alloreactivity. *Nat Rev Immunol* **7**, 942-953 (2007).